

Modeling and Control for the Treatment of Type 1 Diabetes: An Approach Based on Therapy Parameters

THÈSE N° 6084 (2014)

PRÉSENTÉE LE 21 FÉVRIER 2014

À LA FACULTÉ DES SCIENCES ET TECHNIQUES DE L'INGÉNIEUR
INSTITUT DE GÉNIE ÉLECTRIQUE ET ÉLECTRONIQUE
PROGRAMME DOCTORAL EN GÉNIE ÉLECTRIQUE

ÉCOLE POLYTECHNIQUE FÉDÉRALE DE LAUSANNE

POUR L'OBTENTION DU GRADE DE DOCTEUR ÈS SCIENCES

PAR

Alain BOCK

acceptée sur proposition du jury:

Dr A. Karimi, président du jury
Dr D. Gillet, Dr G. François, directeurs de thèse
Prof. M.-O. Hongler, rapporteur
Prof. S. Mougiakakou, rapporteur
Prof. T. Prud'homme, rapporteur
Dr A. Soni, rapporteur



ÉCOLE POLYTECHNIQUE
FÉDÉRALE DE LAUSANNE

Suisse
2014

Fir meng Elteren a meng Schwëster

Acknowledgements

I would like to thank everyone who made this thesis possible and helped me all along the way with their support, expertise and friendship.

I express my deepest gratitude to my thesis directors, Dr Denis Gillet and Dr Grégory François, for allowing me to work on this fascinating project within the React group and the Laboratoire d'Automatique and for guiding me throughout the Ph.D. with their advice and encouragements.

I am very thankful for the fruitful collaboration with Roche Diagnostics who financially supported this thesis. Their interest in this topic is the foundation of my work. In particular, I would like to thank Dr Abhishek Soni and Dr Stefan Weinert in Indianapolis, and Dr Roland Schäfer, Dr Philipp Roebrock, and Dr Gilbert Schiltges in Burgdorf for our enriching work. Special thanks go to Prof. Thierry Prud'homme, for initiating this collaboration and sending me on the right track during the first months.

I would like to thank the members of my jury Prof. Stavroula Mougiakakou, Prof. Max-Olivier Hongler, Prof. Thierry Prud'homme and Dr Abhishek Soni, for reading my thesis and being present at the defense. Your insight and constructive comments have helped to improve this thesis. I also thank Dr Alireza Karimi, the president of the jury.

I am in the fortunate situation of being part of two extraordinary laboratories at the EPFL: the React group and the Laboratoire d'Automatique (LA). The React group is a small and very welcoming research group with great people. Thanks go to the whole group, whose company I enjoyed not only during our dinners and outings, but also during our weekly meetings. The daily breakfasts, "orgies", "remue-méninges" and unique atmosphere made my time in the LA extremely pleasant. Therefore, I express my gratitude to the current and past React and LA family, in particular, Dr Denis Gillet, Prof. Dominique Bonvin, Prof. Roland Longchamp and Prof. Colin Jones for allowing me to work in this environment, but also the secretaries, the technical staff, researchers and, of course, all my colleagues. You will be missed.

During the many years I lived in Lausanne, I was able to make many exceptional friends, so I want to thank: my flatmates and friends in the "al an nei Bourdonnette" for the memorable dinners, parties, and cocktail evenings we had; my crazy training buddies who are always up to

Acknowledgements

no good; the group of veteran Luxembourgers in Lausanne I can always count on; Elementary Penguin for our frenetic jams and inspiring rehearsals; my coffee break-friends for brightening up the grayest workdays; the current and past members of the AELL who made me feel at home in Lausanne; Brass Création, the Avenir d'Aclens, the Echo du Chêne d'Aubonne, and the Big Band of the EJMA for receiving me with arms wide open and introducing me to the authentic Swiss life; the Association du Polyathlon for their events that revealed my limits and taught me how to surpass them; the Association du PolyLiban for the amazing trip to the land of cedars; my American and German friends who gave me the warmest of welcomes during my stays in Indianapolis. However, I shall not forget my oldest friend Joanna for the countless adventures we had together, and my long-time friends in Luxembourg for the fun we have on the rare occasions when I am back. Thank you for the unforgettable moments we have lived together.

Finally, I want to thank my family - Mama, Papa, Tina - for their unlimited support and unconditional love. Without you I would not be anywhere near where I am now.

And last, but definitely not least, I want to thank Ailin. I don't know how I could have done this without you. Your encouragements, your care and your smile are what kept me going. Thank you for always being there for me and for making me happy.

Abstract

Type 1 diabetes is an auto-immune disease that has a significant impact on patients' health and everyday life, and also on health care systems. Since their bodies are unable to control their blood glucose concentrations, patients need to take over this cumbersome task manually and live with the fear of hypo- and hyperglycemia. Counting carbohydrates, pricking their fingers several times per day to measure their blood glucose concentration and injecting insulin are part of their daily routine. This so-called "standard therapy", when applied carefully, leads to acceptable glucose control. However, in order to restore the lost quality of life, to potentially extend their life expectancy, and to avoid medical complications, today's research focuses on the design and the development of an artificial pancreas, a device that automatically controls patient's blood glucose concentrations.

Recent technological breakthroughs, such as insulin pumps and continuous glucose monitoring devices, have paved the way for improved diabetes management, with minimal patient involvement. Nevertheless, advanced blood glucose control methods fail to provide acceptable treatment, whereas standard therapy, which only relies on two parameters, is capable of successfully treating millions of patients. In this context, the aim of this thesis is to design a novel diabetes treatment method that is based on the standard therapy parameters, but takes advantage of the new technology.

In this thesis, the challenges that make glucose control difficult and limit the performances of state-of-the-art control methods, are identified. They are addressed in four independent steps that, when combined, define a new diabetes treatment strategy. First, new models are developed with the objective of improving the quality of the predictions of blood glucose concentration. Inspired by standard therapy knowledge, these simple, identifiable and reliable models are shown to have excellent glucose prediction capabilities and high correlations with physician-set therapy parameters. Meanwhile, they only rely on the identification of four or five parameters. The second step corresponds to the development of a method to design stochastic models, based on continuous deterministic models, motivated by the observed intra-patient variability of blood glucose concentration. When constructed on the basis of the new deterministic prediction models, the resulting stochastic models allow accounting for many sources of uncertainty without requiring additional parameter identification. This way, confidence intervals on predicted blood glucose concentrations are obtained and can be used to make diabetes treatment safer and more robust. Since continuous blood glucose measurements generally exhibit a high level of noise, these measurements have to be filtered before being used for control purposes. This is why the third step proposes to use the stochas-

Abstract

tic model for the design of an extended Kalman filter. Finally, new diabetes-specific control methods are investigated. Open- and closed-loop scenarios that allow successful meal rejections and maintain blood glucose levels close to a specified safe target, are directly derived from the new proposed prediction models. It is observed that meal announcements improve the performance of closed-loop glucose control, but are not mandatory, as the algorithm is shown to successfully reject unannounced meals as well. This novel control approach has the advantage of remaining simple as it only relies on two tuning parameters (with two additional ones for every announced meal type), which are easily obtained using the new prediction models. In other words, no manual tuning of the control algorithm is necessary.

All the proposed approaches are tested on real patient data, on the UVa/Padova simulator, or on both and show excellent performance. In addition, the new closed-loop control algorithms are compared to state-of-the-art controllers and mostly show slightly better results than far more complex controllers.

Keywords: Type 1 Diabetes Mellitus, Modeling, Stochastic Modeling, Control, Extended Kalman Filter, Insulin on Board

Résumé

Le diabète de type 1 est une maladie auto-immune qui a des conséquences sur la santé et la vie quotidienne des personnes atteintes, ainsi que sur les systèmes de santé publique. Comme leur corps n'est plus capable de régler la glycémie de façon naturelle, les patients doivent exécuter eux-mêmes manuellement cette tâche et vivent avec l'angoisse de l'hypo- et de l'hyperglycémie. Compter les hydrates de carbone, se piquer le doigt plusieurs fois par jour pour mesurer le taux de glycémie et injecter de l'insuline, font ainsi partie de leur quotidien. Cette « thérapie standard » conduit, lorsqu'elle est appliquée consciencieusement, à une gestion acceptable de la maladie. Cependant, pour diminuer les effets de la maladie en termes de perte de qualité de vie, augmenter potentiellement l'espérance de vie et éviter les complications médicales, les efforts de recherche se concentrent depuis plusieurs années sur le développement d'un pancréas artificiel, i.e. un appareil dont l'objectif est le réglage automatique de la glycémie.

Des progrès technologiques récents, comme le développement de pompes à insuline et d'appareils de mesure du glucose en continu, ouvrent la voie vers une amélioration du traitement de la maladie en réduisant l'implication du patient à un minimum. Néanmoins, les méthodes de commande avancée de la glycémie ne sont pas encore à même de fournir un traitement acceptable, tandis que la thérapie standard, qui dépend uniquement de deux paramètres, permet de traiter des millions de patients avec succès. Dans ce contexte, le but de cette thèse est de concevoir des nouvelles méthodes de traitement du diabète qui se basent sur les paramètres de la thérapie standard, tout en profitant des progrès technologiques récents.

Dans cette thèse, les défis soulevés par le contrôle automatique de la glycémie et qui limitent les performances des techniques de commande avancée sont identifiés. Des solutions sont proposées qui suivent quatre étapes indépendantes, qui, mises de concert, définissent une nouvelle stratégie pour le traitement de diabète. En premier lieu sont développés deux nouveaux modèles, avec pour objectif l'augmentation de la qualité de prédiction des taux de glycémie. Inspirés par la thérapie standard, ces modèles simples, identifiables et fiables, présentent d'excellentes capacités de prédiction de la glycémie et des corrélations élevées avec les paramètres de thérapie fixés par des médecins. Ils présentent aussi l'avantage que seuls 4 ou 5 paramètres doivent être identifiés. Dans la deuxième étape, une méthode pour construire des modèles stochastiques, basés sur des modèles continus et déterministes, est développée afin de tenir compte de la grande variabilité intra-individuelle. Etant construit sur la base d'un des nouveaux modèles de prédiction, ce modèle stochastique résultant permet de prendre en compte de nombreuses sources d'incertitude, sans pour autant nécessiter l'identification

de paramètres supplémentaires. Ainsi, des intervalles de confiance sur le taux de glycémie prédit sont obtenus qui permettent de rendre le traitement du diabète plus sûr et robuste. Puisque les mesures continues de glucose sont généralement très bruitées, il est nécessaire de les filtrer celles-ci avant de pouvoir les utiliser pour le contrôle de la glycémie. Pour cette raison, au cours de la troisième étape, il est proposé d'utiliser le modèle stochastique pour la construction d'un filtre de Kalman étendu. Finalement, des méthodes de commande automatique spécifiques au traitement du diabète sont étudiées. Des scénarios en boucle ouverte comme en boucle fermée sont dérivés directement des nouveaux modèles de prédiction. Ils permettent de rejeter l'effet des perturbations dues aux repas et de maintenir le taux de glycémie près d'une valeur de référence imposée. On peut observer qu'annoncer les repas améliore la performance de la commande en boucle fermée, mais n'est en rien rédhibitoire, puisque l'algorithme proposé est aussi capable de rejeter l'effet des repas non-annoncés. Cette nouvelle approche a l'avantage de rester simple, puisqu'elle dépend uniquement de deux paramètres à ajuster (avec deux paramètres supplémentaires par type de repas annoncé), qui sont facilement obtenus à l'aide des nouveaux modèles de prédiction. En d'autres termes, l'algorithme de commande n'a pas besoin d'être réglé manuellement.

Toutes les approches proposées dans cette thèse sont testées sur des données cliniques, sur le simulateur UVa/Padova, ou sur les deux. De plus, les nouveaux algorithmes de commande en boucle fermée sont comparés à des contrôleurs récemment publiés dans la littérature et exhibent souvent des résultats légèrement meilleurs que des contrôleurs bien plus complexes.

Mots-clés : Diabète de type 1, modélisation, modélisation stochastique, commande automatique, filtre de Kalman étendu, insuline active restante

Contents

Acknowledgements	v
Abstract	vii
Table of Contents	xi
List of Figures	xv
List of Tables	xix
1 Introduction	1
1.1 Motivation	1
1.1.1 Diabetes Mellitus	1
1.1.2 T1DM treatment	3
1.1.3 Motivation	7
1.2 Challenges in control of T1DM	7
1.2.1 Patient safety	8
1.2.2 Uncertainty	8
1.2.3 Complexity of insulin-glucose dynamics	9
1.2.4 Model identifiability	9
1.2.5 Asymmetric control objective	10
1.2.6 Time delay	10
1.2.7 Control saturation	11
1.3 Contributions	11
1.3.1 Control-specific prediction models of T1DM patients	12
1.3.2 Stochastic Modeling	12
1.3.3 BG Estimation	12
1.3.4 BG Control	12
1.4 Thesis Outline	13
2 Deterministic Modeling	15
2.1 Introduction	15
2.2 State of the art in modeling of the glucoregulatory system	16
2.2.1 Model applications	16
2.2.2 Model structures	17

Contents

2.2.3	Prediction and control specific models	18
2.2.4	Summary	22
2.3	Therapy Parameter-based Model	22
2.3.1	Model derivation	22
2.3.2	Standard therapy	27
2.4	Validation Tools and Methods	30
2.4.1	Validation data	30
2.4.2	Identification method	30
2.4.3	Reliable insulin action	31
2.4.4	Choice of metrics	31
2.5	Validation	32
2.5.1	UVa simulations	32
2.5.2	Clinical data	38
2.5.3	Comparison of results of the UVa simulator data and clinical data	44
2.6	Conclusion	44
3	Stochastic Modeling	47
3.1	Introduction	47
3.2	Stochastic modeling	48
3.2.1	Construction of a stochastic model	48
3.2.2	Propagating uncertainties	49
3.2.3	Parameter identification	50
3.3	Application to the TPM	52
3.3.1	TPM	52
3.3.2	Stochastic model for TPM	52
3.3.3	Relevance of the stochastic model	54
3.4	Stochastic model validation	55
3.4.1	Validation data	55
3.4.2	Validation methods	56
3.5	Results	57
3.5.1	Percentage of measurements inside confidence interval over complete data set	57
3.5.2	Stochastic predictions	62
3.5.3	Other models	64
3.6	Conclusion	66
4	BG estimation	67
4.1	Introduction	67
4.2	Observability	68
4.2.1	State-space representation	68
4.2.2	Observability	70
4.3	Different BG estimators	71
4.3.1	Low-pass filter	71

4.3.2	Luenberger observer	71
4.3.3	Kalman Filter (KF)	72
4.3.4	Extended Kalman Filter with the sTPM (EKF)	74
4.3.5	Extended Kalman Filter with sTPM and added process noise - the Therapy Parameter-based Filter (TPF)	75
4.4	Methods to compare CGM filters	76
4.4.1	Training data	76
4.4.2	Validation data	76
4.4.3	Metrics	77
4.5	Comparison results	77
4.5.1	Scenario 1	77
4.5.2	Scenario 2	79
4.5.3	Scenario 3	80
4.6	Conclusion	80
5	BG Control	83
5.1	Introduction	83
5.2	Open-loop control	84
5.2.1	State of the art	84
5.2.2	TPM-based open-loop therapy	85
5.2.3	CGM augmented open-loop control	97
5.2.4	Implementation on the UVa simulator	97
5.2.5	Results using the UVa simulation	99
5.2.6	Conclusion	99
5.3	Closed-loop control	100
5.3.1	State of the art	100
5.3.2	Closed-loop controllers	104
5.3.3	Evaluation using the UVa simulator	108
5.3.4	Comparative study	115
5.4	Outlook on sTPM-based BG control	122
5.4.1	Pump suspension	122
5.4.2	Open-loop optimal control using sTPM	122
5.4.3	MPC using sTPM	123
5.4.4	SMBG measurement reminder	123
5.4.5	Meal and fault detection	123
5.5	Conclusion	123
6	Conclusion	127
6.1	Summary	127
6.2	Perspectives	129

Contents

A Validation data	131
A.1 UVa/Padova simulator	131
A.1.1 Nominal data set	133
A.1.2 Sensitivity test days	134
A.2 Clinical study	135
B Metrics	137
B.1 MAD	137
B.2 R^2	137
B.3 EGA	138
B.4 BGRI	139
B.5 RMSE	139
B.6 Percentage of time spent within a range of BG concentrations	140
B.7 Mean BG concentrations	140
B.8 Minimum and maximum BG concentration	140
B.9 Boxplot	141
C A Minimal Exercise Extension for Models of the Glucoregulatory System	143
C.1 Introduction	143
C.2 Clinical Study	144
C.2.1 Protocol	144
C.2.2 Analysis	144
C.3 Modeling and Parameter Estimation	145
C.3.1 Model Extension	145
C.3.2 Parameter Identification	146
C.4 Results and Discussion	147
C.4.1 Model Fits	147
C.4.2 Application to new prediction models	147
C.4.3 Model Limitations	148
C.5 Conclusion	148
D Additional UVa comparisons	149
D.1 Wang controller	149
D.2 Grosman controller	150
D.3 Lee controller	150
D.4 Svensson controller	151
E Scenarios	153
E.1 Nominal Scenario	153
E.2 Zarkogianni Scenario	154
E.3 Cameron Scenario	154
E.4 Cormerais Scenario 1 day	154
E.5 Cormerais Scenario 7 days	154

E.6 Lee Scenario	156
E.7 Wang Scenario	157
E.8 Grosman Scenario	157
F Stochastic TPM equations	159
Bibliography	160
Glossary	175
Curriculum Vitae	181

List of Figures

1.1	Simplified version of the BG regulation mechanism in a healthy person.	2
1.2	Illustration of standard therapy.	5
1.3	Illustration of a system.	6
1.4	Illustration of open-loop control for T1DM treatment.	7
1.5	Illustration of closed-loop control for T1DM treatment.	7
1.6	Example of inter-patient variability. The figure shows CGM measurements from the 12 patients of the clinical study described in A.2, with exactly the same meal under standard therapy. BG concentrations are normalized with their respective initial BG concentrations.	9
1.7	The risk function quantifies patient risk as a function of BG concentration. . . .	10
2.1	BG predictions using the LMM with the same insulin sensitivity K_x and inputs, but two different time constants $1/a_x$	25
2.2	BG predictions using the TPM with the same insulin sensitivity K_x and inputs, but two different time constants $1/a_x$	26
2.3	TPM simulations after an insulin bolus (left-hand side) and a meal (right-hand side)	29
2.4	Simulations of the TPM with simultaneous insulin bolus and meal (left) and only an insulin bolus (right). The parameters are chosen as follows: $a_x = 0.04$, $a_g = 0.03$, $\frac{K_g}{K_x} (= I2C) = 0.1$ and K_x is chosen according to legend. The insulin bolus is $2U$ and the meal is $20g$	32
2.5	Boxplot (cf. appendix B.9) of the MAD and R^2 of the data fit of every patient (n=10). Comparison between different prediction models on UVa simulator data.	33
2.6	Comparison of physician-set therapy parameters and identified model parameters to illustrate correlation results on UVa simulator data (n=10).	35
2.7	MAD (top) and % in EGA zone A (bottom) of the averaged model predictions (n=40) for the different prediction models and prediction horizons h on UVa simulator data. Mean values are given on the left, standard deviations on the right.	37
2.8	Example of data fits for different prediction models on clinical data.	38
2.9	Boxplot (cf. appendix B.9) of the MAD and R^2 of the data fit of every patient (n=10). Comparison between different prediction models on clinical data.	39
2.10	Comparison of physician-set therapy parameters and identified model parameters to illustrate correlation results on clinical data.	41

List of Figures

2.11	Example of 90 minute predictions for different prediction models on clinical data.	42
2.12	MAD (top) and % in EGA zone A (bottom) of the averaged model predictions (n=58) for the different prediction models on clinical data. Mean values are given on the left, standard deviations on the right.	43
3.1	Scenario 1: Example of 5 realizations of the sTPM (left) and estimation of 95% confidence interval (right).	55
3.2	Scenario 2: Example of 5 realizations of the sTPM (left) and estimation of 95% confidence interval (right).	55
3.3	Boxplot (cf. appendix B.9) of percentage of measurements inside the 95% confidence interval of all validation data sets (n=40) for cases 1-4.	58
3.4	Examples for cases 1 to 4.	59
3.5	Examples for case 2 when validating over the complete data set.	60
3.6	Examples for case 4 when validating over the complete data set. Both examples show the negative influence of their identical noise realization.	60
3.7	Boxplot (cf. appendix B.9) of expected percentage of measurements inside the 95% confidence interval of all validation data sets for cases 5 to 8.	61
3.8	Comparison of stochastic prediction for cases 5 and 6.	62
3.9	Examples for different cases on 90 minutes prediction horizon.	63
3.10	Prediction results for UVa simulator results (cases 1-4) for different horizons. Means and standard deviations evaluated on all 40 validation sets are given. Mean values are given on the left, standard deviations on the right.	64
3.11	Prediction results for clinical study results (cases 5-8) for different horizons. Means and standard deviations evaluated on all validation sets are given. Mean values are given on the left, standard deviations on the right.	65
3.12	Stochastic prediction results for different models for case 2 and case 6. Mean values are given on the left, standard deviations on the right.	65
4.1	Luenberger observer	72
4.2	Boxplot (cf. appendix B.9) of average percentage in zone A of the EGA and Boxplot of average MAD for scenario 1, corresponding to day 3 of the validation data set.	78
4.3	Example of a BG profile on scenario 1 for adult 5.	78
4.4	Boxplot (cf. appendix B.9) of average percentage in zone A of the EGA and Boxplot of average MAD for scenario 2, corresponding to day 4 of the validation data set.	79
4.5	Example of a BG profile on scenario 2 for adult 6.	79
4.6	Boxplot (cf. appendix B.9) of average percentage in zone A of the EGA and Boxplot of average MAD for scenario 2, corresponding to day 4 of the validation data set.	80
4.7	Example of a BG profile on scenario 2 for adult 6.	81
5.1	Insulin-glucose system with meal disturbance.	86

5.2	Insulin-glucose system with meal disturbance and feed-forward control.	87
5.3	Proportional controller.	104
5.4	The TPC.	107
5.5	Closed-loop controller with announced meal and filter.	109
5.6	Closed-loop controller without meal announcement.	110
5.7	Averages of different metrics as a function of τ	110
5.8	Results for Adult 9 on nominal scenario with TPC TPE	111
5.9	Results for Adult 1 on nominal scenario with TPC TPE	112
5.10	Example of a BG concentration profile for adult 5 on the nominal scenario with the TPC NM (unannounced meals).	115
5.11	Relative BGRI error as a function of the number of repetitions for Adult 1 and a PID controller.	125
A.1	Example of UVa simulation of Adult 6 on nominal day scenario.	133
B.1	Clarke EGA. Figure based on MATLAB code by Edgar Guevara Codina.	138
C.1	Blood glucose concentration and heart rate for patient 9 on day 2. Illustration of linear regression (red line). 1 mmol/l corresponds to 18 mg/dl.	144
C.2	Comparison of slopes for different patients. Values for both exercise sessions and their mean are shown. 1 mmol/l corresponds to 18 mg/dl.	145
C.3	Model fit for patient 9 for both days. 1 mmol/l corresponds to 18 mg/dl.	147

List of Tables

2.1	Comparative table of properties of state-of-the-art models. ✓ indicates that a model verifies a property, × indicates that it does not.	22
2.2	MAD and R^2 indicators (averaged over all patients) for the four investigated models on UVa simulator data.	33
2.3	Identified S_G in 1/min for the TPM+. The parameter is constraint to the interval $[10^{-7}, 1]$ as it needs to be greater than 0, but may take relatively high values. . .	34
2.4	Different correlation factors and their relative p values (in brackets) between therapy parameters provided in the UVa simulator and identified parameters on UVa simulator data (n=10).	34
2.5	Different correlation factors and their relative p values (in brackets) between therapy parameters provided in the UVa simulator and identified parameters on UVa simulator data without Adult 9.	34
2.6	MAD and R^2 indicators (averaged over all patients) for the four investigated models on clinical data.	39
2.7	Identified S_G in 1/min for the TPM+. The parameter is constraint to the interval $[10^{-7}, 1]$	39
2.8	Different correlation factors and their relative p values (in brackets) between physician-set and identified parameters on clinical data.	40
2.9	Comparative table of model properties. ✓ indicates that a model verifies a property, × indicates that it does not.	45
3.1	Possible validation cases	56
3.2	Expected average and median percentage of prediction points within the 95% confidence interval on the maximum prediction horizon.	58
3.3	Expected average and median percentage of prediction points within the 95% confidence interval on the maximum prediction horizon.	61
4.1	Square root of Q_{BG} for all 10 patients in mg/dl.	74
5.1	Identified time constants for TPM on study data in minutes, and their corresponding q . If $q < 1$, it is marked as bold.	89
5.2	Identified time constants for TPM+ on study data in minutes, and their equation q . If $q < 1$, it is marked as bold.	90

List of Tables

5.3	Identified time constants for TPM on UVa simulator data in minutes, and their equation q . If $q < 1$, it is marked as bold.	90
5.4	Adjusted basal rates to have a G_{ss} of 112.5 mg/dl.	98
5.5	Results for all adults of the UVa simulator under for standard therapy on the nominal scenario.	99
5.6	Comparison of BGRI for all adults on nominal scenario.	112
5.7	Comparison of % within target for all adults on nominal scenario.	113
5.8	Comparison of % below target for all adults on nominal scenario.	113
5.9	Results of the nominal scenario without meal announcements comparing the proportional controller (P NM) and the TPC (TPC NM).	114
5.10	Results for the TPC TPF on the nominal scenario with announced meals but different controller sampling times.	116
5.11	Simulation results by Zarkogianni et al. compared to the TPC. Part 1. The mean value is given and the standard deviation is given in parentheses.	118
5.12	Simulation results by Zarkogianni et al. compared to the TPC. Part 2. The mean value is given and the standard deviation is given in parentheses.	118
5.13	Simulation results by Cameron et al. compared to the TPC NM. Part 1.	119
5.14	Simulation results by Cameron et al. compared to the TPC NM. Part 2.	119
5.15	Simulation results by Cormerais and Richard compared to the TPC on the 1 day scenario. Part 1.	120
5.16	Simulation results by Cormerais and Richard compared to the TPC on the 1 day scenario. Part 2.	120
5.17	Simulation results by Cormerais and Richard compared to the TPC on the 7 day scenario. Part 1.	121
5.18	Simulation results by Cormerais and Richard compared to the TPC on the 7 day scenario. Part 2.	121
5.19	Simulation results by Cormerais and Richard compared to the TPC on the 7 day scenario with adult 9 excluded. Part 1.	121
5.20	Simulation results by Cormerais and Richard compared to the TPC on the 7 day scenario with adult 9 excluded. Part 2.	121
6.1	Comparison of identified challenges with the different components designed in this study. ✓ indicates that the challenge is explicitly addressed, while (✓) indicates that its effect is indirectly, or incompletely reduced.	128
6.2	Comparison of identified challenges with a future sTPM-based controller (sTPC). ✓ indicates that the challenge is explicitly addressed, while (✓) indicates that its effect is indirectly, or incompletely reduced.	129
A.1	Default steady-state parameters in the UVa simulator	132
A.2	UVa simulator protocol. Day d , experiment start time t_s , experiment end time t_e , the insulin bolus induced drop in BG Δ_I in mg/dl, the time of the insulin bolus t_I , the CHO induced rise in BG Δ_M in mg/dl, the time of the CHO intake t_M , and the meal duration T_M in minutes are given.	134

A.3	UVa simulator protocol. Day d , experiment start time t_s , experiment end time t_e , the insulin bolus induced drop in BG Δ_I in mg/dl , the time of the insulin bolus t_I , the CHO induced rise in BG Δ_M in mg/dl , the time of the CHO intake t_M , and the meal duration T_M in minutes are given. t_{minBG} and t_{maxBG} are the times at which the minimum or the maximum BG concentration is reached, respectively	134
A.4	Clinical study protocol. The experiment start time t_s , experiment end time t_e , SMBG sampling interval T_s in minutes, availability of CGM data, and the chosen measurement point weight W_i (cf 3.2.3) are specified.	135
C.1	Identified parameters for all patients and respective coefficients of variation (%)	147
D.1	Adaptive basal therapy compared to the TPC and IIAS. Mean and standard deviation for 10 adults is given.	149
D.2	Zone MPC compared to TPC and IIAS. Mean and standard deviation for 10 adults is given.	150
D.3	Controller proposed by Lee et al. compared to TPC. Mean and standard deviation for 10 adults is given.	151
E.1	Nominal scenario protocol	153
E.2	Nominal scenario meal details	153
E.3	Zarkogianni scenario protocol	154
E.4	Zarkogianni scenario meal details	154
E.5	Cameron scenario protocol	155
E.6	Cameron scenario meal details	155
E.7	Cormerais 1day scenario protocol	155
E.8	Cormerais 1day scenario meal details	155
E.9	Cormerais 7day scenario protocol	156
E.10	Lee scenario protocol	156
E.11	Lee scenario meal details	156
E.12	Wang scenario protocol	157
E.13	Wang scenario meal details	157
E.14	Grosman scenario protocol	158
E.15	Grosman scenario meal details	158

1 Introduction

1.1 Motivation

1.1.1 Diabetes Mellitus

Diabetes Mellitus is a metabolic disease characterized by elevated Blood Glucose (BG) concentrations causing acute symptoms such as polyuria (frequent urination), polydipsia (increased thirst), and polyphagia (increased hunger). If these high BG concentrations stay untreated - a condition called hyperglycemia - severe short-term complications including diabetic ketoacidosis and coma may occur. However, long-term complications due to prolonged hyperglycemia are currently the most expensive burden to health care systems and the biggest detriment patient well-being. These complications include cardiovascular diseases, chronic renal failure, and nerve damages, leading among others to blindness, ulceration, amputations, and the need for dialysis.

In 2012, more than 371 million people (International Diabetes Foundation [2011]), i.e. 8.3% of the adult world population, are deemed to suffer from diabetes, most of which in low- and middle- income countries. This enormous, and constantly increasing (Danaei et al. [2011]) prevalence generates global health care expenditures estimated at 465 billion USD in 2011 (expected to rise to 595 billion USD by 2030). These figures highlight the primordial importance of research in diabetes prevention and care.

For a healthy person, the regulation of BG concentrations can be described by the simplified mechanism illustrated in figure 1.1. BG concentrations are kept in balance around 100 mg/dl mainly because of the effects of two hormones: insulin and glucagon. These hormones are produced by the beta- and alpha-cells of the pancreas, respectively. If BG concentration increases, for instance because of a meal, insulin release is stimulated. This insulin mediates the uptake of glucose from the blood to be stocked in the liver and muscles in the form of glycogen, thus reducing BG concentrations to a normal level. If, on the other hand, BG concentrations are low, glucagon is released by the pancreas. Glucagon stimulates the release of the stocked glycogen from the liver and muscles to the bloodstream, thus increasing BG

concentration. This explanation is, of course, an oversimplification as the exact mechanisms are more complex and involve several hormones and external influences. Nevertheless, it is widely admitted that insulin and glucagon are the most significant actors in glucoregulation.

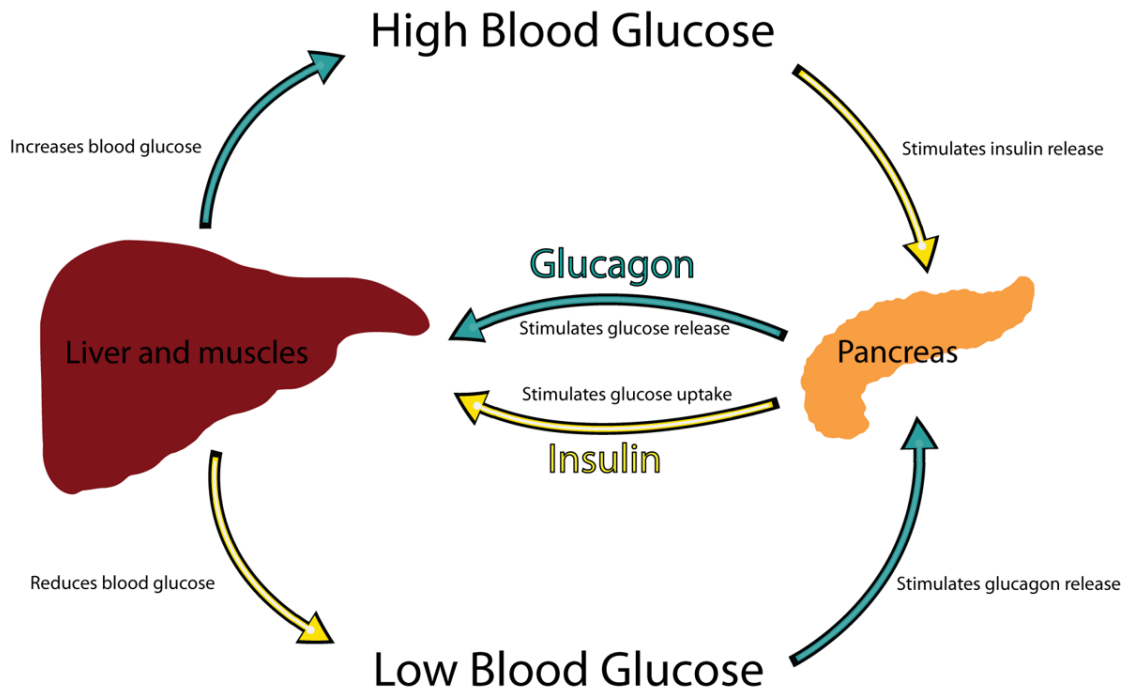


Figure 1.1: Simplified version of the BG regulation mechanism in a healthy person.

Diabetes appears if this equilibrium is disrupted and BG concentration cannot be lowered in an effective way anymore. Three main types of diabetes are defined, based on the cause of the elevated BG concentrations:

- **Type 1 Diabetes Mellitus (T1DM):** Elevated BG concentrations are caused by an autoimmune destruction of insulin producing beta-cells. Consequently, the reduction or absence of insulin production prevents excess glucose in the bloodstream to be stocked inside the liver or muscles. This results in very high BG concentrations that are fatal for the affected individual without treatment. Thus, exogenous insulin injections are vital. T1DM generally first appears at a young age and International Diabetes Foundation [2011] estimates that 78000 children develop T1DM every year. Nearly 10% of diabetic people have T1DM.
- **Type 2 Diabetes Mellitus (T2DM):** A number of lifestyle factors such as diet, physical activity, or stress, as well as genetic predispositions and medical conditions may lead to insulin resistance. In this case, insulin has less effect than for a non-insulin resistant person. This lead to an increase in insulin needs that cannot be met by the pancreatic insulin production, and, in turn, to an insulin deficit with increased BG concentration.

Depending on the severity of the insulin resistance, BG concentrations range from mildly elevated, which is mostly treated by lifestyle changes and medication, to very high, in which case exogenous insulin is needed. The vast majority of people, about 90%, have T2DM.

- **Gestational diabetes:** During pregnancy, 4% of women develop diabetes due to insufficient insulin production and use. While treated during pregnancy, gestational diabetes usually disappears after giving birth.

With exogenous insulin treatment, a new difficulty arises: if too much insulin is injected, BG concentrations can get too low. This condition, called hypoglycemia, is extremely dangerous as severe cases may lead to seizures, coma, or in the worst case even death. Cryer et al. [2003] give a detailed overview of hypoglycemia and related dangers and difficulties.

This thesis is on the treatment of T1DM. Clearly, this challenge should be addressed first as results can later be extended to the treatment of T2DM and other types by considering endogenous insulin production.

1.1.2 T1DM treatment

Until very recently, T1DM was a death sentence for affected people. This only changed with the first extraction of animal-sourced insulin and the first insulin treatment by Banting et al. [1922]. This treatment was improved and led to a significant increase in patients' life expectancy (Joslin [1924]). Over the last century, the treatment kept improving (for example, through the groundbreaking genetically engineered insulin synthesis using *E. coli* bacteria by Goeddel et al. [1979]) together with the understanding of the disease, but it was only The Diabetes Control and Complications Trial Research Group [1993] that showed the enormous benefit of intensive insulin treatment. Keeping BG concentrations as close to normoglycemia as possible significantly delays the onset and slows down the progression of retinopathy, nephropathy, and neuropathy. Nathan et al. [2005] extended these results with longer observations on cardiovascular diseases. As a result, the treatment of patients with T1DM consists in the challenging task of reducing hyperglycemia as much as possible while completely avoiding hypoglycemia.

In the following paragraphs different aspects of T1DM treatment are discussed. First the necessary devices are described and secondly, the different treatment methods are explained.

Devices for T1DM treatment

For T1DM treatment, insulin needs to be infused and BG concentrations need to be measured

Insulin administration Insulin can be administered by several means. Although syringes have been used for a long time for injecting insulin boluses (single doses), they are now widely replaced by insulin pens. For the last decades, the use of insulin pumps has become more and more widespread. These devices allow almost continuous insulin infusion by giving boluses up to every minute. Insulin may be administered (i) subcutaneously (SC), i.e. beneath the skin, (ii) intraperitoneally (IP), i.e. into the membrane of the abdominal cavity, or (iii) intravenously (IV), i.e. directly into the veins. The SC route is the standard for commercial insulin pumps because of the low risk of infections, but has the drawback of relatively slow insulin uptake times. Since fast insulin action reduces the amplitude postprandial BG excursions (as will be shown later), faster IP delivery is being researched and shows promising results, but with the risk of complications (Liebl et al. [2009]). IV infusion is the fastest as it is the closest to healthy insulin delivery, but is only applicable within a clinical setting because of a high risk of infection. In this thesis, therapy using Continuous Subcutaneous Insulin Infusion (CSII) is investigated because of the possibility to infuse insulin almost continuously and because of its widespread acceptance and use.

BG measurements Accurate BG measurements are key for appropriate treatment and avoidance of hypoglycemia. Two main methods are commonly being used: Self Monitoring of Blood Glucose (SMBG) and Continuous Glucose Monitoring (CGM). SMBG consists in measuring the glucose concentration in a small drop of blood obtained by pricking the finger with a lancet. This method is by far the most common because of its relatively good accuracy at reasonable cost. The biggest drawback of this method is that for every measurement, the patient needs to extract a blood drop - a painful procedure. As a result most patients do not take BG measurements very frequently. CGM devices are an alternative that gives almost continuous BG concentrations with less finger pricks, at the price of reduced accuracy and reliability. Also, these devices are relatively expensive and have a time-lag that can be dangerous. These disadvantages explain its slow progression on the market. This work considers both types of measurements.

Diabetes treatment methods

Different T1DM treatment approaches, ranging from currently applied methods to active research fields, are introduced in this paragraph.

Standard therapy Currently, standard therapy - as it will be called in this thesis - is the norm when it comes to T1DM treatment. This therapy is also referred to as basal/bolus therapy or Multiple Daily Injections (MDI), if performed using insulin pens or syringes. The principle is to split insulin treatment into two parts as illustrated in figure 1.2.

- **basal insulin** is insulin that acts relatively uniformly throughout the day and should keep patients fasting BG concentration close to the optimum. Patients using syringes or

pens inject long-acting insulin once or twice a day while CSII-treated patients use the insulin pump to adjust the basal rate in an "optimal" manner. Currently, the ability to change the basal insulin whenever needed is a major advantage of CSII over syringes or pens. A good overview of CSII treatment is given by Marcus [2013].

- **bolus insulin** is insulin that is injected in order to counteract the effect of meals. The carbohydrates (CHO) contained in meals are processed by the digestive system and release glucose into the bloodstream. In order to avoid hyperglycemia, this major disturbance needs to be counteracted by injecting a well-chosen quantity of fast-acting insulin using a syringe, pen, or insulin pump. This quantity is based on the quantity of ingested CHO and the pre-meal BG concentration. To compute the correct insulin amount, the patient has to take an SMBG measurement before each meal.

The Diabetes Control and Complications Trial Research Group [1993] that standard therapy is effective. However, this method can be enhanced by taking into account the additional information provided by CGM devices on the one hand, and by making meal rejections more effective on the other hand. Indeed, according to Prud'homme et al. [2011] these have a lot of room for improvement, as different meal speeds are not taken into account in standard therapy.

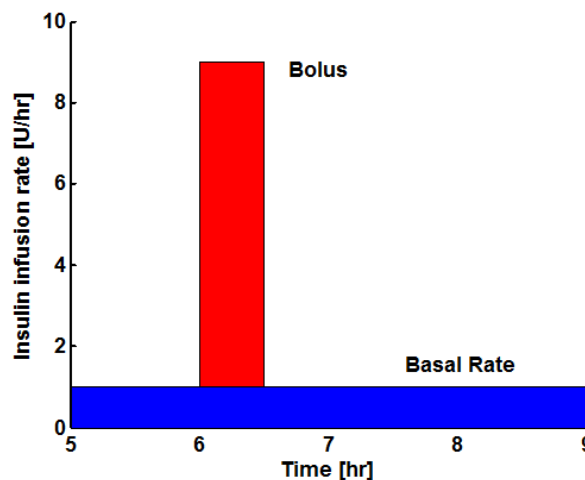


Figure 1.2: Illustration of standard therapy.

Short introduction to systems and control Before describing more elaborate control methods, control-specific concepts and vocabulary are introduced. In the context of control, a **system**, represented in figure 1.3, is an object of interest (it can be many different things) upon which different actions can be taken - the **inputs** u - and that shows or gives different reactions - the **outputs** y . The inputs are defined by the fact that they can be manipulated from outside the system, while the outputs are defined by the property that they can be observed from outside the system. Additionally, **disturbances** may apply to the systems. These are generally

unknown, but have a measurable effect on the outputs. For example, in this thesis, the system is part of the human endocrine system, the inputs are mainly insulin injection and meal intake, the output is BG concentration, and the disturbance is the measurement noise or other unknown excitations that have an effect on BG concentration.

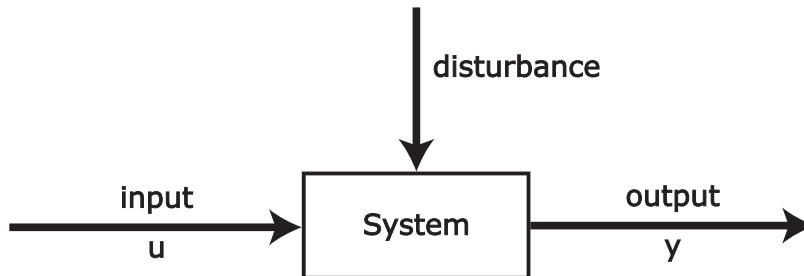


Figure 1.3: Illustration of a system.

Often, the behavior of a system is studied and described mathematically. This description is called a **model**, and it should reproduce the outputs of a system, based on the inputs, as accurately as possible. However, quite often, models are not capable of capturing the whole behavior of a system, either because it is too complex, or because disturbances are too important.

A system is called **static** if its outputs at a given time are influenced by the inputs at that time, only. In a **dynamical** system, however, the outputs are determined by current and past inputs.

A **controller** is used to adjust a system's inputs, in order to obtain desired outputs. This system is called controlled system. A controller itself can be considered as a system, whose output is the controlled system's input. If the controller's inputs depend directly on the controlled system's outputs, then the controller is called a **closed-loop** controller, otherwise it is called an **open-loop** controller. The output value that a closed-loop control algorithm is intended to reach is called a **setpoint**.

Open-loop control In control theory, an open-loop controller is a controller that computes system inputs based on the current system state and a model. In the context of T1DM treatment, open-loop control means that future insulin infusions are computed using current BG measurements and past insulin infusions, as illustrated in figure 1.4. Hence, standard therapy is a good example of open-loop control applied at every SMBG measurement and using a simple static model for BG prediction. However, other implementations than standard therapy exist for open-loop control and the use of different BG prediction and state estimation methods may improve treatment. These improvements should result in reduced hypo- and hyperglycemia. Open-loop control is currently not a very active field of research, despite its potential improvements over standard therapy.

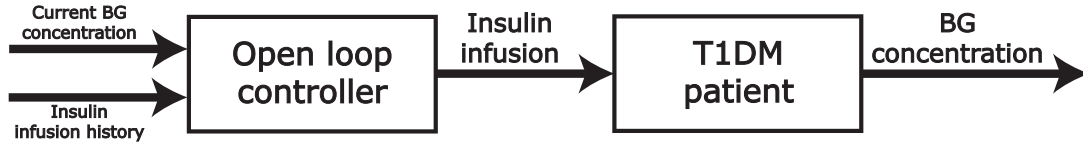


Figure 1.4: Illustration of open-loop control for T1DM treatment.

Closed-loop control In closed-loop control, a continuous or frequently sampled measurement is used to compute the system input continuously or at the same sampling rate, respectively. For closed-loop T1DM treatment, continuous measurements, i.e. a CGM device, is required. The resulting feedback structure, shown in figure 1.5, potentially leads to dramatic performance improvements and better disturbance rejection, although guaranteeing patient safety is still an open issue. The goal of a closed-loop treatment is to reproduce the behavior of a healthy pancreas as close as possible while minimizing patient involvement. Therefore, it is also referred to as the Artificial Pancreas (AP). It should be noted that, strictly speaking, open-loop control is actually closed-loop, as BG measurements are taken into account. However, because of the long and irregular sampling times, it is generally considered as open-loop.

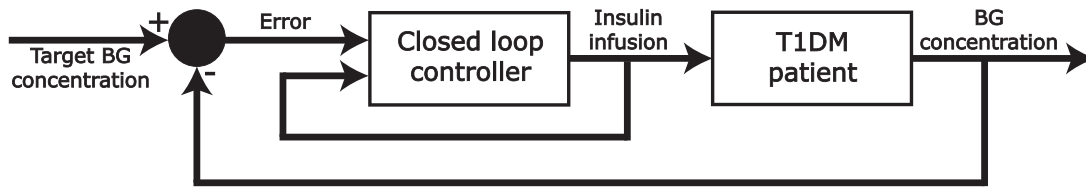


Figure 1.5: Illustration of closed-loop control for T1DM treatment.

1.1.3 Motivation

Diabetes is a disease with an enormous human and economic impact, but its current treatment is suboptimal, as it does not fully embrace the possibilities offered by insulin pumps and CGM devices. Thus, research to improve the treatment has a lot of potential to positively affect patients lives while reducing the health care burden. For these reasons, this thesis aims at making the treatment of patients with T1DM more effective. For this purpose, new BG prediction algorithms and new open- and closed-loop control strategies using the SC-SC route (i.e. SC measurements and SC insulin infusion), are explored. The ultimate goal is the design of an AP.

1.2 Challenges in control of T1DM

The quest for the AP has been ongoing for more than 3 decades and an enormous amount of time and money was spent. Still, there is no AP commercially available. Among the numerous scientific bottlenecks limiting the development of an AP, some are inherent to the difficulties

associated with BG control. The main challenges encountered during AP development and addressed in this thesis are described below.

1.2.1 Patient safety

BG control is vital and there is no room for mistakes. Patients' lives are at stake and BG control must be absolutely reliable and safe. This is why medical research is strictly regulated by different agencies such as the American Food and Drug Administration (FDA). These necessary, but heavy, regulations slow down the development process as clinical studies and new products need to be thoroughly tested and approved.

1.2.2 Uncertainty

BG concentrations as well as BG measurements are subject to a great number of uncertainties that make it very difficult to ascertain patient safety.

- **Inter-patient variability:** Patients differ significantly from one to another and need to have an individualized treatment. These differences have physiological and life-style related reasons and are significant: inter-patient variability for insulin absorption may have a coefficient of variation (CV) between 20-45% in a clinical environment (Heinemann [2002]). This uncertainty might even be higher for complete BG dynamics (i.e. not only insulin absorption) and in an out-patient setting. For this reason, if a model-based approach is used, it is necessary that the model parameters can be reliably determined for any patient on the basis of the available measurements: the model should be identifiable. An example of inter-patient variability is given in figure 1.6.
- **Intra-patient variability:** Even if the same treatment is applied and the same meals are taken, the BG concentration profile of a patient can vary significantly over consecutive and identical days. This glucose variability is related among others to changes in insulin sensitivity, but also insulin therapy (Vora and Heise [2013]). Heinemann [2002] quantifies this variability with a CV between 15 and 25% for insulin absorption in a clinical setting. Such variability is considerable and may lead to hypoglycemia.
- **Measurement noise:** BG measurements, when using SMBG or CGM, are very noisy. The ISO 15197 norm prescribes that 95% of measurements should be within 20% of the exact value if the reference BG > 75 mg/dl and within ± 15 mg/dl if BG ≤ 75 mg/dl. However, neither most SMBG devices (Freckmann et al. [2010]), nor CGMs (Freckmann et al. [2013]) currently fulfill this norm.
- **Meal announcement errors:** Most T1DM methods rely on meal announcements for which patients need to estimate the CHO content of the meal they are about to ingest. However, such an estimation is extremely difficult and even an experienced patient may considerably under- or overestimate the CHO content. Kildegaard et al. [2007]

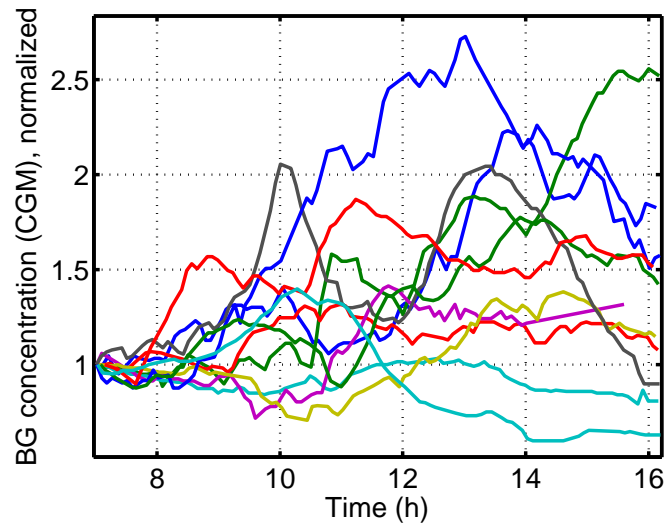


Figure 1.6: Example of inter-patient variability. The figure shows CGM measurements from the 12 patients of the clinical study described in A.2, with exactly the same meal under standard therapy. BG concentrations are normalized with their respective initial BG concentrations.

report an average intra-individual variation in meal announcements of 30%, which has a significant impact on the performances of the treatment.

- **Meal uptake rate variability:** Depending on the meal, the rate of glucose appearance in the bloodstream may vary considerably, as shown by Prud'homme et al. [2011]. This is quantified by the Glycemic Index (GI) that can be accounted for when predicting the effect of the meal. Nevertheless, this source of uncertainty remains and is mainly addressed by the use of different sets of model parameters associated with the corresponding meals.

1.2.3 Complexity of insulin-glucose dynamics

The relationship between insulin and glucose, i.e. the system to be controlled, is extremely complex. Even if some models were designed with the goal to mimic the glucoregulatory system with as much detail and physiological accuracy as possible (the model by Sorensen [1985] being the most notable example), they still cannot fully explain the observed variability. It is thus impossible to model the system in such a way that BG concentrations can be precisely predicted.

1.2.4 Model identifiability

Most control methods use a model to predict BG concentrations. As this model needs to be individualized, it is necessary that its parameters can be determined based on given measurements: the model needs to be identifiable. Mostly only BG measurements are available

because other measurements, such as tracer measurements, are expensive and thus not possible for a large population. This limitation prohibits the use of complex model structures and limits BG prediction capabilities. Model identifiability needs to be considered during model and experiment design.

1.2.5 Asymmetric control objective

Control theory mostly assumes that the control objective is symmetric around the setpoint (the value the controller tries to reach). In other words, undershoots of the system output are admissible if they allow faster convergence to the setpoint. However, the risk for a patient is not a symmetric function of the deviation of BG concentration, and undershoots mostly go hand in hand with hypoglycemia. In fact hypoglycemia is much more dangerous than hyperglycemia. The work of Kovatchev et al. [2000] led to the definition of an indicator of risk as a function of BG concentration. This risk function is depicted in figure 1.7, and is described in more detail in appendix B.4. It can be observed that, for example, a concentration of 50 mg/dl is as risky as a concentration of 240 mg/dl, while the risk is zero at 112.5 mg/dl. Therefore, traditional control algorithms need to be applied with caution.

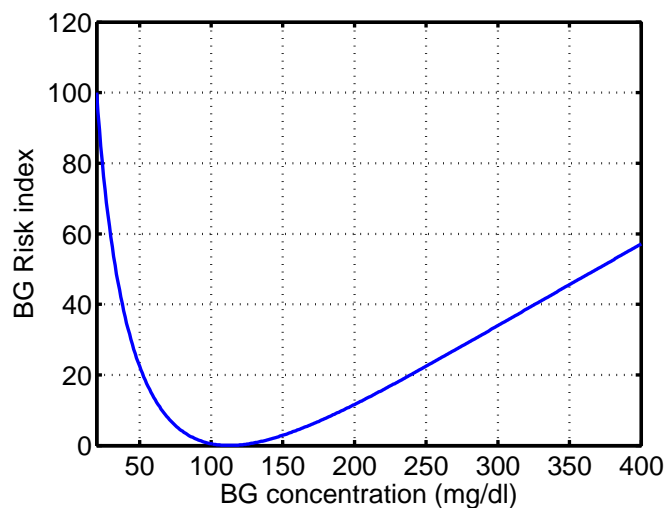


Figure 1.7: The risk function quantifies patient risk as a function of BG concentration.

1.2.6 Time delay

Time delays are detrimental to control performance. Intuitively this is well illustrated by an example given by Longchamp [2010]: Taking a shower is a case of closed-loop control as a target water temperature should be reached by adjusting the tap and feeling the temperature on the skin. This system has a time delay as the effect of the adjustment of the tap is not felt instantaneously, but only after several seconds. As a consequence, while setting the water temperature, one might over-adjust, but only feel this when the water gets too hot or cold. As

a reaction, one tends to over-adjust in the other direction and come back close to the original opening of the tap, hence creating an oscillating system fueled by over-adjustments. For T1DM control such oscillation must be avoided as they may lead to hypoglycemia or even loss of controller stability.

During T1DM treatment, time delays have two different origins:

- **SC infusion** During CSII, insulin is injected subcutaneously. Consequently, the insulin needs to be transported from the SC compartment into the bloodstream and it takes some time for the injected insulin to have an effect on BG concentrations. This delay is generally estimated to be around 20 minutes.
- **SC measurement** When using a CGM device, BG concentration is measured within the SC tissue, and not in the plasma. The glucose contained in the blood must first get into the interstitial fluids, which takes some time. Recently, Basu et al. [2013] estimated this delay to be 5 to 6 minutes for patients at fasting state (i.e. who did not eat or take an insulin bolus in the recent past)). However these values might be larger when large BG variations occur.

Overall, delays of up to 30 minutes between the insulin injection and the measurement of its effect can be observed. This is a substantial duration, especially considering that, for example, during exercise BG can drop easily by 60 mg/dl during 30 minutes (cf. figure C.1).

1.2.7 Control saturation

In closed-loop control, the control variable can generally take both, positive and negative values around its operating point. However, insulin injection can only take positive values as no insulin can be removed from the body. This saturation makes BG control difficult because, again, BG concentration undershoots need to be avoided at any price. Such an input saturation is a strong non-linearity that makes the application of standard control methods inappropriate and dangerous.

In other words, BG concentration can be lowered by an AP, but they cannot be automatically increased. The most common ways to increase BG concentration are through CHO intake or a glucagon shot, but these need to be administered manually. El-Khatib et al. [2010] use a second pump for automated glucagon injection, but this technique is not widely accepted, yet.

1.3 Contributions

This thesis proposes to improve the treatment of T1DM while addressing most of the aforementioned challenges using a complete method that leads to state-of-the-art BG control

without the need of manual parameter tuning, while making physician supervision more accessible. The contributions of this work are found in the fields of research discussed in below:

1.3.1 Control-specific prediction models of T1DM patients

New control-oriented prediction models are proposed. These models allow the identification of parameters that are directly linked to standard therapy parameters using exclusively BG measurements. Two versions of the **Therapy Parameter-based Model** (TPM) were designed to predict the effect of insulin injections and CHO intake on BG concentrations.

- **TPM** has only 4 parameters to identify and is best used for predicting BG concentrations of patients within the University of Virginia/Padova simulator (UVa simulator) - the FDA approved *in silico* simulator designed to test control algorithms, and described in A.1.
- **TPM+** has 5 parameters to identify and is recommended for prediction of real patient's BG concentrations.

Additionally, in the context of this work, a model extension for predicting the **effect of physical activity** on BG concentrations was proposed and is given in appendix C.

1.3.2 Stochastic Modeling

A method to design a **stochastic model** based on a given continuous deterministic model (not forcibly T1DM related) is proposed and validated. This method reliably computes **confidence intervals** on system states based on previous measurements.

This method is applied to the TPM to create the **stochastic Therapy Parameter-based Model** (sTPM).

1.3.3 BG Estimation

An Extended Kalman Filter (EKF)-based **Therapy Parameter-based Filter** (TPF) is proposed to process CGM data. It takes into account past insulin injections and CHO intake information to generate improved BG estimations. The TPF is derived using the sTPM.

1.3.4 BG Control

Based on the TPM and the TPF, several novel control approaches are proposed using both, open- and closed-loop control.

- **Open-loop:** Standard therapy was extended to reject meal disturbances in a more

effective way, especially in the case of very slow acting meals i.e. with a low GI.

- **Closed-loop:** A new **Therapy Parameter-based Controller** (TPC) continuously rejects announced and unannounced disturbances based on the TPM.

1.4 Thesis Outline

The thesis is organized as follows:

Chapter 2 discusses the design of deterministic models that leads to the TPM and TPM+. These new models are identified and their fitting and prediction capabilities are assessed with real clinical data as well as UVa simulator data.

In chapter 3, the method to build stochastic models based on parametric uncertainty is introduced and applied to the TPM to obtain the sTPM. Results are then validated using both clinical and UVa simulator data.

The use of an EKF in combination with the TPM or sTPM to improve the estimation of BG concentrations given by CGM devices is discussed in chapter 4. The TPC is shown to be effective in UVa simulator data.

All previous results are then combined in chapter 5 to provide a T1DM treatment strategy. Open-loop control and closed-loop options are introduced and assessed with the UVa simulator. Results are compared to state-of-the-art controllers.

Finally, a conclusion is drawn in chapter 6 and an outlook on possible future work is given.

2 Deterministic Modeling

2.1 Introduction

The development of reliable BG prediction models, that can be used e.g. in bolus calculators, educational tools, insulin pump suspension algorithms and closed-loop BG controllers, is a very active research field and many prediction models are now available in the literature, among which the most commonly used are undoubtedly compartmental models. These models, whose complexities rise from the simplicity of the Bergman Minimal Model (BMM), proposed by Bergman et al. [1979], to the complexity of the models of Hovorka et al. [2002] or Dalla Man et al. [2007], e.g., show potentially good prediction capabilities as long as they can be personalized (Fischer et al. [1987]). The personalization of the corresponding model parameters is only possible if, together with BG, additional measured quantities, such as insulin concentrations and tracer measurements, are available. Unfortunately this is rarely the case and prediction models that are identifiable with only BG measurements should be preferred. This justifies the widespread use of black-box models, such as auto-regressive models (Finan et al. [2009]), or Neural Networks (NN) (Daskalaki et al. [2011]). These models, however, have the disadvantage that their parameters cannot be linked to physically observable quantities. As a result, identification errors which result in unlikely parameters cannot be easily detected and predictions may become dangerously corrupted.

In this context, one of the main contributions of this thesis is to propose new compartmental models that can be identified using only BG measurements. Their simple linear structure, together with their low number of model parameters and states, facilitates the identification step and prevents fitting measurement noise. These new models also have the proven property that their model parameters are related to the standard therapy parameters, which have a physiological meaning. These are very valuable model properties for applications like continuous glucose measurement signal filtering, BG control (automated pancreas or open-loop control), state estimation, bolus calculators, or pump suspension algorithms.

This chapter starts by a review of the state of the art in modeling of the glucoregulatory system in section 2.2. In section 2.3, the new therapy parameter-based models are presented and the

link between its parameters and standard therapy parameters is discussed. In section 2.4, the identification method, and the evaluation metrics are described. The validation method of the new models is presented in section 2.5. This validation is performed in 3 successive steps: (i) the models are fitted to the UVa simulator and study data, (ii) the correlation between model and therapy parameters is verified, and (iii) model predictions are analyzed and compared. We conclude the chapter in section 2.6 and give an outlook on future work.

Most of the research and results presented in this chapter were published by Bock et al. [2013].

2.2 State of the art in modeling of the glucoregulatory system

To improve the treatment of patients with T1DM it is essential to have a good understanding of the dynamics of BG concentrations. As discussed before, this is made complicated by the extreme complexity and variability of the system. Despite these difficulties, many models of a wide range of complexity have been developed over the past decades. These models have all been designed for a specific applications, even if some were rightfully used beyond their initial scope. It is important to choose or design a model according to the intended use. The different applications of glucose-insulin models are reviewed and, for each, the commonly used models are given. Most of these models have a modular structure that is described, and, subsequently, prediction models are discussed in more detail and their properties compared to those requested for an appropriate prediction model.

2.2.1 Model applications

Several categories of models can be classified by decreasing complexity:

Physiological models The goal of this type of model is to follow the underlying principles of the glucoregulatory system. This means that the system is represented in the most detailed way, with all organs and associated transfer rates being modeled. As a consequence, these models generally rely on a very large number of model parameters and equations. The trouble is that these parameters are almost impossible to identify and population parameters are used. Hence, the individualization of these models is nearly impossible. Examples are developed by Sorensen [1985], or by Kim et al. [2007], who focus on the effect of exercise on the glucoregulatory system.

***In silico* simulation models** This type of model aims at generating BG profiles of virtual patients as a response to several stimuli, such as CHO intake or insulin infusions. This allows testing different therapies and controllers in the context of pilot studies. As an example, the UVa simulator by Kovatchev et al. [2009], based upon a model by Dalla Man et al. [2007] has been accepted by the United States FDA to replace animal testing in preclinical studies and is

2.2. State of the art in modeling of the glucoregulatory system

currently widely used for testing closed-loop therapies. Another model that is frequently used for this purpose was developed by Hovorka et al. [2002] and was implemented by Wilinska et al. [2010]. Models used in this framework generally rely on many parameters, whose identification requires complex and expensive experiments. For this reason, identification is only performed to generate a population of virtual patients. The model equations generally maintain a certain degree of physiological accuracy, i.e. the different states mostly represent the actual concentrations in the human body. A comparative overview of the most common simulation models is given by Colmegna and Sánchez Peña [2013].

Models for educational purposes Many people may not know how BG concentrations change when CHO are ingested or insulin is injected. To make them aware of the consequences of their different actions, educational simulators are used. These do not need to be perfectly accurate, nor to be individualized, but should only allow the prediction of the main tendencies. Most models qualify for this use, but there are also models, like the KADIS model by Rutscher et al. [1994] or the AIDA model by Lehmann and Deutsch [1991] that were specifically designed for this purpose.

Models for parameter identification In some cases it is important to determine the value of a given physiological parameter that is deemed to be useful for therapy or research. One way to obtain these values is to design a model that is sensitive to this parameter and to use clinical data. The most well-known example is the BMM that is designed to estimate insulin sensitivity. These models are generally tailored for a precise experimental setup (an intravenous glucose-tolerance test in the case of the BMM) and a predefined parameter.

Prediction and control specific models One of the most interesting properties of a model - and especially of those proposed in this thesis - is the ability to predict future BG values based on past data. These predictions can be used for multiple purposes, such as model-based control, bolus calculators, pump suspension algorithms and hypoglycemia warnings. Generally speaking, when models give accurate BG predictions, they are very well suited for BG control. As for the best model to use for this task, there is currently no consensus. Many different and opposing options are available, which are discussed with more details in 2.2.3. Again, important properties are that they should be identifiable on BG measurements only, and computationally cheap, while being robust against inter- and intra-patient variability.

2.2.2 Model structures

Most models discussed previously are designed in a modular way. This means that they are composed of several sub-models, which, in general, are interchangeable. In this section, the most common sub-models are introduced.

Glucose-insulin sub-models The glucose-insulin sub-model is the central part of T1DM patient models. The inputs are the plasma insulin concentration and the meal related glucose appearance rate, and the output is the BG concentration. The most used glucose-insulin sub-models are the BMM by Bergman et al. [1981], the Hovorka model (Hovorka et al. [2002]) and parts of the model by Dalla Man et al. [2007].

Insulin absorption sub-models Insulin absorption sub-models provide the evolution of the plasma insulin concentration as a function of subcutaneous or intravenous insulin injection. The output of these models can thus directly be used as an input for the glucose-insulin sub-model, whenever plasma insulin concentration is not measured. A good review is given by Nucci and Cobelli [2000], and Wilinska et al. [2005].

CHO sub-models To model the effect of meals on BG concentrations, most sub-models only focus on the CHO content of the ingested meal. The input of these sub-models is the CHO ingestion rate while the output is the glucose appearance rate. These sub-models can be combined with a glucose-insulin sub-model. Good examples are the Dalla Man Model, and the control model by Hovorka et al. [2004].

Exercise sub-models Physical activity has a significant influence on BG concentrations. For the moment, this is rarely taken into account by models. However, some models that quantify the effect of exercise exist, even if their inclusion into a glucose-insulin sub-model can be rather complex. Breton [2008], Hernández-Ordoñez and Campos-Delgado [2008], Roy [2008], and Balakrishnan et al. [2013] have contributed to this field, and an exercise model, which is discussed in appendix C, was designed during this thesis.

CGM sub-models As discussed in 1.2.6, CGM does not provide a direct measurement of the BG concentration, but the BG concentration in the interstitial tissue. To account for the dynamics between the different tissues and of the sensor itself, sub-models are being used. The UVa simulator, for example, uses the model by Breton and Kovatchev [2008].

Other sub-models There are several other factors that influence BG concentrations and some have been modeled. Examples are Free Fatty Acids by Roy [2008] or stress by Finan et al. [2010].

2.2.3 Prediction and control specific models

Since the objective of this thesis is to improve the treatment of patients with T1DM using control, the focus is on prediction- and control-specific models. Indeed, with most control

2.2. State of the art in modeling of the glucoregulatory system

methods, the quality of the prediction model has a critical influence on the control performances: a rudimentary control algorithm with an accurate model generally outperforms a perfect control method that is based on an inaccurate model. Hence, the availability of a tailored model to do control is a necessary, but not a sufficient condition for all reasonable model-based controller design.

The following specifications are required to address the challenges introduced in 1.2:

- **Personalizable:** Considering the large inter-patient variability (1.2.2), a prediction model needs to be easily adaptable to each patient.
- **Identifiable:** It is necessary that the personalized parameters of a prediction model can be identified (1.2.4) despite the large uncertainty. In order to improve patient safety (1.2.1), reliable insulin action identification is the most important property.
- **Acceptable predictions:** Despite the high complexity of the glucoregulatory system (1.2.3), the dynamics of a prediction model need to be good enough to lead to realistic and acceptable BG predictions.
- **Optional: Related to therapy parameters:** A direct relation between personalized parameters and commonly used therapy parameters is highly desirable. This would allow to either use physicians expertise to help tuning model parameters, or, conversely to facilitate model parameter validation by physicians.
- **Optional: Linear:** Linearity is a property that makes control more convenient and leads to many other useful properties. This feature is not mandatory, but desired if compatible with the other properties.

A first step is thus to review existing prediction models and assess if they fulfill the necessary specifications. In a second step, new models are designed, if required.

A recent and detailed review of models used for control was done by Balakrishnan et al. [2011] and a review including model-based control methods can be found in Lunze et al. [2012].

Prediction models can be divided into two categories, black box models, which do not rely on any physiological or other external knowledge and model structures, and grey box models whose dynamics and parameters are based on incomplete knowledge of the system. White box models, which rely solely on first principles, are not feasible in the context of modeling the glucoregulatory system because of the very high system complexity.

Black box models

Different families of black box models exist and have been used for prediction and control of BG concentration.

Autoregressive (AR) models Autoregressive models have linear dynamics that are defined by parameters, which are identified on training data. The main tuning parameter set by the user is the order of the model. Autoregressive models with exogenous inputs (ARX) are also widely used, as those by Finan et al. [2009], Ståhl and Johansson [2010], or Finan [2008]. Estrada et al. [2010] used an ARX model with adaptive parameters, while Cescon [2011] developed an Autoregressive–moving-average with exogenous inputs (ARMAX) model in her thesis. Bunesco et al. [2013] used an Autoregressive Integrated Moving Average (ARIMA) model in combination with support vector regression.

The main advantages of autoregressive models are that they are simple to implement, need minimal user input, and are computationally cheap. However, the main drawback is that the different parameters do not have a direct physiological meaning that might be validated by a physician, and meanwhile, often, identifications do not lead to reliable results, as shown by Finan et al. [2009]. Finally, only short prediction horizons give results that are sufficiently realistic.

Artificial NN Artificial NN are models used mainly in machine learning. Their structure is inspired from nervous systems and allows reproducing nonlinear observations. In the field of BG predictions, this is a very convenient tool, as more complex behaviors than with autoregressive models can be obtained. Daskalaki et al. [2011] show that performance of artificial NN is superior to ARX models for certain uses. Huang et al. [2010], and Zecchin et al. [2012] have shown a performance gain when combining artificial NN with a gray box model. Disadvantages of artificial NN are that its parameters do not have an explicit physiological meaning, making it difficult to evaluate their pertinence. Additionally, the computational load and the complexity of the controller design increase.

Support Vector Regression (SVR) Bunesco et al. [2013] used SVR to build prediction models. However, this led to better performances than AR models only when combined with a grey box model.

Grey box models

Grey box models are not based on first principles, but use available physiological knowledge, leading to models of varying complexity. A great number of such models can be found in the literature, but not all of them are suited for BG prediction and control. The most commonly used (although not forcibly the most suited) ones are introduced here.

Bergman-based models Though Bergman et al. [1979] originally designed the BMM to provide estimations of insulin sensitivities based on intravenous glucose tolerance tests in dogs and subsequently in humans (Bergman et al. [1981]), it has been widely used for BG

2.2. State of the art in modeling of the glucoregulatory system

prediction and control in many different variants by Cormerais and Richard [2012], Percival et al. [2008], François et al. [2003], Owens et al. [2006], Dua et al. [2006], Hughes et al. [2010].

What makes the BMM appealing for prediction and control is mainly its simple structure and its widespread acceptance, although, to be used as a prediction model, it requires additional sub-models for meal contributions, insulin dynamics and, optionally, physical activity (Bock et al. [2011]). However, according to Pilonetto et al. [2003], the identification of BMM parameters is only possible with a priori knowledge. Identifiability can be improved by using sub-models (e.g. Kanderian et al. [2009]), provided the insulin concentration profile $I(t)$ is available. This is unfortunately not the case in practice, as $I(t)$ is not measured, and the identifiability of the BMM is still an issue.

Hovorka-based models Hovorka et al. [2002] designed a model based on tracer measurements gathered from clinical experiments. This is a relatively complex model that is characterized by a triple insulin action. It was designed to reproduce the observations made on real patients and was mainly meant to be used as a virtual patient, but is used quite frequently for control as well. Hovorka et al. [2004] used it for nonlinear Model Predictive Control (MPC) with online parameter estimation. Another example where the Hovorka model is linearized is given by Boiroux et al. [2010a].

Using the Hovorka model as a prediction model is relatively difficult as the full model needs to be identified on the basis of expensive tracer measurements. One alternative is to identify a small subset of the model parameters, while using population values for the others.

Dalla Man-based models Dalla Man et al. [2007] developed a model to simulate the evolution of BG concentrations after meals for healthy and T2DM subjects and identified model parameters based on triple tracer measurements that are collected in an extensive subject database. Next, the model was extended to take into account subjects with T1DM by removing the endogenous insulin production and adding exogenous insulin infusion. The most prominent use of this model is in the FDA approved UVa/Padova Type 1 Diabetes Metabolic Simulator described in appendix A.1.

Although it is not a prediction model, the Dalla Man model is frequently the model used for MPC. In the linear MPC by Magni et al. [2007], and in its improved version by Soru et al. [2012], a linearized version of the Dalla Man model with mean population parameters is used. Because it is impossible to identify individual model parameters, it is the control method that is personalized, instead of the model. Bondia et al. [2011] used the Dalla Man model with other sub-models to generate interval predictions.

The advantage of the Dalla Man model is that it is well accepted and leads to good results on the UVa simulator because they are based on the same dynamics. Nevertheless, because of its complex structure, it is impossible to identify parameters and predictions may prove to be

inaccurate.

van Heusden model A control-specific model was designed in the frequency domain by van Heusden et al. [2012]. Their goal was to obtain an accurate model close to the cutoff frequency that improves robustness either for different individuals or for a whole population. The optional individualization is done using only the patients Total Daily Insulin (TDI). This model is an interesting option for the use in control, however its prediction capabilities are limited (as the model is not designed to do predictions) and the effect of CHO intake is not modeled.

2.2.4 Summary

Many prediction and control-specific models exist to date. However, so far, none fulfill all the requirements necessary to do reliable control of BG concentrations as recalled in Table 2.1. For this reason there is a need for a new identifiable model that is simple and gives acceptable predictions.

	AR	ANN	SVR	BMM	Hovorka	Dalla Man	van Heusden
Personalizable	✓	✓	✓	✓	✓	✓	✓
Identifiable	✓	✓	✓	×	×	×	N/A
Acceptable predictions	×	×	×	×	×	×	×
Related to therapy param.	×	×	×	✓	✓	✓	✓
Linear	✓	×	×	×	×	×	✓

Table 2.1: Comparative table of properties of state-of-the-art models. ✓ indicates that a model verifies a property, × indicates that it does not.

2.3 Therapy Parameter-based Model

In what follows, two models, the TPM and the TPM+, which fulfill the requirements defined in 2.2.3, are derived from the BMM and the relationship between the TPM parameters and physician-set therapy parameters is shown.

2.3.1 Model derivation

Bergman Minimal Model (BMM)

The initial point of the model design is the widely accepted BMM (cf 2.2.3). One variation of its equations is as follows:

$$\dot{G}(t) = -X(t)G(t) - S_G G(t) + U_{endo} \quad (2.1)$$

$$\dot{X}(t) = -p_2(X(t) - S_I I_p(t)) \quad (2.2)$$

where G is the BG concentration in $mg \cdot dl^{-1}$, X is the insulin action in min^{-1} , S_G is the glucose effectiveness at zero insulin in min^{-1} , S_I is the insulin sensitivity in $U^{-1} \cdot min^{-1} \cdot l$, U_{endo} is the endogenous glucose production in $mg \cdot dl^{-1} \cdot min^{-1}$, and p_2 is the inverse of the time constant of the insulin action in min^{-1} . I_p is the plasma insulin concentration in U/l .

To be used as a prediction model, the BMM needs to be extended with sub-models to account for insulin absorption and CHO intake.

Minimal model (MM)

Prud'homme et al. [2011] recently extended the BMM by substituting the insulin action and insulin absorption models by a 2nd-order insulin action model and by adding the 2nd-order linear carbohydrates (CHO) sub-model by Hovorka et al. [2004], resulting in the following set of ODEs:

$$\dot{G}(t) = -K_x X(t)G(t) - S_G G(t) + U_{endo} + K_g U_G(t) \quad (2.3)$$

$$\dot{U}_G(t) = -a_g U_G(t) + a_g U_{G,1}(t) \quad (2.4)$$

$$\dot{U}_{G,1}(t) = -a_g U_{G,1}(t) + a_g U_{CHO}(t) \quad (2.5)$$

$$\dot{X}(t) = -a_x X(t) + a_x X_1(t) \quad (2.6)$$

$$\dot{X}_1(t) = -a_x X_1(t) + a_x U_I(t) \quad (2.7)$$

where the new states are the gut glucose absorption U_G in $g \cdot min^{-1}$, the intermediate gut glucose absorption $U_{G,1}$ in $g \cdot min^{-1}$, and the intermediate insulin action X_1 in $U \cdot min^{-1}$. X is now given in $U \cdot min^{-1}$. Additional model parameters are introduced: the meal sensitivity K_g in $mg \cdot dl^{-1} \cdot g^{-1}$, the inverse of the meal time constant a_g in min^{-1} , the insulin sensitivity K_x in U^{-1} (different from S_I), and the inverse of the insulin absorption/action time constant a_x in min^{-1} . The manipulated inputs are the subcutaneous insulin infusion, U_I in $U \cdot min^{-1}$ and the carbohydrate intake rate U_{CHO} in $g \cdot min^{-1}$. This model will be referred to as the Minimal Model (MM) hereafter.

The fact that the insulin concentration - which is neither measured nor used - is not explicitly modeled improves the identifiability of this model compared to models using the original BMM insulin action of Equation (2.2).

However, the results presented by Prud'homme et al. [2011] show that, despite improved identifiability and the use of prior knowledge, the resulting predictions are still unsatisfactory and lead to sub-optimal insulin infusions. Another drawback of the MM lies in the behavior induced by the bilinear term of Equation 2.3 (Equation 2.1 for the BMM). While according to the term $-K_x X(t)G(t)$, high BG values should lead to high insulin effect and vice-versa, the opposite effect has been observed in practice (Unger and Grundy [1985]). Especially prolonged hyperglycemia blunts the effect of insulin.

Linear Minimal Model (LMM)

A simple yet effective approach to circumvent the limitations of both the BMM and MM is to linearize the BG equation. As linearity is also advantageous for identification and control purposes (Hernjak and Doyle III [2005]), several linearized versions of the minimal model are available in the literature. Fernandez et al. [2007] have shown that the performances of both the BMM and the LMM are comparable, though none fits all the available data. Linearized minimal models were also used by Percival et al. [2008] for predicting BG, but with limited success.

The LMM presented here and used thereafter is a linear version of the MM that reads:

$$\dot{G}(t) = -K_x X(t) - S_G G(t) + U_{endo} + K_g U_G(t) \quad (2.8)$$

$$\dot{U}_G(t) = -a_g U_G(t) + a_g U_{G,1}(t) \quad (2.9)$$

$$\dot{U}_{G,1}(t) = -a_g U_{G,1}(t) + a_g U_{CHO}(t) \quad (2.10)$$

$$\dot{X}(t) = -a_x X(t) + a_x X_1(t) \quad (2.11)$$

$$\dot{X}_1(t) = -a_x X_1(t) + a_x U_I(t) \quad (2.12)$$

with the insulin sensitivity K_x now being in $mg \cdot dl^{-1} \cdot U^{-1}$,

Despite the removal of the bilinear term, the LMM is still not very efficient in terms of steady-state predictions. In fact, if no insulin bolus is infused and no meal is ingested, steady-state BG concentration is obtained by setting all inputs and time derivatives to 0 in Equations (2.8) to (2.12) and reads:

$$G_{ss} = \frac{U_{endo}}{S_G} \quad (2.13)$$

Typical values of G_{ss} are around $100 mg \cdot dl^{-1}$, when adequate basal insulin is infused (cf. 2.3.2).

As such, the steady-state BG concentration predicted by the LMM does not depend on a patient's initial BG. In fact, all the aforementioned models predict recovery even when a patient in hyperglycemic condition does not take counteractive actions. This is in contradiction with practical observations that showed that in such a case, the patient will typically remain in hyperglycemic condition (Cescon et al. [2013]). Also, the parameters U_{endo} and S_G directly influence the identification of insulin and meal parameters, which makes identification particularly prone to model mismatch - which is inevitable in such a high noise and disturbance-rich environment. Indeed, the couples of insulin and meal time constants and sensitivities, i.e. (a_x, K_x) and (a_g, K_g) , respectively, are dependent. This latter issue is illustrated by figure 2.1, where it is shown that the time constant $1/a_x$ influences the amplitude of an insulin injection-related drop in BG. To obtain meaningful model parameters the amplitude and the rate of the effect of meal and/or insulin on BG concentration have to be decoupled, which furthermore increases correlation with therapy parameters (cf. 2.5.1 and 2.5.2). Therefore this influence

should be eliminated, making a_x and a_g independent of the respective response amplitudes.

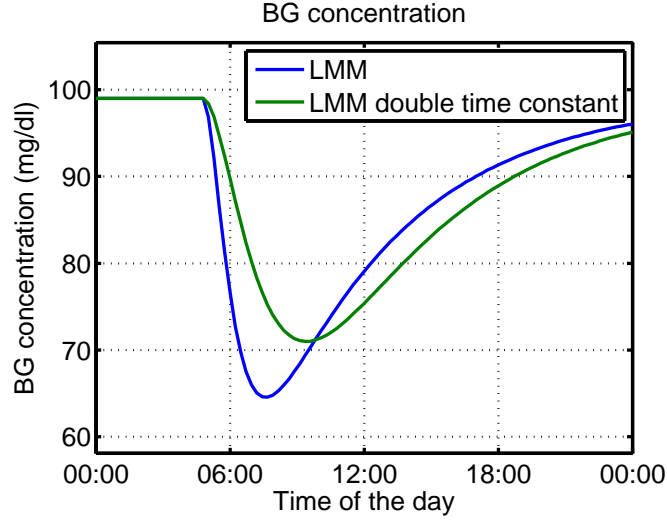


Figure 2.1: BG predictions using the LMM with the same insulin sensitivity K_x and inputs, but two different time constants $1/a_x$.

Therapy Parameter-based Model (TPM)

To improve the LMM, it is proposed to remove U_{endo} and S_G , leading to the following set of ODEs:

$$\dot{G}(t) = -K_x X(t) + K_g U_G(t) \quad (2.14)$$

$$\dot{U}_G(t) = -a_g U_G(t) + a_g U_{G,1}(t) \quad (2.15)$$

$$\dot{U}_{G,1}(t) = -a_g U_{G,1}(t) + a_g U_{CHO}(t) \quad (2.16)$$

$$\dot{X}(t) = -a_x X(t) + a_x X_1(t) \quad (2.17)$$

$$\dot{X}_1(t) = -a_x X_1(t) + a_x U_I(t) \quad (2.18)$$

The removal of U_{endo} and S_G leads to the following changes in the properties of the resulting dynamical model:

- After an insulin bolus or a meal, BG drops or rises, respectively, as a second-order dynamical system.
- G_{ss} only varies with K_x , K_g , and the initial BG concentration:

$$G_{ss} = G(0) - K_x U_{I,tot} + K_g U_{CHO,tot} \quad (2.19)$$

where $G(0)$ is the initial BG, $U_{I,tot} = \int_0^{t_f} U_I(t) dt$ is the total amount of infused insulin between the initial time and the final time t_f , and $U_{CHO,tot} = \int_0^{t_f} U_{CHO}(t) dt$ is the total amount of ingested CHO between the initial time and the final time t_f .

- As depicted in Figure 2.2, the sensitivities are now decoupled from their respective time constants. The BG excursion amplitude depends on the amount of insulin and K_x only and is independent of a_x , while the BG excursion speed depends on a_x only.
- The number of parameters to identify has been reduced from 6 to 4.

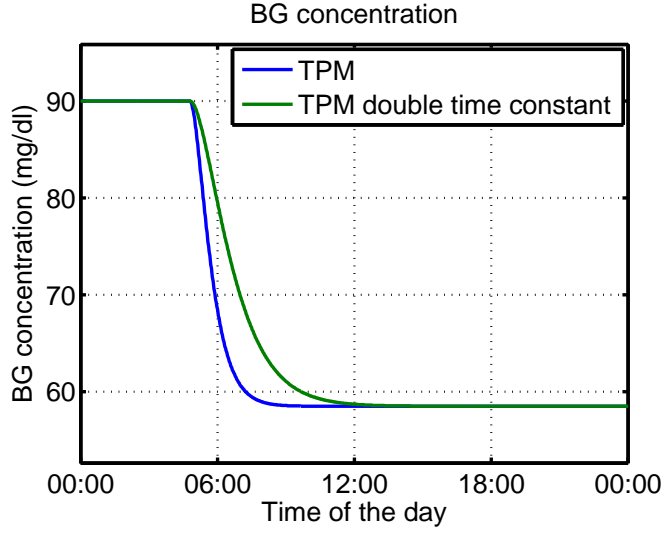


Figure 2.2: BG predictions using the TPM with the same insulin sensitivity K_x and inputs, but two different time constants $1/a_x$.

By coincidence, Kirchsteiger et al. [2011a] used the same model as the TPM to predict BG concentrations on real patient data. However, neither a comparison to other models was performed, nor a link to therapy parameters was established.

Percival et al. [2010] developed a similar model with first-order dynamics and a pure time delay. However, the corresponding simulated BG profiles are not smooth and the time delay is difficult to identify. Also, their correlation analysis showed that the identified parameters were not significantly correlated to therapy parameters. Of note is that this model was also used by Cescon et al. [2013] as a prediction model.

Cescon et al. [2012] used a similar model to the TPM, but proposed a first order sub-system with integral behavior. This model was also considered as an alternative to the TPM, but showed slightly inferior prediction capabilities. However, it may be a good choice if a model with a low number of states is required.

Extended therapy parameter-based model (TPM+)

While stripping the LMM of its S_G and U_{endo} parameters made steady-state properties more realistic and predictions more accurate, in some cases it is advantageous to keep the S_G parameter in the model. This introduces a pole with time constant S_G that replaces the

integrator of the TPM. This is consistent with the observation made by Cescon et al. [2013] that the integral effect of the model by Percival et al. [2010] may be replaced by a very slow pole.

The proposed model is given as

$$\dot{G}(t) = -K_x X(t) - S_G G(t) + K_g U_G(t) \quad (2.20)$$

$$\dot{U}_G(t) = -a_g U_G(t) + a_g U_{G,1}(t) \quad (2.21)$$

$$\dot{U}_{G,1}(t) = -a_g U_{G,1}(t) + a_g U_{CHO}(t) \quad (2.22)$$

$$\dot{X}(t) = -a_x X(t) + a_x X_1(t) \quad (2.23)$$

$$\dot{X}_1(t) = -a_x X_1(t) + a_x U_I(t) \quad (2.24)$$

Two remarks are in order for frequently identified values of S_G :

- $S_G = 0$. In this case the TPM+ is the same as the TPM.
- S_G very small. It can be derived from 2.13 that G_{ss} is zero and hence BG always converges to 0 mg/dl. This may be an unrealistic value, but as shown in 2.5.1 and 2.5.2, it is not detrimental for diabetes treatment as it tends to underestimate BG concentration, mostly leading to benign treatment decisions. The small value of S_G guarantees a relatively slow convergence to this value, such that therapy parameters may still be identified and BG concentrations stay realistic on a moderate prediction horizon.

2.3.2 Standard therapy

In the following paragraphs, the principles of the standard bolus and insulin pump therapy are described and it is shown how therapy parameters are related to the parameters of the TPM and TPM+.

Standard therapy definition

Patients with T1DM:

- Take a SMBG measurement (G_m) before a meal, or whenever they suspect their BG to be out of range,
- Compare G_m to the target BG (G_t), and compute the difference: $\Delta G = G_m - G_t$,
- Compute the correction bolus as $U_{I,corr} = \Delta G / CF$, with CF being the correction factor in $mg \cdot dl^{-1} \cdot U^{-1}$. I_{corr} may be negative if the patient plans to ingest a meal.
- Compute the meal bolus as $U_{I,meal} = I2C \cdot CHO$, with $I2C$ being the insulin-to-carbohydrates ratio in $U \cdot g^{-1}$, and CHO being the corresponding weight of carbohydrates in g.

- Inject the bolus $U_I = U_{I,corr} + U_{I,meal}$ using their insulin pump or pen.

Indeed, CF and $I2C$ correspond to the therapy parameters and are set by a physician. CF quantifies the drop in BG resulting from a 1U insulin injection (U corresponds to the "insulin unit", the international unit of insulin) at steady-state, while $I2C$ indicates how much insulin should be injected per gram of ingested CHO. $MS = I2C \cdot CF$ can thus be defined as the meal sensitivity, which indicates the increase in BG per gram of ingested carbohydrates.

From the viewpoint of systems theory, a way to interpret the standard therapy parameters MS and CF is by assimilating them to the parameters of a static model, identified by physicians, that maps the amount of insulin to the future steady-state BG.

Basal insulin

With an insulin pump, insulin may be infused almost continuously. This basal rate is useful in that it counteracts circadian variations in insulin sensitivity, such as the dawn effect. It is generally tuned by a physician in such a way that, in the absence of disturbances (such as meals or physical activity), BG stays approximately at the target value throughout the day. Hereafter, we will always assume a properly set basal rate. In this case, basal insulin is not considered as an input, i.e. inputs correspond exclusively to insulin boluses.

The proper adjustment of the basal rate is all but trivial and requires an experienced physician and lengthy patient observations. Currently, basal adjustments are also a field of research with a strong impact on diabetes treatment, especially in the case of open-loop treatment. For example methods such as run-to-run are proposed by Palerm et al. [2008].

Relation between therapy parameters and the TPM

Proposition 1. *The TPM parameter K_x is equal to the therapy parameter CF .*

Proof. If a 1U insulin bolus is infused at $t = 0$, $U_I(s) = 1$ and, in the absence of previous insulin boluses and meals, CF , according to the definition given in 2.3.2, is given as:

$$CF = -(G(\infty) - G(0)) \quad (2.25)$$

where $G(\infty)$ is the BG at steady-state and $G(0)$ the initial BG.

Using the Laplace transform of the TPM equations 2.14, 2.17, and 2.18:

$$G(s) = -\frac{K_x}{s\left(1 + \frac{1}{a_x}s\right)^2} U_I(s) + \frac{1}{s} G(0) \quad (2.26)$$

Applying the final value theorem leads to:

$$\begin{aligned} G(\infty) &= \lim_{s \rightarrow 0} sG(s) \\ &= -\lim_{s \rightarrow 0} \frac{K_x}{\left(1 + \frac{1}{a_x} s\right)^2} - G(0) \\ &= -K_x - G(0) \end{aligned}$$

Thus,

$$K_x = -(G(\infty) - G(0)) = CF \quad (2.27)$$

□

Proposition 2. *The TPM parameter K_g is equal to the therapy parameter MS .*

Proof. If 1g of CHO is ingested at $t = 0$, and in the absence of previous insulin boluses and meals, MS , according to its definition (see Section 2.3.2), reads:

$$MS = G(\infty) - G(0) \quad (2.28)$$

The rest of the proof is straightforward and is similar to that of Proposition 1. □

As shown, the therapy parameters CF and MS correspond by construction to the model parameters K_x and K_g of the TPM, respectively. Both indicate how much BG will drop or rise, respectively, in between consecutive steady states. In other words, the TPM may be considered as a dynamical extension of the standard, static, therapy model. This property is illustrated in Figure 2.3, while experimental verification of this link is presented in section 2.5.2.

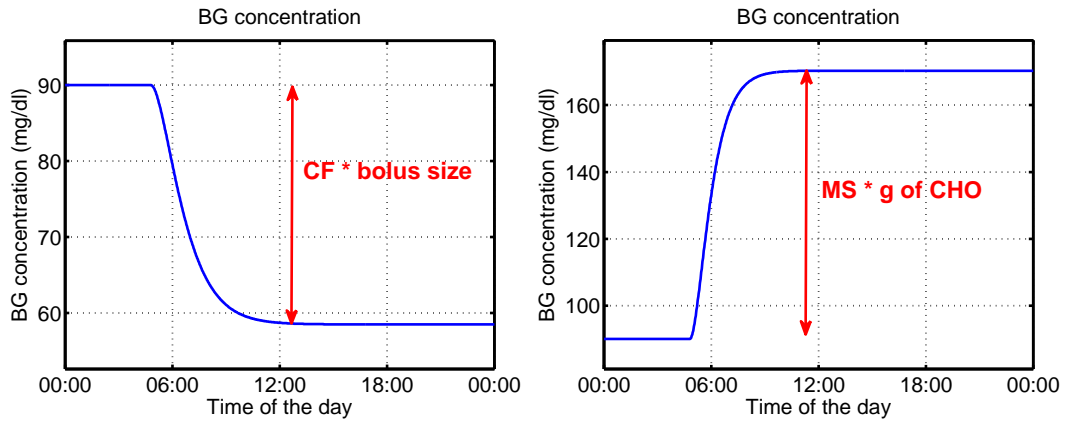


Figure 2.3: TPM simulations after an insulin bolus (left-hand side) and a meal (right-hand side)

The link between therapy and model parameters is very valuable, because TPM parameters have a physical meaning that is recognized by physicians and may therefore be accepted more easily. On the other hand, a priori knowledge of the physician-set therapy parameters can be used, if available, to improve the reliability of the TPM parameters.

The relation between therapy parameters and TPM+ parameters cannot be shown in the general case. In the case where S_G equals zero, the TPM+ is equal to the TPM and the two propositions hold. However, in the opposite, this cannot be verified, but the fact that TPM+ properties are very close to those of the TPM as long as S_G is small explains a good correlation with therapy parameters as shown in 2.5.1 and 2.5.2.

2.4 Validation Tools and Methods

This section describes the data used for the validation of the TPM and TPM+ as well as the practical methods and tools.

2.4.1 Validation data

Data from two different sources is used:

- Simulated BG profiles generated with the UVa simulator show how the proposed models perform on this widely accepted tool. More details concerning the UVa simulator are given in appendix A.1 and the 4 day nominal scenario specified in A.1.1 is used for cross-validation. The noiseless measurements of the 10 adults are used and are sampled with a period of 15 minutes.
- Data from 10 of the 12 patients from the clinical study described in appendix A.2 are used to validate the TPM and the TPM+ on real patient data.

2.4.2 Identification method

Model parameters identification is performed by minimizing the following weighted least squares objective function J :

$$J(\theta) = \sum_{d=1}^D \alpha_d J_d(\theta) \quad (2.29)$$

where θ is the vector of model parameters to estimate ($\theta = [a_x \ a_g \ K_x \ K_g]^T$ for the TPM, e.g.), D is the number of days, α_d is the weight associated to day d , and J_d is defined for each day d :

$$J_d(\theta) = \sum_{i=1}^{N_d} (G_{d,i} - \hat{G}_{d,i}(\theta))^2 \quad (2.30)$$

where N_d is the number of BG measurements for day d , $G_{d,i}$ and $\hat{G}_{d,i}$ are the measured and simulated BG concentrations on day d , respectively.

The optimal values θ^* are such that they minimize the cumulated (and weighted) prediction error:

$$\min_{\theta} J(\theta) = \sum_{d=1}^D \left(\alpha_d \left(\sum_{i=1}^{N_d} (G_{d,i} - \hat{G}_{d,i}(\theta))^2 \right) \right) \quad (2.31)$$

$$\text{s.t.} \quad \text{Model Equations} \quad (2.32)$$

where the Model Equations (Equations (2.14)-(2.18) for the TPM, e.g.) are integrated to compute the predicted values $\hat{G}_{d,i}(\theta)$ at the sampling instant i of day d under the same conditions than the corresponding measured values $G_{d,i}$, for any choice of θ .

2.4.3 Reliable insulin action

Particular attention has to be paid to the estimation of insulin action, as, for instance, underestimating the insulin effect increases the risk of overdosing insulin. It is made more complicated when meals and insulin boluses are taken simultaneously, since the effects of carbohydrates and insulin cancel each other out, especially if they act at similar speeds. Note that this remark further justifies the choice of slow meals in the context of the clinical study associated with this thesis, as the meals taken by the subjects were mostly slower than the insulin actions.

This difficulty to identify insulin parameters - worsened by the high noise level - is depicted in Figure 2.4. It is shown that when the meal and the bolus are taken simultaneously, the simulated BG does not change significantly when K_x is doubled, while the right-hand side plot shows the large sensitivity of the simulated BG profile to a change in K_x when the meal and the bolus are taken separately. In other words, Figure 2.4 illustrates how difficult it is to reliably identify K_x on the basis of BG measurements if the meal and the bolus are taken simultaneously. Indeed, in such a case, it is possible to estimate the ratio $\frac{K_g}{K_x}$ that corresponds to $I2C$, but not K_x (corresponding to CF). This difficulty was also discussed by Finan et al. [2007].

To circumvent this problem, the only solution is to perform insulin sensitivity tests, where a bolus without a corresponding meal is infused.

2.4.4 Choice of metrics

In this validation, we propose to assess the quality of the LMM, the MM and the TPM by three different indicators, Mean Absolute Difference (MAD), coefficient of determination (R^2), and Error Grid Analysis (EGA), which are detailed in the appendix B.

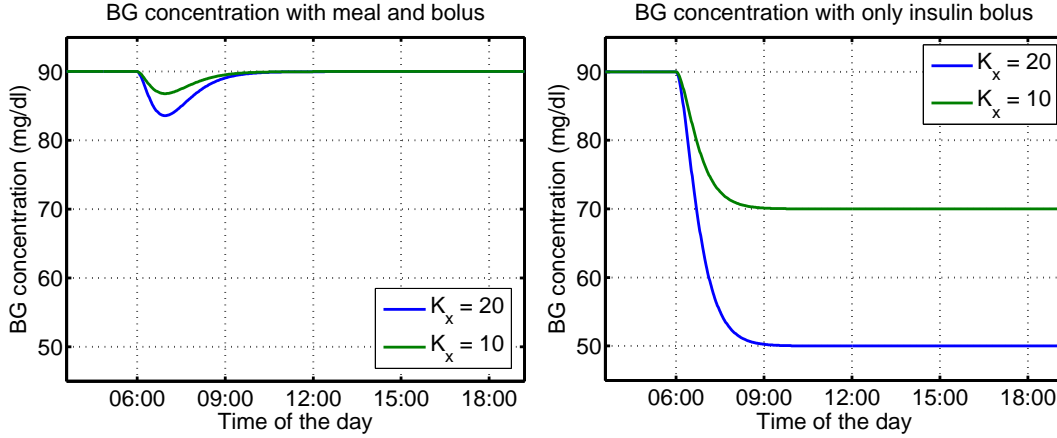


Figure 2.4: Simulations of the TPM with simultaneous insulin bolus and meal (left) and only an insulin bolus (right). The parameters are chosen as follows: $a_x = 0.04$, $a_g = 0.03$, $\frac{K_g}{K_x} (= I2C) = 0.1$ and K_x is chosen according to legend. The insulin bolus is $2U$ and the meal is $20g$.

2.5 Validation

The validation of the TPM is performed with the UVa simulator data described in A.1 and the clinical study data discussed in A.2 and follows 3 separate steps: (i) the data fits are analyzed, (ii) the correlation between therapy and model parameters is checked, and (iii), model predictions are evaluated.

2.5.1 UVa simulations

Data fit

The main difference between the TPM and the other models lies in the absence of endogenous glucose production and glucose effectiveness at zero insulin, resulting in different behavior at steady-state. The TPM+ also has a particular steady-state behavior, as it slowly converges to the unrealistic value of 0 mg/dl. The UVa model, however, has a similar steady-state behavior than the MM and LMM, which cannot be reproduced by the TPM or the TPM+. For this reason, for this validation, no insulin sensitivity tests are considered with the UVa simulator since the TPM and TPM+ do not have the appropriate dynamics to fit such data. This situation is not optimal and may result in unreliable insulin action, as explained in 2.4.3, but the challenge is the same for each tested model.

For the identification of UVa simulator data, the weight associated to the different days is equal, i.e. $\alpha_d = 1$ for all days d . Data from the last 4 days ($D = 4$), i.e. the test days with meals and insulin boluses, are used for the evaluation of fitting performance, leading to one parameter set for each patient. Initial BG is computed via linear interpolation between the values just before and right after the first measurement used for identification. The initialization of the

other states is performed by propagating past model inputs.

Table 2.2 shows that LMM and the MM have comparable fitting capabilities on UVa simulator data, while the TPM and TPM+ are slightly less accurate. This was expected since the number of model parameters of the TPM and TPM+ are lower. However, as it will be seen in sections 2.5.1 and 2.5.1, this small decrease in the fitting capability is largely compensated by the improvement in the identifiability of the parameters and in the prediction performances.

	TPM	TPM+	LMM	MM
MAD in mg/dl	7.02	7.04	5.00	5.30
R^2 in %	89.5	89.6	94.8	94.0

Table 2.2: MAD and R^2 indicators (averaged over all patients) for the four investigated models on UVa simulator data.

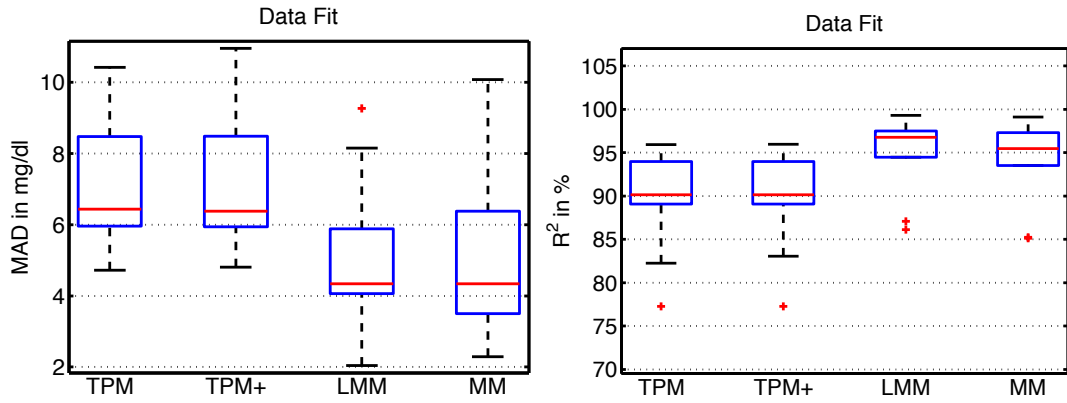


Figure 2.5: Boxplot (cf. appendix B.9) of the MAD and R^2 of the data fit of every patient ($n=10$). Comparison between different prediction models on UVa simulator data.

Indeed, good model fits do not necessarily imply good model predictions. With a high number of parameters, a model is typically able to generate many different BG profiles, leading to good data fits even though the dynamics of the model are not appropriate. However, in such a case, model predictions will not be good when the data set used for validation differs from that used for identification. Conversely, a model with less parameters may have inferior fitting capabilities but better predictions capabilities if its dynamics are more appropriate. This effect increases with the presence of measurement noise (which is high in our case), because having more parameters to identify increases the risk of fitting the noise. To summarize, a model with more appropriate dynamics, but less parameters will have potentially worse data fits, but better model predictions than a model with a high number of parameters, but less appropriate dynamics. The variability on parameter identifications is similar for all models as shown in figure 2.5 and shows few significant outliers.

The results for the TPM and TPM+ are almost identical. This is explained by the identified values of the S_G parameter for the TPM+ given in table 2.3. The identified values are always very close to zero, showing that for UVa simulation data the TPM and TPM+ are equivalent,

Chapter 2. Deterministic Modeling

even though the TPM+ has one additional parameter to identify.

Adult	1	2	3	4	5	6	7	8	9	10
S_G	10^{-5}	$8.7 \cdot 10^{-7}$	10^{-7}	10^{-7}	10^{-7}	$6.5 \cdot 10^{-5}$	10^{-7}	$4 \cdot 10^{-5}$	0.00017	10^{-7}

Table 2.3: Identified S_G in 1/min for the TPM+. The parameter is constraint to the interval $[10^{-7}, 1]$ as it needs to be greater than 0, but may take relatively high values.

Correlation analysis

In this subsection, we experimentally verify the relation between the therapy parameters provided in the UVa simulator and those identified using the models by analyzing their correlation. As in 2.5.1, D equals 4 and α_d equals 1 for all day d . It is not clear how the therapy parameters provided in the UVa simulator were determined, but simulations tend to show that they are accurate.

The results are summarized in Table 2.4 and illustrated in Figure 2.6.

	Correction factor	Ins-to-carb ratio	Meal sensitivity
MM	-0.20 (0.58)		-0.02 (0.95)
LMM	0.14 (0.70)	0.98 ($2.6 \cdot 10^{-7}$)	0.11 (0.77)
TPM	0.91 (0.0002)	0.99 ($1.6 \cdot 10^{-8}$)	0.71 (0.2)
TPM+	0.91 (0.0002)	0.97 ($1.7 \cdot 10^{-6}$)	0.67 (0.03)

Table 2.4: Different correlation factors and their relative p values (in brackets) between therapy parameters provided in the UVa simulator and identified parameters on UVa simulator data (n=10).

In the results of figure 2.6, it can be observed that for the LMM and the MM, there is one outlier patient, who corresponds to Adult 9 of the UVa standard database. This subject was previously identified as an abnormal subject by Cameron et al. [2011]. The structure of the two models does not allow to identify this subject, which results in unrealistic parameter values. This outlier heavily influences the comparison of correlation factors given in table 2.4. For this reason, the correlation analysis without Adult 9 is shown separately in table 2.5.

	Correction factor	Ins-to-carb ratio	Meal sensitivity
MM	0.77(0.014)		0.62 (0.075)
LMM	0.86 (0.0028)	0.99 ($9.76 \cdot 10^{-7}$)	0.69 (0.038)
TPM	0.90 (0.00078)	0.99 ($1.01 \cdot 10^{-7}$)	0.74 (0.023)
TPM+	0.91 (0.00074)	0.99 ($1.80 \cdot 10^{-7}$)	0.73 (0.025)

Table 2.5: Different correlation factors and their relative p values (in brackets) between therapy parameters provided in the UVa simulator and identified parameters on UVa simulator data without Adult 9.

When not considering Adult 9, the identified parameters of all models (except K_g of the MM) are correlated ($p < 0.05$) to their respective values given by the UVa simulator. However,

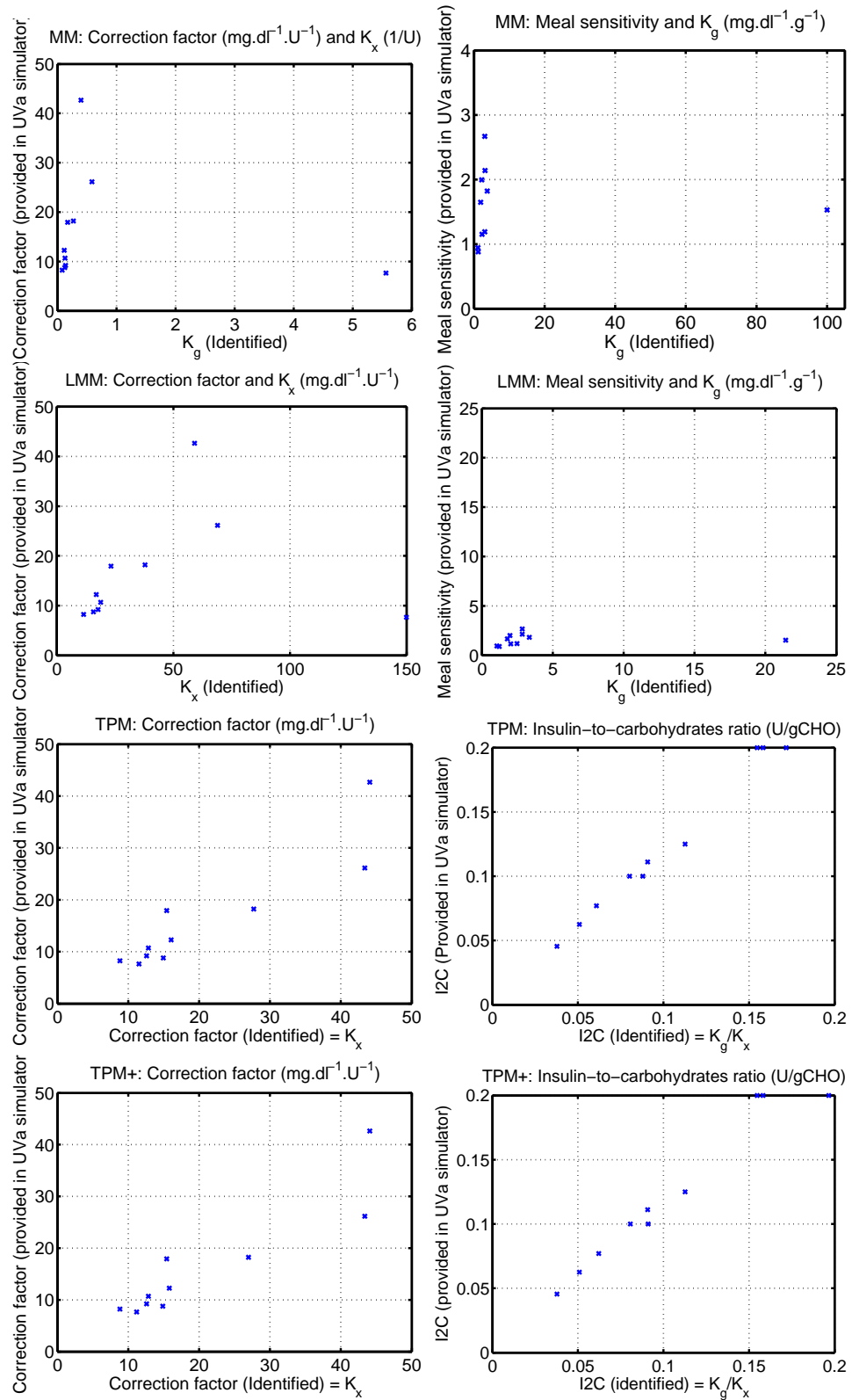


Figure 2.6: Comparison of physician-set therapy parameters and identified model parameters to illustrate correlation results on UVa simulator data (n=10).

the correlation factors of the TPM and TPM+ are much higher than those of the other two models, indicating that the TPM and TPM+ have the ability to reliably identifying therapy parameters. These are excellent results for the TPM and TPM+, considering that no specific insulin sensitivity tests are included in the identification. It should be noted that TPM and TPM+ parameters for Adult 9 were correctly identified. The correlation factors for the LMM are higher than those of the MM, indicating that its structure is more appropriate. Also, the insulin-to-carbohydrates ratio is accurately identified by the LMM, which indicates that, as discussed in 2.4.3, the LMM is not capable to reliably identify K_g and K_x in the absence of insulin sensitivity tests.

Removing Adult 9 from the data fit analysis (2.5.1) does not significantly change the results, since its data fits were only a little below average for all models.

Again, results for the TPM and TPM+ are very close. The reason is the same as discussed for the data fits, where S_G was close to 0 in most cases.

BG predictions

In this section, the prediction capabilities of the TPM and TPM+ are compared to those of the MM and the LMM.

To obtain reliable results, the data used for the identification (training data) should not be used for validation (validation data). In this study, we perform cross-validation: in the case of UVa simulator data, model parameters are identified on 3 data sets and validated on the 4th, for all possible permutations of the data sets. Thus, we obtain 4 parameters sets with the corresponding predictions for every subject, leading to a total of 40 different parameter sets.

Given a prediction horizon of h minutes, model predictions are done as follows:

- A validation data set with corresponding model parameters (identified on training data) for a given patient and day is chosen.
- For every BG measurement we start by simulating the model h minutes earlier. The initial BG values are set to the measured value preceding the h -minute simulation (this is different to the identification because future values are assumed unknown). All other states are initialized using simulations with model inputs, dating back several hours before the beginning of the simulation.
- The BG value after the h -minute simulation is the predicted BG and coincides with an experimental measurement point.
- The evaluation metrics are evaluated on all prediction points.
- Finally, the results are averaged over all parameters sets for comparison purposes.

For comparison, we also show the results of a Zero Order Hold (ZOH) model, which is often used as a reference. It consists in setting the predicted BG value to the initial BG value. In other words, we consider constant BG concentrations over the prediction horizon.

Predictions are performed with horizons rising from $h = 15$ minutes to $h = 165$ minutes with 15 minute increments. The predictions of all models are compared in Figure 2.7, where (i) the MAD, which measures the prediction fit quality, and (ii) the percentage of predictions in Clarke EGA zone A, which quantifies patient safety, are depicted.

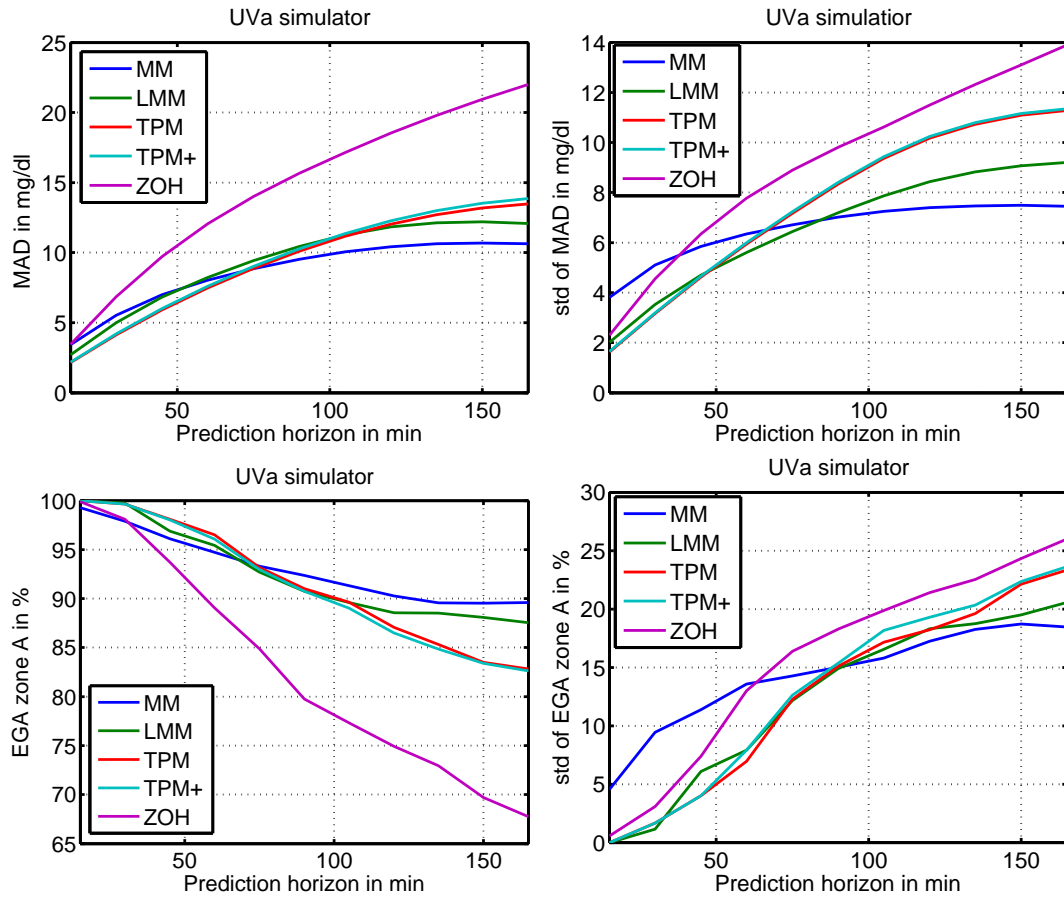


Figure 2.7: MAD (top) and % in EGA zone A (bottom) of the averaged model predictions ($n=40$) for the different prediction models and prediction horizons h on UVa simulator data. Mean values are given on the left, standard deviations on the right.

For small prediction horizons (up to 60 minutes), the TPM and TPM+ give better MAD values than all other models. For longer prediction horizons, the MM is the most effective, followed by the LMM and the TPM and TPM+. The standard deviations are given to evaluate the variability of the predictions and it shows that for short predictions, the TPM and the TPM+ are the most consistent, while the MM is more reliable for longer prediction horizons.

The percentage in zone A of the Clarke EGA shows similar results. This is caused by the

steady-state behavior of the MM that is closer to that of the UVa simulator model (which always converges to a value independently of the inputs) than the TPM or the TPM+. All model predictions, except for the ZOH, are within zones A and B of the EGA. Overall, the difference between the different models is small.

If Adult 9 is disregarded, results do not change significantly.

It can be concluded that for predicting BG on UVa simulator data, the TPM is an excellent choice because, despite having less parameters, worse data fits, and a model structure that is not fully compatible with the UVa simulator model, it is superior or comparable to the other models in terms of prediction performance and therapy parameter correlation.

2.5.2 Clinical data

Data fit

For the clinical study, the data fits are computed as described in 2.5.1, with a few differences: (i) the model parameters are identified with $D = 7$ (i.e. the full data set is used). (ii) As discussed in section 2.4.3, to be able to identify K_x , the sensitivity tests described in A.2 were performed. However, 2 sensitivity test days out of 7 were insufficient. For this reason, the weight of the insulin sensitivity test days was increased by 5 - the value that led to the best results. Thus, the objective function defined in Equation (2.31) used $\alpha_4 = \alpha_5 = 5$ and $\alpha_d = 1$ otherwise. Ideally, more sensitivity tests should be performed, so that they outweigh the meal tests.

Examples of data fits are given in Figure 2.8, while Table 2.6 compares the performances of the TPM, the TPM+, the LMM, and the MM in terms of the MAD and R^2 indicators.

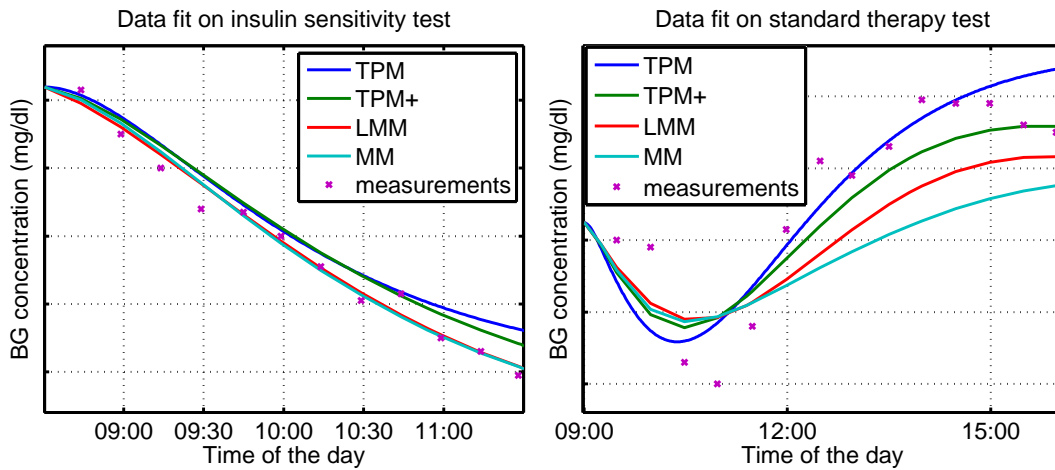


Figure 2.8: Example of data fits for different prediction models on clinical data.

The LMM and the TPM+ show the best fitting capabilities. Hence, the structure of the LMM is more appropriate than the structure of the MM, as both have 6 parameters to identify.

	TPM	TPM+	LMM	MM
MAD in mg/dl	12.89	10.90	10.56	12.09
R^2 in %	72.42	80.76	81.16	76.15

Table 2.6: MAD and R^2 indicators (averaged over all patients) for the four investigated models on clinical data.

However, the TPM+, with only 5 parameters to identify, has almost the same fitting capabilities than the LMM and should therefore be preferred. The performances of the TPM and the MM are comparable, with a slight advantage for the MM. Figure 2.9 depicts the variability of data fits, that is the lowest for the LMM and the TPM+ and increases for the MM and the TPM. A higher variability is due to a higher number of patients that were more difficult to fit. However, it will be seen in sections 2.5.2 and 2.5.2 that this is not detrimental neither to parameter identification nor to model prediction, the reason being that some patients have intrinsically higher variability in their BG concentrations.

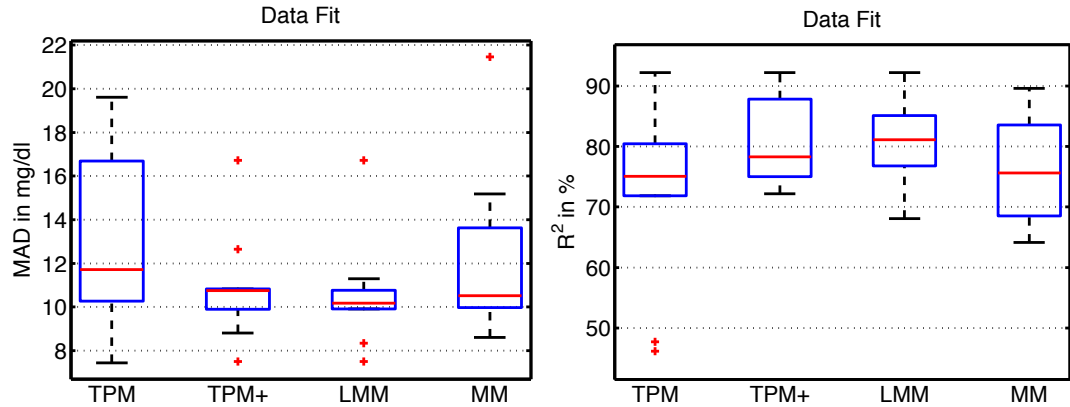


Figure 2.9: Boxplot (cf. appendix B.9) of the MAD and R^2 of the data fit of every patient ($n=10$). Comparison between different prediction models on clinical data.

While identifying the LMM, for 4 patients out of 10, the values of S_G and U_{endo} collapsed to 0, with the consequence that the LMM becomes identical to the TPM and that the corresponding model fits are very close. A similar observation is made for the TPM+, where the S_G parameter converges to 0 for 3 out of 10 patients, as shown in table 2.7.

Patient	1	2	3	4	5	6	7	9	11	12
S_G	0.0007	10^{-7}	0.00003	10^{-7}	0.0006	10^{-7}	0.0008	0.0017	0.0006	0.0010

Table 2.7: Identified S_G in 1/min for the TPM+. The parameter is constraint to the interval $[10^{-7}, 1]$.

Correlation analysis

The correlation analysis is performed similarly to the case of the UVa simulator data in section 2.5.1. The identification of the TPM and TPM+ parameters uses the full set of data, i.e. $D = 7$, and the same α .

The results are summarized in Table 2.8 and illustrated in Figure 2.10.

	Correction factor	Ins-to-carb ratio	Meal sensitivity
MM	0.16 (0.67)		0.57 (0.09)
LMM	0.47 (0.17)	0.78 (0.0077)	0.52 (0.13)
TPM	0.89 (0.00055)	0.89 (0.00055)	0.85 (0.002)
TPM+	0.91 (0.0003)	0.79 (0.0062)	0.84 (0.002)

Table 2.8: Different correlation factors and their relative p values (in brackets) between physician-set and identified parameters on clinical data.

The parameters of the MM are not correlated with the physician-set parameters and the correlation of the CF is very low, indicating a dangerously unreliable insulin action. Also, the identified values of K_x have some outliers with very high values (compared to the corresponding physician-set counterparts), which can be due to high values of U_{endo} . The meal sensitivity on the other hand has a higher correlation factor, although the results from Figure 2.10 show that the K_g parameter has low sensitivity. High K_g values should lead to high K_x values (cf. 2.4.3), but this is not the case, probably due to high values of S_G . The overestimation of the meal effect has to be avoided as it can lead to the computation of potentially massive insulin doses.

Similar results were found for the identification of K_g with the LMM. Though the correlation of K_x and the correction factor are improved by the LMM structure, this improvement does not lead to significant correlations.

Correlation results for the TPM and the TPM+ are very similar and all model parameters are significantly correlated with the therapy parameters. In some cases however, the modeled insulin sensitivity seems to underestimate the value set by the physician. At this point it is hard to know whether the real value is overestimated by the physician (for safety purposes), or underestimated by the model (or both). The TPM and TPM+ also slightly overestimate the I2C set by the physician. In the context of BG control, this results in higher insulin injections. For this study this is not detrimental as insulin boluses are generally too small during the standard therapy experiments.

We can conclude that with the TPM and the TPM+, parameters are more reliably and safely identified, compared to the LMM and MM. This is a clear hint that the TPM and TPM+ model structure is more appropriate for BG predictions. Conversely, this nice feature could make these new models a valuable tool for assisting physicians in determining the therapy parameters.

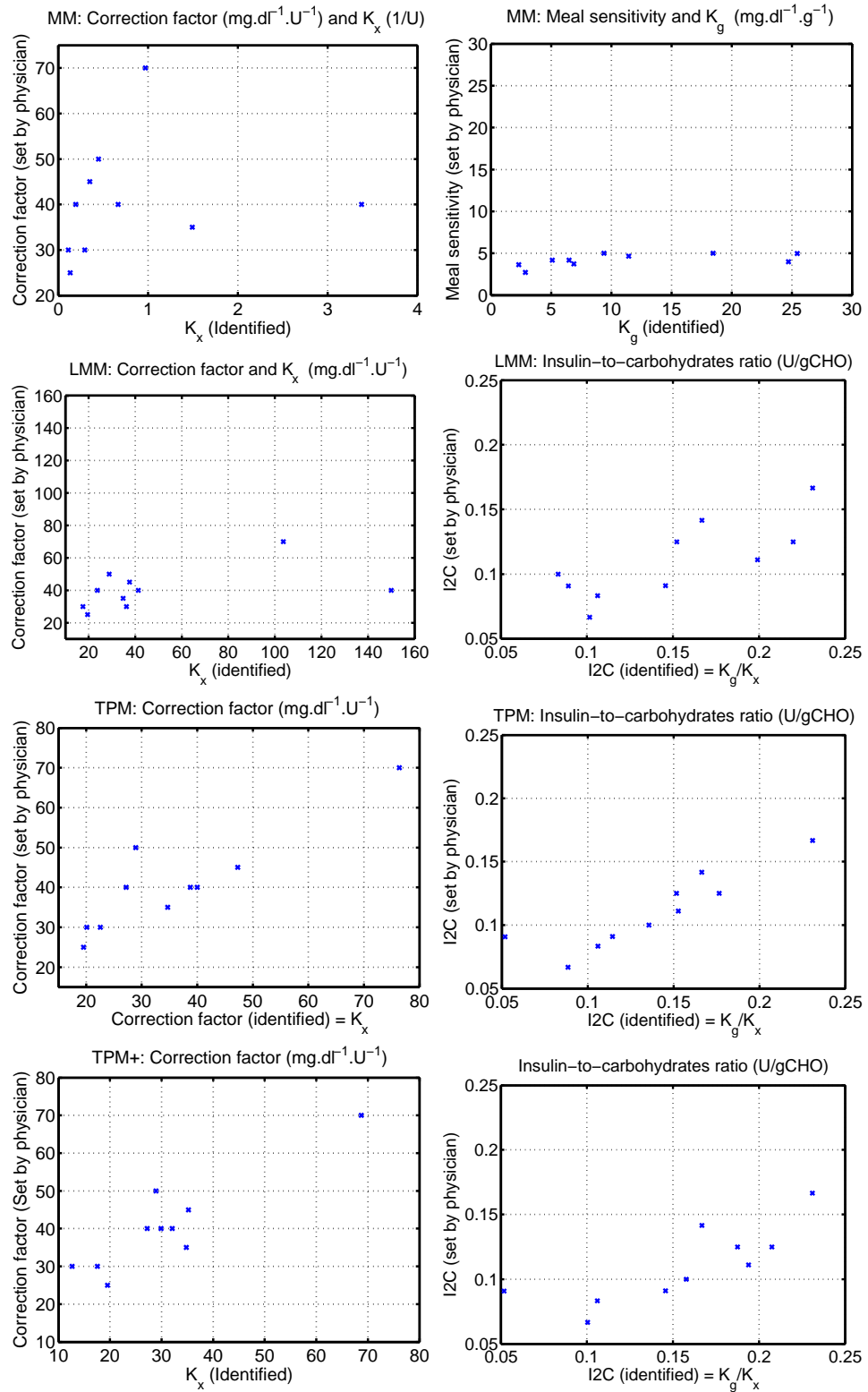


Figure 2.10: Comparison of physician-set therapy parameters and identified model parameters to illustrate correlation results on clinical data.

BG predictions

The BG prediction analysis follows the principles described in section 2.5.1, but again with α chosen as in 2.5.2. Also, the cross-validation leads to up to 7 parameter sets per patient and thus to a total of 58 parameter sets.

Two examples of BG predictions with $h = 90$ are plotted in Figure 2.11, with on the left-hand side a relatively good prediction and on the right-hand side a less successful one.

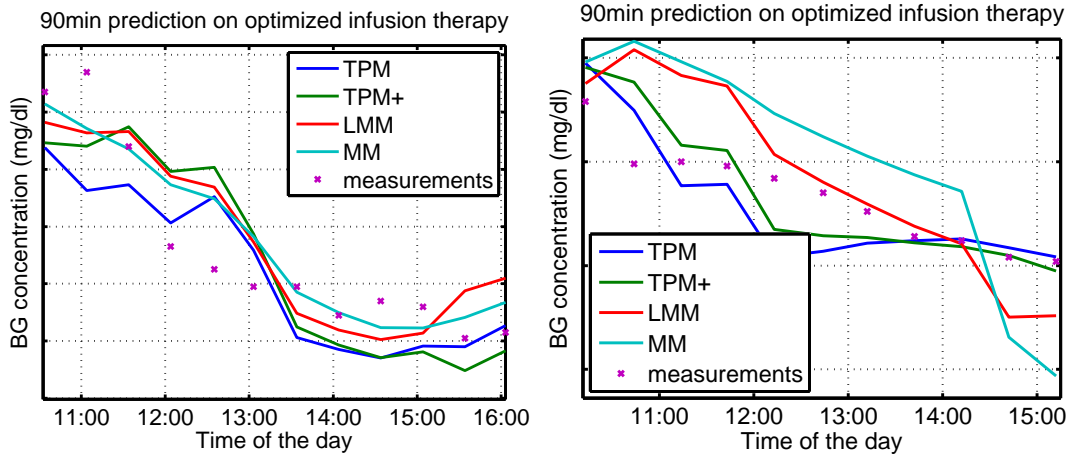


Figure 2.11: Example of 90 minute predictions for different prediction models on clinical data.

As the BG concentration is initialized with real measurements, it is noisy. This directly influences BG predictions and can sometimes lead to wrong predictions. This does not preclude the representativity of the comparison since the same initialization method is applied to every tested model.

As can be seen in figure 2.12, according to the mean MAD and percentage of predictions in zone A of the EGA, the TPM+ has better prediction performance and with smaller standard deviations than all other considered models. The TPM and LMM are almost equal, the latter only having a slightly lower standard deviation. The MM is less effective, especially with small prediction horizons, where predictions are worse than with the ZOH. The mean percentage of predictions in EGA zone A leads to a similar conclusion - this time the TPM being marginally better and having smaller standard deviations than the LMM.

On average, 97% of predictions for TPM+, TPM and LMM are in zones A and B for the EGA. This means that nearly no wrong treatment decisions would be taken, even for long prediction horizons. The MM goes down to 94%, whereas the ZOH goes to 88%.

Predictions do not significantly differ between the four models - a difference occurs mainly if, during the identification of a model, the global minimum of the identification problem corresponds to physiologically unrealistic parameters. This happens mostly with the MM and is due to the model dynamics that are not compatible with the measurements. These outliers

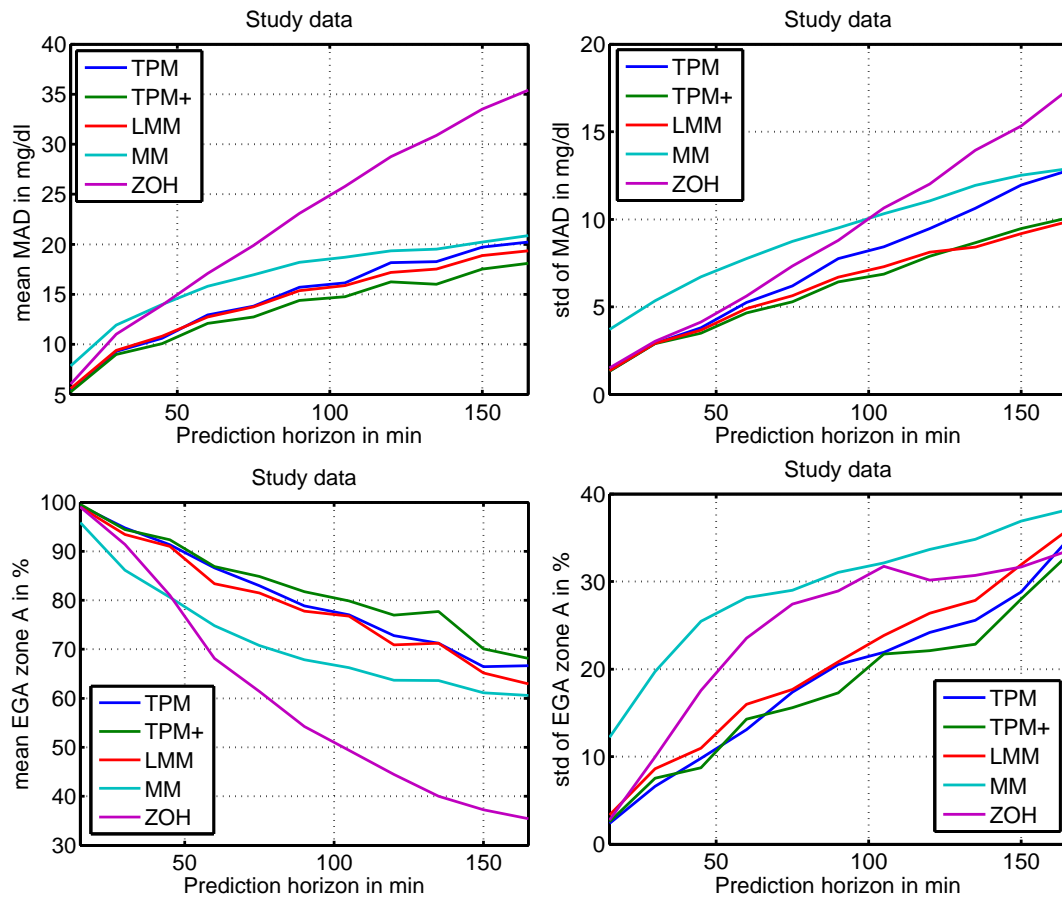


Figure 2.12: MAD (top) and % in EGA zone A (bottom) of the averaged model predictions (n=58) for the different prediction models on clinical data. Mean values are given on the left, standard deviations on the right.

result in worse average performance outcomes and are the main reason for the differences between the different models in figure 2.12.

Overall, the TPM always shows superior or comparable prediction capabilities. This is particularly interesting considering that only 4 parameters have to be identified. This compensates for the slightly inferior fitting capabilities. The TPM+ on the other hand is superior to all other tested models, but has 5 parameters to identify. Hence the TPM+ should be preferred for long prediction horizons, while the TPM is the model of choice if computational resources are scarce or prediction horizons are shorter.

As a concluding remark, it should be noted that the different days of the clinical study were very similar, which most likely makes predicting BG easier. With more varied scenarios, some of the tested models could prove inappropriate. It would therefore be interesting to test the model in a more diverse setting, similar to the analysis on the UVa simulator data, however this is not possible with the currently available data.

2.5.3 Comparison of results of the UVa simulator data and clinical data

The results obtained with the UVa simulator data and clinical data are consistent. Because of improved BG predictions, parameter correlation, and the reduced number of parameters, the TPM is the best choice on UVa simulator data and clinical data, while the TPM+ should be preferred for long-horizon predictions for real patients. Another main difference between results on the UVa simulator data and clinical data is the relative performance of the LMM and the MM: LMM is better on clinical data, while the MM is better on UVa simulator data. This is probably due to the fact that the MM dynamics are closer to the UVa simulator and to its non-linearities, while the LMM dynamics are closer to real human glucose dynamics.

2.6 Conclusion

The TPM and the TPM+ measure up to the expectations of being reliable but simple prediction models identifiable on BG measurements only. Stripping the models to a bare minimum (they can hardly be any simpler) allows reliable parameter identification, even in the presence of the characteristic high noise levels in BG measurements. We linked the model parameters directly to physician-set therapy parameters and showed their strong correlation. This adds another safety layer to the resulting model identification and the model may easily be personalized.

As expected, model fits were slightly worse than with other models - a result of the lower number of parameters. However, model predictions were on par or better than the alternatives. A higher number of parameters is therefore not necessary.

Predictions are used to calculate insulin doses and as such are critical for patient safety. If carefully identified, the TPM and the TPM+ lead to reliable insulin sensitivity estimation, which is rarely the case with the other models (identified under the same conditions). Additionally,

the TPM and the TPM+ have the property of only predicting an increase of BG concentration in case of a meal. The possibility of predicting an erroneous increase in BG is thus eliminated and hypoglycemia might be avoided in certain cases, especially when used in closed-loop controllers. Insulin infusions based on the TPM or the TPM+ are therefore safer than with conventional models.

The properties of the four prediction models are summarized and compared in Table 2.9, according to the features discussed in 2.2.3.

	MM	LMM	TPM	TPM+
Personalizable	✓	✓	✓	✓
Acceptable predictions	×	✓	✓	✓
Acceptable data fits	✓	✓	✓	✓
Identifiable	×	✓	✓	✓
Correlation with therapy parameters	×	×	✓	✓
Linear	×	✓	✓	✓
Number of parameters to identify	6	6	4	5

Table 2.9: Comparative table of model properties. ✓ indicates that a model verifies a property, × indicates that it does not.

The TPM and the TPM+ have been tailor-made for the use in state estimation, predictive control, and recommendation methods, e.g. MPC, optimal control, or pump suspension algorithms. These applications are the topic of chapters 4 and 5.

Future work will address the following points:

- The available clinical data used for validation was very similar from one day to the other. The TPM should be tested on more random test days to show its full potential.
- The TPM should be tested on different meals and the meal sub-model should be adapted if necessary. Additionally, to address the meal uptake rate variability introduced in 1.2.2, a meal library could be established, as proposed by Dassau et al. [2008].
- It was demonstrated that the TPM is an excellent tool to determine patient's therapy parameters and this property could be further developed to assist physicians in determining these parameters.
- The previous point may as well be reversed: T1DM patients should have good estimates of their therapy parameters that were set by physicians. If the TPM is used on these patients, the available therapy parameters can be used as prior knowledge to facilitate model parameter identification and increase its robustness.

3 Stochastic Modeling

3.1 Introduction

In chapter 2, many of the challenges identified in section 1.2 are addressed and overcome. However, the large uncertainty described in section 1.2.2 makes accurate BG predictions difficult and requires a probabilistic approach.

Inter-patient variability is taken into account by identifying individual model parameters for each patient. However, this requires models with very specific properties such as the TPM. Meal uptake rate variability can be addressed by identifying model parameters for different types of meals and constructing a meal library (Dassau et al. [2008], Prud'homme et al. [2011]). However, methods to quantify intra-patient variability are more difficult and rarely found in the literature. Such methods aim to find confidence intervals on predicted BG concentrations. One possibility to address this problem is by applying modal interval analysis (García-Jaramillo et al. [2012], Gardeñes et al. [2001]), which leads to models computing the upper and lower limits on BG, based on any deterministic model and on model parameter bounds. This method is computationally efficient, but difficult to set up. Additionally, no experimental verification, nor method to determine parameter intervals is given. Kirchsteiger et al. [2011b] addressed the problem in a similar way by computing upper and lower bounds, based on TPM parameter identification. Another approach is to add process noise to transform Ordinary Differential Equations (ODEs) into Stochastic Differential Equations (SDEs) and to identify the process noise amplitude as proposed by Klim [2009]. However, finding this amplitude is not straightforward. A similar approach by Cameron [2010] uses a multi-model method, but is computationally demanding. Finally, it is also possible to estimate uncertainties using linear regression prediction methods. However, according to Cameron et al. [2008], this method is only reliable for short prediction horizons of up to 20 minutes .

In this chapter a complete procedure to estimate the quality of BG predictions as a function of time by constructing a stochastic model and quantifying model uncertainties is proposed. The ODEs of a well-chosen continuous and deterministic model are transformed into SDEs by adding parametric uncertainties. Model parameter uncertainties are estimated during

standard parameter identification and, as a consequence, no additional parameters need to be identified. The uncertainties are propagated using EKF theory.

This chapter is structured as follows: first, in section 3.2, the stochastic model, the uncertainty estimation, and the covariance propagation are introduced. Then, in section 3.3 and the proposed method is applied to the TPM. In section 3.4, predictions using the newly designed sTPM are done and validated using simulated and clinical data. Finally, conclusions are drawn and future work is proposed in section 3.6.

3.2 Stochastic modeling

3.2.1 Construction of a stochastic model

The construction of a stochastic model is based on a well-chosen deterministic model. The latter one should be continuous and expressed as:

$$\dot{\mathbf{x}}(t) = f_{det}(\mathbf{x}(t), \mathbf{u}(t), \boldsymbol{\theta}), \quad (3.1)$$

where \mathbf{x} is the vector of n states, t is the time, \mathbf{u} is the m -dimension input vector, $\boldsymbol{\theta}$ is a vector containing p model parameters, and f_{det} is a differentiable function that defines the model dynamics. In this chapter only, vectors and matrices are represented in bold. One of the states in \mathbf{x} should be the BG concentration. If this model is well chosen, it gives appropriate BG predictions. Nevertheless, because of the random nature of human glycemia, these predictions will rarely be accurate and a stochastic model is useful to evaluate the quality of the deterministic predictions. For this reason, it is useful to turn the deterministic model into a stochastic one of the form

$$\dot{\mathbf{x}}(t) = f_{sto}(\mathbf{x}(t), \mathbf{u}(t), \mathbf{w}(t), \boldsymbol{\theta}), \quad (3.2)$$

where $\mathbf{w}(t) \sim \mathcal{N}(\mathbf{0}, \mathbf{Q})$, \mathbf{Q} is the covariance matrix of a multivariate zero-mean Gaussian, and f_{sto} is a differentiable function that defines the model dynamics. Now $\mathbf{x}(t)$ is a random variable whose distribution is analyzed and propagated through time.

The biggest challenge in estimating the quality of BG predictions is to model how the uncertainty $\mathbf{w}(t)$ affects the BG concentration. Often a zero-mean univariate Gaussian is added to the BG state and all other states remain unchanged Klim [2009]. It is difficult to choose a numerical value for this Gaussian's standard deviation σ and it requires additional and computationally important identification steps. Moreover, with this approach, the uncertainty is independent of model inputs, even though meal inputs are a more important source of uncertainty than insulin injections, for example.

In order to define a meaningful and easy-to-identify alternative, it is proposed to consider the parametric uncertainty of the model parameters. So, to obtain a stochastic model, $\boldsymbol{\theta}$ is

replaced by a normally distributed parameter vector Θ in equation 3.1, defined as

$$\Theta \sim \mathcal{N}(\theta, \mathbf{Q}) \quad (3.3)$$

$$\sim \theta + \mathbf{w}(t) \quad (3.4)$$

In other words, a Gaussian term is added to every parameter Θ_i , such that $\Theta_i = \theta_i + w_i$, where $\mathbf{w} = \begin{bmatrix} w_1 & \dots & w_p \end{bmatrix}^T$ has the covariance matrix \mathbf{Q} . Thus the uncertainty on several parameters can be correlated. The strong assumption that the parameters are normally distributed presents the biggest drawback of the proposed method, as physiological parameters are often found to be log-normally distributed Zhang and Popp [1994]. However, as shown in section 3.4, results are convincing.

If the deterministic model is linear with respect to its parameters, equation 3.2 can be written as

$$d\mathbf{x}(t) = f_{det}(\mathbf{x}(t), \mathbf{u}(t), \theta) dt + g(\mathbf{x}(t), \mathbf{u}(t), \theta) d\mathbf{w}(t) \quad (3.5)$$

where \mathbf{w} is a standard Brownian motion vector of dimension p and covariance matrix \mathbf{Q} , and g is a deterministic function. f_{det} is called the *drift* function and quantifies the deterministic part of the model, same as in equation 3.1. g is called *diffusive* function and quantifies the uncertainty of the different states.

To simulate the stochastic model, the Euler-Maruyama scheme can be used, for instance. The simulations could then be used for different Monte Carlo methods. These have the advantage of giving accurate results, but at a high computational price.

3.2.2 Propagating uncertainties

If the complete distribution of the states is not necessarily needed, but the propagation of its variance is sufficient, the computational burden of Monte Carlo simulations can be considerably alleviated by propagating the covariance using EKF theory (Simon [2006]). The model designed in the previous section is not forcibly linear. In the case of non-linearities, finding the evolution of the states and its uncertainties needs the application of a non-linear version of the KF. For this reason, the model is linearized along the estimated trajectory and \mathbf{A} and \mathbf{L} are defined:

$$\mathbf{A}(t) = \left. \frac{\partial f_{sto}(t)}{\partial \mathbf{x}(t)} \right|_{\hat{\mathbf{x}}(t), \mathbf{w}_0} \quad (3.6)$$

and

$$\mathbf{L}(t) = \left. \frac{\partial f_{sto}(t)}{\partial \mathbf{w}(t)} \right|_{\hat{\mathbf{x}}(t), \mathbf{w}_0}, \quad (3.7)$$

where $\hat{\mathbf{x}}(t)$ is the estimated state vector $\mathbf{x}(t)$ at time t . The estimated trajectory has no process noise, hence $\mathbf{w}_0 = \mathbf{0}$. Furthermore,

$$\tilde{\mathbf{Q}}(t) = \mathbf{L}(t)\mathbf{Q}\mathbf{L}(t)^T. \quad (3.8)$$

The state estimation is the same as for the deterministic model and the state covariance $\mathbf{P}(t)$ propagates over time, giving the following set of equations to integrate:

$$\dot{\hat{\mathbf{x}}}(t) = f_{sto}(\hat{\mathbf{x}}(t), \mathbf{u}(t), \mathbf{w}_0, \boldsymbol{\theta}) \quad (3.9)$$

$$\dot{\mathbf{P}}(t) = \mathbf{A}(t)\mathbf{P}(t) + \mathbf{P}(t)\mathbf{A}(t)^T + \tilde{\mathbf{Q}}(t), \quad (3.10)$$

where $\mathbf{w}_0 = \mathbf{0}$. The initial conditions for $\hat{\mathbf{x}}(t)$ are set using BG measurements and state propagation using past inputs, while the initial conditions for $\mathbf{P}(t)$ are determined by covariance propagation using past inputs.

Using the covariance matrix, the standard deviation on the BG state can be isolated and thus, its uncertainty estimated at every point in time. Furthermore, the distribution of the uncertainty of the states over time is assumed to follow a normal distribution. This is a strong assumption, but allows computing confidence intervals on BG concentration. It might not hold for models with strong non-linearities, nevertheless, if the model is linear and linearly parameterized, this is not an approximation and exact results are found.

The 95% confidence interval is defined by

$$P(\hat{x}_{BG}(t) - 1.96\sigma_{BG}(t) \leq x_{BG}(t) \leq \hat{x}_{BG}(t) + 1.96\sigma_{BG}(t)) = 0.95, \quad (3.11)$$

where \hat{x}_{BG} is the estimated BG state and σ_{BG} is the standard deviation of \hat{x}_{BG} . $\sigma_{BG} = \sqrt{P_{BG}}$, where P_{BG} is the variance of \hat{x}_{BG} , whose value is found on the BG element of the diagonal of \mathbf{P} . The upper 95% confidence limit is thus $\hat{x}_{BG}(t) + 1.96\sigma_{BG}(t)$ and the lower one is $\hat{x}_{BG}(t) - 1.96\sigma_{BG}(t)$.

In order to compute the confidence intervals, $\frac{n(n+1)}{2}$ additional differential equations need to be integrated. Including the n equations from the deterministic model, a total of $\frac{n(n+3)}{2}$ ODEs need to be integrated over the desired time horizon.

3.2.3 Parameter identification

The performance of the proposed stochastic model depends largely on the quality of the estimated parameter vector $\boldsymbol{\theta}$ and its covariance matrix \mathbf{Q} . The following paragraphs show how to find them.

Estimation of θ

Similarly as in section 2.4.2, a non-linear weighted least squares method that minimizes the objective function J is used to estimate θ for a given patient:

$$J(\theta) = \sum_{i=1}^N W_i (G_i - \hat{x}_{BG}(\theta, t_i))^2 \quad (3.12)$$

where N is number of available BG measurements, G_i is the i -th BG measurement, W_i is the weight associated to the measurement G_i , and $\hat{x}_{BG}(\theta, t_i)$ is the predicted BG value at the measurement time t_i .

Finally the optimization problem may be written as:

$$\min_{\theta} J(\theta) \quad (3.13)$$

$$\text{s.t.} \quad \dot{\hat{\mathbf{x}}}(t) = f_{det}(\hat{\mathbf{x}}(t), \mathbf{u}(t), \theta). \quad (3.14)$$

Thus, the deterministic model equations need to be integrated over an appropriate time horizon and the resulting estimated glucose state is used to compute the value of the objective function.

Estimation of \mathbf{Q}

It is proposed to use the inverse of the Fisher information matrix \mathcal{J} to estimate \mathbf{Q} .

The Cramér-Rao bound gives a lower bound on \mathbf{Q} :

$$\mathbf{Q} \geq \mathcal{J}^{-1}. \quad (3.15)$$

To estimate \mathbf{Q} , it is assumed that the Cramér-Rao bound is attained

$$\mathbf{Q} = \mathcal{J}^{-1}, \quad (3.16)$$

where \mathcal{J} is defined as

$$\mathcal{J} = \mathbf{S}_{BG}(\theta, t_i) \begin{pmatrix} \frac{W_1}{\sigma_1^2} & 0 & 0 \\ 0 & \ddots & 0 \\ 0 & 0 & \frac{W_N}{\sigma_N^2} \end{pmatrix} \mathbf{S}_{BG}(\theta, t_i)^T, \quad (3.17)$$

and σ_i is the standard deviation of the measurement error of the i^{th} data point and

$$\mathbf{S}_{BG}(\boldsymbol{\theta}, t_i) = \frac{\partial \hat{x}_{BG}(\boldsymbol{\theta}, t_i)}{\partial \boldsymbol{\theta}} \quad (3.18)$$

are the partial derivatives of the estimated BG concentration with respect to the parameter vector $\boldsymbol{\theta}$, which is a $p \times N$ matrix. They can be determined by integrating the sensitivity equations with respect to $\boldsymbol{\theta}$ at the measurement times t_i :

$$\mathbf{S}(\boldsymbol{\theta}, t) = \frac{\partial f_{det}(\mathbf{x}(t), \mathbf{u}(t), \boldsymbol{\theta})}{\partial \mathbf{x}} \mathbf{S}(\boldsymbol{\theta}, t) + \frac{\partial f_{det}(\mathbf{x}(t), \mathbf{u}(t), \boldsymbol{\theta})}{\partial \boldsymbol{\theta}} \quad (3.19)$$

where $\mathbf{S}(\boldsymbol{\theta}, t) = \frac{\partial \hat{\mathbf{x}}(\boldsymbol{\theta}, t)}{\partial \boldsymbol{\theta}}$. These $n \cdot p$ equations to integrate may be computed by hand or symbolic mathematical software and are very useful to compute the gradient via forward sensitivity analysis that can be used in the minimization of J .

3.3 Application to the TPM

The proposed method for estimating confidence intervals is illustrated by an application to the TPM. This is not only an example, but the TPM is recommended as an excellent choice for stochastic predictions. Of note is that the application to the TPM+ can be performed in an analogous way.

3.3.1 TPM

As a reminder, the TPM equations (2.14 to 2.18) are

$$\dot{G}(t) = -K_x X(t) + K_g U_G(t) \quad (3.20)$$

$$\dot{U}_G(t) = -a_g U_G(t) + a_g U_{G,1}(t) \quad (3.21)$$

$$\dot{U}_{G,1}(t) = -a_g U_{G,1}(t) + a_g U_{CHO}(t) \quad (3.22)$$

$$\dot{X}(t) = -a_x X(t) + a_x X_1(t) \quad (3.23)$$

$$\dot{X}_1(t) = -a_x X_1(t) + a_x U_I(t). \quad (3.24)$$

The state vector is defined as $\mathbf{x} = \begin{bmatrix} G & U_G & U_{G,1} & X & X_1 \end{bmatrix}^T$, the model parameters vector as $\boldsymbol{\theta} = \begin{bmatrix} K_g & a_g & K_x & a_x \end{bmatrix}^T$, and the input vector as $\mathbf{u} = \begin{bmatrix} U_{CHO} & U_I \end{bmatrix}^T$.

3.3.2 Stochastic model for TPM

To turn the TPM into the stochastic TPM (sTPM), $\boldsymbol{\theta}$ is replaced by its stochastic version $\boldsymbol{\Theta}$ (cf equation 3.4), where the parameter uncertainty vector is defined as $\mathbf{w} = \begin{bmatrix} w_{K_g} & w_{a_g} & w_{K_x} & w_{a_x} \end{bmatrix}^T$

and w_i is the uncertainty of parameter i . The sTPM can be written as:

$$\dot{G}(t) = -(K_x + w_{K_x})X(t) + (K_g + w_{K_g})U_G(t) \quad (3.25)$$

$$\dot{U}_G(t) = (a_g + w_{a_g})(U_{G,1}(t) - U_G(t)) \quad (3.26)$$

$$\dot{U}_{G,1}(t) = (a_g + w_{a_g})(U_{CHO}(t) - U_{G,1}(t)) \quad (3.27)$$

$$\dot{X}(t) = (a_x + w_{a_x})(X_1(t) - X(t)) \quad (3.28)$$

$$\dot{X}_1(t) = (a_x + w_{a_x})(U_I(t) - X_1(t)) \quad (3.29)$$

Since the TPM is linearly parameterized, therefore a drift and a diffusion function can be defined according to equation 3.5. f_{det} is the deterministic part of equations 3.25 to 3.29 and is thus the same as the deterministic TPM defined in equations 3.20 to 3.24:

$$f_{det}(t) = \begin{bmatrix} -K_x X(t) + K_g U_G(t) \\ -a_g U_G(t) + a_g U_{G,1}(t) \\ -a_g U_{G,1}(t) + a_g U_{CHO}(t) \\ -a_x X(t) + a_x X_1(t) \\ -a_x X_1(t) + a_x U_I(t) \end{bmatrix}. \quad (3.30)$$

The diffusion function, which models the uncertainties, is given by

$$g(t) = \begin{bmatrix} -w_{K_x} X(t) + w_{K_g} U_G(t) \\ -w_{a_g} U_G(t) + w_{a_g} U_{G,1}(t) \\ -w_{a_g} U_{G,1}(t) + w_{a_g} U_{CHO}(t) \\ -w_{a_x} X(t) + w_{a_x} X_1(t) \\ -w_{a_x} X_1(t) + w_{a_x} U_I(t) \end{bmatrix}. \quad (3.31)$$

Since the TPM is linear, the covariance propagation proposed in 3.2.2 is not an approximation, but gives an exact result. Thus, equation 3.6 gives

$$\mathbf{A} = \begin{bmatrix} 0 & K_g & 0 & -K_x & 0 \\ 0 & -a_g & a_g & 0 & 0 \\ 0 & 0 & -a_g & 0 & 0 \\ 0 & 0 & 0 & -a_x & a_x \\ 0 & 0 & 0 & 0 & -a_x \end{bmatrix}, \quad (3.32)$$

and equation 3.7 reads:

$$\mathbf{L}(t) = \begin{bmatrix} U_G(t) & 0 & -X(t) & 0 \\ 0 & U_{G,1}(t) - U_G(t) & 0 & 0 \\ 0 & U_{CHO}(t) - U_{G,1}(t) & 0 & 0 \\ 0 & 0 & 0 & X_1(t) - X(t) \\ 0 & 0 & 0 & U_I(t) - X_1(t) \end{bmatrix}. \quad (3.33)$$

It should be noted, that \mathbf{A} is time invariant, while \mathbf{L} depends on the states. This introduces a non-linearity in the covariance propagation equations, hence evaluating the stochastic model of a linear and linearly parameterized model does not result in a set of linear equations.

The initial values for these equations may be found by propagating past model inputs. However, the initial uncertainty on the BG state, $P_{BG,0}$, should be set according to the relative accuracy of the glucose meter. According to Freckmann et al. [2010], for the used SMBG device, 95% of BG measurements are within $r = 10\%$ of the accurate value, while, according to Damiano et al. [2012], $r = 20\%$ for CGM data (even though this value could be higher). Hence, because the distribution is assumed to be Gaussian,

$$P_{BG,0} = \left(\frac{rG_0}{1.96} \right)^2 \quad (3.34)$$

where G_0 is the measured BG value at initial time.

The complete equations resulting from equation 3.10 are given in appendix F.

3.3.3 Relevance of the stochastic model

To illustrate the benefits of the stochastic model, examples based on model parameters identified on CGM data from patients of the clinical study described in A.2 are considered. Two different scenarios are analyzed: In both scenarios, the patient ingests 50g of CHO one hour after the start of the experiment and applies standard therapy, i.e. infuses the amount of insulin calculated using the insulin-to-carb ratio (cf. 2.3.2). The CGM measurement relative error was chosen to be 20% corresponding to the ISO 15197 norm and a target BG of 100 mg/dl is used.

- *Scenario 1:* The chosen patient's effect of insulin is faster than the effect of the meal ($a_x > a_g$). The deterministic TPM predicts safe treatment, however it does not take into account any source of variability. Different realizations of the sTPM in figure 3.1 show that the treatment may lead to hypoglycemia in some cases. The 95% confidence interval indicates that the risk of hypoglycemia is higher than 2.5 %.
- *Scenario 2:* If the effect of the meal is faster than the one of the insulin ($a_x < a_g$), which is the case for some of the patients, there is a significant risk of hyperglycemia, as illustrated in figure 3.2.

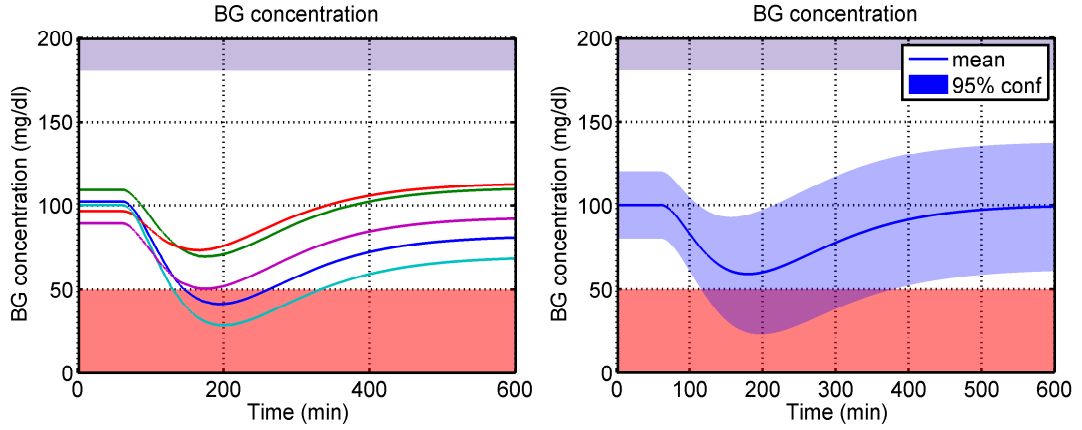


Figure 3.1: Scenario 1: Example of 5 realizations of the sTPM (left) and estimation of 95% confidence interval (right).

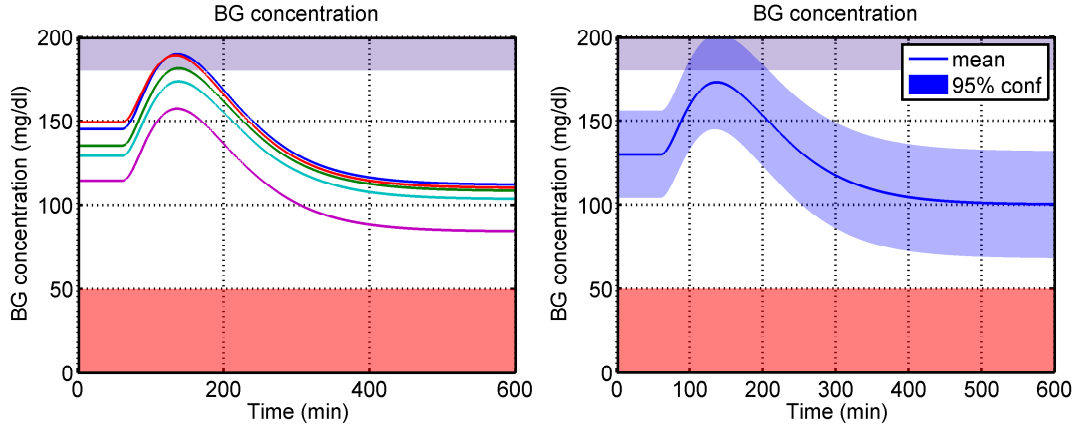


Figure 3.2: Scenario 2: Example of 5 realizations of the sTPM (left) and estimation of 95% confidence interval (right).

These two scenarios show that there is a risk of hypo- and hyperglycemia, respectively, if standard therapy is applied. The proposed stochastic model allows to quantify this risk and may allow reducing it.

3.4 Stochastic model validation

3.4.1 Validation data

The data used to evaluate the proposed stochastic model comes from two different sources: (i) the nominal data set generated using the UVa simulator, defined in appendix A.1.1 and (ii) the clinical study described in appendix A.2.

3.4.2 Validation methods

Cross-validation

One should never use data for validation that was previously used for parameter identification. Since 4 days of UVa simulator data and 7 or 6 days for study data (for SMBG and CGM data, respectively) are available, cross-validation is performed. This consists in identifying model parameters on all but one day and using the additional day for validation. This procedure is done such that every day is used for validation once. This way, a maximum of 4 validations for every adult on the UVa simulator can be obtained, which leads to a total of 40 experiments. For clinical study data, this would add up to 70 (respectively 60 for CGM data), however, because, for some patients some days were disregarded, the number of separate validations is 58 (respectively 52 for CGM data). These results are then averaged in order to evaluate performance.

Choice of identification and validation data

For each of the two data sources, two different measurements are available: the exact BG and CGM for the UVa simulator, and SMBG and CGM measurements for clinical study data. This means that there are 8 possible validation cases (cf table 3.1) depending on what measurements are used for identification and validation. For the sake of brevity, only a few cases are

case	data origin	identification data	validation data
1	UVa simulator	exact BG	exact BG
2	UVa simulator	CGM	exact BG
3	UVa simulator	exact	CGM
4	UVa simulator	CGM	CGM
5	clinical study	SMBG	SMBG
6	clinical study	CGM	SMBG
7	clinical study	SMBG	CGM
8	clinical study	CGM	CGM

Table 3.1: Possible validation cases

analyzed in detail. The main goal of the proposed method is to obtain probabilistic estimations of the patient's actual BG concentration. These estimations should be as exact as possible when parameters are identified on measurements. For this reason, stochastic predictions should always be compared with the most accurate measurement that is available. Therefore, only cases 2,5, and 6 are analyzed in detail and the other cases are used to show particular model properties.

The initialization of G and P_{BG} is always done with respect to the measurements used for identification. This means that if parameters are identified on CGM, exact, or SMBG data, then G is initialized with CGM, exact, or SMBG measurements, respectively. P_{BG} is initialized according to equation 3.34 with $r=20\%$, $r=0\%$, or $r=10\%$, respectively.

The way the data was collected plays a crucial role in analyzing the results. It is, for instance, straightforward to decide whether exact data generated by the UVa simulator lies within an estimated confidence interval or not. However, inexact measurements, such as CGM or SMBG measurements, make this task more complicated. The measurement noise is normally distributed and the variance for SMBG and CGM measurements G_i are $\sigma_{SMBG} = \frac{0.1G_i}{1.96}$ and $\sigma_{CGM} = \frac{0.2G_i}{1.96}$, respectively. This entails that it is impossible to give an exact value for the percentage of BG concentrations within the predicted confidence interval. On the other hand, it is possible to give its expected value, denoted $p_{95\%}$. Since the exact, and not the measured BG concentration lies inside the confidence interval, is of interest, it can be assumed that $G_{e,i} \sim \mathcal{N}(G_i, \sigma_i^2)$, where $G_{e,i}$ is the exact BG concentration at time t_i . p_i is the probability of $G_{e,i}$ being inside the confidence interval. If \bar{x}_{BG} and \underline{x}_{BG} are the upper and lower bounds of the estimated confidence interval, respectively, then p_i is given by the normal cumulative distribution function:

$$p_i = P(\underline{x}_{BG,i}(t) < G_{e,i} \leq \bar{x}_{BG,i}) \quad (3.35)$$

$$= P(G_{e,i} \leq \bar{x}_{BG,i}) - P(G_{e,i} \leq \underline{x}_{BG,i}) \quad (3.36)$$

where

$$P(X \leq a) = \frac{1}{2} \left[1 + \operatorname{erf} \left(\frac{a - G_i}{\sqrt{2\sigma_i^2}} \right) \right] \quad (3.37)$$

Finally the expected value of the percentage of points within the confidence interval is

$$p = \frac{1}{N} \sum_{i=1}^N p_i \quad (3.38)$$

If the stochastic model fulfills our assumptions and a 95% confidence interval is used, then $p \approx 95\%$.

3.5 Results

3.5.1 Percentage of measurements inside confidence interval over complete data set

First, in order to validate the proposed method for computing confidence intervals, the accuracy of the stochastic predictions over the whole duration of the available data sets (i.e. from t_s to t_e) is evaluated. Cross validation (cf 3.4.2) is performed and for every validation data set the percentage of data points within the estimated confidence interval is computed and averaged over all combinations and patients.

UVa simulator data

Results for cases 1 to 4, defined in table 3.1, are given in table 3.2 and figure 3.3. Examples of simulations over the complete time horizon are given in figure 3.4 for different cases. Cases 1 and 2 are most relevant, because they compare predictions to the exact BG concentration.

case	% mean	% median	n
1	0	0	40
2	97.73	100	40
3	0	0	40
4	84.13	85.00	40

Table 3.2: Expected average and median percentage of prediction points within the 95% confidence interval on the maximum prediction horizon.

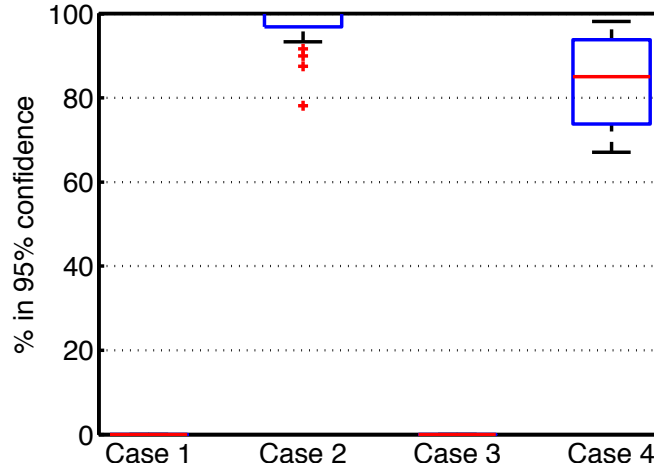


Figure 3.3: Boxplot (cf. appendix B.9) of percentage of measurements inside the 95% confidence interval of all validation data sets ($n=40$) for cases 1-4.

- Case 1: In this case, exact measurements were used to identify model parameters. When calculating \mathbf{Q} using equation 3.17 and $\sigma_i = 0$ for all measurements, the Fisher information matrix will be independent of both the model and the measurements. \mathbf{Q} is in fact a zero matrix and, as a consequence, the stochastic term of the stochastic model is zero. Hence, the model simplifies to the deterministic TPM and it is impossible to estimate confidence intervals. This can be explained by the fact that the parameter covariance matrix is assumed to be equal to the inverse Fisher information matrix even though it actually gives a lower bound on this matrix. If measurements are noiseless, this lower bound is equal to zero because, if an appropriate model is available, the model parameters can be identified perfectly. However, because of the model mismatch between the TPM and the UVa simulator model, this lower bound will not be reached. Hence, it is recommended not to use the sTPM when using exact measurements.
- Case 2 evaluates the efficiency of using CGM data for identification through comparison

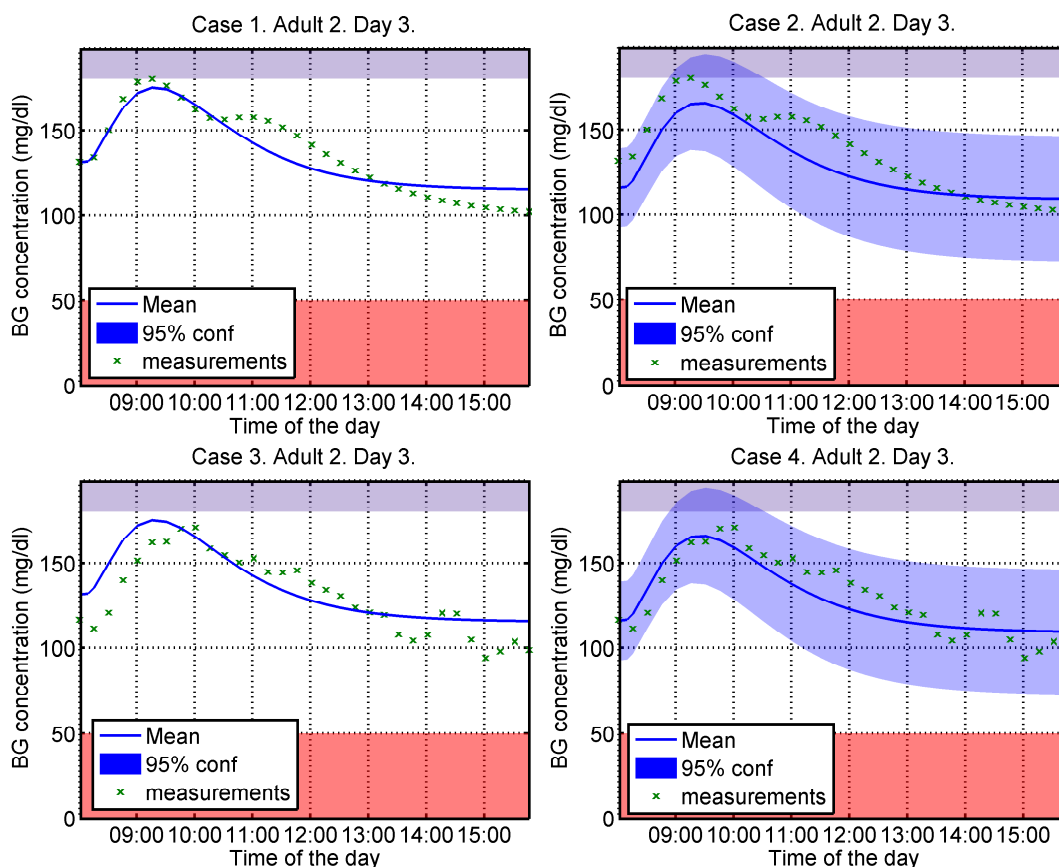


Figure 3.4: Examples for cases 1 to 4.

with exact BG concentrations. Results are very good, considering that the analysis on the maximum prediction horizon is strongly dependent on the inaccurate initial BG measurement. The percentage of points within the confidence interval is even too high, which indicates that confidence intervals may be too large. However, a visual inspection of figure 3.5 shows that the intervals are not overly large.

Some subjects from the UVa simulator population, such as adult 9 (which has already been identified as a complicated patient in section 2.5), have dynamics that cannot be reproduced by the TPM. Figure 3.5 shows that adult 9 has a pronounced two-peak response to a meal. Hence, its dynamics are only partially captured by the TPM and the confidence intervals are only partially appropriate. The proposed method thus only performs well if the deterministic model is adapted to the data.

- Case 3 has little interest as CGM data would never be used if exact data was available. Again uncertainty is estimated to be zero, for the same reasons as described for case 1.
- Case 4 is important because in a closed-loop setting only CGM is available. Similarly to case 2, CGM noise has an important influence on BG initialization. Additionally, the results depend on the different noise realizations during the experiment. Since this

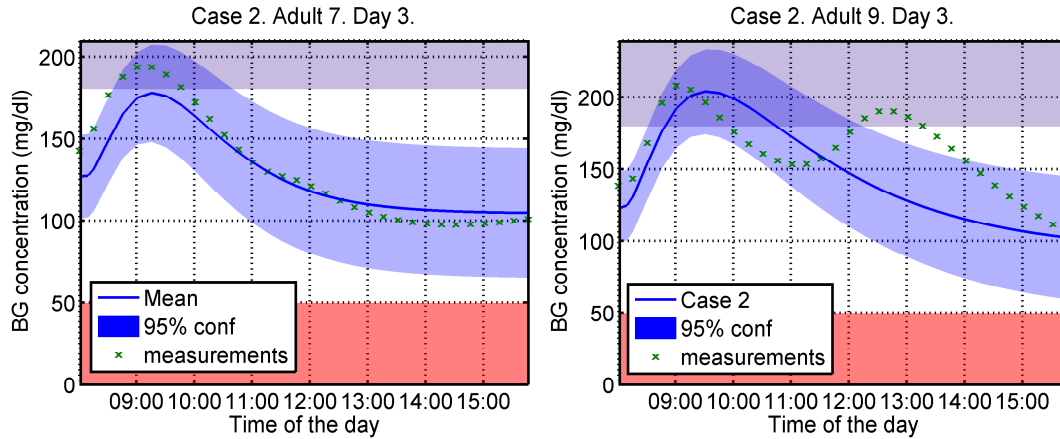


Figure 3.5: Examples for case 2 when validating over the complete data set.

realization is the same for all patients, the noise influence is not averaged out. Figure 3.6 gives an example that shows the negative influence of unfavorable noise realization, which explains the low percentage values in table 3.2.

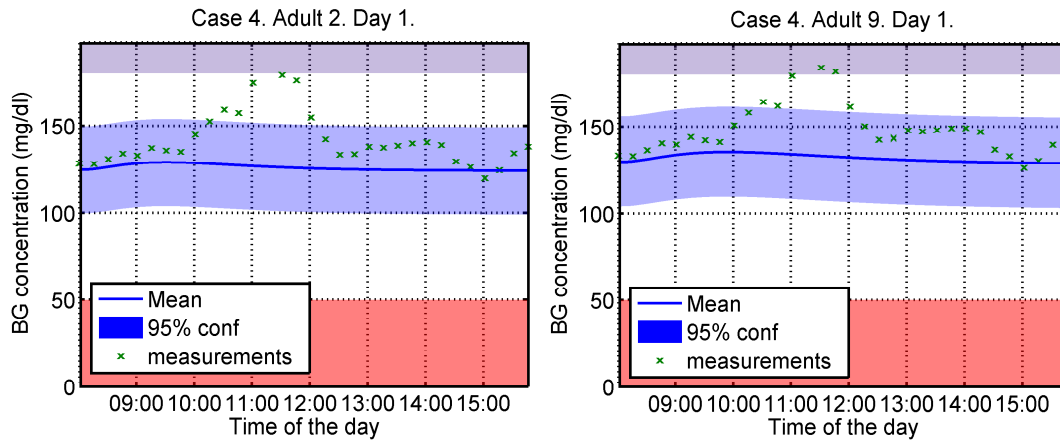


Figure 3.6: Examples for case 4 when validating over the complete data set. Both examples show the negative influence of their identical noise realization.

Overall, the performance of the sTPM is very good on the UVa simulator when CGM data was used for identification.

Study data

The results of the study data analysis are given in table 3.3 and figure 3.7. There is little difference between validating on SMBG and CGM data, as both measurement types have a significant level of noise. Results are generally slightly better with SMBG measurements, because of the increased confidence in measurement accuracy. Only cases 5 and 6 are discussed in

more detail as the discussion is analogous for cases 7 and 8.

The expected percentage of points within the 95% confidence interval is acceptable for data identified using SMBG or CGM measurements. Several outliers, visible in figure 3.7, occur and have a strong influence on the average value. Therefore, the median, which is more robust against outliers, is also given.

case	% mean	% median	n
5	71.25	73.38	58
6	78.80	89.68	52
7	63.58	67.38	52
8	74.80	79.67	52

Table 3.3: Expected average and median percentage of prediction points within the 95% confidence interval on the maximum prediction horizon.

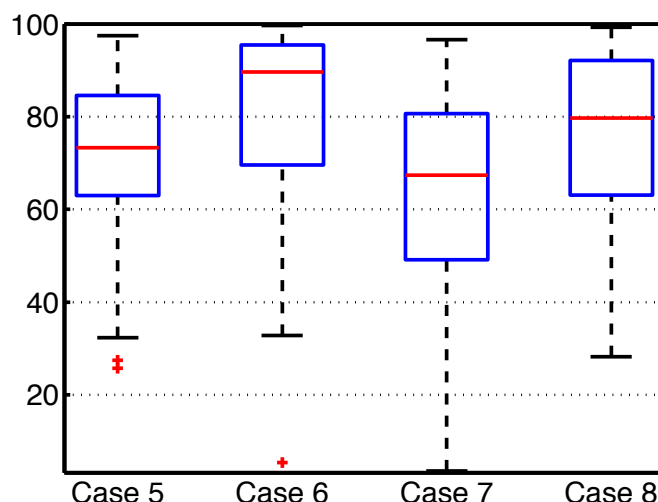


Figure 3.7: Boxplot (cf. appendix B.9) of expected percentage of measurements inside the 95% confidence interval of all validation data sets for cases 5 to 8.

For case 5, results are good, but not perfect, as the expected percentage of points within the confidence interval is lower than 95%. A possible explanation is that the amplitude of the SMBG measurement noise is underestimated.

Case 6 shows better results. This is due to the fact that the assumptions on measurement noise are more appropriate. Nevertheless, results are not perfect, mainly because of the reduced quality of the parameter identification on CGM measurements. This is illustrated in figure 3.8: Case 5, identified on SMBG measurements, has better deterministic predictions, but narrower confidence intervals than case 6, which is identified on noisier and unreliable CGM data.

As a conclusion, on real patient data, BG uncertainty can be predicted with acceptable accuracy using SMBG, as well as CGM data. Analysis shows that, as expected, best results are obtained for parameters identified on accurate and frequently sampled data. Ideally, SMBG data with

increased sampling rate or CGM data on more days should be used.

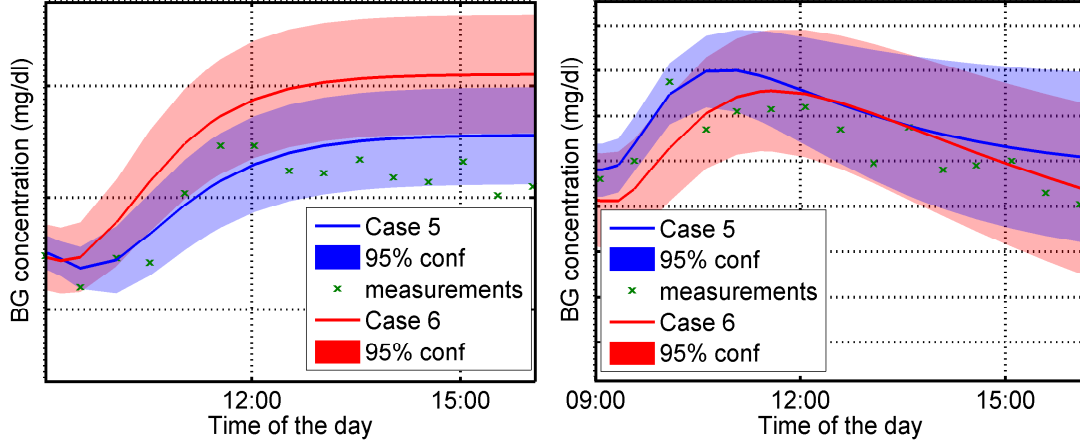


Figure 3.8: Comparison of stochastic prediction for cases 5 and 6.

3.5.2 Stochastic predictions

The analysis of the results over the maximum prediction horizon performed in 3.5.1 is a good indicator for uncertainty predictions performance. However, to get more insight, an analysis of the performance over well-defined prediction horizons is performed. In particular, the effects of measurement noise will be filtered out, leading to more representative results.

To do stochastic predictions, the following procedure is followed for every combination of identified model parameters and validation data set, and for every measurement G_i in the validation data set: A simulation is started h minutes before t_{G_i} , where t_{G_i} is the time of the measurement G_i and h is the prediction horizon. The inputs are propagated to initialize the insulin and CHO sub-systems and their respective covariance elements. The BG measurement preceding $t_{G_i} - h$ is used to define the initial BG and BG variance. As a consequence, to have a BG measurement to initialize the model, t_{G_i} has to be greater than $h + t_i$. The simulation is then run for h minutes and the final BG and confidence interval are compared to the measurement G_i . The results are then averaged for all measurement points, for all cross-validation permutations, and for all patients. Finally, the resulting value of points within the confidence interval and its standard deviation are plotted as a function of the prediction horizon. As illustration, examples of 90-minute predictions are given in figure 3.9.

The results for different prediction horizons on UVa simulator data are given in figure 3.10. In accordance with what was found in 3.5.1, case 1 and 3 cannot give confidence intervals and percentages of points within are zero. Case 2 (the most relevant one) shows excellent results over all horizons and case 4 gives good results that become even better when h increases. This improvement is due to the vanishing influence of the initial BG, and to the more favorable CGM noise realizations. The standard deviation indicates that the variability of the stochastic

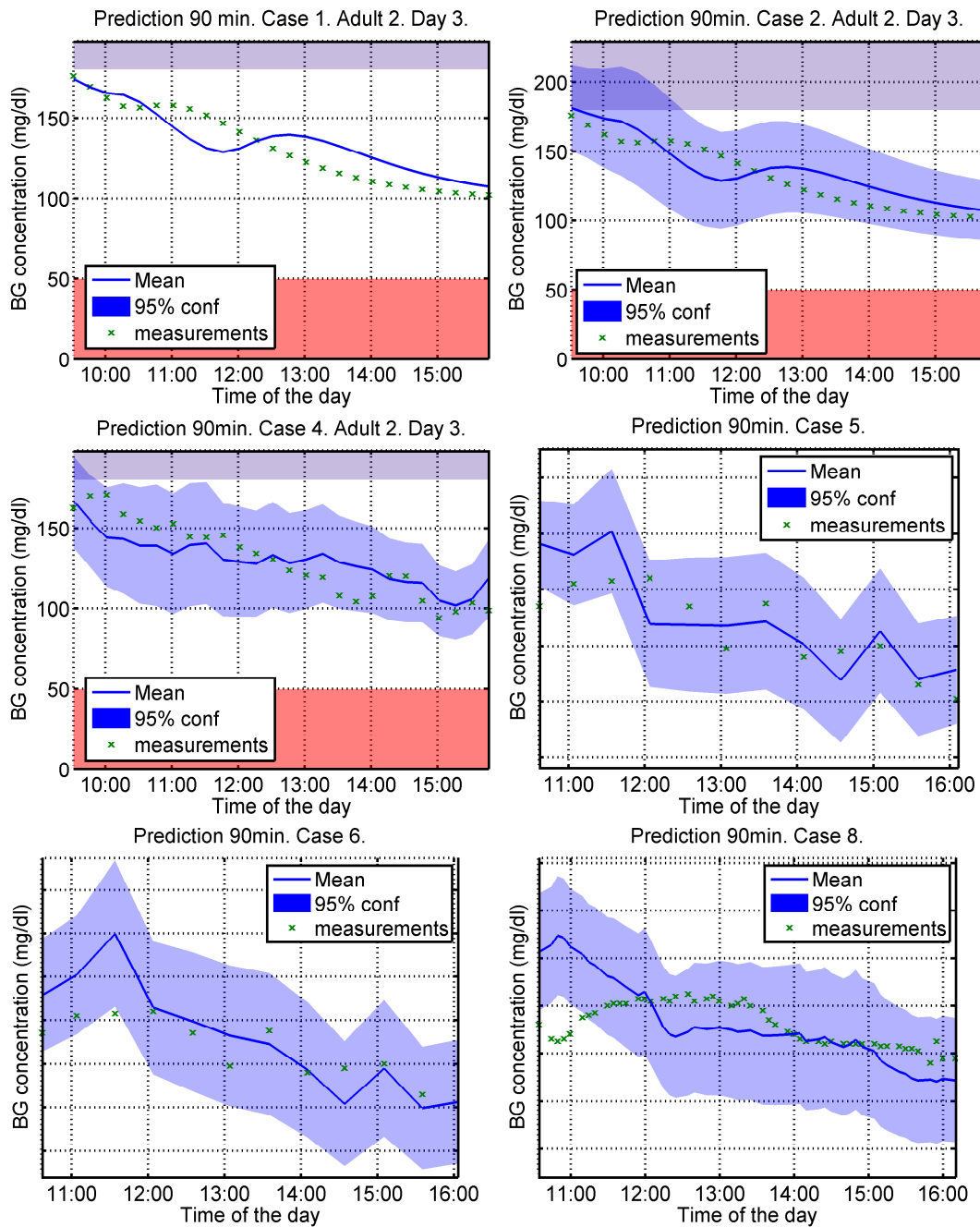


Figure 3.9: Examples for different cases on 90 minutes prediction horizon.

predictions rises with low prediction horizons and reaches a maximum value for $h > 150$ minutes. This indicates that predictions are stable, even for long horizons. The overall level of variability is acceptably small.

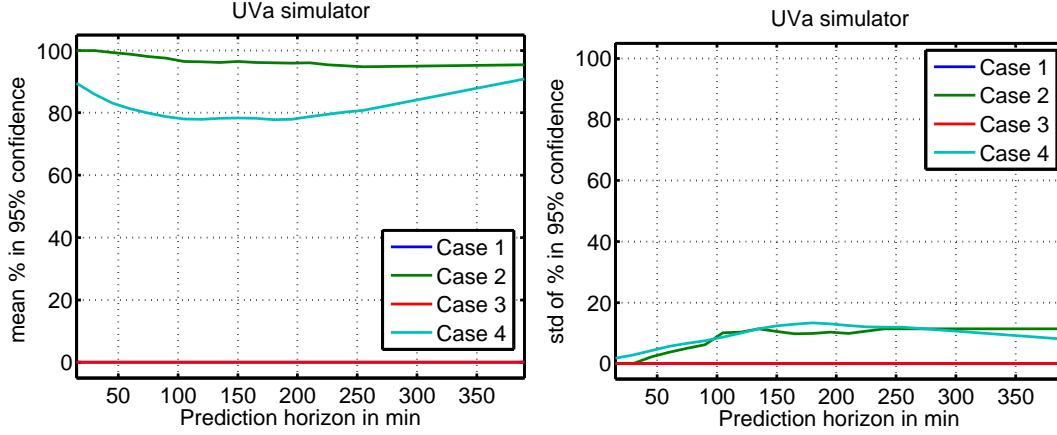


Figure 3.10: Prediction results for UVa simulator results (cases 1-4) for different horizons. Means and standard deviations evaluated on all 40 validation sets are given. Mean values are given on the left, standard deviations on the right.

Figure 3.11 depicts the results obtained with study data. Again, these results are in agreement with those of section 3.5.1: Cases 6 and 8 have a higher percentage of points within the 95% confidence interval because the uncertainty was estimated to be larger with CGM measurements. Cases 5 and 7 show a lower percentage of points within the confidence interval, but this is caused by the SMBG measurement error that was probably larger than the used value of 10%. The quality of the predictions is very good nevertheless, as the percentage of points within the 95% confidence interval does not depend much on h . The standard deviation is shown to increase with h . This is comparable to results on the UVa simulator. However, in this case, the value of the standard deviation is higher, because of the higher variability and noise level in the study data.

3.5.3 Other models

The proposed method to evaluate the prediction quality was also tested on other models (figure 3.12). Results on the LMM, the MM, and the TPM+ (see 2.3.1) show acceptable results. The TPM+ gives almost identical results than the TPM. However, since the other models, LMM and MM, led to inferior deterministic predictions, the performance of the corresponding stochastic model is also lower. The LMM, as defined in equations 2.8 to 2.12, does not have a linear parameterization. Therefore, the application of the EKF is an approximation. The MM is non-linear and results in additional approximations compared to the TPM.

These results show that the method performs well even in case of mild non-linearities, especially if the deterministic model has intrinsically good prediction capabilities, but also that the

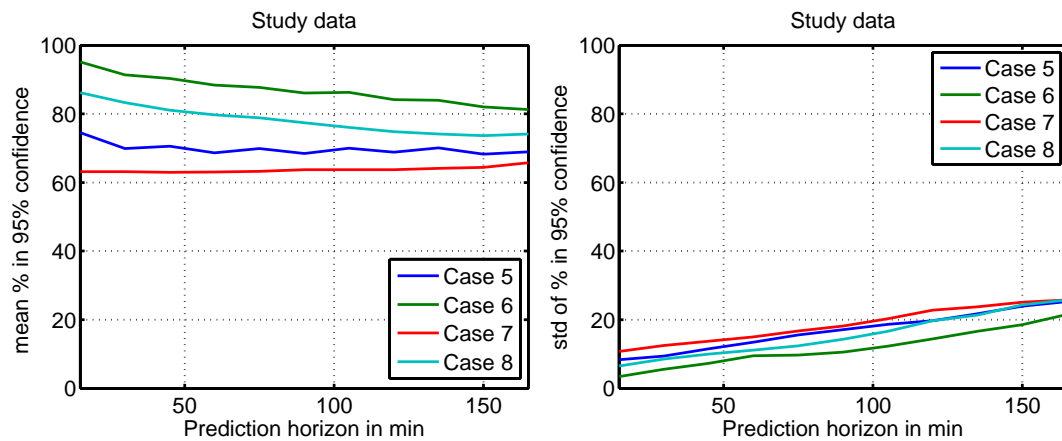


Figure 3.11: Prediction results for clinical study results (cases 5-8) for different horizons. Means and standard deviations evaluated on all validation sets are given. Mean values are given on the left, standard deviations on the right.

quality of the deterministic model plays an important role.

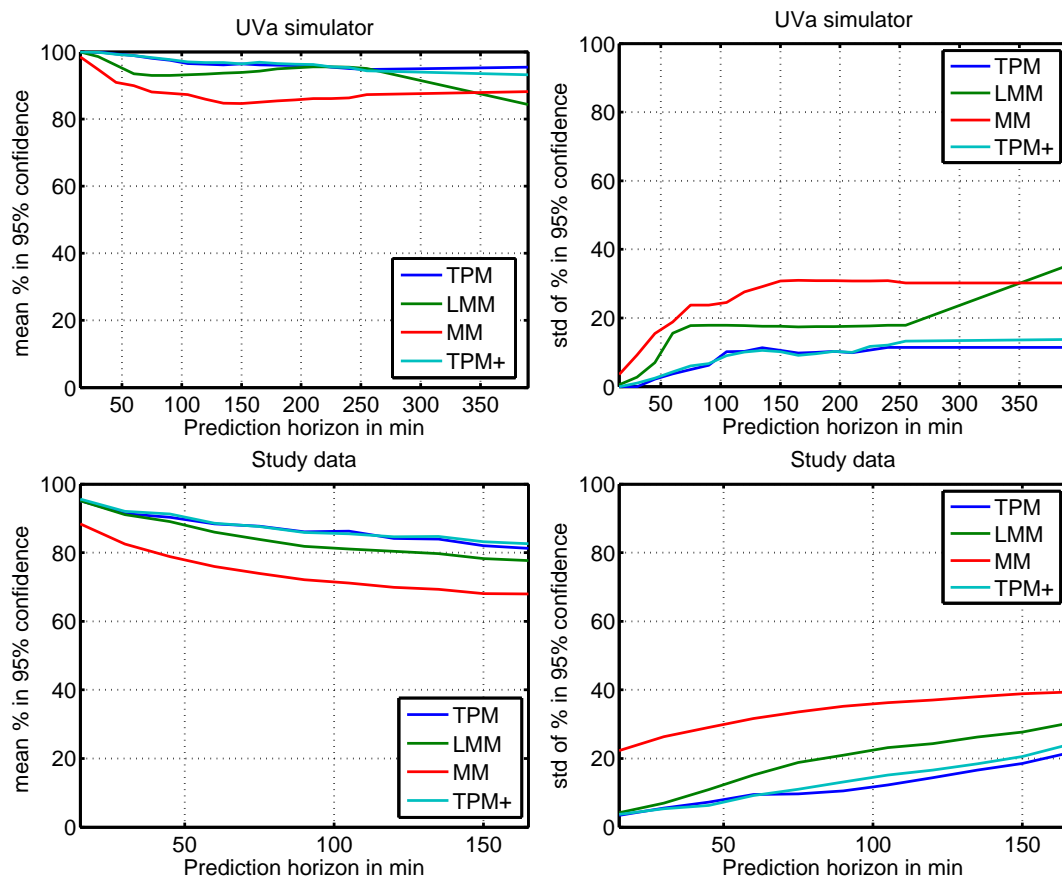


Figure 3.12: Stochastic prediction results for different models for case 2 and case 6. Mean values are given on the left, standard deviations on the right.

3.6 Conclusion

A novel method, to construct a stochastic model based on parametric uncertainty and to propagate these uncertainties, was presented and applied to the TPM. This new approach allows computing confidence intervals on BG concentrations in a simple, yet effective way. It performs as expected, although the designed stochastic models are always just as good as their underlying deterministic models. As such, it is important that the latter be adapted to the modeled system. Validation was performed on UVa simulator data, as well as clinical data and results for both were good for the relevant cases. Since clinical data contains more unpredictable events, estimation results were slightly worse than with UVa simulator data.

The estimation of BG uncertainty is an invaluable addition to improve diabetes treatment. The use of the stochastic information allows reducing patient's hypo- and hyperglycemia risk, especially in combination with a CGM device. However, the expected percentage of points within the 95% confidence interval is not 95% as it should be, if all assumptions were satisfied. Hence, more than 5% of the points lie outside the estimated confidence interval. This has numerous causes, such as non-Gaussian noise, different sources of non-linearities, or exceptional intra-patient variability. Nevertheless, using the stochastic information is beneficial in all circumstances: if the uncertainty is reliably estimated, patients can be treated while considerably reducing hypo- and hyperglycemia risk. Furthermore, if the uncertainty is estimated to be larger than it actually is, patients still have a lowered risk for large glycemic deviations, but may need to take more SMBG measurements to reduce the conservatism of the resulting recommendations of insulin injections. If uncertainties are underestimated, on the one hand, treatment is still safer than without uncertainty estimations and, on the other hand, if a CGM device is used, inaccuracies can immediately be detected and parameters can be adapted accordingly.

The newly designed sTPM will be used for new applications in the two following chapters.

It should be noted that the application field of this new method is not limited to diabetes management, but may be applied to any process in which a large uncertainty is present and needs to be estimated. Also, the application is not limited to parametric uncertainty, but can be extended to take input uncertainty into account. For example the uncertainty in meal amounts, discussed in section 1.2.2, could be addressed.

4 BG estimation

4.1 Introduction

One of the objectives of this thesis is to improve the treatment of diabetes using control methods. However, in order to do control - may it be standard therapy, open-loop, or closed-loop control - good quality BG, or full state estimation (i.e. estimating all states and not only BG) are essential. The most straightforward way to obtain BG estimations is to use one of the measurement devices described in 1.1.2: SMBG is commonly used for standard therapy or open-loop control, while CGM is required for an AP, but is also useful for open-loop control.

However, with these devices, measurement noise contributes to the uncertainty that makes BG control a challenge, as described in 1.2.2. The measurement noise is detrimental to treatment and its impact should be minimized. Since SMBG measurements are taken irregularly with potentially low sampling frequency, it is almost impossible to improve these measurements significantly. CGM measurements, on the other hand, have a sampling time of about one minute, but have a rather large noise level. This sampling time is much smaller than what would be required for treatment, as an AP is usually sampled every 5 minutes, even though 20 minutes would be sufficient (cf. 5.3.3). Therefore, the redundant measurements can be used to filter out high measurement noise and improve the BG estimates at the relevant instants. For some closed-loop controllers, it is also necessary to have access to the full system state, in which case, a complete state estimation using CGM measurements can be done.

In the literature, CGM data is almost always filtered or used for state estimation, and the most commonly used technique is by far the Kalman filter (KF). There are many different implementations such as, for example, a KF with adaptive signal-to-noise ratio by Facchinetti et al. [2011]. Knobbe and Buckingham [2005] propose an EKF, i.e. a non-linear KF, and Kuure-Kinsey et al. [2006] discuss a dual-rate KF that takes into account both CGM measurements and SMBG calibration measurements. While most of these filters work relatively well, their performance still depends on the underlying model. However, as discussed and shown in chapter 2, the models, typically used for control or prediction, are not very well adapted to these tasks and may lead to unacceptable results. Another drawback is that these models do

not account for other available information like insulin infusions or meal intakes.

In this chapter, in order to improve the available BG concentration information, several well-known estimation techniques of varying complexity are adapted for diabetes treatment. The individualized TPM, TPM+, or sTPM that allow better model predictions and take inputs such as meal announcements or insulin infusions into account are at the heart of these techniques. The BG concentrations estimated using the proposed filters are shown to be superior for diabetes treatment (evaluated using the Clarke EGA described in B.3) as demonstrated on the UVa simulator.

This chapter is organized as follows: First, in section 4.2, the observability of the TPM and the TPM+ is verified as this is a necessary condition for the application of most state estimation algorithms. Section 4.3 describes the different estimators that will then be compared on UVa simulator data in section 4.5, using the methods described in section 4.4. Final considerations are made and a conclusion is drawn in section 4.6.

4.2 Observability

The proposed model-based estimation techniques require the deterministic part of the model to be observable - a property that is further defined below. A first step for checking model observability is to put it into the standard linear state-space form.

4.2.1 State-space representation

The state-space representation was already introduced in equation 3.1 in its general form. However, since the TPM and the TPM+ are linear, the linear state-space representation, which is fully specified by the definition of 3 matrices, can be used.

The linear state-space equations are defined as follows where the output is considered to be linear with respect to the states:

$$\dot{\mathbf{x}}(t) = \mathbf{A}\mathbf{x}(t) + \mathbf{B}\mathbf{u}(t) \quad (4.1)$$

$$\mathbf{y}(t) = \mathbf{C}\mathbf{x}(t), \quad (4.2)$$

where \mathbf{A} is the n -by- n state matrix, with n being the number of states, \mathbf{x} is the n -by-1 state vector, \mathbf{B} is the n -by- m input matrix, with m being the number of inputs, \mathbf{u} is the m -by-1 input vector, \mathbf{y} is the p -by-1 output vector, with p being the number of outputs, and \mathbf{C} is the p -by- n output matrix.

The two new control-specific models, designed in chapter 2, are given in this representation below. Since only BG concentration is assumed to be measured, the output is the BG concentration state G .

- **TPM**, as defined in equations 2.14 to 2.18: $n = 4$, $m = 2$, $p = 1$,

$$\mathbf{x}(t) = \begin{bmatrix} G(t) & U_G(t) & U_{g1}(t) & X(t) & X_1(t) \end{bmatrix}' \quad (4.3)$$

$$\mathbf{u}(t) = \begin{bmatrix} U_{CHO}(t) & U_I(t) \end{bmatrix}' \quad (4.4)$$

$$y(t) = G(t) \quad (4.5)$$

$$\mathbf{A} = \begin{bmatrix} 0 & K_g & 0 & -K_x & 0 \\ 0 & -a_g & a_g & 0 & 0 \\ 0 & 0 & -a_g & 0 & 0 \\ 0 & 0 & 0 & -a_x & a_x \\ 0 & 0 & 0 & 0 & -a_x \end{bmatrix} \quad (4.6)$$

$$\mathbf{B} = \begin{bmatrix} 0 & 0 \\ a_g & 0 \\ 0 & 0 \\ 0 & 0 \\ 0 & a_x \end{bmatrix} \quad (4.7)$$

$$\mathbf{C} = \begin{bmatrix} 1 & 0 & 0 & 0 & 0 \end{bmatrix}. \quad (4.8)$$

$y(t)$ is no longer a vector, since only one output is considered.

- **TPM+** as defined in equations 2.20 to 2.24: $n = 4$, $m = 2$, $p = 1$,

$$\mathbf{x}(t) = \begin{bmatrix} G(t) & U_G(t) & U_{g1}(t) & X(t) & X_1(t) \end{bmatrix}' \quad (4.9)$$

$$\mathbf{u}(t) = \begin{bmatrix} U_{CHO}(t) & U_I(t) \end{bmatrix}' \quad (4.10)$$

$$y(t) = G(t) \quad (4.11)$$

$$\mathbf{A} = \begin{bmatrix} -S_G & K_g & 0 & -K_x & 0 \\ 0 & -a_g & a_g & 0 & 0 \\ 0 & 0 & -a_g & 0 & 0 \\ 0 & 0 & 0 & -a_x & a_x \\ 0 & 0 & 0 & 0 & -a_x \end{bmatrix} \quad (4.12)$$

$$\mathbf{B} = \begin{bmatrix} 0 & 0 \\ a_g & 0 \\ 0 & 0 \\ 0 & 0 \\ 0 & a_x \end{bmatrix} \quad (4.13)$$

$$\mathbf{C} = \begin{bmatrix} 1 & 0 & 0 & 0 & 0 \end{bmatrix}. \quad (4.14)$$

4.2.2 Observability

A system defined by equations 4.1 and 4.2 is observable if, for any initial state $\mathbf{x}(0)$, there exists a finite real number T , such that the knowledge of the input vector $\mathbf{u}(t)$ and of the output vector $y(t)$, $\forall 0 \leq t < T$, allows determining the initial state $\mathbf{x}(0)$ in a unique way. This property is shown to be verified if the observability matrix

$$\mathcal{O} = \begin{bmatrix} \mathbf{C} \\ \mathbf{CA} \\ \mathbf{CA}^2 \\ \vdots \\ \mathbf{CA}^{(n-1)} \end{bmatrix} \quad (4.15)$$

has full rank, i.e. its determinant is non-zero. For most estimation methods, observability is a necessary condition. For this reason, the observability of the TPM and the TPM+ need to be verified.

TPM For the TPM, the observability matrix is:

$$\mathcal{O}_{TPM} = \begin{bmatrix} 1 & 0 & 0 & 0 & 0 \\ 0 & K_g & 0 & -K_x & 0 \\ 0 & -K_g a_g & K_g a_g & K_x a_x & -K_x a_x \\ 0 & K_g a_g^2 & -2K_g a_g^2 & -K_x a_x^2 & 2K_x a_x^2 \\ 0 & -K_g a_g^3 & 3K_g a_g^3 & K_x a_x^3 & -3K_x a_x^3 \end{bmatrix} \quad (4.16)$$

This matrix has full rank as long as $a_x \neq a_g$ and all parameters are non-zero.

TPM+ For the TPM+, the observability matrix is:

$$\mathcal{O}_{TPM+} = \begin{bmatrix} 1 & 0 & 0 & 0 & 0 \\ -S_G & K_g & 0 & -K_x & 0 \\ S_G^2 & -K_g(S_G + a_g) & K_g a_g & K_x(S_G + a_x) & -K_x a_x \\ -S_G^3 & K_g a_g^2 + K_g S_G(S_G + a_g) & -K_g a_g(S_G + 2a_g) & -K_x a_x^2 - K_x S_G(S_G + a_x) & K_x a_x(S_G + 2a_x) \\ S_G^4 & -K_g(S_G + a_g)(S_G^2 + a_g^2) & K_g a_g(S_G^2 + 2S_G a_g + 3a_g^2) & K_x(S_G + a_x)(S_G^2 + a_x^2) & -K_x a_x(S_G^2 + 2S_G a_x + 3a_x^2) \end{bmatrix} \quad (4.17)$$

Again, this matrix has full rank as long as $a_x \neq a_g$ and all parameters, except S_G , are non-zero. When $S_G = 0$, the TPM+ is indeed the TPM and $\mathcal{O}_{TPM+} = \mathcal{O}_{TPM}$.

Consequently, the system is almost always observable, as it is unlikely that both time constants are exactly identical. Parameters (S_G excepted) are identified such that they cannot be zero. If both time constants have similar values, some numerical problems may occur, though.

4.3 Different BG estimators

Now that the conditions for observability have been verified, the different BG estimators that will be compared on the UVa simulator in this chapter, can be introduced in the following paragraphs, ordered by increasing complexity. Since these estimators are evaluated on UVa simulator data, the TPM is used as a prediction model, but can be replaced by the TPM+ if real patient data is to be used.

4.3.1 Low-pass filter

The most obvious and simple way to filter a noisy signal with high sample frequency is to use a traditional low-pass filter, such as a Butterworth filter. This kind of filter damps all information with a frequency higher than the so-called cutoff frequency. This results in a smoother signal, but a delay will appear. The cutoff frequency ω_c , which is the tuning parameter, should be slightly higher than the frequency corresponding to the system's smallest time constant. A first-order filter is typically chosen to reduce filter latency. The problem with this approach is that such a filter introduces a new delay that is relatively long if the cutoff frequency is low. For this reason a model-based method is probably better suited for this purpose. Also, the low-pass filter is sensitive to sensor dropouts because no model information is used. The transfer function of the low-pass filter is:

$$H(s) = \frac{1}{\frac{1}{\omega_c}s + 1}. \quad (4.18)$$

The time constant of the filter was chosen to be 10% faster than the fastest system time constant (which is around 20 minutes on UVa simulator data).

4.3.2 Luenberger observer

A classical state-space observer such as the Luenberger observer is a common candidate for determining unmeasured states or filtering measurements, and is used by Svensson [2013], e.g.. The estimation achieved using the following continuous-time equations

$$\dot{\hat{\mathbf{x}}}(t) = \mathbf{A}\hat{\mathbf{x}}(t) + \mathbf{B}\mathbf{u}(t) + \mathbf{L}(y(t) - \mathbf{C}\hat{\mathbf{x}}(t)), \quad (4.19)$$

where $\hat{\mathbf{x}}$ is the estimated state and \mathbf{L} is the n -by- p observer gain matrix. In other words, a Luenberger observer is based on open-loop observer that is corrected using the weighted estimation error. A schematic representation of this observer is given in figure 4.1.

The performance of this estimator depends, on the one hand, on the model that is being used (in this case the new prediction models), and, on the other hand, on the tuning of the \mathbf{L} matrix. In the context of this thesis, as only BG concentration is measured, p equals 1 and, therefore, \mathbf{L} is a vector of dimension 5. This means that the system to be observed has multiple

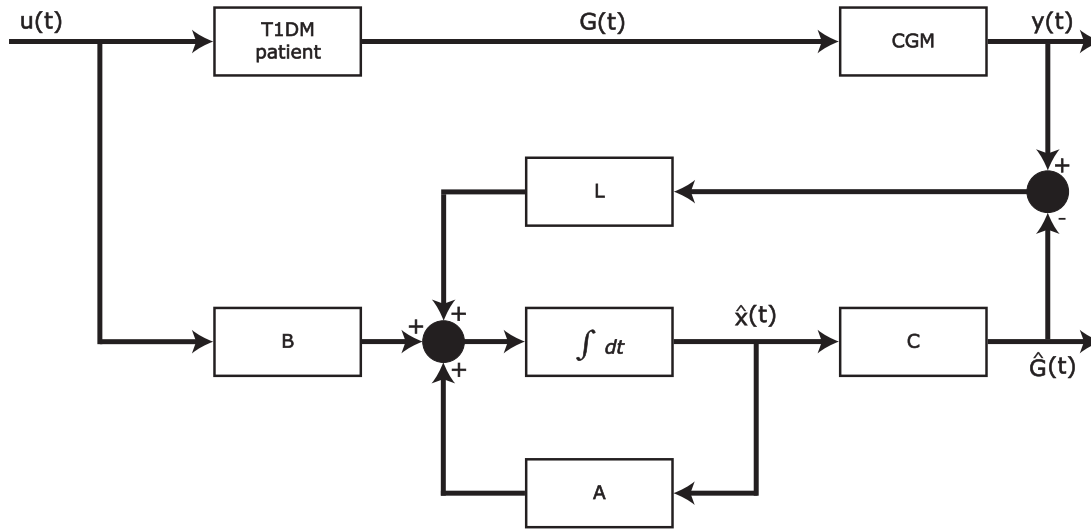


Figure 4.1: Luenberger observer

inputs and a single output (MISO system). As a consequence, the Ackermann formula and the duality between controller and observer may be used to find the observer gain \mathbf{L} (Longchamp [2010]). When using the Ackermann formula, the observer dynamics are specified by placing its poles. In a continuous-time setup, the closer the values of the poles are to $-\infty$, the closer the observer is to being a dead-beat observer and to exactly following the measurements.

The performance of the observer relies crucially on the placement of the poles. However, a dead-beat observer is not desired, as our measurements are noisy and our model is not perfect. The model should have some influence on the estimator behavior, hence, the poles need to be closer to 0, but still negative. The goal is to find the right balance between CGM measurements and model-based predictions to generate the best possible BG concentration estimate. An identical value, corresponding to a time constant of 40 minutes, was chosen for all 5 poles as this value has shown the best results.

4.3.3 Kalman Filter (KF)

The Luenberger observer is a deterministic observer that does not take into account neither the quality of model predictions, nor the quality of the measurements. This is manually and indirectly tuned by the user. As a consequence, the Luenberger observer may still be improved and its tedious tuning may be simplified by the use of a KF.

The KF, described among many others by Simon [2006], is a well-known filter that allows making estimations using weighted contributions from both model predictions and measurements. The weights are determined by the specified measurement and process noise covariance matrices, R and Q_{KF} , respectively. The discretized KF is applied to the discrete

system defined by:

$$\mathbf{x}_k = \Phi \mathbf{x}_{k-1} + \Gamma \mathbf{u}_{k-1} + \mathbf{w}_{k-1} \quad (4.20)$$

$$\mathbf{y}_k = \mathbf{C} \mathbf{x}_k + \mathbf{v}_k \quad (4.21)$$

$$E(\mathbf{w}_k \mathbf{w}_j') = \mathbf{Q}_{KF} \delta_{k-j} \quad (4.22)$$

$$E(\mathbf{v}_k \mathbf{v}_j') = \mathbf{R} \delta_{k-j} \quad (4.23)$$

$$E(\mathbf{w}_k \mathbf{v}_j') = \mathbf{0}, \quad (4.24)$$

where Φ and Γ are the discretized matrices corresponding to \mathbf{A} and \mathbf{B} , respectively. \mathbf{x}_k , \mathbf{u}_k , \mathbf{w}_k , and \mathbf{y}_k are $\mathbf{x}(t)$, $\mathbf{u}(t)$, $\mathbf{w}(t)$, and $\mathbf{y}(t)$ at the k^{th} sampling time. $\mathbf{v}(k)$ is the measurement noise at the k^{th} sampling time. \mathbf{w}_k and \mathbf{v}_k are Gaussian random variables whose covariance matrices are defined by equations 4.22 to 4.24 and are thus uncorrelated. δ_{k-j} is the Kronecker delta that equals $\mathbf{1}$ if $k = j$ and $\mathbf{0}$ otherwise.

The discrete-time KF is given by equations 4.25 to 4.21, for each sampling time k .

$$\mathbf{P}_k^- = \Phi \mathbf{P}_{k-1}^+ \Phi' + \mathbf{Q}_{KF} \quad (4.25)$$

$$\mathbf{K}_k = \mathbf{P}_k^- \mathbf{C} (\mathbf{P}_k^- \mathbf{C}' + \mathbf{R})^{-1} \quad (4.26)$$

$$\hat{\mathbf{x}}_k^- = \Phi \hat{\mathbf{x}}_{k-1}^+ + \Gamma \mathbf{u}_{k-1} \quad (4.27)$$

$$\hat{\mathbf{x}}_k^+ = \hat{\mathbf{x}}_k^- + \mathbf{K}_k (\mathbf{y}_k - \mathbf{C} \hat{\mathbf{x}}_k^-) \quad (4.28)$$

$$\mathbf{P}_k^+ = (\mathbf{I} - \mathbf{K}_k \mathbf{C}) \mathbf{P}_k^- \quad (4.29)$$

$$\hat{\mathbf{y}}_k = \mathbf{C} \hat{\mathbf{x}}_k^+, \quad (4.30)$$

where \mathbf{P}_k is $\mathbf{P}(t)$ at $t = t_k$, and \mathbf{K} is the Kalman filter gain. Since, during one KF iteration, \mathbf{P}_k and $\hat{\mathbf{x}}_k$ are updated, the superscripts $-$ and $+$ denote the values before and after the variable update, respectively.

In this work, the discrete-time KF equations are applied to the TPM in discretized state-space formulation. The discretization at a 1-minute sampling time, corresponding to the UVa simulator, is evaluated numerically. Initial values are chosen as follows:

$$\hat{\mathbf{x}}_0^+ = \begin{bmatrix} G_0 & 0 & 0 & 0 & 0 & 0 \end{bmatrix}' \quad (4.31)$$

$$\mathbf{P}_0^+ = \begin{bmatrix} \sigma_{G,0}^2 & 0 & 0 & 0 & 0 & 0 \\ 0 & 0 & 0 & 0 & 0 & 0 \\ 0 & 0 & 0 & 0 & 0 & 0 \\ 0 & 0 & 0 & 0 & 0 & 0 \\ 0 & 0 & 0 & 0 & 0 & 0 \end{bmatrix}, \quad (4.32)$$

where, G_0 is the initial measurement of BG, and $\sigma_{G,0}^2$ is the variance attributed to G_0 .

The two tuning parameters \mathbf{Q}_{KF} and \mathbf{R} are chosen as follows:

$$\mathbf{Q}_{KF} = \begin{bmatrix} Q_{BG} & 0 & 0 & 0 & 0 & 0 \\ 0 & 0 & 0 & 0 & 0 & 0 \\ 0 & 0 & 0 & 0 & 0 & 0 \\ 0 & 0 & 0 & 0 & 0 & 0 \\ 0 & 0 & 0 & 0 & 0 & 0 \end{bmatrix} \quad (4.33)$$

$$Q_{BG} = \text{cf. table 4.1} \quad (4.34)$$

$$R = 100. \quad (4.35)$$

The value of Q_{BG} is determined using the Root Mean Square Error (RMSE) of 1-minute ahead predictions on UVa data, which reflects how well the TPM allows doing short predictions for each patient. A generic value of 0.04 (mg/dl)^2 also gives good results whenever a personalization is not possible. The value of R is found by assuming that 95% of measurements are within 20% and that the average BG concentration is approximately 100 mg/dl:

$$R = \left(\frac{0.2}{1.96} 100 \right)^2 \approx 10^2. \quad (4.36)$$

It should be noted that a KF assumes a white Gaussian noise for both process and measurement noise. However, this is only an assumption, as both of these noises are known to be correlated. For example, the CGM noise in the UVa simulator is generated using the model developed by Breton and Kovatchev [2008] that uses colored noise.

Adult	1	2	3	4	5	6	7	8	9	10
$\sqrt{Q_{BG}}$	0.297	0.234	0.205	0.159	0.147	0.186	0.299	0.227	0.228	0.195

Table 4.1: Square root of Q_{BG} for all 10 patients in mg/dl.

4.3.4 Extended Kalman Filter with the sTPM (EKF)

The sTPM explicitly models process noise as a function of time. Specifically, after a bolus or a meal, the confidence in the model decreases, as the outcome becomes less predictable. This information may directly be used in a KF. However, the sTPM, as described in chapter 3, is not linear because of the time and state dependence of the stochastic term. For this reason, an EKF has to be used. As already mentioned, the sTPM being linearly parameterized, this is not an approximation.

The sTPM can be expressed as:

$$\mathbf{x}_k = \Phi \mathbf{x}_{k-1} + \Gamma \mathbf{u}_{k-1} + \mathbf{L}_{k-1} \mathbf{w}_{k-1} \quad (4.37)$$

$$y_k = \mathbf{C} \mathbf{x}_k + \nu_k, \quad (4.38)$$

where \mathbf{L}_k is the discrete version of $\mathbf{L}(t)$ defined in equation 3.33 that depends on \mathbf{x}_k and \mathbf{u}_k . The process noise is now defined by $E(\mathbf{w}_k \mathbf{w}_j') = \mathbf{Q} \delta_{k-j}$.

Because the EKF can account for non-linearities, the measurement noise variance can be expressed as a function of BG concentration, based on the ISO 15197 norm that imposes a 20% error:

$$R_k = \left(\frac{0.2}{1.96} G_k \right)^2, \quad (4.39)$$

where G_k is the BG concentration at the k^{th} sample. As a consequence, high BG measurements have higher uncertainty than lower ones.

The EKF is given by the following equations:

$$\mathbf{P}_k^- = \Phi \mathbf{P}_{k-1}^+ \Phi' + \mathbf{L}_{k-1} \mathbf{Q} \mathbf{L}_{k-1}' \quad (4.40)$$

$$\mathbf{K}_k = \mathbf{P}_k^- \mathbf{C} (\mathbf{P}_k^- \mathbf{C}' + \hat{y}_k R_k \hat{y}_k)^{-1} \quad (4.41)$$

$$\hat{\mathbf{x}}_k^- = \Phi \hat{\mathbf{x}}_{k-1}^+ + \Gamma \mathbf{u}_{k-1} \quad (4.42)$$

$$\hat{\mathbf{x}}_k^+ = \hat{\mathbf{x}}_k^- + \mathbf{K}_k (\mathbf{y}_k - \mathbf{C} \hat{\mathbf{x}}_k^-) \quad (4.43)$$

$$\mathbf{P}_k^+ = (\mathbf{I} - \mathbf{K}_k \mathbf{C}) \mathbf{P}_k^- \quad (4.44)$$

$$\hat{y}_k = \mathbf{C} \hat{\mathbf{x}}_k^+. \quad (4.45)$$

\mathbf{Q} is determined using the inverse Fisher information matrix as described in section 3.4. Initial values for x and P are the same as for the KF.

4.3.5 Extended Kalman Filter with sTPM and added process noise - the Therapy Parameter-based Filter (TPF)

As the noise level in the EKF can be shown to be insufficient (section 4.5), the process noise used for the KF and for the EKF can be combined to have a more realistic noise term. In this case, the noise term $\mathbf{L}_{k-1} \mathbf{w}_{k-1}$ is augmented by increasing the dimension of \mathbf{L}_k and \mathbf{Q} by one. This can easily be done by adding a term to equation 4.40. This new EKF will be referred to as Therapy Parameter-based Filter (TPF). Its equations can be written as:

$$\mathbf{P}_k^- = \Phi \mathbf{P}_{k-1}^+ \Phi' + \mathbf{L}_{k-1} \mathbf{Q} \mathbf{L}_{k-1}' + \mathbf{Q}_{KF} \quad (4.46)$$

$$\mathbf{K}_k = \mathbf{P}_k^- \mathbf{C} (\mathbf{P}_k^- \mathbf{C}' + \hat{y}_k R_k \hat{y}_k)^{-1} \quad (4.47)$$

$$\hat{\mathbf{x}}_k^- = \Phi \hat{\mathbf{x}}_{k-1}^+ + \Gamma \mathbf{u}_{k-1} \quad (4.48)$$

$$\hat{\mathbf{x}}_k^+ = \hat{\mathbf{x}}_k^- + \mathbf{K}_k (\mathbf{y}_k - \mathbf{C} \hat{\mathbf{x}}_k^-) \quad (4.49)$$

$$\mathbf{P}_k^+ = (\mathbf{I} - \mathbf{K}_k \mathbf{C}) \mathbf{P}_k^- \quad (4.50)$$

$$\hat{y}_k = \mathbf{C} \hat{\mathbf{x}}_k^+, \quad (4.51)$$

where \mathbf{Q}_{KF} is given in equation 4.33. Initial values for \mathbf{x} and \mathbf{P} are the same as for the KF.

4.4 Methods to compare CGM filters

As was already explained in section 2.5 and 3.4, the data used to determine model parameters should never be used to validate results. For this reason, separate sets of training data and validation data are generated using the UVa simulator. The methods are not tested on real patient data because no accurate reference measurements are available. As such, this analysis is limited to the UVa simulator and results are only valid within this scope. Therefore, the TPM and the sTPM are used, rather than the TPM+ that would be recommended on real patient data. To compare the results for different filters, several metrics are necessary that are discussed in this section.

4.4.1 Training data

The proposed filters (except the Butterworth filter) are based on models, whose parameters need to be identified for every subject out of the 10-patient database of the UVa simulator. For this reason, the model parameters are identified on different sensitivity test days, which are specified in more detail in appendix A.1.2. These test days consist in 3 insulin sensitivity and 3 meal sensitivity tests, performed to obtain reliable insulin action (cf. 2.4.3).

As explained in 2.5.1, neither the TPM, nor the TPM+ is able to fit sensitivity test data, because their dynamics are not fully compatible with the UVa simulator model. Nevertheless, it is possible to fit these models on sensitivity test data when the BG measurements taken after the maximum or minimum of the meal or insulin sensitivity test, respectively, are discarded. This procedure leads to accurate model parameters that have very reliable insulin action. To identify the parameters, an analogous procedure to that of section 2.4.2 was used.

Simulated CGM measurements are used for parameter identification. This makes the identification of the parameter covariance matrix possible, with the approach of section 3.2.3.

4.4.2 Validation data

To validate and compare the proposed filtering algorithms, 4 consecutive days of UVa simulator data are available. These are described in more detail in appendix A.1.1 and consist in 3 standard therapy days and one day with "random" insulin infusions and meal intakes. The simulated CGM results are filtered and compared to the exact BG values.

The validation relies on 3 scenarios, each leading to slightly different results and showing advantages and drawbacks of the different formulations:

- *Scenario 1:* Data from the third standard therapy day illustrates how the filters compare

in a setting with little excitation.

- *Scenario 2:* An experiment on the random day shows how the filters perform in a setting with rich inputs.
- *Scenario 3:* A continuous data set comprising all 4 uninterrupted validation days gives an overview of the overall performance and is indeed the most meaningful scenario.

4.4.3 Metrics

The percentage of points within zone A of the Clarke EGA (B.3) is used primarily as a metric, since it is the most clinically relevant one, i.e. it provides direct information on the quality of the treatment. The MAD (B.1) is analyzed in order to have a more rigorous comparison, as the EGA is partly an empiric tool.

4.5 Comparison results

The next step is to run the proposed filters with previously identified parameters on the different scenarios, defined for the validation data sets, and compare the outcomes using EGA and MAD.

4.5.1 Scenario 1

For the first scenario, a standard therapy meal experiment from the third day of the validation data set is considered. Results are given in figure 4.2 and are illustrated in figure 4.3.

The Butterworth filter leads to worse results than the raw CGM measurements. This is caused by the long time delay (of about 30 minutes) observed after a meal-induced rise in BG concentration. Results for the other filters show that taking into account the inputs and using an appropriate model solves this problem. The Luenberger observer has good filtering properties, but is unmatched by the KF. Surprisingly, results for the EKF are bad. This may be explained by analyzing figure 4.3: the EKF has excellent filtering properties shortly after the meal, when uncertainty on model predictions is high, as modeled by the sTPM. However, 7 hours after the meal, the BG concentrations start to rise again - a behavior that is not forcibly observed on real patients and that the TPM is not capable of reproducing - while a relatively high confidence in the model is assumed. As a consequence, the filtered BG concentration does not follow the CGM signal, but stays close to the concentrations predicted by the TPM. For this reason, additional process noise needs to be considered (in addition to the one estimated by the sTPM). Therefore, in order to add some uncertainty that would account for the observed model mismatch, the process noise used for the KF is added to the EKF to create the TPF. With this scenario, the performance of the resulting filter is comparable to that of the KF. Indeed, the KF has a better percentage in EGA zone A while the TPF has a lower MAD.

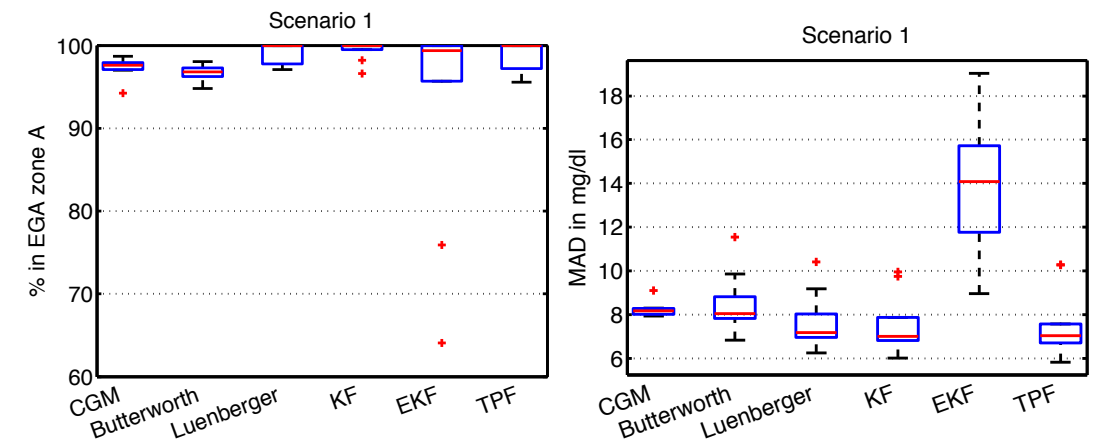


Figure 4.2: Boxplot (cf. appendix B.9) of average percentage in zone A of the EGA and Boxplot of average MAD for scenario 1, corresponding to day 3 of the validation data set.

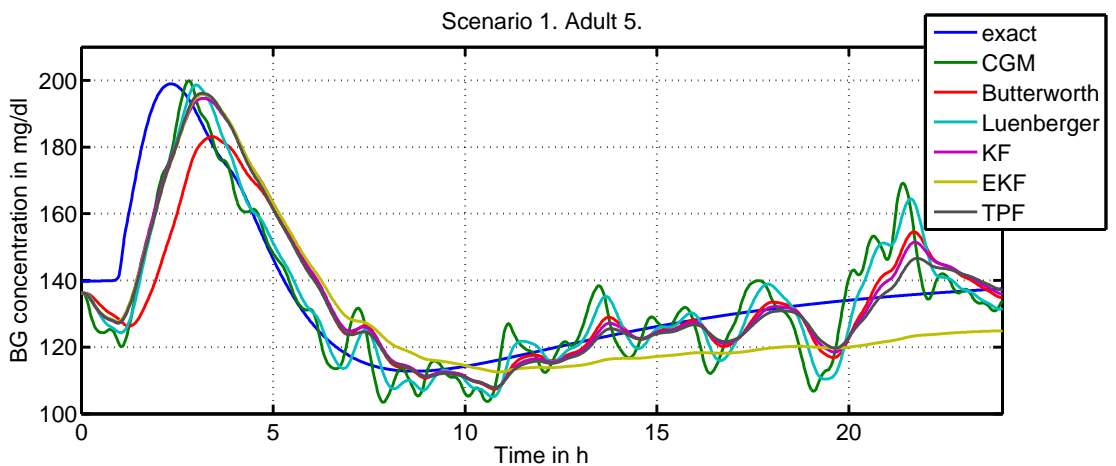


Figure 4.3: Example of a BG profile on scenario 1 for adult 5.

4.5.2 Scenario 2

Scenario 2 incorporates frequent system excitation as opposed to scenario 1 and its single meal. The results are given in figure 4.4 and are illustrated in figure 4.5.

In this case the EKF has the best filtering properties for the two metrics, closely followed by the TPF. These results can be explained by the more accurate TPM predictions for this data set combined with the larger confidence intervals due to the richer input data. As a consequence, these filters should be very well suited for an application in an AP, as inputs are very rich in this case, too. The KF and Luenberger observer also exhibit good performance and improve the results compared to raw CGM measurements, while the simple low-pass filter shows some weaknesses.

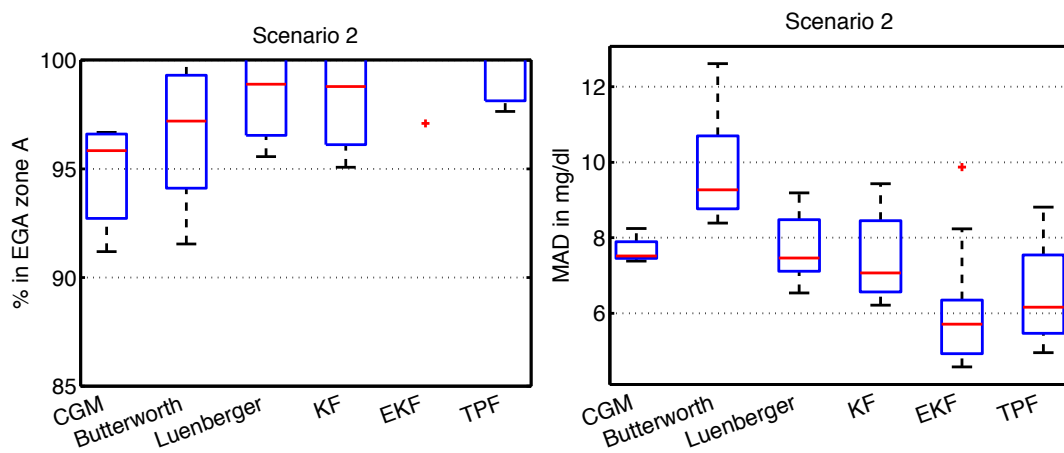


Figure 4.4: Boxplot (cf. appendix B.9) of average percentage in zone A of the EGA and Boxplot of average MAD for scenario 2, corresponding to day 4 of the validation data set.

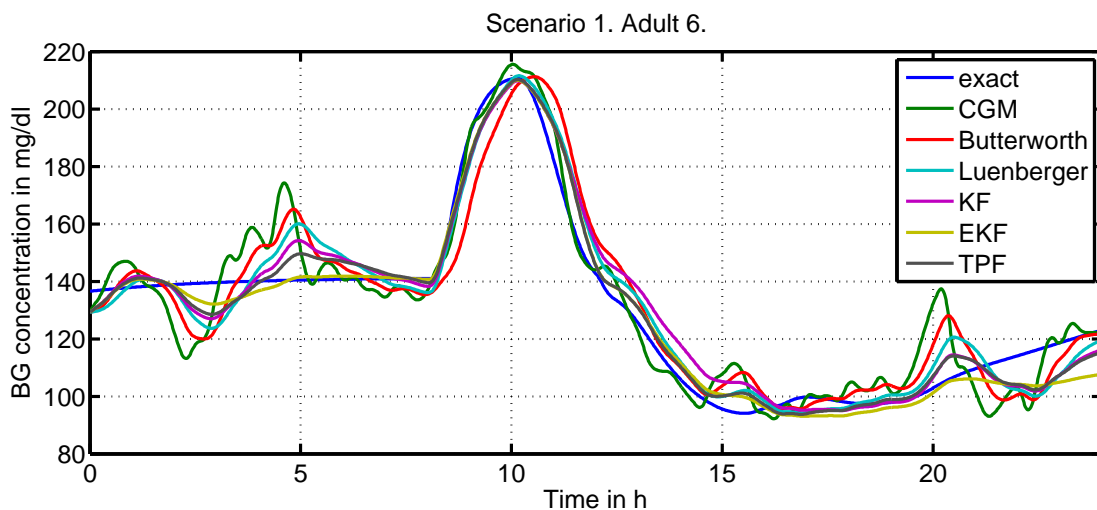


Figure 4.5: Example of a BG profile on scenario 2 for adult 6.

4.5.3 Scenario 3

For this scenario, which considers all 4 consecutive validation days, the results are given in figure 4.6 and are illustrated in figure 4.7.

This scenario leads to the most general results, whereas the previous scenarios are intended to show the different properties of the filters. The TPF has the most accurate and the most reliable BG estimation properties and should therefore be used in the context of BG control. If a simpler estimator is required, the KF also performs well on most data sets.

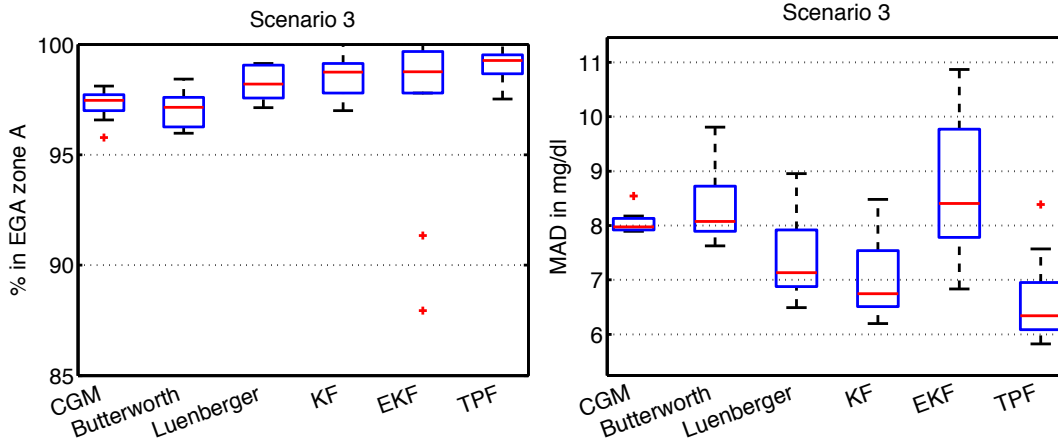


Figure 4.6: Boxplot (cf. appendix B.9) of average percentage in zone A of the EGA and Boxplot of average MAD for scenario 2, corresponding to day 4 of the validation data set.

4.6 Conclusion

The previous sections have highlighted the benefits of the use of the TPF for a well-performing AP, and, at the same time, nicely illustrate a possible application of the sTPM. The new filter, based on the EKF and the new sTPM, with additional added process noise, proves to be the best and most versatile filter for estimating the BG concentrations based on UVa simulator-generated CGM measurements. This is especially true for rich input signals commonly used in an AP. However, in the case of less rich inputs, the simpler KF is shown to be comparable in terms of performance.

Several remarks need to be made concerning the preceding analysis:

- The TPF was validated on simulated UVa data, only. It is unknown whether results are applicable to real patients, especially considering the limitations of the UVa metabolic model and CGM error model. While results are very promising and are used for further testing on the UVa simulator, additional experiments and validations need to be performed to determine the best filter for a real patient. For instance, the addition of the process noise in the TPF might become unnecessary, as the TPM's dynamics are closer

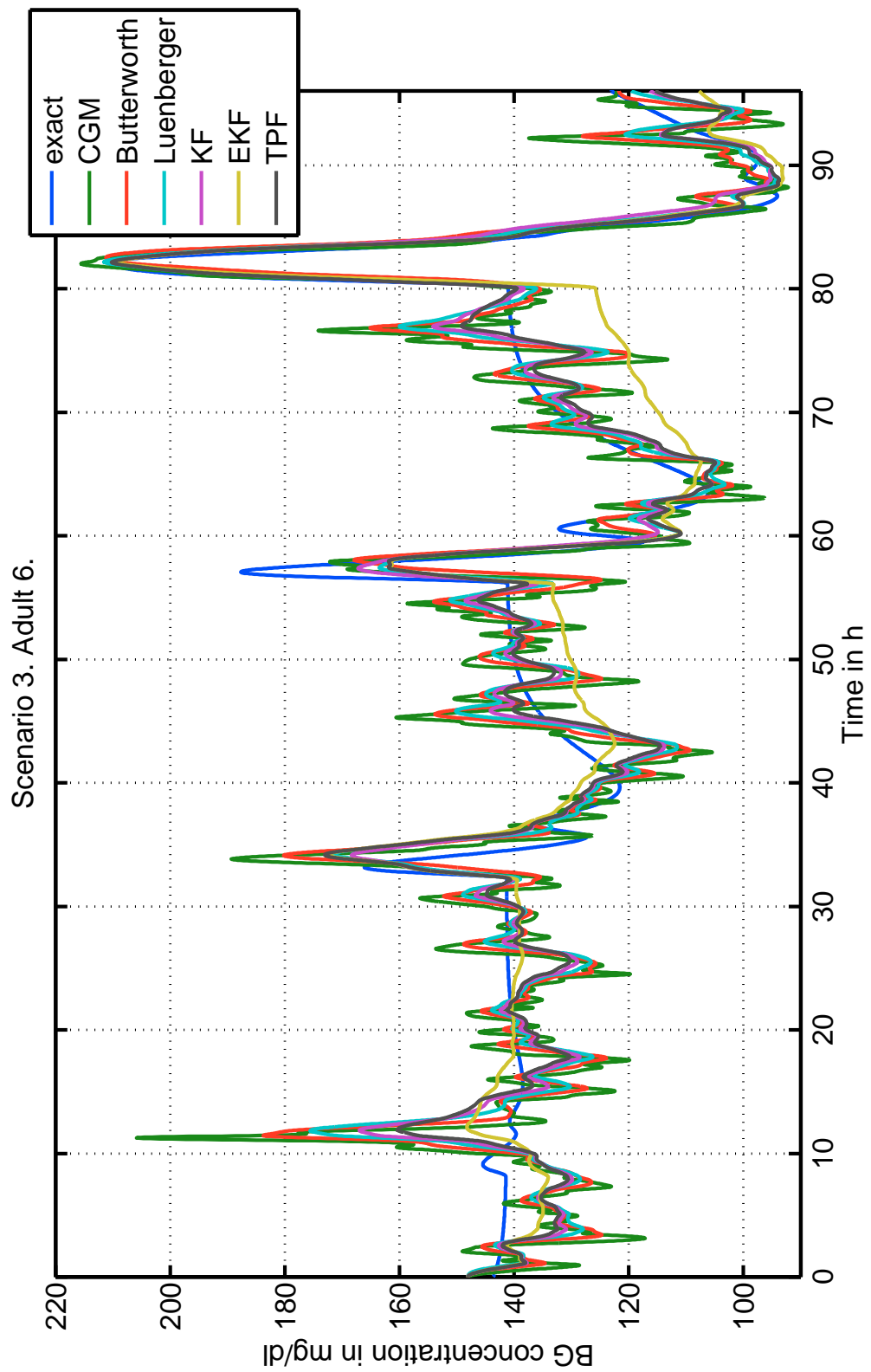


Figure 4.7: Example of a BG profile on scenario 2 for adult 6.

to those of a real patient.

- The proposed TPF relies on meal announcements and insulin infusion profiles. However, in a real setting, meal announcements may be absent or wrong. In this case, the TPF would not perform properly anymore and would underestimate the effect of a meal. While this would lead to lower post-prandial insulin doses using an AP, BG control would be less effective, but would, nevertheless, remain safe. On the other hand, the TPF can be used to detect such unannounced meals by determining when the estimated BG concentration is not consistent with the measured BG concentration anymore. Similarly, sensor anomalies and unexpected BG excursions can be detected and, thus, necessary counteractive measures can be taken.
- The measurement noise considered in the TPC is assumed to be white, uncorrelated, Gaussian noise. However, the noise modeled in the UVA simulator by Breton and Kovatchev [2008] is clearly correlated. Hence, the use of a KF with correlated noise, as described by Simon [2006], for example, should be investigated.
- In section 2.5, the initial states of the TPM and the TPM+ were fixed using noisy CGM or SMBG measurements. The TPF can be used to improve this initialization and potentially the resulting data fits, parameter correlation, and model predictions.

5 BG Control

5.1 Introduction

The central part of T1DM treatment is the control algorithm, which needs to be safe (avoid hypoglycemia) and perform well (minimize hyperglycemia). Currently, standard therapy (described in section 2.3.2) is the most common treatment. However, there is room for improvement for two main reasons.

First, standard treatment does not make full use of the available continuous insulin infusion capabilities offered by insulin pumps and does not systematically take into account the information from CGM devices. For this reason, a tremendous research effort for developing an AP is currently being done and involves a number of institutions funded, for instance, by the European Commission (AP@home, DIAdvisor), or the JDRF (iAP).

Secondly, the quality of a patient's treatment depends largely on the patient's know-how for the estimation of CHO, and on the willingness to take frequent measurements and calculate the corresponding insulin doses. For this reason, an automatization procedure requiring minimal patient involvement could substantially improve the treatment of the patients.

There are two main control approaches to improve T1DM treatment (which were briefly introduced in section 1.1.2):

- **Open-loop control** is characterized by the absence of fully automated BG treatment decisions. The patient or the physician determine and/or validate every insulin injection and function as a final safety layer. Standard therapy is a form of open-loop control that has proven to perform with reasonable performance. Nevertheless, improvements in the form of bolus calculators are being developed and are partially already implemented on commercial insulin pumps. While these bolus calculators are valuable tools for T1DM patients, the potential of the insulin pumps and the CGM devices are not fully exploited so far. For these reasons, a TPM-based open-loop control algorithm is presented and tested on the UVa simulator.

- **Closed-loop control** is defined by the possibility of the controller to actively take treatment decisions. It is generally characterized by the use of CGM readings to generate almost continuously adapted insulin infusions. Considering the frequency of the CGM readings, it is impossible for anyone to validate insulin doses, and the system needs to be fully autonomous. Only for some variants, patients are required to announce meals. Despite the huge and prolonged effort to develop an out-patient AP, no device is commercially available for now. Since the AP has become technically possible with new CGM augmented insulin pumps, the bottleneck are BG control algorithms and the strong regulations to certify such potentially harmful devices. The number of proposed algorithms is large and first versions of closed-loop controllers are being successfully tested on humans, although a close review reveals that most APs have a large potential for improvement. In what follows, the TPM is used to design control approaches that are simple and reliable, and, which are tested on the UVa simulator.

The unavailability of the AP can be explained by the challenges identified in section 1.2. The inter-patient variability, the meal uptake variability, the complexity of the system, and the identifiability have already been addressed in this thesis by developing the TPM and the TPM+. The stochastic model reduces the effects of intra-patient variability, meal announcement errors, and system complexity, while improving patient safety. The TPF filters part of the measurement noise without adding time delay. The remaining open issues, which are the asymmetric control objective, the time delay and the saturation, will be resolved in this chapter, while patient safety is further improved.

This chapter is organized as follows: First, in section 5.2, the state of the art in open-loop control is discussed and TPM-based improvements are derived and tested. In section 5.3, current closed-loop approaches are analyzed and a new controller, the TPC, is designed, tested, and compared to state-of-the-art controllers. Then, an outlook on other TPM- and sTPM-based approaches is given in section 5.4, and conclusions are drawn in 5.5.

5.2 Open-loop control

5.2.1 State of the art

Standard therapy as described in section 2.3.2 is a very effective and well accepted open-loop control strategy. A first step in making this therapy more reliable is to integrate a bolus calculator into the BG meter. This helps patients with diabetes to compute their insulin bolus correctly, based on their CF and I2C. Recently, more and more insulin pump manufacturers have been offering hybrid devices with coupled insulin pump and SMBG (or recently even CGM) meter. This allows so-called "**smart**" **insulin pumps**, which not only compute the appropriate insulin bolus based on standard therapy, but also verify if no insulin is being stacked. Insulin stacking occurs when a patient applies standard therapy while there is still some active insulin in the bloodstream. This is quite likely to happen since even fast-

acting insulin keeps on acting after several hours. The excess insulin administrated because of stacking is a very likely cause of hypoglycemia. The currently available smart insulin pumps use the concept of Insulin On Board (IOB), introduced by Ellingsen et al. [2009], which quantifies how much insulin is active in the body. This method is effective, but there are no guidelines to tune the insulin action duration (the only parameter), even though this parameter may vary significantly from one patient to another. Zisser et al. [2008] give an overview over current smart insulin pumps.

While smart insulin pumps are simple, yet effective ways to obtain appropriate BG control, more complex methods potentially lead to improved results and were already explored 15 years ago by Hejlesen et al. [1997], e.g. . In this context, a model-based **optimal control** approach is often adopted, such as proposed by Prud'homme et al. [2011], for which, BG concentrations are predicted over a prolonged horizon and an insulin infusion profile is computed in order to minimize a BG-specific cost function. This approach allows optimizing BG control following various, especially slow or "difficult", meals. However, optimal control-based methods were shown to lead to inappropriate results, mostly as a result of inappropriate BG prediction models and unreliable insulin action (cf. 2.4.3).

A first improvement of open-loop control strategies is obtained by using the information provided by **CGM** devices. The efficacy of CGM-augmented standard therapy is shown to improve T1DM treatment to the point of potentially justifying healthcare reimbursement (Heinemann and Devries [2013]). By using a BG estimator, as discussed in chapter 4, CGM measurements can also be used to obtain more accurate BG estimations. Vereshchetin et al. [2013] proposed this approach to treat MDI users, while Patek et al. [2011] applied it in an optimal control setting. Additionally, the CGM data can be used to generate different alarms in case of dangerous situations that would typically remain unnoticed otherwise.

Considering the large potential for improvement, in the context of this thesis, open-loop controllers are designed with the objective of enhancing standard therapy and potentially taking CGM information into account.

5.2.2 TPM-based open-loop therapy

The main difficulty in designing an optimal control approach in open-loop control is the choice of an appropriate BG prediction model. For this reason, the TPM, a new prediction model was developed in chapter 2. In this section a novel open-loop therapy is deduced directly from the TPM equations, rather than using the TPM for optimization. Because of the TPM's simple structure, the optimal treatment can be determined analytically.

Feed-forward meal disturbance rejection

The principle of feed-forward control is to compute current and future system inputs based on prior knowledge. In this case, this translates to computing the required insulin infusion

based on a prediction model. Generally speaking, and especially in the presence of complex models, it is impossible to do this analytically. However, with the TPM, this becomes indeed possible and an "optimal meal rejection" can be computed using the Laplace transform.

The TPM is defined in equations 2.14 to 2.18, which can be written in the Laplace domain:

$$G(s) = -\frac{K_x}{s(\frac{1}{a_x}s + 1)^2}U_I(s) + \frac{K_g}{s(\frac{1}{a_g}s + 1)^2}U_{CHO}(s). \quad (5.1)$$

The insulin action and meal effect time constants are defined as $\tau_x = \frac{1}{a_x}$ and $\tau_g = \frac{1}{a_g}$, respectively. Thus, equation 5.1 can be rewritten as

$$G(s) = -\frac{K_x}{s(\tau_x s + 1)^2}U_I(s) + \frac{K_g}{s(\tau_g s + 1)^2}U_{CHO}(s). \quad (5.2)$$

If $I(s) = -\frac{K_x}{s(\tau_x s + 1)^2}$ is defined as the system to be controlled, i.e. the glucose-insulin sub-system, and $D(s) = \frac{K_g}{s(\tau_g s + 1)^2}$ as the system disturbance (corresponding to the meal disturbance), equation 5.2 can be written as:

$$G(s) = I(s)U_i(s) + D(s)U_{CHO}(s). \quad (5.3)$$

This is graphically represented in figure 5.1. It is possible to determine the feed-forward

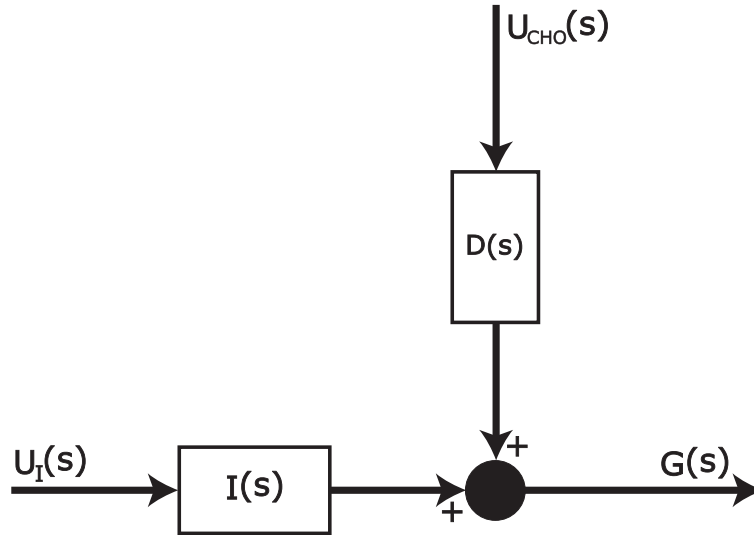


Figure 5.1: Insulin-glucose system with meal disturbance.

control $U_0(s)$ such that the disturbance is perfectly canceled. This is possible because the meal input U_{CHO} is assumed to be known with sufficient accuracy. Hence, $U_0(s)$ is found by equating the system output with feed-forward control with the disturbance-free system (cf. figure 5.2):

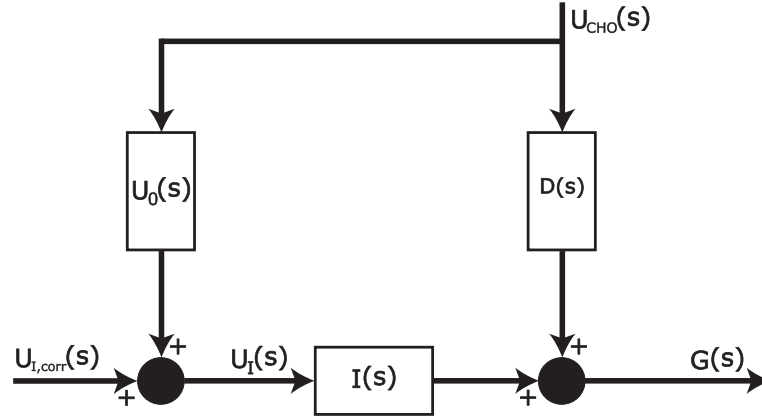


Figure 5.2: Insulin-glucose system with meal disturbance and feed-forward control.

$$I(s)(U_I(s) + U_0(s)U_{CHO}(s)) + D(s)U_{CHO}(s) = I(s)U_I(s) \quad (5.4)$$

$$I(s)U_I(s) + U_0(s)U_{CHO}(s)I(s) + D(s)U_{CHO}(s) = I(s)U_I(s) \quad (5.5)$$

$$U_0(s)I(s) = -D(s) \quad (5.6)$$

$$U_0(s) = -\frac{D(s)}{I(s)}. \quad (5.7)$$

Using the definition of $D(s)$ and $I(s)$, equation 5.7 becomes

$$U_0(s) = -\frac{D(s)}{I(s)} \quad (5.8)$$

$$= \frac{\frac{K_g}{s(\tau_g s + 1)^2}}{-\frac{K_x}{s(\tau_x s + 1)^2}} \quad (5.9)$$

$$= -\frac{K_g (\tau_x s + 1)^2}{K_x (\tau_g s + 1)^2} \quad (5.10)$$

$$= -I2C \frac{(\tau_x s + 1)^2}{(\tau_g s + 1)^2} \quad (5.11)$$

This feed-forward control $U_0(s)$ perfectly counteracts any announced meal disturbance.

Marchetti et al. [2008] propose a very similar feed-forward control, where the feed-forward is a first-order system with different time constants than in 5.11.

The expression of $U_0(s)$ can be transformed back into the time domain if U_{CHO} is an impulse. This is the case if meal duration is considered as being infinitely small. This approximation allows finding an analytic time-domain solution for the optimal meal rejection. Since the Laplace transform of a Dirac impulse $\delta(t)$ is 1, $U_{CHO}(s) = 1$ if 1 g of CHO are ingested at the

initial time ($t = 0$). Using any symbolic computation software, one obtains:

$$U_0(t) = I2C \left(\frac{\tau_x^2}{\tau_g^2} \delta(t) + (\tau_g - \tau_x) \frac{(\tau_g t - \tau_x t + 2\tau_g \tau_x)}{\tau_g^4} e^{-\frac{t}{\tau_g}} \right) \quad (5.12)$$

$$= I2C \left(\frac{\tau_x^2}{\tau_g^2} \delta(t) + \frac{(\tau_g - \tau_x)^2}{\tau_g^4} t e^{-\frac{t}{\tau_g}} + 2\tau_x \frac{\tau_g - \tau_x}{\tau_g^3} e^{-\frac{t}{\tau_g}} \right) \quad (5.13)$$

The solution from equations 5.12 and 5.13 needs to be scaled to the total amount of CHO ingested, when more than 1 g is ingested.

Equation 5.13 consists of three terms:

- The first term is a bolus that is given simultaneously to the meal. It can be observed that this bolus is smaller than $I2C$ (for $\delta = 1$ g), if insulin action is faster than CHO action ($\tau_x < \tau_g$), the same if the two time constants are identical, and larger if $\tau_g < \tau_x$.
- The second term is always greater than or equal to 0 and is part of an insulin infusion profile.
- The third term is positive if $\tau_x < \tau_g$ and negative otherwise. It is the second part of an insulin infusion profile.

Using the final value theorem, it can be observed that $\int_0^\infty U_0(t) dt = I2C$. This means that the total amount of insulin is always equal to $I2C$, the optimal bolus that would have been infused for standard therapy.

However, depending on the value of $q = \frac{\tau_x}{\tau_g}$, the ratio of the two time constants, several cases can be distinguished:

- $q < 1$: In this case, insulin acts faster than the meal effect and the therapy resulting from the TPM leads to an initial bolus $q \cdot I2C$, smaller than $I2C$, followed by a positive insulin infusion profile that perfectly counteracts the meal disturbance.
- $q = 1$: In this case, insulin action and meal effect have the same time constant and an optimal bolus at the same time as the meal is enough to counteract the meal disturbance. In fact the second and third terms of equation 5.13 are 0.
- $q > 1$: This case is more complex: In fact, the meal acts faster than the insulin, which entails that it is impossible to perfectly counteract the meal disturbance. Since the TPM is linear, the optimal profile computed in equation 5.13 leads to an initial bolus that is greater than $I2C$, followed by a partially negative insulin infusion. In fact the second term of equation 5.12 is negative for $0 < t < \frac{2\tau_x}{q-1}$, where t is the time after the meal. Since the required insulin infusion becomes negative, this treatment is not recommended and might become dangerous, because of controller saturation. Indeed,

the initial bolus is larger than $I2C$, but negative insulin is not infused because of the input saturation - in the case of basal insulin, a slightly negative infusion makes sense - resulting in hypoglycemia. As a conclusion, if $q > 1$ standard therapy should be applied. It is impossible to do better, while maintaining patient safety. In fact, the option to infuse insulin before the meal intake may result in improved treatment outcomes, but is considered unsafe (as a patient may be prevented from taking a planned meal) and does not have an analytic solution.

Finally, feed-forward control using the TPM can be summarized:

$$\text{If } q \leq 1 : U_0(t) = I2C \left(\frac{\tau_x^2}{\tau_g^2} \delta(0) + \frac{(\tau_g - \tau_x)^2}{\tau_g^4} t e^{-\frac{t}{\tau_g}} + 2\tau_x \frac{\tau_g - \tau_x}{\tau_g^3} e^{-\frac{t}{\tau_g}} \right) \\ \text{else } U_0(t) = I2C \cdot \delta(0).$$

Using an analogous development, feed-forward control for the TPM+ can be shown to be identical.

Feed-forward using TPM or TPM+ has only advantages over standard therapy. A next step is to verify whether identified parameter values from the clinical study data and UVa simulator data allow this advantage over standard therapy. The value of q depends, on the one hand, on the insulin absorption and action rates of an individual, and, on the other hand, on the individual and meal-specific CHO absorption rate. To evaluate typical values of q , parameter values for the different available data sets (cf. appendix A) are given for all patients for the different data sets:

Clinical study data The clinical study was designed to test optimal control solutions in open-loop. During the study design, it was already clear that such a method would only make sense for relatively slow meals. For this reason, a meal with low GI was chosen. Identified TPM and TPM+ model parameters are given in table 5.1 and 5.2, respectively. They show that, for the study data, only 4 or 5 out of 10 patients, for the TPM and TPM+, respectively, can have perfect disturbance rejection using a variable insulin infusion profile, while the others would rely on standard therapy to reject meals.

Patient	1	2	3	4	5	6	7	9	11	12
τ_x	52	48	72	197	26	37	49	37	89	53
τ_g	69	69	55	33	44	34	46	37	102	35
q	0.77	0.69	1.29	6.03	0.60	1.07	1.07	1.00	0.87	1.53

Table 5.1: Identified time constants for TPM on study data in minutes, and their corresponding q . If $q < 1$, it is marked as bold.

Chapter 5. BG Control

Patient	1	2	3	4	5	6	7	9	11	12
τ_x	62	48	73	197	28	37	51	46	110	61
τ_g	83	69	57	33	54	34	49	50	131	37
q	0.75	0.69	1.29	6.03	0.52	1.08	1.05	0.93	0.84	1.67

Table 5.2: Identified time constants for TPM+ on study data in minutes, and their equation q . If $q < 1$, it is marked as bold.

UVa simulator sensitivity tests In the UVa simulator there is only the choice for one type of meal: a quite fast meal, as seen in table 5.3. The model parameters are those used in chapter 4 and were identified on CGM measurements taken during the sensitivity test days specified in appendix A.1.2. Parameter values from table 5.3 show that $q > 1$ for all patients and, thus, having a variable insulin infusion profile as feed-forward control does not make sense, and that standard therapy should therefore be preferred.

Adult	1	2	3	4	5	6	7	8	9	10
τ_x	96	53	51	56	62	71	56	63	79	65
τ_g	23	38	27	27	26	46	37	21	30	27
q	4.13	1.39	1.89	2.11	2.39	1.54	1.51	3.04	2.60	2.37

Table 5.3: Identified time constants for TPM on UVa simulator data in minutes, and their equation q . If $q < 1$, it is marked as bold.

Complex feed-forward insulin profiles are only useful if insulin action is faster than the meal effect. However, this is rarely the case, as shown above. Therefore, in most cases, standard therapy is the best choice for feed-forward control. This justifies the development of faster acting insulin and insulin delivery methods, which is a very active research field. Improvements were obtained with super-fast inhaled insulin by The Doyle Group and the Sansum Diabetes Research Institute [2013], by heating the insulin injection site (Raz et al. [2009]), or through IP insulin infusion. This paves the way for more effective T1DM treatment.

Setpoint adaptation

It has been shown that, according to the TPM and the TPM+, it is impossible to maintain a constant BG after a meal, if the insulin action is slower than the meal action ($q > 1$). As a consequence, it is physically impossible to maintain the target BG concentration over time using current insulins. For this reason, after a meal, the setpoint should be modified in order to be reachable and to avoid giving massive insulin doses. In the following paragraphs this setpoint adaptation is derived from the TPM and the TPM+.

Default setpoint The setpoint for BG control has to be set by a physician, according to his personal knowledge of a given patient. In this thesis, the value of 112.5 mg/dl is chosen, because it is the value that minimizes the Blood Glucose Risk Index (BGRI), defined in appendix

B.4. Svensson [2013], or Weinzimmer et al. [2008], propose to use different setpoints during the night to avoid nocturnal hypoglycemia.

Setpoint adaptation Two separate cases are distinguished for determining if, and how, the setpoint should be adapted.

- $\tau_x \leq \tau_g$, i.e. $q \leq 1$: In this case it is straightforward to find the setpoint value. Since the disturbance rejection is able to perfectly counteract the meal effect, the setpoint is constant and equal to the optimal BG concentration, i.e. 112.5 mg/dl if the BGRI is to be minimized.
- $\tau_x > \tau_g$, i.e. $q > 1$: This case is far more common than the previous one and is systematic on the UVa simulator. To have perfect rejection of the meal disturbance, negative insulin would need to be administered, following a large bolus. Since this is not possible, the standard bolus should be given. However, this entails that it is not possible to keep BG constant anymore and the setpoint should be adapted such that it can be followed.

To compute this setpoint adaptation, the increase in BG resulting from feed-forward control needs to be calculated. It consists of the sum of the disturbance and the resulting BG from the feed-forward control. Hence, the setpoint adaptation $S(s)$ is:

$$S(s) = U_0(s)I(s)U_{CHO}(s) + D(s)U_{CHO}(s) \quad (5.14)$$

$$= (U_0(s)I(s) + D(s))U_{CHO}(s). \quad (5.15)$$

Since $q > 1$, $U_0(s) = I2C$, and equation 5.15 can be rewritten:

$$S(s) = (I2C \cdot I(s) + D(s))U_{CHO}(s). \quad (5.16)$$

For the TPM:

$$S_{TPM}(s) = \left(I2C \left(-\frac{K_x}{s(\tau_x s + 1)^2} \right) + \frac{K_g}{s(\tau_g s + 1)^2} \right) U_{CHO}(s) \quad (5.17)$$

$$= \frac{K_g}{s} \left(\frac{1}{(\tau_g s + 1)^2} - \frac{1}{(\tau_x s + 1)^2} \right) U_{CHO}(s) \quad (5.18)$$

$$= \frac{K_g}{s} \left(\frac{(\tau_x s + 1)^2 - (\tau_g s + 1)^2}{(\tau_g s + 1)^2 (\tau_x s + 1)^2} \right) U_{CHO}(s) \quad (5.19)$$

$$= K_g \frac{(\tau_x - \tau_g) [(\tau_x + \tau_g)s + 2]}{(\tau_g s + 1)^2 (\tau_x s + 1)^2} U_{CHO}(s). \quad (5.20)$$

U_{CHO} can be approximated by an impulse input if the duration of the meal is very small. In this case, the calculations can be done by choosing an amplitude of 1 and an impulse time equal to 0, because the linearity allows scaling and time-shifting. Hence,

$U_{CHO}(t) = \delta(t)$, and $U_{CHO}(s) = 1$. In this case, the inverse Laplace transform leads to the time-domain response:

$$S_{TPM}(t) = K_g \left[\left(1 + \frac{t}{\tau_x} \right) e^{-t/\tau_x} - \left(1 + \frac{t}{\tau_g} \right) e^{-t/\tau_g} \right]. \quad (5.21)$$

The same calculations are made for the TPM+, for which $I_{TPM+}(s) = -\frac{K_x}{(s+S_G)(\tau_x s+1)^2}$ is defined as the system to be controlled, i.e. the glucose-insulin sub-system, and $D_{TPM+}(s) = \frac{K_g}{(s+S_G)(\tau_g s+1)^2}$ as the system disturbance. Equation 5.2 can be written as:

$$G_{TPM+}(s) = I_{TPM+}(s)U_i(s) + D_{TPM+}(s)U_{CHO}(s), \quad (5.22)$$

and the appropriate setpoint adaptation is:

$$S_{TPM+}(s) = K_g \frac{s}{s+S_G} \frac{(\tau_x - \tau_g) [(\tau_x + \tau_g)s + 2]}{(\tau_g s + 1)^2 (\tau_x s + 1)^2} U_{CHO}(s). \quad (5.23)$$

The time domain solution for the TPM+ may be computed using symbolic software, but is not given here, as the expression is relatively complex.

Summary Finally, the BG concentration setpoint G_{SP} is defined as the target BG concentration plus the setpoint adaptation:

$$G_{SP}(s) = G_t + S(s). \quad (5.24)$$

Hence, for the TPM:

$$\begin{aligned} \text{If } q \leq 1 : G_{SP}(s) &= 112.5 \text{ mg/dl} \\ \text{else } G_{SP}(s) &= 112.5 \text{ mg/dl} + K_g \frac{(\tau_x - \tau_g) [(\tau_x + \tau_g)s + 2]}{(\tau_g s + 1)^2 (\tau_x s + 1)^2} U_{CHO}(s), \end{aligned}$$

while for the TPM+:

$$\begin{aligned} \text{If } q \leq 1 : G_{SP}(s) &= 112.5 \text{ mg/dl} \\ \text{else } G_{SP}(s) &= 112.5 \text{ mg/dl} + K_g \frac{s}{s+S_G} \frac{(\tau_x - \tau_g) [(\tau_x + \tau_g)s + 2]}{(\tau_g s + 1)^2 (\tau_x s + 1)^2} U_{CHO}(s). \end{aligned}$$

Corrective insulin

In the previous paragraphs, an optimal meal disturbance rejection has been designed, based on the TPM or the TPM+. This new method either leads to a perfect meal rejection, or to an adaptation of the controller setpoint. Nevertheless, this method only works well, if the model is sufficiently close to the real BG concentrations. However, it is known that, because of the

huge system complexity and uncertainty, the TPM and TPM+ will only lead to an approximate, yet reliable prediction. For this reason, a corrective insulin dose should be computed at every insulin injection, using the same concept as in standard therapy (cf. 2.3.2). This corrective insulin dose $U_{I,corr}$ can be improved using the new models, by taking into account the system's initial state.

The TPM without the meal sub-model, corresponding to $I(s)$ is given by

$$\dot{G} = -K_x X(t) \quad (5.25)$$

$$\dot{X}(t) = -\frac{1}{\tau_x} X(t) + \frac{1}{\tau_x} X_1(t) \quad (5.26)$$

$$\dot{X}_1(t) = -\frac{1}{\tau_x} X_1(t) + \frac{1}{\tau_x} U_I(t). \quad (5.27)$$

The Laplace transform with non-zero initial conditions leads to

$$sG(s) = -K_x X(s) + G_0 \quad (5.28)$$

$$sX(s) = -\frac{1}{\tau_x} X(s) + \frac{1}{\tau_x} X_1(s) + X_0 \quad (5.29)$$

$$sX_1(s) = -\frac{1}{\tau_x} X_1(s) + \frac{1}{\tau_x} U_I(s) + X_{1,0}, \quad (5.30)$$

where G_0 , X_0 , and $X_{1,0}$ are the respective initial conditions for the different states.

Hence,

$$G(s) = -K_x \frac{X(s)}{s} + \frac{G_0}{s} \quad (5.31)$$

$$X(s) = \frac{X_1(s) + \tau_x X_0}{\tau_x s + 1} \quad (5.32)$$

$$X_1(s) = \frac{U_I(s) + \tau_x X_{1,0}}{\tau_x s + 1}. \quad (5.33)$$

Substituting equation 5.33 into equation 5.32:

$$X(s) = \frac{U_I(s) + \tau_x X_{1,0} + \tau_x (\tau_x s + 1) X_0}{(\tau_x s + 1)^2}, \quad (5.34)$$

and substituting equation 5.34 into equation 5.31, the full expression for G , for all initial conditions, is obtained.

$$G(s) = -K_x \left(\frac{U_I(s) + \tau_x X_{1,0} + \tau_x (\tau_x s + 1) X_0}{s(\tau_x s + 1)^2} \right) + \frac{G_0}{s} \quad (5.35)$$

$$= -\frac{K_x}{s(\tau_x s + 1)^2} U_I(s) - K_x \frac{\tau_x X_{1,0} + \tau_x (\tau_x s + 1) X_0}{s(\tau_x s + 1)^2} + \frac{G_0}{s} \quad (5.36)$$

$$= I(s) U_I(s) - \tau_x K_x \frac{X_{1,0} + (\tau_x s + 1) X_0}{s(\tau_x s + 1)^2} + \frac{G_0}{s} \quad (5.37)$$

Chapter 5. BG Control

This means that the complete expression for G is the sum of I , the insulin subsystem with initial conditions set to zero, and two further terms setting the initial conditions.

Next, this expression is used to find the insulin quantity necessary to reach the BG concentration setpoint. The setpoint should be reached at least when time goes to infinity:

$$G_{SP} = G(\infty). \quad (5.38)$$

Using the final value theorem:

$$G_{SP} = \lim_{s \rightarrow 0} sG(s) \quad (5.39)$$

$$= \lim_{s \rightarrow 0} \left(-\frac{K_x}{(\tau_x s + 1)^2} U_I(s) - K_x \tau_x \frac{X_{1,0} + (\tau_x s + 1)X_0}{(\tau_x s + 1)^2} + G_0 \right) \quad (5.40)$$

$$= K_x (\lim_{s \rightarrow 0} U_I(s)) - K_x \tau_x (X_{1,0} + X_0) + G_0. \quad (5.41)$$

Hence,

$$\lim_{s \rightarrow 0} U_I(s) = -\frac{1}{K_x} (G_{SP} - G_0) - \tau_x (X_{1,0} + X_0), \quad (5.42)$$

and from the definition of the Laplace transform:

$$\lim_{s \rightarrow 0} U_I(s) = \int_0^\infty U_I(t) dt. \quad (5.43)$$

Finally,

$$\int_0^\infty U_I(t) dt = -\frac{1}{K_x} (G_{SP} - G_0) - \tau_x (X_{1,0} + X_0). \quad (5.44)$$

This means that, according to the TPM, the total amount of insulin that needs to be administered in order to reach the BG concentration setpoint is composed of two terms:

1. the difference between the setpoint and current BG concentration divided by K_x (which is the same as the CF), which corresponds exactly to the correction term of standard therapy.
2. the opposite of the sum of X and X_1 at the initial time, multiplied by the insulin time constant τ_x . The next step is to show how these initial values of X and X_1 can be estimated using insulin infusion history.

X and X_1 are taken from the Laplace transform of the TPM equations:

$$X(s) = \frac{X_1(s)}{\tau_x s + 1} \quad (5.45)$$

$$X_1(s) = \frac{U_I(s)}{\tau_x s + 1}. \quad (5.46)$$

Thus,

$$X(s) + X_1(s) = \frac{X_1(s)}{\tau_x s + 1} + \frac{U_I(s)}{\tau_x s + 1} \quad (5.47)$$

$$= \frac{U_I(s)}{(\tau_x s + 1)^2} + \frac{U_I(s)}{\tau_x s + 1} \quad (5.48)$$

$$= \frac{\tau_x s + 2}{(\tau_x s + 1)^2} U_I(s). \quad (5.49)$$

Therefore, in Laplace domain, the second term of equation 5.44 corresponds to:

$$\tau_x(X(s) + X_1(s)) = \frac{\tau_x^2 s + 2\tau_x}{(\tau_x s + 1)^2} U_I(s), \quad (5.50)$$

and is evaluated at time $t = 0$ using past insulin injections information.

Finally, the quantity of corrective insulin to be injected at time $t = 0$ is

$$U_{I,corr} = -\frac{1}{K_x}(G_{SP} - G_0) - \tau_x(X_{1,0} + X_0), \quad (5.51)$$

because, considering the dynamics of the TPM that make insulin overshoots impossible, the fastest way to reach the setpoint BG concentration is by infusing the insulin as early as possible.

The same calculation cannot be done for the TPM+. In fact,

$$\int_0^\infty U_I(t) dt = -\infty, \quad (5.52)$$

because the TPM+ converges to 0 if times goes to infinity. Hence, a constant negative insulin infusion would be required after some time. Nevertheless, using $U_{I,corr}$ in the context of the TPM+ can still be recommended, as long as S_G is sufficiently small.

Insulin on board

IOB is a concept that was introduced by Ellingsen et al. [2009], and was already described in the state of the art in section 5.2.1. There are several methods to predict how much insulin stays active in the bloodstream after a given time. They range from linear to non-linear curves, but almost all rely on a single time constant. The difficulty is to estimate this time constant such that a compromise between performance and safety is obtained. For this reason, it is proposed to use the TPM to evaluate the IOB, based on the identified model parameters. IOB is the amount of injected insulin $\frac{U_I(s)}{s}$, minus the insulin that has already acted $-\frac{I(s)}{K_x} \cdot U_I(s)$,

corresponding to the drop in BG divided by the insulin sensitivity:

$$IOB(s) = \frac{U_I(s)}{s} + \frac{I(s)}{K_x} \cdot U_I(s) \quad (5.53)$$

$$= \left(\frac{1}{s} - \frac{1}{s(\tau_x s + 1)^2} \right) \cdot U_i(s) \quad (5.54)$$

Thus,

$$\frac{IOB(s)}{U_I(s)} = \left(\frac{1}{s} - \frac{1}{s(\tau_x s + 1)^2} \right) \quad (5.55)$$

$$= \frac{\tau_x^2 s^2 + 2\tau_x s}{s(\tau_x s + 1)^2} \quad (5.56)$$

$$= \frac{\tau_x^2 s + 2\tau_x}{(\tau_x s + 1)^2} \quad (5.57)$$

This value corresponds exactly to the expression of the right hand side term of equation 5.50 and corresponds to the second term of the corrective insulin $U_{I,corr}$ that can now be written as

$$U_{I,corr} = -\frac{1}{K_x} (G_{SP} - G_0) - IOB(0), \quad (5.58)$$

where $IOB(0)$ is the insulin on board at the initial time. It should be noticed that IOB only depends on the time constant τ_x .

Open-loop control summary

An open-loop control strategy was derived from the TPM, leading to an optimization-free, model-based treatment that augments standard therapy by adding safety and performance enhancements, and does not rely on CGM. This treatment will be referred to as the Therapy Parameter-based Controller in Open-Loop (TPC OL).

It is composed of 3 new parts that are added to standard therapy:

1. Meal disturbances are rejected by the following feed-forward control administered after the meal intake time and multiplied by the mass of ingested CHO:

$$\text{If } q \leq 1 : U_0(t) = I2C \left(\frac{\tau_x^2}{\tau_g^2} \delta(t) + \frac{(\tau_g - \tau_x)^2}{\tau_g^4} t e^{-\frac{t}{\tau_g}} + 2\tau_x \frac{\tau_g - \tau_x}{\tau_g^3} e^{-\frac{t}{\tau_g}} \right)$$

$$\text{else } U_0(t) = I2C \cdot \delta(t).$$

This enhances performance, especially in the case of a slow meal ($q < 1$).

2. The BG concentration setpoint is adapted by adding the term $S(s)$ to the target BG

concentration:

$$\text{With the TPM: } S(s) = K_g \frac{(\tau_x - \tau_g) [(\tau_x + \tau_g)s + 2]}{(\tau_g s + 1)^2 (\tau_x s + 1)^2} U_{CHO}(s)$$

$$\text{With the TPM+: } S(s) = K_g \frac{s}{s + S_G} \frac{(\tau_x - \tau_g) [(\tau_x + \tau_g)s + 2]}{(\tau_g s + 1)^2 (\tau_x s + 1)^2} U_{CHO}(s).$$

This improves patient safety because it reduces the injected insulin bolus if a meal is taken while the previous meal has still an effect.

3. Finally the insulin on board is subtracted from the standard therapy correction factor.

$$IOB(s) = \frac{\tau_x^2 s + 2\tau_x}{(\tau_x s + 1)^2} U_I(s) \quad (5.59)$$

5.2.3 CGM augmented open-loop control

The proposed open-loop strategy can be applied using exclusively SMBG measurements. However, if CGM measurements are available, they can be directly integrated into the existing strategy using the TPF of chapter 4. This filter can be used to improve BG estimation at the treatment time.

5.2.4 Implementation on the UVa simulator

To evaluate the proposed open-loop control method, a clinical study would need to be carried out. However, since this is not possible within this thesis, the treatment strategy is evaluated on the UVa simulator described in detail in appendix A.1. The nominal scenario, detailed in E.1, is used for this validation. Several points need to be specified first:

Target BG concentration The target BG concentration G_t is 112.5 mg/dl in this thesis. This value was chosen because it is the value that minimizes the patient risk according to Kovatchev et al. [2000], as further explained in appendix B.4.

Basal rate correction For the new open-loop controller, the basal rate is adjusted such that the target BG concentration of 112.5 mg/dl is obtained when no meals and no additional insulin affect the system. The personalized basal rates are given in table 5.4.

Evaluated open-loop controllers

The open-loop controllers that are evaluated on the UVa simulator are:

Adult	$U_{I,b}$ in U/h
1	1.500
2	1.600
3	1.733
4	1.048
5	1.683
6	1.850
7	1.450
8	1.396
9	1.450
10	1.501

Table 5.4: Adjusted basal rates to have a G_{ss} of 112.5 mg/dl.

UVa simulator standard therapy (UVa ST) The results from the new open-loop strategy are tested against the standard open-loop algorithm implemented by default in the UVa simulator. The basal rate is the predefined basal rate that keeps the unperturbed subject at a given basal BG concentration, which is around 140 mg/dl (cf. A.1). The meal bolus is given by multiplying the given I2C with the amount of ingested CHO. No corrective insulin is injected. This means that this method is fully open-loop, since it does not rely on any measurements at all.

Standard therapy based on TPM parameters (TPM ST) UVa ST is not the standard therapy described in 2.3.2, because no corrective insulin is given. For this reason, standard therapy using the parameters identified with the TPM and the adjusted basal rate are applied to the UVa simulator. This should indicate how standard therapy performs on the UVa simulator. It should be noted that there is still a difference compared to the original standard therapy in that, on the simulator, CGM measurements are used instead of SMBG measurements. This should have a negative effect on performance, as CGM is less accurate than SMBG. The model parameters result from the sensitivity tests described in A.1.2 and were already used in chapter 4.

TPM-based open-loop control (TPC OL) The TPC OL is constructed as in 5.2.2. The same parameter set than for the TPM ST is used. Again, simulated CGM measurements are used, since no SMBG measurements are available in the UVa simulator.

TPM-based open-loop control with TPF (TPC TPF-OL) This controller is the same as the TPC OL, with the exception that the TPF is used for estimating BG concentrations, instead of using raw CGM data.

5.2.5 Results using the UVa simulation

Simulation results for UVa ST and TPM ST are given in table 5.5. The control methods are evaluated based on the BGRI (cf. appendix B.4) and the percentage of time within target and below target (more detail in appendix B.6). According to all averaged metrics, standard therapy performs not as well as the measurement-free UVa ST. Indeed, for the UVa ST, the average BGRI and the time spent in hypoglycemia are lower, while the time spent within the target range is higher. This holds when results are averaged over all patients, as well as when the atypical adult 9 is discarded. The main reason is the increase in the basal insulin for the TPM ST, combined with the large oscillations observed on the UVa simulators dynamics (as illustrated in A.1). Both of these bring BG concentrations closer to, and sometimes beyond, the hypoglycemic limit. It should be noted that in 7 out of 10 patients, TPM ST has a better or comparable BGRI than the UVa ST, and the three outliers are responsible for the increased average BGRI. A slightly lower basal insulin rate would probably improve these results.

Adult	BGRI		% in tar		% below tar	
	ST UVa	ST TPM	ST UVa	ST TPM	ST UVa	ST TPM
1	3.14	6.15	92.85	83.13	0	16.87
2	1.41	5.23	100	82.05	0	17.95
3	1.41	0.79	100	100	0	0
4	1.9	1.45	91.7	94.9	0	0
5	1.29	1.02	100	100	0	0
6	2.8	2.87	89.93	88.62	0	11.38
7	1.19	1.59	100	95.35	0	4.65
8	1.33	1.06	100	100	0	0
9	4.33	4.67	83.17	84.69	8.64	9.79
10	3.08	1.9	88.23	98.47	0	1.53
Av.	2.19	2.67	94.59	92.72	0.86	6.22
Av. No 9	1.95	2.45	95.86	93.61	0.00	5.82

Table 5.5: Results for all adults of the UVa simulator under for standard therapy on the nominal scenario.

5.2.6 Conclusion

A complete open-loop strategy has been developed starting from the TPM equations. This strategy extends the existing standard therapy by introducing new performance enhancing and patient risk reducing measures. The method may be interpreted as an augmented bolus calculator and could easily be implemented in an insulin pump, thanks to its low computational cost.

However, simulations revealed that standard therapy does not perform well on the UVa simulator. This shows the simulator's limits, as this therapy works well on real patients. Nevertheless the UVa simulator provides some insight into how control methods perform.

5.3 Closed-loop control

5.3.1 State of the art

A detailed review of existing closed-loop control methods is not be given here, as the number of such algorithms and related simulation and clinical studies is huge. The aim of this section is rather to introduce the different available options for the design of an AP algorithm and to give examples. This will justify the choices made and the goals set for the design of the proposed control algorithms.

For a more detailed review, the interested reader is referred to recent works by Lunze et al. [2012] for a technical review, or by Bequette [2012] for a broader overview. Cobelli et al. [2011] review the past efforts in designing an AP, introduce the current projects and give an outlook on future works. Renard et al. [2013] make an update of recent progress in the development of an AP, with focus on the advances in out-patient studies.

In the following paragraphs, different aspects of closed-loop BG control are discussed and recent examples are given.

Degree of automation

According to the definition of closed-loop control in this thesis (cf. section 5.1), an AP is a device that takes control actions without previous patient interaction. Therefore, there are many different degrees of automation and complexity that define several classes of APs.

Pump suspension algorithms are probably the most simple and intuitive forms of an AP. These algorithms shut of the basal insulin infusion if certain conditions such as the passing of a low BG concentration threshold, or hypoglycemia predictions, are met. Devices with automated pump shutoff are currently on the market, and have recently been approved by the FDA. For this reason, the manufacturer, Medtronic [2013], is marketing their pump suspend algorithm as "the world's first breakthrough in Artificial Pancreas technology". This very simple solution (even though more complex variations, such as proposed by Cameron et al. [2012], for example, exist) is only a first step towards reaching the full potential of an AP.

A next degree of automation are **overnight BG controllers** that control nocturnal BG concentrations and actively administer insulin when required. BG concentrations are easier to manage overnight than during the day, as no major system disturbances occur. Overnight controllers are currently being investigated and many studies have recently been published, such as those by Elleri et al. [2011], by O'Grady et al. [2012], by Capel et al. [2013], or by Nimri et al. [2013].

A further degree in automation is reached using a full **AP with meal announcements**, meaning that insulin infusion is completely automatized and the patient only provides information on his meal intakes and, possibly, on his physical activity. As a consequence, the involvement is

the same as with a standard therapy, but the treatment quality is potentially improved. This is the most common type of AP currently investigated.

A **fully automated AP** is the last step in the development of closed-loop control. In this case, the patient does not have to take any action at all - as if he had an artificial pancreas. These controllers should eventually reproduce the functionality of a healthy pancreas and allow patients with T1DM to live their lives without the limitations of diabetes. Unfortunately, with the current limitations of the SC-SC route and its resulting time delays, the performance of a healthy pancreas cannot be reached.

Type of controller

The type of controller is an important choice to make for the design of an AP. A short overview is given below.

Proportional-Integral-Derivative (PID) controller The classical PID controller is by far the most used controller and is often applied for BG control, as well. Many PID tuning methods exist - the recent variants by Weinzimer et al. [2008], or by Lee et al. [2013] should be noted. The PID is a very simple and well-accepted controller that has a few important drawbacks, when it comes to resolving the challenges in BG control of section 1.2. Indeed, the PID controller is not well suited for systems with large time delays (1.2.6), or with control saturation (1.2.7). Additionally, the PID controller is designed for symmetric problems, which makes safe control more difficult (1.2.5) and requires robust design methods, resulting in reduced performance. However, PID controllers may give acceptable results, if appropriate feed-forward is applied and no large, unexpected BG excursions occur.

Model Predictive Control (MPC) MPC is the most promising control algorithm for the use in BG control. It allows considering constraints, saturations, asymmetric control objectives, and non-linear models. MPC has none of the drawbacks of the PID controller. This explains why MPC is currently the most used for BG controller and is implemented in various forms as illustrated by the following recent examples:

- Soru et al. [2012] use a linear unconstrained MPC using the linearized Dalla Man model
- Zarkogianni et al. [2011] use an adaptive non-linear MPC
- Grosman et al. [2011] introduce a multi-zone MPC that has a different behavior depending on the patient's glycemia
- Cameron et al. [2011] model the prediction uncertainty and use it to minimize patient risk.

With MPC, an optimization problem is solved at every sampling time. A given cost function is minimized in order to compute optimal insulin infusions. This cost function relies on model-based predictions and is generally minimized under constraints, e.g. saturation.

However, as promising as the MPC concept is, results still lag behind expectations. The main reason is the lack of appropriate prediction models - the most critical part in MPC - as will be explained below. Another drawback is that MPC is computationally expensive, and the price increases with the number of constraints, model non-linearities, and model order.

Other controllers Many other approaches are being tried for BG control, but are used much less. Examples are Error Dynamics Shaping (EDS) proposed by Cormerais and Richard [2012], fuzzy logic used by Miller et al. [2011] or partially by Zarkogianni et al. [2011], or robust methods, such as sliding mode control, as described by Abu-Rmieleh and Garcia-Gabin [2012].

Choosing the model

Almost all of the applied methods are, to some extent, model-based. Therefore, the crucial question on what model to use arises. The different available models were discussed in detail in 2.2.3. The impact of an inappropriate prediction model was experienced by Dassau et al. [2012], whose MPC only gave benign insulin infusions because of an IOB safety measure. Another example is the MPC by Soru et al. [2012] that needs therapy parameter-based feed-forward control to work properly - which contradicts the concept of the MPC. In fact, the model of an MPC should give appropriate insulin doses, even in the presence of a meal. If feed-forward is used, a much simpler controller is typically sufficient.

In some cases, the model is not identifiable on BG measurements only, or appropriate training data is not available. Population model parameters can be used in this case, or, as proposed by Soru et al. [2012], the cost function may be personalized. Considering the large inter-patient variability, these solutions are generally sub-optimal and should therefore only be used if personalized model parameters cannot be obtained.

Meal announcements

Currently, T1DM patients always need to estimate the CHO content of meals and deduce the amount of insulin to infuse. When designing an AP, one needs to decide whether the AP should do this task itself. Meal announcements go hand in hand with feed-forward control, while unannounced meals are more difficult to reject and lead to higher postprandial BG concentration peaks. If meals are not announced, meal detection algorithms (e.g. citeBoiroux2010a), or probabilistic meal predictors (e.g. Hughes et al. [2010]), can lead to better BG control. Weinzimer et al. [2008], or Campetelli et al. [2013] consider the option to infuse feed-forward insulin 15 or 60 minutes before the meal, respectively. If the ingested meal has a high GI (i.e. a fast meal), this improves results even further, but increases the risk of

hypoglycemia, if the meal is finally not taken.

Adaptive methods

Adaptive methods are used for two main different purposes, i.e. either to account for the shift in parameter values that naturally occurs over time, or to reject disturbances. The first case can be done by methods such as run-to-run (R2R), as investigated by François et al. [2003], or Daskalaki et al. [2012]. In this case, parameters only change slowly with time constants of the order of days. This is an important feature that makes frequent re-identifications of model parameters useless and improves treatment quality. However, the changes in parameters need to be closely monitored to avoid safety problems. In the second case, the time constant of parameter changes are much shorter and parameters may vary significantly in a very short time. Such a method is proposed by Turksoy et al. [2013], for instance. Zarkogianni et al. [2011] adapt MPC parameters using NN and fuzzy logic when model predictions are no longer accurate. Since parameters change in the order of minutes, it is impossible to check the validity of parameters, thus adding another risk factor to the treatment.

Controller validation

The ideal way to evaluate the performance of a controller is to do a clinical study. Some MPCs were recently tested within the context of large scale projects, such as AP@home, the iAP project, or others (Elleri et al. [2012], Dassau et al. [2012], Luijf et al. [2013]). Even the feasibility of out-patient AP use (Kovatchev et al. [2013]), or closed-loop control for T2DM (Kumareswaran et al. [2013]), is being explored. Unfortunately, most researchers do not have the funds and the expertise to do clinical studies. For this reason, the UVa simulator, described in appendix A.1, is an alternative to showcase the potential of a given control algorithm. Many simulation studies were done either on the 100- or the 10-patient population, and published. Nevertheless, these results are only an indicator for potentially good results and clinical studies are still required to validate the most promising methods.

Conclusion of the state of the art: BG control goals

Designing a controller for diabetes treatment involves making choices beforehand. In the previous section, some of the most important aspects were introduced. Considering the advantages and disadvantages of these different points, this thesis aims at finding or designing the "best" control method, based on the TPM that was specifically developed for this use in chapter 2. The controller should be able to handle scenarios with announced and unannounced meals. In other words, control should be better if a patient announces his meal, but it should remain acceptable whenever he does not. For the time being, a method with fixed parameters is considered, but can be extended to an adaptive scheme, with large time constants. As a clinical study is not possible within this small-scale project, the proposed

controllers are validated on the UVa simulator.

5.3.2 Closed-loop controllers

The different controllers that are tested on the UVa simulator, are introduced in this section. All these controllers are based on the open-loop controller TPC OL introduced in the previous sections. The core idea is that the TPC OL gives appropriate feed-forward control and adapts the setpoint accordingly. The most important insulin doses will be given by the feed-forward, and, hence, the controller should never need to take excessive control action. Thus it should only focus on setpoint tracking.

Proportional controller

The proportional controller is simple, but effective. It is a special case of the PID controller, where the integral and derivative terms are zero. The controller multiplies the tracking error by a gain K_P :

$$U_{I,corr}(s) = K_P (G_{SP}(s) - \hat{G}(s)). \quad (5.60)$$

The gain of the controller K_P is chosen as:

$$K_P = -\frac{1}{\tau \cdot K_x} \quad (5.61)$$

where K_x is the insulin sensitivity and τ is the controller time constant in minutes. This controller is depicted in figure 5.3. The controller gain is thus inversely proportional to the correction factor, i.e. the more sensitive the patient is to insulin, the less insulin will be injected. The introduction of the time constant τ is necessary to tune the aggressiveness of the controller. In fact, if the time constant is chosen to be smaller than τ_x , the closed-loop system tries to reject disturbances faster than in open-loop, which would inevitably lead to undesired BG concentration undershoots. Therefore, τ should be greater than τ_x . A value between 150 and 350 minutes should perform well and the best value can be determined manually.

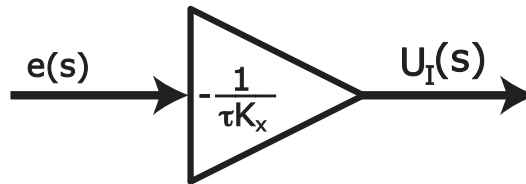


Figure 5.3: Proportional controller.

Steady-state error At this point, a question that may arise with the use of a proportional controller without an integral term (as well as the controllers presented in what follows), is

whether there is steady-state error, i.e. a difference between setpoint and BG concentration when the closed-loop system is at steady state. As explained by Longchamp [2010], steady-state error is zero, if the *type* of the open-loop system $K(s)H(s)$ is greater or equal than one. The *type* is defined as the number of integrators in the transfer function, where $K(s)$ is the transfer function of the controller and $H(s)$ is the open-loop transfer function of the controlled system. If $H(s)$ corresponds to the TPM:

$$K(s)H(s) = K_P I(s) \quad (5.62)$$

$$= -K_P \frac{K_x}{s(\tau_x s + 1)^2}, \quad (5.63)$$

which contains an integral term $\frac{1}{s}$ and, hence, there will not be any steady-state error. However, the real patient dynamics are sometimes closer to the TPM+ dynamics and in that case:

$$K(s)H(s) = -K_P \frac{K_x}{(s + S_G)(\tau_x s + 1)^2} \quad (5.64)$$

whose type is 0, potentially leading to steady-state errors. The same goes for an application on the UVa simulator that does not have integral dynamics, either. To get rid of the steady-state error, an integrator term could be added to the controller. However, this leads to decreased controller robustness and the control saturation possibly leads to integral windup. An anti-reset windup helps in the latter case, but the decreased patient safety does not justify the use of an integral term.

Finally, this approach does not eliminate the steady-state error, it, however, reduces its effect. The key is that, if feed-forward control at steady-state is set to maintain the BG concentration at the target, then steady-state error is zero at this target BG. In other words, there will be no steady-state error at the target BG, if basal insulin infusion is set to stabilize the patient at this concentration. This can easily be done on the UVa simulator through the choice of the basal rate (cf. table 5.4). For real patient data, this is more difficult as a physician needs to tune the basal rate, or it can be set by more complex methods, such as R2R proposed by Palerm et al. [2008].

Therapy Parameter-based Controller (TPC)

Concept description The TPC is a new control algorithm that is directly inspired by standard therapy and, more specifically, by the concept of the corrective bolus. In standard therapy, at certain times, such as before meals, BG concentration is measured and, according to the difference to the target BG, corrective insulin $U_{I,corr}(t)$ is administered. As described in section 2.3.2, this corrective bolus is computed as:

$$U_{I,corr}(t) = \frac{e(t)}{K_x}, \quad (5.65)$$

where e is the difference between the setpoint and the measured BG. The idea of the TPC is to apply this treatment, not only at specific times, but at every sampling time (or continuously). In other words this leads to a proportional controller with gain $\frac{1}{K_x}$. Of course, the application of this controller can be dangerous:

- The controller gain is large compared to other PID controllers. This will most likely lead to BG concentration undershoots.
- Negative insulin boluses are only possible to a very limited extent, depending on the basal insulin infusion. Larger negative boluses cannot be administered and control needs to avoid any BG concentration undershoots to maintain patient safety.
- This controller does not account for the time delays (~ 20 min) in insulin action. This can lead to insulin stacking, where full correction boluses are given despite active insulin being on board. This is a serious issue, even for patients following standard therapy, and is unacceptable for the described controller.

To prevent this insulin stacking, the TPM allows estimating by how much BG concentration is expected to drop, using the IOB introduced in 5.2:

$$IOB(s) = \frac{\tau_x^2 s + 2\tau_x}{(\tau_x s + 1)^2} U_I(s) \quad (5.66)$$

The transfer function to compute IOB is defined as:

$$H_{IOB}(s) = \frac{\tau_x^2 s + 2\tau_x}{(\tau_x s + 1)^2}. \quad (5.67)$$

Now, to obtain the TPC, the computed insulin amount is reduced by the amount of active insulin:

$$U_I(s) = \frac{e(s)}{K_x} - H_{IOB}(s)U_I(s) \quad (5.68)$$

$$(1 + H_{IOB}(s))U_I(s) = \frac{e(s)}{K_x} \quad (5.69)$$

$$U_I(s) = \frac{e(s)}{K_x(1 + H_{IOB}(s))}. \quad (5.70)$$

The TPC, which is depicted in figure 5.4, can also be interpreted as a closed-loop version of the TPC OL that is evaluated at specified sampling times. The estimation of the current BG may come directly from the CGM device, or may be filtered by the TPF, depending on what information is available. IOB can be estimated using the TPF and equation 5.71, which results in an estimate that is corrected by CGM measurements.

$$IOB(s) = \tau_x(\hat{X}(s) + \hat{X}_1(s)), \quad (5.71)$$

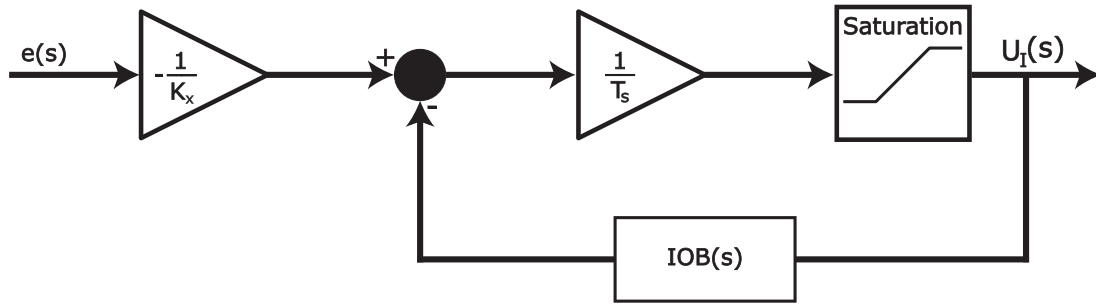


Figure 5.4: The TPC.

where the hat indicates that values are estimated by the TPE. Nevertheless, in this thesis, IOB is estimated in open-loop, i.e. by integrating equation 5.66. This is considered to be safe, as this prevents unmodeled dynamics or CGM dropouts from having an effect on the safety-critic IOB estimate.

Note that, as represented in figure 5.4, the computed insulin dose that is the difference between the corrective insulin and the insulin on board, need to be divided by the sampling time T_s in order to transform the required bolus into an insulin infusion rate.

One of the main advantages of the TPC is that it does not require any manual tuning. The two only parameters, K_x and τ_x can reliably identified using the TPM.

It is necessary to put the saturation directly into the controller in order to have correct IOB estimations. It should be remarked that the IOB value may be negative, in the case where insulin infusions are lower than the basal rate. This has the consequence that the controller shows less overshoots when recovering from low BG concentrations than a pump suspension algorithm.

Wang et al. [2010] proposed a similar approach combined with a meal detection algorithm, while León-Vargas et al. [2013] proposed to use IOB in combination with a PD controller and an adaptive scheme.

Meal rejection The TPC may be used with or without meal announcements. In the absence of meal information, the TPC is applied as such, but if information is available, feed-forward control and setpoint adaptation (described in section 5.2.2) can be used. This adds two parameters (K_g and a_g) to the controller, for each considered type of meal. There is also the option of using meal detection algorithms (Boiroux et al. [2010b]).

Comparison with classical PID control The TPC has some very interesting properties that a classical PID controller is unable to obtain. The main advantage of the TPC is that it gives a relatively aggressive first bolus and stays defensive afterwards. As a consequence, this

controller is perfectly suited for rejecting unannounced meals with relatively small reaction times. The PID, on the other hand, needs to be tuned robustly, because it is prone to large oscillations otherwise. As a consequence, PID controllers always react slowly to perturbations such as meals, and, thus, performance is considerably reduced.

However, as there is always a compromise between performance and robustness, the TPC also has some disadvantages. The TPC manages the rejection of real perturbations very well, but is sensitive to sensor noise. This means that, if a CGM is used, there is a risk that the controller gives too much insulin if there is a short spike in CGM readings. This is mostly benign except when the patient already has a relatively low BG concentration. However, the impact of this drawback may be reduced using good CGM filters and possibly two CGM devices simultaneously, as it has been proposed in recent studies (Kovatchev et al. [2013], for example).

If the TPC is still too aggressive, several measures can be taken:

- K_x can be increased.
- τ_x can be increased.
- The lower 95% confidence estimate of the BG concentration can be used instead of the estimated average BG.

5.3.3 Evaluation using the UVa simulator

Implementation

The implementation of the TPC is the same as for the TPC OL given in 5.2.4, with the exception that it is generally sampled with $T_s = 5$ minutes and uses CGM measurements. The analyzed scenario is described in E.1 and is used as a nominal scenario on which all available controllers are evaluated and compared.

The sampling time was chosen, because this is the most used value in control-related published works. However, considering the dominant time constant, this choice might not be the best: because CGM measurements are noisy with frequencies higher than the glucoregulatory system cutoff frequency, measurement noise is not filtered and leads to a noisy input signal. In control theory, the sampling frequency ω_s is chosen such that $10\omega_0 < \omega_s < 20\omega_0$, where ω_0 is the closed-loop system's cutoff frequency (Longchamp [2010]). When considering the sampling period T_s this can be written as $\frac{\tau_{CL}}{3.2} < T_s < \frac{\tau_{CL}}{1.6}$, where τ_{CL} is the closed-loop time constant. τ_{CL} is expected to be close to, or larger, than the TPM's fastest time constant, i.e. the minimum of τ_x and τ_g . According to table 5.1, this should be around 20 minutes on clinical study parameters and, according to table 5.3, around 15 minutes on the UVa simulator. These values may need to be adapted for each patient.

To compare the different controllers, the BGRI (defined in appendix B.4) and the percentage

of time spent in hypo- an normglycemia (as specified in appendix B.6) are provided. Average values are given with and without adult 9. In fact, for some controllers, this subject becomes unstable and suffers from irreversible hypoglycemia. Since this adult is often considered as an outlier, results are more meaningful if this subject is discarded.

Tested controllers

The seven following controllers (described in section 5.3.2) are evaluated with the UVa simulator. The implementation scheme is given in figure 5.5, where the "Controller", and "Filter" blocks are modified according to the chosen controller configuration.

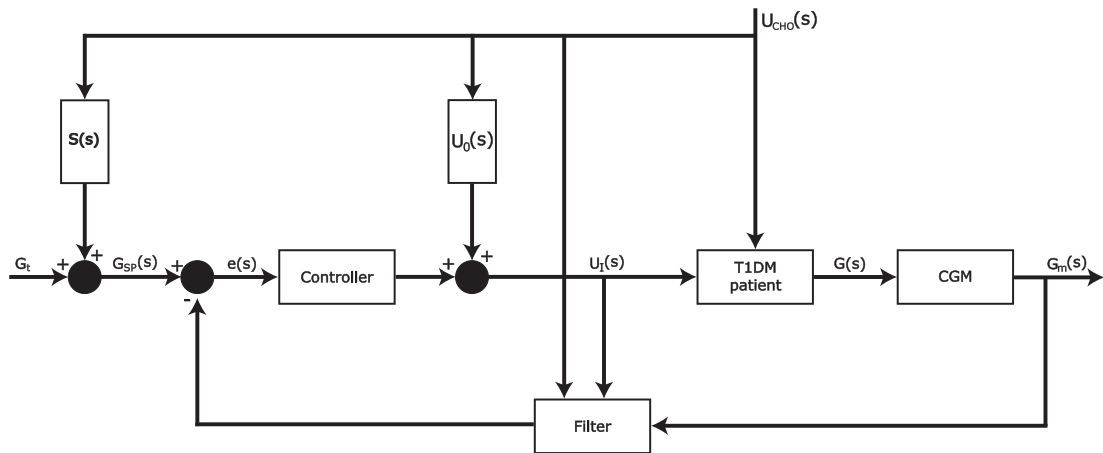


Figure 5.5: Closed-loop controller with announced meal and filter.

- **P** - proportional controller with announced meals and unfiltered CGM data.
- **P TPF** - proportional controller with announced meals. CGM data is filtered by the TPF (described in section 4.3.5).
- **TPC** - TPC with announced meals and unfiltered CGM data.
- **TPC KF** - TPC with announced meals. CGM data is filtered by the KF (described in section 4.3.3).
- **TPC TPF** - TPC with announced meals. CGM data is filtered by the TPF (described in section 4.3.5).

When meals are not announced, the complete controller can be represented as in figure 5.6. This time, only the "Controller" block needs to be changed to correspond to the different controller variants.

- **P NM** - P with No Meals announced. CGM data remains unfiltered.

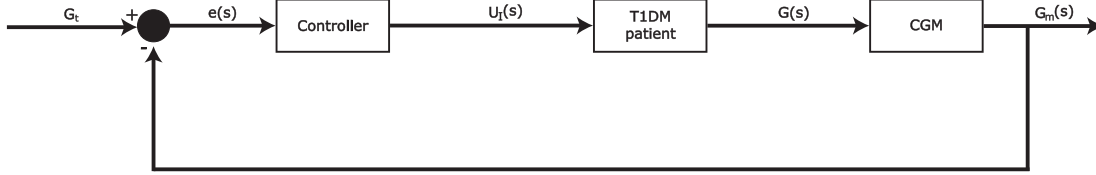


Figure 5.6: Closed-loop controller without meal announcement.

- **TPC NM** - TPC with No Meals announced. CGM data remains unfiltered.

Determination of τ for the P controller

A first step is to find the best value of the time constant τ , used for the P controller. Several values for τ are tested on the simulator and compared using the percentage of time spent in different regions and the BGRI.

Adult 9 was excluded when calculating the BGRI, because his treatment significantly improved with increasing τ , which is in contradiction with all the other patients. This did not influence the time spent in different regions much.

The value for τ is chosen equal to 250 minutes because it gives consistently good results, as illustrated in figure 5.7.

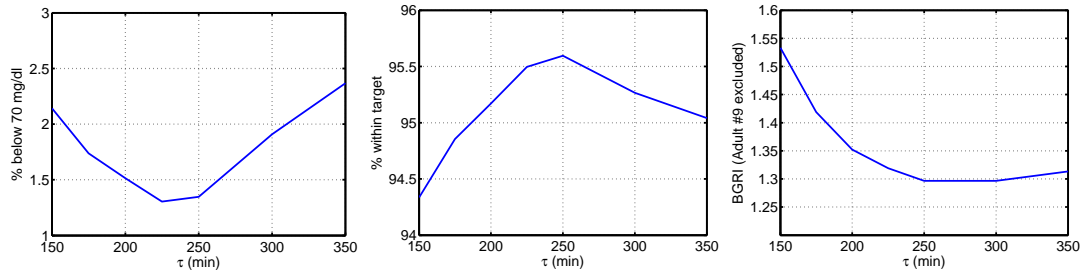


Figure 5.7: Averages of different metrics as a function of τ .

Announced meals

First, the controllers are compared when meals are announced. Results are given in tables 5.6, 5.7, and 5.8. The OL has a considerably higher BGRI than all there controllers and the time spent in target is relatively low. Hence, it can be concluded that all controllers perform better than the default open-loop controller provided within the UVa simulator. P gives respectable results, considering its very simple nature, but surprisingly, the addition of a CGM filter does not lead to a lower BGRI. The different TPC variants give the best results on all metrics, except for time spent in hypoglycemia, even if this time is extremely low. Adding a CGM filter the TPC leads to excellent results. Several remarks are in order:

- The time spent in hypoglycemia is higher when using the designed controllers, compared to standard open-loop control, while time in target is higher. This means that hyperglycemia was significantly reduced. If time in hypoglycemia needs to be reduced, an increased setpoint value can be used.
- Out of the 10-adult population, several patients are more difficult to control:
 - Most of the time, Adult 9 is unstable. This is caused by the highly unusual dynamics of this individual, characterized by a very large second postprandial peak in BG concentrations, as can be observed in figure 5.8 at midnight. This problem could be solved if a different meal model was used for computing the setpoint adaptation. For instance, a double peak model with higher order could be fitted to the measurements.

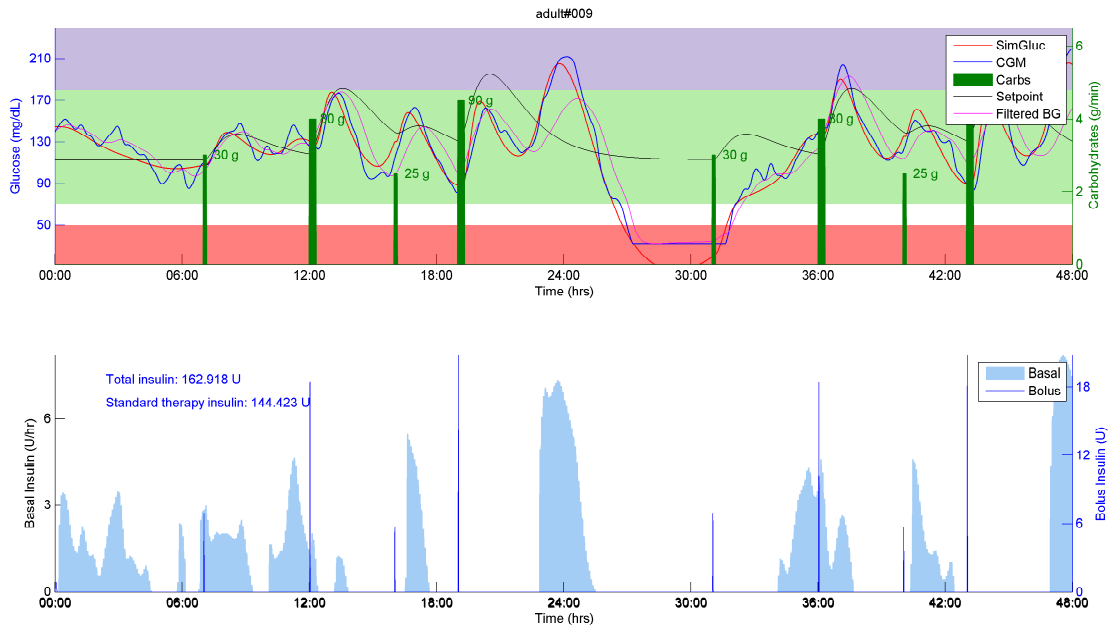


Figure 5.8: Results for Adult 9 on nominal scenario with TPC TPE

- Adult 1 also has a double-peak meal response similar to Adult 9. However, in this case, this second peak is smaller and would normally not lead to bad results. For Adult 9, the second peak coincides with a very unfavorable CGM reading, which amplifies the second peak such that it leads to an insulin injection. The combination of these circumstances leads to mild nocturnal hypoglycemia. Since the same seed was used for all CGM noise simulations, the unfavorable CGM measurements will be found for all the investigated controllers at this time.

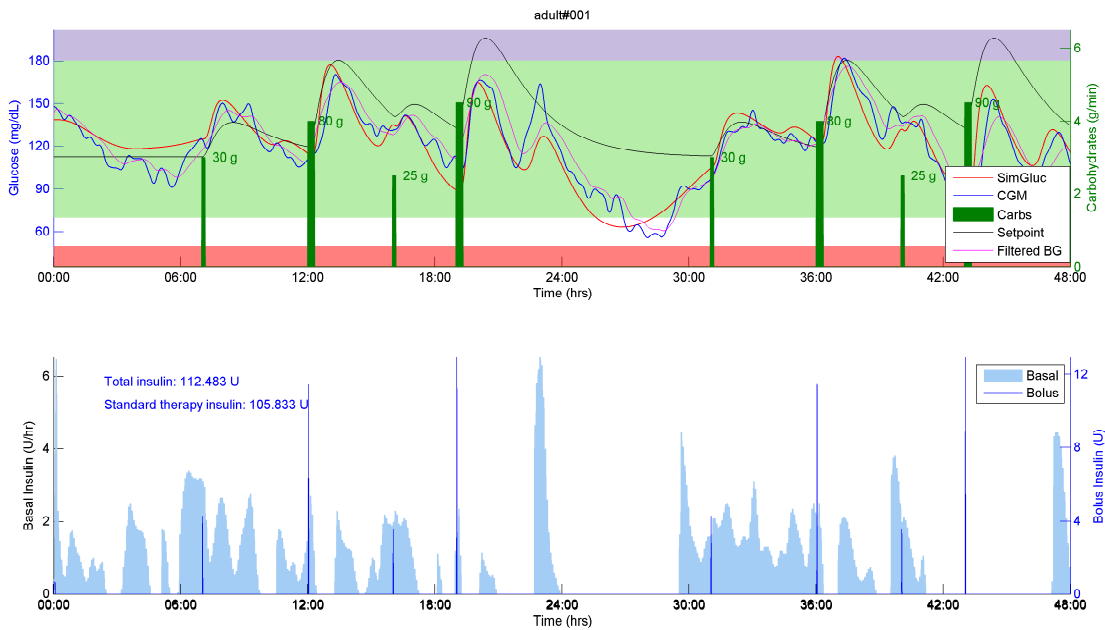


Figure 5.9: Results for Adult 1 on nominal scenario with TPC TPE.

Adult	OL	P	P EKF	TPC	TPC KF	TPC EKF
1	3.14	2.22	2.3	2.64	1.84	1.77
2	1.41	0.82	1.3	0.89	0.60	0.57
3	1.41	1.06	1.05	0.89	0.89	0.86
4	1.90	1.24	1.39	1.00	0.94	0.95
5	1.29	1.01	0.74	0.74	0.69	0.68
6	2.80	1.81	1.69	1.08	1.07	1.06
7	1.19	1.20	1.19	0.39	0.50	0.51
8	1.33	0.57	0.69	0.86	0.62	0.59
9	4.33	6.24	6.21	889.70	1509.33	16.94
10	3.08	1.74	1.71	1.51	1.48	1.47
Av.	2.19	1.79	1.83	89.97	151.80	2.54
Av. No 9	1.95	1.30	1.34	1.11	0.96	0.94

Table 5.6: Comparison of BGRI for all adults on nominal scenario.

5.3. Closed-loop control

Adult	OL	P	P EKF	TPC	TPC KF	TPC EKF
1	92.85	94.31	92.99	89.66	93.13	93.61
2	100	100	94	100	100	100
3	100	98.47	98.58	100	100	100
4	91.7	93.61	93.93	94.79	94.52	94.52
5	100	98.72	100	100	100	100
6	89.93	96.49	94.59	100	100	100
7	100	100	100	100	100	100
8	100	100	100	100	100	100
9	83.17	79.07	81.99	51.82	51.68	81.85
10	88.23	95.28	96.11	97.36	97.67	97.95
Av.	94.59	95.60	95.22	93.36	93.70	96.79
Av. No 9	95.86	97.43	96.69	97.98	98.37	98.45

Table 5.7: Comparison of % within target for all adults on nominal scenario.

Adult	OL	P	P EKF	TPC	TPC KF	TPC EKF
1	0	1.28	4.76	9.55	6.07	5.62
2	0	0	6	0	0	0
3	0	0	0	0	0	0
4	0	0	0	0	0	0
5	0	0	0	0	0	0
6	0	2.08	5.41	0	0	0
7	0	0	0	0	0	0
8	0	0	0	0	0	0
9	8.64	10.1	10.03	46.03	45.44	12.08
10	0	0	0	0	0	0
Av.	0.864	1.35	2.62	5.56	5.15	1.77
Av. No 9	0	0.37	1.80	1.06	0.67	0.62

Table 5.8: Comparison of % below target for all adults on nominal scenario.

Unannounced meals

The ultimate goal of an AP is to be completely autonomous and to rely on no user input, like meal announcements. For this reason, the controllers are also tested without meal announcements, which makes the problem more challenging. In this case, results cannot be compared to standard therapy, since the latter relies on meal announcements. Also, the previously used CGM filters cannot be used anymore, because they rely on meal announcements, too. An option to explore then is to use meal detection algorithms. Comparative results are given in table 5.9, and an example of a typical BG concentration profile is given in figure 5.10.

As expected, BG excursions are bigger. However, the TPC performs much better than the P controller now, while the difference was less pronounced in the case announced meals. This illustrates that a PID controller requires a good feed-forward control, and that the TPC has excellent meal rejection properties, even when meals are not announced. Also, for the TPC, time spent in hypoglycemia is barely more elevated when meals are not announced than when they are. This shows the TPC's good safety properties with respect to unexpected perturbations.

Adult	BGRI		% in tar		% below tar	
	P NM	TPC NM	P NM	TPC NM	P NM	TPC NM
1	4.79	4	78.31	81.05	10	10.59
2	3.02	1.66	84.24	96.63	0	0
3	5.21	2.12	67.65	89.07	4.58	0
4	7.46	3.49	69.7	85.21	0	0
5	4.25	1.96	81.53	89.55	0.66	0
6	9	5.29	54.15	76.36	6.56	0
7	4.47	1.95	75.49	88.79	1.74	0
8	1.71	1.18	100	100	0	0
9	19.14	746.51	48.91	45.89	12.08	46.06
10	6.86	4.13	59.46	77.72	5.8	4.13
Av.	6.59	77.23	71.94	83.03	4.14	6.08
Av. No 9	5.20	2.86	74.50	87.15	3.26	1.64

Table 5.9: Results of the nominal scenario without meal announcements comparing the proportional controller (P NM) and the TPC (TPC NM).

Increased sampling time

Previously, it was deduced that a sampling time of 15 minutes should be appropriate on the UVa simulator. A comparison between previous results with $T_s = 5$ and simulations with $T_s = 20$ minutes is given in table 5.10. It shows that increasing the sampling time from 5 to 20 minutes has a negligible effect on BG control quality. Since 20 minutes is more than the required 15 minutes, results show that the TPC is robust, even when the measurements are slightly under-sampled.

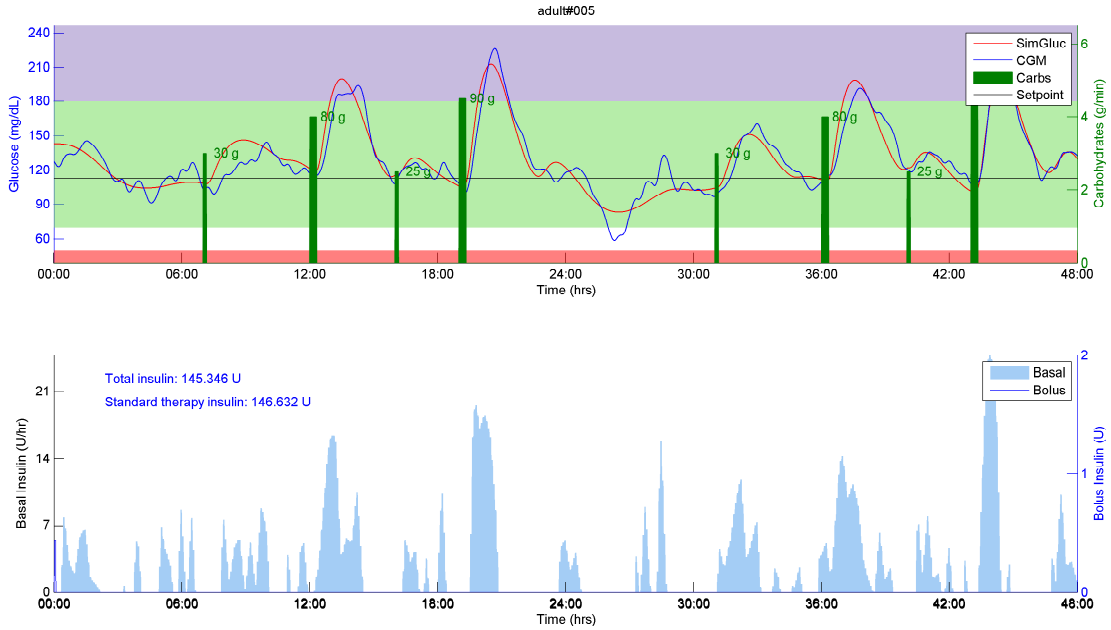


Figure 5.10: Example of a BG concentration profile for adult 5 on the nominal scenario with the TPC NM (unannounced meals).

Nevertheless, for the sake of comparison, T_s is kept equal to 5 minutes since this is, again, the most used value in the literature.

5.3.4 Comparative study

The UVa simulator is used by a number of researchers to assess the performance of their closed-loop controllers. Unfortunately, comparisons are difficult to perform for the following reasons:

- Even though Patek et al. [2009] published some guidelines, unfortunately, the use of the UVa simulator is not standardized and everyone uses different scenarios.
- Two different versions of the simulator exist: one with 300 subjects and one with 30 subjects, each composed to equal parts of adults, children and adolescents. The 300 subject simulator is not available for everyone and is reserved mainly for the iAP consortium. As a consequence, their results cannot be compared to others in a fair way.
- It is common that the 30 subject simulator is customized, in order to introduce circadian variations, for example. This allows testing the robustness of a controller, but makes fair comparisons impossible.

Finally, only seven publications that use the 10 adults of the unmodified 30-subject simulator can be found so far. However, for four of these seven publications, those by the Doyle group, a

Adult	BGRI		% in tar		% below tar	
	$T_s = 5$	$T_s = 20$	$T_s = 5$	$T_s = 20$	$T_s = 5$	$T_s = 20$
1	1.77	1.81	93.61	93.13	5.62	6.07
2	0.57	0.66	100	100	0	0
3	0.86	0.92	100	100	0	0
4	0.95	0.96	94.52	94.52	0	0
5	0.68	0.67	100	100	0	0
6	1.06	1.12	100	100	0	0
7	0.51	0.63	100	100	0	0
8	0.59	0.59	100	100	0	0
9	16.94	17.77	81.85	81.43	12.08	12.25
10	1.47	1.49	97.95	98.85	0	0
Av.	2.54	2.66	96.79	96.79	1.77	1.83
Av. No 9	0.94	0.98	98.45	98.50	0.62	0.67

Table 5.10: Results for the TPC TPF on the nominal scenario with announced meals but different controller sampling times.

simulator with different subjects than the version used in this thesis seems to have been used. Results are very bad compared to other publications, and the difficult patients, identified above, do not coincide. For this reason, these works were not considered (see appendix D).

In the end, three publications with plausible results were kept, for which comparisons are discussed in this section.

Zarkogianni controller

Zarkogianni et al. [2011] propose the Insulin Infusion Advisory System (IIAS), which is based on a non-linear MPC. They use a hybrid model, composed of two compartmental models for SC insulin kinetics and gut glucose absorption, respectively, and recurrent NN to combine them with CGM measurements. The cost function penalizes hyper- and hypoglycemia, while parameters are tuned on-line using an adaptive fuzzy logics-based approach.

Detailed specifications of the scenario are given in E.2. The simulated results are given in tables 5.11 and 5.12. The default open-loop control implemented in the UVa simulator is given as well and allows verifying that identical UVa simulator versions were used.

Accurate meal announcement As a first experiment, the controller is tested with accurate meal announcements. When comparing the three TPC variants, it can be observed that results improve with the complexity of the CGM filter. This is illustrated by the value of the time spent within the different zones and the risk indexes, but also by the reduced standard deviations.

When comparing the best variant of the TPC to the IIAS, results are mostly on par. Only the average BGRI is a clearly better with the TPC. This is due to the BG concentrations being closer

to the target BG for a longer time, which can also be deduced from the reduced standard deviations of mean BG concentrations.

As expected, open-loop control is inferior to the closed-loop methods.

Meal overestimated by 40% Zarkogianni et al. demonstrate their controller's robustness to meal estimation errors by overestimating meals by 40%. Results for the TPC TPF, where the announced meal is 1.4 times the actual meal, are given for comparison. In this case, as expected, the TPC TPF has a lower mean BG concentration, because more insulin was injected at meal time. The TPC TPF can effectively reject such mismatches.

The results for the IIAS are very good, but are less intuitive. Against expectations, mean BG is increased, while pre- and post-meal BG concentrations are lowered compared to exact meal announcements.

Meal underestimated by 40% Zarkogianni et al. also simulated the case where meal announcements are underestimated, i.e. only 60 % of the actual meal is announced. Results for the TPC TPF are excellent, and, as expected mean BG concentrations are bigger than for the correct announcements. As a consequence, the time spent in hypoglycemia is reduced, while time in hyperglycemia is slightly increased.

Results for the IIAS are inferior to the TPC EKF, and characterized by an increase in hypo- as well as hyperglycemia. As a consequence, most other metrics give worse, but acceptable results.

Conclusion The TPC generated slightly better control results than the IIAS despite being considerably simpler and computationally more efficient. If BG concentrations below target should be avoided, the setpoint of the TPC may be increased. However, when meal announcements were underestimated, the IIAS showed some weaknesses, while the TPC TPF could successfully cope with both, under- and overestimation.

It should be noted that Zarkogianni et al. compared their results to those by Wang et al. [2009] and those by Grosman et al. [2010]: These were added to the comparisons in appendix D.

Cameron controller

Cameron et al. [2011] have developed the Extended MPC (EMPC) that explicitly minimizes the risk of hypo- and hyperglycemia by estimating BG prediction uncertainty. A complex multi-model approach was developed to detect meals and to predict BG concentrations and uncertainty. The cost function depends directly on a risk, computed using the uncertainty and a newly defined risk function, close to the one introduced by Kovatchev et al. [2000].

	Mean BG	Pre meal BG	Post meal BG	% below target
Correct				
TPC	114.72 (6.17)	109.46 (9.08)	128.53 (11.31)	2.64 (5.16)
TPC KF	115.62 (5.38)	109.85 (9.52)	130.30 (9.98)	1.79 (3.94)
TPC TPF	115.83 (5.36)	110.07 (9.56)	130.55 (9.91)	1.57 (3.64)
IHAS	112.25 (9.06)	114.27 (12.31)	139.78 (9.19)	0 (0)
Open-Loop	130.50 (6.92)	124.4 (6.65)	145.16 (10.8)	1.14 (3.61)
40% over				
TPC TPF	107.67 (6.11)	103.03 (10.32)	119.73 (9.81)	3.85 (5.1)
IHAS	117.54 (7.91)	105.57 (8.99)	132.26 (12.68)	1.01 (1.51)
40% under				
TPC TPF	124.28 (5.85)	115.98 (9.59)	141.45 (11.62)	1.37 (3.28)
IHAS	120.28(10.61)	110.11 (11.13)	137.44 (14.3)	5.15 (5.07)

Table 5.11: Simulation results by Zarkogianni et al. compared to the TPC. Part 1. The mean value is given and the standard deviation is given in parentheses.

	% above tar	% within tar	LBGI	HBGI	BGRI
Correct					
TPC	0.68 (1.36)	96.69 (5.08)	1.06 (1.82)	0.53 (0.29)	1.59 (1.89)
TPC KF	0.73 (1.40)	97.48 (4.08)	0.68 (0.95)	0.56 (0.31)	1.24 (1.11)
TPC TPF	0.74 (1.39)	97.69 (3.83)	0.61 (0.78)	0.57 (0.31)	1.17 (0.95)
IHAS	2.51 (2.76)	97.49 (2.76)	0.35 (0.35)	1.09 (0.64)	1.45 (0.66)
Open-Loop	3.68 (3.78)	95.17 (5.59)	0.30 (0.48)	1.65 (0.71)	1.96 (0.91)
40% over					
TPC TPF	0.27 (0.82)	95.88 (5.06)	1.46 (1.44)	0.34 (0.20)	1.80 (1.47)
IHAS	2.4 (3.13)	96.58 (2.83)	0.72 (0.34)	0.92 (0.62)	1.64 (0.66)
40% under					
TPC TPF	2.05 (3.10)	96.58 (4.69)	0.40 (0.56)	1.12 (0.55)	1.51 (0.92)
IHAS	4.36 (4.43)	90.48 (6.66)	0.99 (0.41)	1.27 (0.86)	2.26 (1.1)

Table 5.12: Simulation results by Zarkogianni et al. compared to the TPC. Part 2. The mean value is given and the standard deviation is given in parentheses.

Cameron et al. compare their EMPC to a classical MPC and a PID controller. Additionally, they give an optimized basal/bolus (BB) insulin injection that was found using retrospective optimization. Hence, BB is considered an upper limit in possible performance.

Adult 9, who already caused inconsistent results on the nominal scenario, was discarded by Cameron et al. as an outlier with unlikely dynamical properties, and was not used for analysis.

They also use a modified BGRI, proposed by Magni et al. [2007], which they consider more relevant for control purposes. To be able to perform comparisons, the same metric is adopted here (detailed in B.4), for this scenario, only.

The comparisons of the controllers tested by Cameron et al. and the TPC NM (meals are not announced in the Cameron scenario) are given in tables 5.13 and 5.14. When considering the average percentage of time spent in the different regions, the TPC NM performs very well, surpassing all controllers used by Cameron et al. and the % within target almost reaches the level of BB. However, because different risk indexes were used, TPC NM performance is inferior to the EMPC in terms of BGRI. This is due to the fact that the modified BGRI is 0 for a BG concentration of 140 mg/dl but the target BG of the TPC NM is set to 112.5 mg/dl. For this reason, the target BG was raised to 140 mg/dl (though basal insulin was left unchanged). This reveals to be a drastic increase, because, even if the modified BGRI is lower for the TPC NM $G_t = 140$ than for the EMPC, percentages of time spent in different regions are worsened. As a compromise, a value with a target BG concentration of 125 mg/dl was tried and it surpassed the EMPC for all considered metrics.

controller	mean BG	pre meal BG	% bel tar	% bel 50mg/dl	% within tar
PID	156	142	0	0	72.6
MPC	151	135	0.15	0	79.4
EMPC	147	135	0.7	0	84.3
BB	140	127	0	0	92
TPC NM	134	131	0.14	0	90.3
TPC NM $G_t = 125$	142	139	0	0	85.2
TPC NM $G_t = 140$	153	150	0	0	78.6

Table 5.13: Simulation results by Cameron et al. compared to the TPC NM. Part 1.

controller	LBGI (mod)	HBGI (mod)	BGRI (mod)	BGRI
PID	0.61	2.38	2.99	N/A
MPC	1.19	1.86	3.05	N/A
EMPC	1.1	1.41	2.51	N/A
BB	0.49	0.78	1.27	N/A
TPC NM	2.06	0.90	2.96	2.58
TPC NM $G_t = 125$	1.10	1.31	2.41	3.23
TPC NM $G_t = 140$	0.45	1.99	2.44	4.39

Table 5.14: Simulation results by Cameron et al. compared to the TPC NM. Part 2.

Cormerais controller

Cormerais and Richard [2012] apply EDS to the BMM and validate it on the UVa simulator. EDS is a nonlinear state feedback method that is based on the idea of imposing certain dynamic properties to the error. The BMM was identified on UVa simulator-generated training data. One parameter, the aggressiveness of the controller, needs to be tuned manually, and additionally, the target BG concentration is manually adjusted to obtain improved results. All of these values are set using a "trial and error procedure" through different tests on the simulator that would as well be applicable to a real patient, without endangering him. The proposed controller does not need any meal announcements. However, it is unclear how all the necessary state estimations are performed.

Cormerais and Richard use two different scenarios to demonstrate their controller's abilities: a 1 day and a 7 day scenario.

1 day scenario This scenario is defined in appendix E.4 and is composed of a single day with 3 typical meals. Results are in tables 5.15 and 5.16. The TPC NM shows lower averaged performance for all given metrics. Since the pre-meal BG concentration is about the same for both controllers, but the post-meal BG concentration is much higher, the main difference lies within the meal rejection capabilities of both controllers. Considering that meals are not announced, EDS results are outstanding. In order to obtain comparable post-meal and maximum BG concentrations, the target BG concentration of the TPC NM was reduced to 100mg/dl. However, in this case, the risk of hypoglycemia increases.

	mean BG	pre m BG	post m BG	% bel tar	% ab tar	% bel 50mg/dl
Cormerais	126.58	104.21	164.52	0.0	4.3	0.0
TPC NM	130.02	104.67	181.84	0.5	8.7	0.0
TPC NM $G_t = 100$	119.87	94.19	169.52	1.9	6.0	0.0

Table 5.15: Simulation results by Cormerais and Richard compared to the TPC on the 1 day scenario. Part 1.

	% within tar	LBGI	HBGI	BGRI	min BG	max BG
Cormerais	95.7	0.11	1.45	1.56	91.1	187.7
TPC NM	90.8	0.24	2.11	2.35	83.1	202.8
TPC NM $G_t = 100$	92.1	0.57	1.43	2.00	74.9	189.6

Table 5.16: Simulation results by Cormerais and Richard compared to the TPC on the 1 day scenario. Part 2.

7 day scenario This second scenario is designed to show the robustness of EDS with respect to meal variability. The meal amounts and meal times are randomly modified and meals of up to 120g of CHO are ingested. This puts an increased strain on the tested controllers and, as shown in tables 5.17 and 5.18, leads to higher BGRI values. In this case, the different versions

5.3. Closed-loop control

of the TPC NM show an important deficiency, caused again by adults 9 (that was manually tuned in EDS to be stable). For this reason, averaged metrics where adult 9 was not considered are compared in tables 5.19 and 5.20. In this case, results for the TPC NM are acceptable, but still inferior to EDS that allows very narrow BG control.

	7 days	mean BG	pre m BG	post m BG	% bel tar	% ab tar	% bel 50mg/dl
Cormerais		124.63	104.82	165.64	0.00	6.63	0.00
TPC NM		118.69	98.72	170.68	9.54	9.89	7.08
TPC NM $G_t = 100$		108.73	89.00	159.54	13.13	7.08	7.33

Table 5.17: Simulation results by Cormerais and Richard compared to the TPC on the 7 day scenario. Part 1.

	7 days	% within tar	LBGI	HBGI	BGRI	min BG	max BG
Cormerais		93.37	0.35	1.59	1.94	75.57	232.25
TPC NM		80.57	110.48	2.12	112.60	58.10	249.59
TPC NM $G_t = 100$		79.80	100.80	1.53	102.33	50.98	237.30

Table 5.18: Simulation results by Cormerais and Richard compared to the TPC on the 7 day scenario. Part 2.

	7 days no 9	mean BG	pre m BG	post m BG	% bel tar	% ab tar	% bel 50mg/dl
Cormerais		123.18	102.48	165.48	0.00	6.09	0.00
TPC NM		127.44	105.52	183.99	2.75	10.56	0.05
TPC NM $G_t = 100$		116.75	95.10	171.98	6.48	7.59	0.31

Table 5.19: Simulation results by Cormerais and Richard compared to the TPC on the 7 day scenario with adult 9 excluded. Part 1.

	7 days no 9	% within tar	LBGI	HBGI	BGRI	min BG	max BG
Cormerais		93.91	0.35	1.46	1.82	75.94	230.82
TPC NM		86.69	0.76	2.26	3.02	64.56	252.63
TPC NM $G_t = 100$		85.92	1.54	1.63	3.16	56.66	239.97

Table 5.20: Simulation results by Cormerais and Richard compared to the TPC on the 7 day scenario with adult 9 excluded. Part 2.

EDS conclusion EDS is a very promising control strategy for the use on the UVa simulator. Performance metrics show irreproachable results. Compared to the well-performing TPC NM, EDS has the drawback of needing manual parameter tuning that requires expert knowledge and a trial and error approach. Additionally, it is based on the BMM that was shown to have inappropriate dynamics for the use in real patients, so EDS performance would need to be validated in a clinical setting.

5.4 Outlook on sTPM-based BG control

The TPC, based on the deterministic TPM, shows promising results on the UVa simulator, but several sTPM-based control methods and applications have the potential to improve diabetes treatment even further. These approaches are shortly introduced, but not covered in detail in this thesis.

5.4.1 Pump suspension

The sTPM introduces the possibility to monitor the uncertainty of the BG concentration on top of simple BG predictions. This can be put to good use in the context of pump suspension algorithms. The recently FDA-approved algorithm by Medtronic [2013], for example, suspends the insulin pump if the BG concentration passes a predefined threshold. Because of the important delays in the system (cf. 1.2.6) this preventive action may occur too late and hypoglycemia may occur, even though to a lesser extent. Model predictions could thus be used to predict and avoid future hypoglycemia by acting before its occurrence (Cameron et al. [2012]). The sTPM allows adding an additional layer to such a suspension algorithm by predicting the risk of hypoglycemia, instead of the simple prediction of the most likely BG concentration. The TPF would be an ideal candidate to give such predictions, although the algorithm that defines the needed actions still has to be developed.

5.4.2 Open-loop optimal control using sTPM

In section 5.2, the optimal feed-forward control for meal disturbance rejection has been designed. However, if the additional uncertainty information provided by the sTPM was taken into account, the optimal feed-forward control would change, depending on the chosen cost function. To solve this problem, an optimization would need to run after each SMBG measurement in order to compute the optimal insulin infusion (Prud'homme et al. [2011]). For example, good results would be expected by minimizing the cost function J_{sTPM} on a control and prediction horizon h_c :

$$J_{sTPM}(U_I) = \sum_{k=0}^{N_c} (kov(\overline{G}(k, U_I)) + kov(\underline{G}(k, U_I))), \quad (5.72)$$

where N_c is the number of samples within h_c , kov is the Kovatchev risk function given in appendix B.4, \overline{G} is the estimated upper 95% confidence limit, \underline{G} is the estimated lower 95 % confidence limit, and U_I is the insulin infusion profile. This cost function would ensure that the patient's risk is minimal. If uncertainty would be zero, the method would impose a target BG of 112.5 mg/dl, while this value would increase with uncertainty.

5.4.3 MPC using sTPM

Just like the TPC is a regularly sampled version of the TPC OL, an MPC is a regularly sampled version of open-loop optimal control. This means that the open-loop optimal control method using the sTPM, described in the previous paragraph, can be generalized to give an MPC based on the sTPM. This stochastic Therapy Parameter-based Controller (sTPC) would explicitly minimize the patient risk in a similar way as Cameron et al. [2011] and improve safety, compared with the TPC.

5.4.4 SMBG measurement reminder

The sTPM provides a quality evaluation for BG predictions. This property can be used for a SMBG measurement reminder. If the confidence in predictions gets too low, the patient could be asked to take a SMBG measurement. A drawback of such a method is that, if a patient's parameters are prone to be relatively uncertain, these reminders may be given at a high frequency, which may be annoying for the patient. However these frequent measurements could be used to update the model parameters, thus reducing the number of future reminders.

This idea can be extended using CGM measurements: the TPF can be run to update uncertainties and, when CGM measurements start falling outside the confidence region, a new calibration SMBG measurement can be requested.

5.4.5 Meal and fault detection

A CGM device, in combination with the TPF, can be used for detecting unexpected BG measurements. If stochastic model predictions do not coincide with the CGM measurements anymore, the patient may, for example, have taken a meal, have been doing some exercise, or have a problem with his insulin pump, or CGM device. Detecting unannounced meals, and reminding patients to announce them, may lead to improved BG control as suggested by the results of section 5.3.3.

5.5 Conclusion

The new TPM equations were used to construct an optimal open-loop control strategy that allows keeping BG concentrations as close to the target BG as possible. The resulting TPC OL adds three features to conventional standard therapy:

- Feed-forward for meal disturbance rejection.
- Setpoint adaptation in case a meal disturbance cannot fully be rejected.
- Improved insulin correction using TPM-based IOB.

The open-loop control strategy was then extended to construct a closed-loop controller, referred to as the TPC, which applies TPC OL at each CGM sampling time. Additionally, the TPF was used to filter CGM measurements and improve BG estimation. This AP is a very simple and effective method that requires minimal computational resources. The tuning of these controllers can be fully automatized and no manual tuning is necessary. However, manual tuning is still possible, because only two intuitive parameters need to be set in the TPC NM, while two more for every additional type of meal to be announced.

The open challenges defined in the state of the art (5.3.1) are addressed by the new controllers: the combination of the methods introduced in the TPC OL and TPC is designed such that hyperglycemia is rejected as fast as possible while always avoiding BG concentrations lower than the setpoint. Hence the **asymmetric control objective** is considered directly in the controller's structure. As a consequence, BG concentrations that are lower than the setpoint should never occur and negative insulin infusions should never be required, if the TPM is accurate. Nevertheless, if this happens, because of unmodeled effects, required negative insulin infusions will be small and can be applied by reducing the basal rate. Using this mechanism, the negative effect of the **control saturation** is reduced to a minimum. Finally, the **time delay** of the effect of insulin infusions on the BG concentration is taken into account through the time constant of the IOB.

The new controllers were evaluated on the UVa simulator, showing that

- Standard therapy, which is successfully used for real patients, shows bad performance on the UVa simulator, revealing one of the limits of the simulator. TPC OL probably does not lead to much better results.
- The TPC gives excellent results on the UVa simulator with both announced and unannounced meals, reducing patient risk (lower BGRI) and improves treatment quality (increased % of time in target range). These results are confirmed by a comparison with other published controllers that are considerably more complex, but show slightly inferior results, with the exception of EDS that shows better results.

Several remarks are in order:

- The TPC OL and TPC are based on the TPM and are the best possible solutions with this model. However, since it is not accurate, resulting control will not be perfect, either. However, since the TPM is the model showing best prediction capabilities (cf. chapter 2), the derived controllers perform quite well.
- Controller testing is only done on the UVa simulator. While this gives first insight into a controller's behavior, it is not a reliable measure of controller performance. The results are only valid within the UVa simulator framework, but will be different for real patients. This is especially true for TPM-based controllers, as there is a significant mismatch

between the TPM and the UVa model. It should be noted that almost all published model-based controllers rely on models that are adapted to the UVa simulator model dynamics. In particular, the EDS procedure is based on the BMM, whose dynamics are closer to the UVa simulator model's. Hence EDS performance may be lower for real patients.

- The CGM noise simulated in the UVa simulator is based on a random number generator (Breton and Kovatchev [2008]). This generator uses a seed upon which the sequence of random numbers is based. As a consequence, the UVa simulator results depend significantly on the chosen seed. Unfortunately, most studies with the UVa simulator do not specify which seed was used, which makes it impossible to reproduce the results and makes comparisons rather difficult. Probably, most authors used the default seed which is random and different for each simulation. Svensson [2013] mentions that the same seed was used for all simulations, but does not provide it. In this work, for single repetition experiments, the seed was always set to 1, allowing valid comparisons within the scope of this work.

However, to get truly comparable results, simulations should be repeated until the average of a metric over all repetitions stays stable. The necessary number of repetitions is determined using figure 5.11, which shows the evolution of the average risk index error (taken with respect to the last found value) as a function of the number of repetitions for Adult 1 and a PID controller. It can be seen that after about a hundred repetitions this error is less than 2%, which is considered to be sufficient. This figure may also depend on the different controllers and scenarios, and the 100 repetitions should be checked for consistency. Ideally, all simulations in this thesis should have been repeated at least 100 times, especially to have a fairer comparison with other controllers. Unfortunately, this was not possible mainly because of computation time considerations.

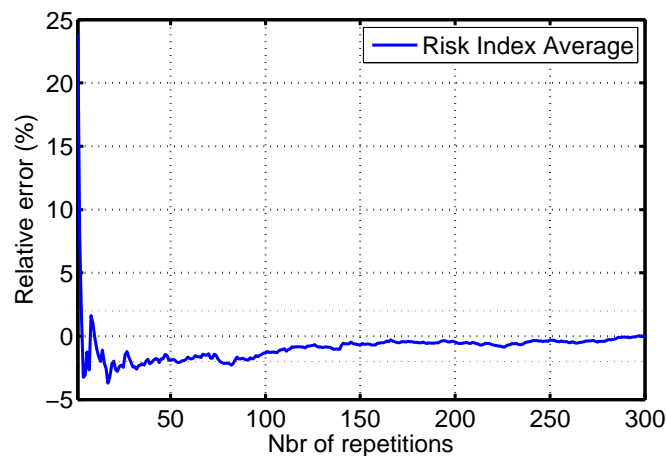


Figure 5.11: Relative BGRI error as a function of the number of repetitions for Adult 1 and a PID controller.

- The proposed control algorithms are relatively safe since they are directly inspired by standard therapy (considered as safe), but have additional safety measures such as the IOB and the adapted setpoint. Nevertheless, safety cannot always be guaranteed and, for unfortunate circumstances or, in case of unexpected BG dynamics, excessive insulin doses may be administered. The example of adult 9 illustrates this danger, even though his meal response appears to be exceptional. A sTPM-based control algorithm may be able to supply this final security layer.

6 Conclusion

6.1 Summary

This thesis proposes an AP that tackles most important challenges of BG control (section 1.2) by using standard therapy, a reliable and widely used treatment method. The therapy parameters are explicitly introduced into the proposed method in order to create a well-accepted, intuitive, and reliable treatment option.

Several components, sharing the concept of therapy parameters, were developed and combined to create a complete treatment approach: the AP is fully specified and does not need any additional, manual tuning. The only requirement is an appropriate data set to identify the model parameters. The components are the following:

- Prediction models (**TPM** and **TPM+**) directly based on therapy parameters.
- BG estimator for filtering CGM measurements (**TPF**) based on the prediction models.
- Open- and closed-loop control algorithm (**TPC**) based on the prediction models.

These components address several of the above-mentioned challenges, as illustrated in table 6.1. The **uncertainty** is split into different categories that are separately addressed by some of the proposed components: Inter-patient variability is considered by identifying parameters for every individual instead of using population parameters. Hence, the therapy is individualized and differences between patients have no influence on their therapy. Intra-patient variability is not taken into account in the proposed controller, yet, measurement noise is being filtered out using the TPC. Meal announcement errors are not taken into account directly, either. However, it was shown that the TPC has good performance, even if meals are not announced at all, making the TPC robust against meal announcement errors. Meal uptake variability is considered by identifying new model parameters for every type of meal, and, indirectly, by the meal rejection properties of the TPC. This is done analogously to the individual identification for the different patients, but cannot be demonstrated in this thesis, because the necessary

Chapter 6. Conclusion

data is missing. The **complexity of the dynamics** is not completely accounted for, but, as the TPC has excellent disturbance rejection capabilities, the influence of unexpected dynamics is reduced. The **identifiability** is greatly improved by the proposed structure of the TPM and the TPM+. Additionally, the quality of the identification can easily be verified by comparing identified parameters to therapy parameters. The **asymmetric control objective** is taken into account by the TPC, which was specifically designed to perform well in this particular setting. Indeed, the TPC is intended to prevent overly large insulin injections, and, hence, to prevent BG concentrations from reaching a hypoglycemic state. The **time delay** effects are addressed by the use of the IOB, which uses a model that takes into account the time delay in order to estimate how much insulin is still going to act in the future. Additionally, the TPF reduces the influence of the time delay on the BG estimation, when compared to conventional filters. Finally, the **control saturation** is generally avoided because of the TPC's capability to reduce BG concentration undershoots. This goes hand in hand with the asymmetric control objective.

Challenge	TPM(+)	TPF	TPC	Combined	sTPM
Patient safety			(✓)	(✓)	
Uncertainty					
Inter-patient variability	✓			✓	
Intra-patient variability					✓
Measurement noise		✓		✓	✓
Meal announcement errors			(✓)	(✓)	✓
Meal uptake variability	✓		(✓)	✓	
Complexity of dynamics			(✓)	(✓)	(✓)
Identifiability	✓			✓	✓
Asymmetric control objective			✓	✓	
Time delay		(✓)	✓	✓	
Control saturation			✓	✓	

Table 6.1: Comparison of identified challenges with the different components designed in this study. ✓ indicates that the challenge is explicitly addressed, while (✓) indicates that its effect is indirectly, or incompletely reduced.

These components are combined to create a very efficient BG control method, as shown on the UVa simulator. Nevertheless, some open challenges remain: the intra-patient variability and the meal announcement errors have not yet been accounted for.

For this reason, a stochastic term was modeled and added to the TPM, resulting in the sTPM. This allows quantifying the uncertainty on BG concentrations by propagating parameter and input uncertainties, as well as measurement noise. This way, some of the unmodeled complexity of the system are also considered and opens the way to even safer control methods.

6.2 Perspectives

This thesis results in a promising control algorithm built upon a new reliable prediction model. Nevertheless, patient safety may still be improved. Therefore, the ultimate goal of designing an AP usable in an outpatient setting has not yet been fully reached and several further steps are suggested for future work.

A first solution to use this controller in combination with an independent safety supervision module, such as proposed in the modular framework introduced by Patek et al. [2012].

Another option to further improve patient safety is to design a control algorithm that directly uses the information generated by the sTPM to compute safer insulin infusions. Such a sTPC could be based on optimal control or MPC, as explained in section 5.4. If the pieces of the puzzle could be gathered, a safe closed-loop control algorithm might be attainable, as illustrated in table 6.2:

Challenge	TPM(+)	TPF	sTPM	sTPC	Combined
Patient safety				✓	✓
Uncertainty					
Inter-patient variability	✓				✓
Intra-patient variability			✓		✓
Measurement noise		✓	✓		✓
Meal announcement errors			✓		✓
Meal uptake variability	✓				✓
Complexity of dynamics			(✓)		(✓)
Identifiability	✓				✓
Asymmetric control objective				✓	✓
Time delay		(✓)		✓	✓
Control saturation				✓	✓

Table 6.2: Comparison of identified challenges with a future sTPM-based controller (sTPC). ✓ indicates that the challenge is explicitly addressed, while (✓) indicates that its effect is indirectly, or incompletely reduced.

Nevertheless, the system complexity is so huge that it will never be possible to be completely protected against unexpected BG excursions. Its influence can only be reduced by an appropriate and sufficiently robust control algorithm.

Other points need to be addressed in the future:

- Model parameters are known to drift over time, as a patient's physiological parameter also change. For this reason, an adaptive parameter estimation should be implemented on the TPM. This method may also allow initializing the controller without the need for a training data set.
- The TPC was tested exclusively on the UVa simulator and is therefore only validated

in the light of the known limitations of this simulator. In order to truly validate the proposed algorithms, they would need to be tested on real patients. It should be noted that the TPM was designed on real patient data and not on UVa simulations. As a consequence, the potential of the TPM and of related control methods is certainly higher on real data.

- The effect of exercise is one of the external disturbances with a significant effect on BG concentrations and whose cause may be measured. For this reason, an exercise model that follows the design methods of the TPM should be designed.
- The proposed models and controllers should not only be tested on the adult population of the UVa simulator, but also on the children and adolescents. Good results would indicate good robustness of the proposed methods, because these patients are more difficult to control, because of their increased insulin sensitivity and variability.

A Validation data

A.1 UVa/Padova simulator

The FDA-approved *in silico* testing of diabetes control strategies in order to replace pre-clinical animal testing. The approved software is called the UVa/Padova simulator (referred to as the UVa simulator in this thesis) and is based on a high-order model by Dalla Man et al. Dalla Man et al. [2007]. This simulator, also known as the Type 1 Diabetes Metabolic Simulator, is currently the most important benchmark for control strategy evaluation, and it is important for proposed methods to perform well on generated simulator data.

The UVa simulator exists in two versions: a 300- and a 30-subject version. The larger version is reserved for selected research groups only, while the smaller version is used in this work. Out of the 30 available subjects, there are 10 adults, 10 children, and 10 adolescents. Only the 10 adults are considered here for the following reasons: (i) It is computationally more efficient to do the first tests on less subjects, (ii) children and adolescents are more difficult to control and the simplest case should be analyzed first, and (iii) most published controllers were validated on adult data only (as for the ones compared in section 5.3.4).

The UVa simulator allows interactions with the virtual subject population by setting an insulin injection rate (the insulin profile can be adapted at a sampling time of 1 minute and at increments of 0.05 U/h) or by determining the CHO intake rate. Only a single type of mixed meal is available. The provided outputs are BG concentrations, both exact and CGM measurements. An example of such an output is given in figure A.1. The CGM measurements are based on a model by Breton and Kovatchev [2008] that uses the exact values to generate the noisy ones colored noise and a stochastic process. This stochastic process is simulated based on the initial seed of a random number generator. In this thesis, this seed was always chosen equal to 1.

The dynamics of the underlying model are non-linear and relatively complex. Nevertheless, insulin and meal sensitivities only change to limited degree over the BG concentration range. For this reason, the developers are able to provide values for CF and I2C that are appropriate.

Appendix A. Validation data

In addition to these two parameters, corresponding basal insulin and steady-state BG values are given (cf table A.1). These indicate the BG concentration that is reached if the indicated basal insulin is infused.

In the UVa simulator software, so-called scenarios need to be defined on which experiments are run. These can either provide the timing and amounts of the complete model inputs (CHO and insulin) to be used for data generating tests, or just give meal information and rely on a closed-loop controller to provide insulin infusions. In this thesis, a nominal scenario and a sensitivity test scenario are used to generate identification data and are specified in sections A.1.1 and A.1.2, respectively.

Adult	G_{ss} in mg/dl	$U_{I,b}$ in U/h
1	138.56	1.267
2	136.45	1.369
3	147.10	1.425
4	150.69	0.887
5	142.67	1.179
6	135.64	1.724
7	135.26	1.371
8	143.23	1.141
9	145.08	1.133
10	152.83	1.018

Table A.1: Default steady-state parameters in the UVa simulator

To illustrate several properties of the simulator, a data set from the nominal scenario is shown in figure A.1. A first observation is that CGM noise sometimes takes highly unlikely values, such as after 10h for example. At this time exact BG concentration rises by 5 mg/dl, while the CGM measurements show a rise of 60 mg/dl - more than 10 times the actual excursion and a relative error in BG concentration of nearly 50 %. Of course such noise levels make BG control difficult and require the controllers to be highly robust. Another observation can be made when an "optimal" bolus is given with a meal, as observed after 33 and 57 hours. This results in considerable BG concentration undershoot 2-3 hours after the meal that take around 10 hours to recover. These undershoots have an amplitude as big as the BG peak caused by the meal. This phenomenon is generally not observed to such an extent for real patients and makes BG control more difficult, again.

The UVa simulator has several limitations, because not all of a patients dynamics are captured by the model. Some of these limitations are that:

- Only a single type of meal is available, even though there are important differences from one type of meal to another.
- The model is completely deterministic and therefore, the intra-patient variability cannot be modeled. In other words, if a patient does the same things two days in row, his exact

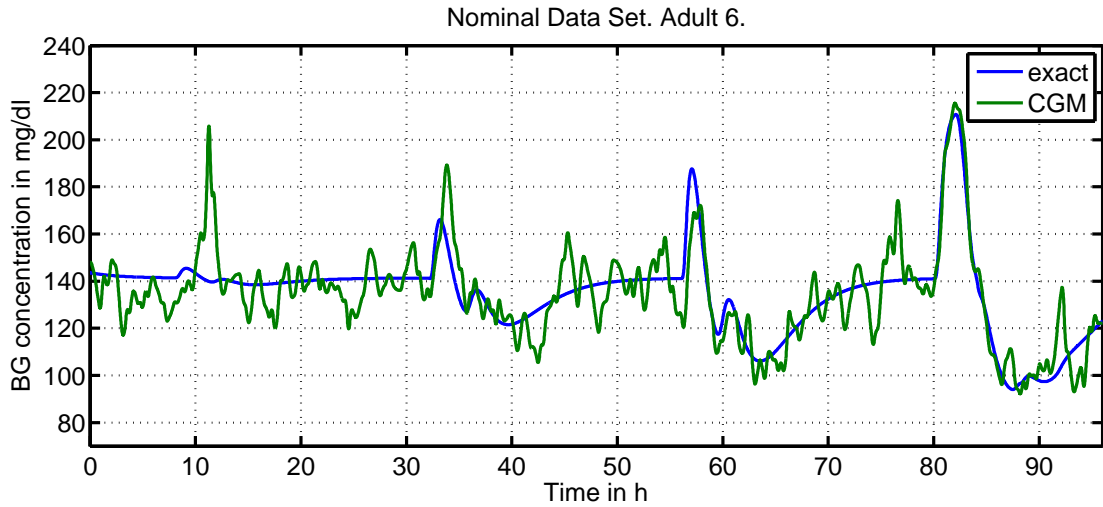


Figure A.1: Example of UVa simulation of Adult 6 on nominal day scenario.

BG concentration will be the same on both days.

- The model parameters are time-invariant. As a consequence, effects related to the circadian rhythm, like the dawn phenomenon (increased BG concentration early in the morning) are not modeled.
- Disturbances, other than meals, such as physical activity or stress, are not modeled, thus ignoring these potentially dangerous situations.

Overall, the absence of some sources of uncertainty is balanced by the increased and sometimes unexpected randomness of the CGM noise. This reduces the effect of some of the limitations and makes the simulator more realistic.

A.1.1 Nominal data set

Four consecutive days with meal and insulin inputs as defined in table A.2 are generated. These are then separated into 4 days with start and end times also given in table A.2. These experiments result in BG concentrations that have a wide range, such that the non-linearities of the UVa simulator model are not avoided.

The 10 available adults were used and basal rates were set to the default values in the UVa simulator (cf A.1).

These 4 days have been chosen in the following way:

- The **first three days** are similar. An insulin bolus and a meal are taken simultaneously. The insulin bolus is chosen such that it decreases BG concentrations by the specified

Appendix A. Validation data

d	t_s	t_e	Δ_I	t_I	Δ_M	t_M	T_M
1	8 AM	4 PM	10	8 AM	10	8 AM	10
2	8 AM	4 PM	70	8 AM	70	8 AM	20
3	8 AM	4 PM	120	8 AM	120	8 AM	10
4	8 AM	11 PM	100	10 AM	80	8 AM	10
			5	2 PM	20	2 PM	15
			10	3 PM	10	6 PM	20
			15	4 PM			

Table A.2: UVa simulator protocol. Day d , experiment start time t_s , experiment end time t_e , the insulin bolus induced drop in BG Δ_I in mg/dl , the time of the insulin bolus t_I , the CHO induced rise in BG Δ_M in mg/dl , the time of the CHO intake t_M , and the meal duration T_M in minutes are given.

amount, calculated using the CF that is given in the simulator. The meals are then given such that they counteract these boluses based on the $I2C$ provided in the simulator.

- The **fourth day** spans the whole palette of BG concentrations and incorporates different amounts of carbohydrate ingestion and insulin injections. The goal is to have a day that differs from the others in order to make validation more difficult.

A.1.2 Sensitivity test days

The sensitivity test days are generated in the same way as the first three days of the nominal test. However, this time, the meals and insulin doses were not taken simultaneously, but on separate days, as specified in table A.3. The goal of this experiment is to observe the effect of meals and insulin separately and over a broad range of possible amounts.

d	t_s	t_e	Δ_I	t_I	Δ_M	t_M	T_M
1	8 AM	t_{minBG}	10	8 AM			
2	8 AM	t_{minBG}	70	8 AM			
3	8 AM	t_{minBG}	120	8 AM			
4	8 AM	t_{maxBG}			10	8 AM	10
5	8 AM	t_{maxBG}			70	8 AM	20
6	8 AM	t_{maxBG}			120	8 AM	10

Table A.3: UVa simulator protocol. Day d , experiment start time t_s , experiment end time t_e , the insulin bolus induced drop in BG Δ_I in mg/dl , the time of the insulin bolus t_I , the CHO induced rise in BG Δ_M in mg/dl , the time of the CHO intake t_M , and the meal duration T_M in minutes are given. t_{minBG} and t_{maxBG} are the times at which the minimum or the maximum BG concentration is reached, respectively

A.2 Clinical study

Clinical data used in this thesis is extracted from a mono-center and open-label study, designed to evaluate an investigational meal bolus advice method, similar to that of Prud'homme et al. [2011]. 12 subjects with type 1 diabetes mellitus followed the same 10-day procedure, summarized in table A.4:

- *Clinical habituation phase*: The objective of the 3 preliminary days was to get the subjects used to the clinical environment and changes in their daily routine. Meanwhile, physicians adjusted the therapy parameters. On day 3, an additional basal rate test was performed to verify and adapt the basal rate. The patients' basal rate was carefully tuned by physicians such that, without insulin infusions or CHO ingestion, BG stays approximately constant across the day. Data from these days is not considered on this thesis.
- *Sensitivity tests*: On days 1 and 2, insulin sensitivity tests were performed, i.e. patients received an isolated insulin shot, followed by BG monitoring. The goal was to observe the effect of insulin without the influence of any meal disturbance, which is key for obtaining reliable insulin action parameters (2.4.3). Whenever necessary, the basal rate was slightly reduced a few hours before the test, so that at 8:30 AM a corrective bolus could be infused. Until 11:30 AM, the sampling period for SMBG measurements was set equal to 15 minutes.
- *Standard therapy days*: On days 3 and 4, standard therapy was applied (2.3.2). At 9:00 AM, the subjects received the test meal and infused their standard insulin bolus. BG was measured every 30 minutes until 4:00 PM.
- *Optimized insulin infusion days*: On days 5 to 7, optimized insulin patterns were infused under the same meal and BG measurements conditions than before. The therapy consisted of small insulin boluses, potentially administered every 30 minutes until 2:00 PM.

day	t_s	t_e	T_s	CGM	W_i
1,2	8:30 AM	11:30 AM	15	✓	5
3,4	9:00 AM	4:00 PM	30	✓	1
5,6	9:00 AM	4:00 PM	30	✓	1
7	9:00 AM	4:00 PM	30	×	1

Table A.4: Clinical study protocol. The experiment start time t_s , experiment end time t_e , SMBG sampling interval T_s in minutes, availability of CGM data, and the chosen measurement point weight W_i (cf 3.2.3) are specified.

SMBG measurements were performed with Accu-Chek[®] Combo meters, and CGM measurements with a Dexcom[®] SEVEN[®] PLUS. It should be noted that CGM data is not available on day 7.

Appendix A. Validation data

The test meals were always the same fatty, heavy and long-lasting meals (750 kcal with 25-30% carbohydrates, 15-20% protein, and 55-60% fat). This is a very slow acting meal, i.e. a meal with low GI where the rise in BG is slow, chosen intentionally to show the benefits of an insulin infusion pattern, which only exists if the insulin action is faster than the meal effect.

The following data were not considered for model validation:

- Data collected after a hypoglycemic intervention.
- Data collected after the intake of medication.
- Data with very high variability and unexplained BG excursions.

Of note is that this corresponds to the exclusion of 2 subjects. Overall, the standard therapy parameter I2C was often underestimated leading to high BG concentrations, most likely due to the slow nature of the selected meal. Therapy parameter values were updated on a day-to-day basis. However, in this thesis, only one single therapy parameter value is considered per patient.

The insulin sensitivity tests have a weight W_i that is 5 times the weight of the other days. This increased importance given to the identification quality of the insulin subsystem is vital to have a reliable identification of insulin action.

The data from this study are very well suited to analyze parameter correlations and compare deterministic and stochastic model predictions since:

- insulin sensitivity tests were performed (cf. 2.4.3).
- the patients had the same meal several times on consecutive days, which prevents that parameters change significantly over the course of the study.
- the basal rates and therapy parameters were very well adjusted by physicians.
- two different insulin infusion strategies were used.

The latter is interesting in that, generally speaking, if all study days are similar, models that have good data fits generate good predictions even if they have inappropriate dynamics. On the other hand, an even more diversified study design with, e.g., modified meal sizes, more patients and more insulin sensitivity test days, would improve the quality of the data further.

B Metrics

In this thesis, many different metrics are used, in order to quantify the quality of data fits, BG predictions and control performance. A good overview of many metrics is given by Del Favero et al. [2012]. Additionally, Del Favero et al. propose an extension of existing metrics to incorporate a glucose specific penalty, although this is not necessary in this thesis, since hypo- and hyperglycemia conditions rarely occurred in the data sets. In the following sections, the different metrics used along this document are introduced.

B.1 MAD

The MAD, in mg/dl, is used to compare data fits, as well as model predictions resulting from the different investigated models. It is defined as:

$$\text{MAD} = \frac{1}{N} \sum_{t=1}^N |G(t) - \hat{G}(t)| \quad (\text{B.1})$$

where N denotes the number of samples. It measures the mean absolute deviation between an estimated and an exact BG concentration. Hence, the lower its value, the better the results.

B.2 R^2

The coefficient of determination R^2 in % is used to compare data fits, as well as model predictions resulting from the different investigated models. It is defined as:

$$R^2 = 100 \left(1 - \frac{\frac{1}{N} \sum_{t=1}^N (G(t) - \hat{G}(t))^2}{\frac{1}{N} \sum_{t=1}^N (G(t) - \bar{G})^2} \right) \quad (\text{B.2})$$

where \bar{G} is the average BG: $\bar{G} = \frac{1}{N} \sum_{t=1}^N G(t)$. A value of 100% is equivalent to a perfect fit, while bad fits may have negative values. This method is more sensitive to outliers, because of its quadratic term.

B.3 EGA

As BG predictions are thought to be, in the ideal case, used in the same way as BG measurements, they should also be evaluated using the EGA, proposed by Clarke et al. [1987], which is used to assess the performances of BG meters. BG measurements are compared to reference BG measurements and are classified via a grid, represented in figure B.1 that rates resulting treatment decisions.

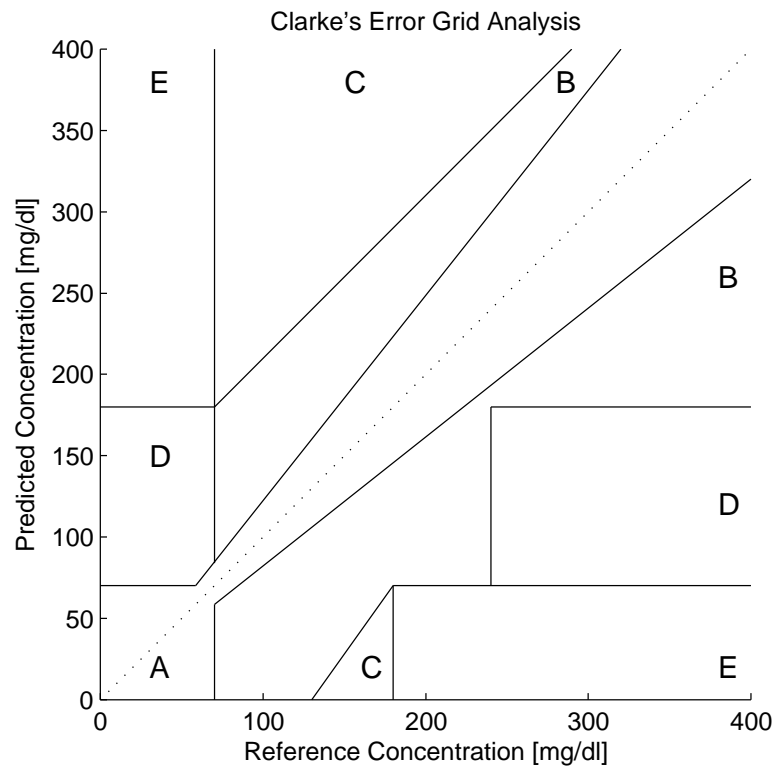


Figure B.1: Clarke EGA. Figure based on MATLAB code by Edgar Guevara Codina.

- If the measurement is "clinically accurate", i.e. if it deviates by no more than 20%, it is classified in zone A. If 95% of the measurements are in zone A, the BG meter is approximately achieving the standards of the ISO 15197 norm. However, as shown by Freckmann et al. [2010], many current BG meters do not fulfill this norm.
- If a measurement is "clinically appropriate", i.e. if it would lead to benign or no treatment, it is classified in zone A and B.
- All other zones are considered potentially dangerous and should therefore be avoided.

Clearly, it is highly desired to obtain as many predictions in zone A as possible, and to avoid zones other than A or B.

B.4 BGRI

The BGRI was introduced by Kovatchev et al. [2000] and is well recognized as a reliable indicator of the clinical adequacy of a BG profile. As such the BGRI is implemented in the UVa simulator as one of the main performance metrics. It is defined using a risk function r given in equation B.4 and represented in figure 1.7.

$$f(G) = 1.509 [(\ln(G))^{1.084} - 5.381] \quad (\text{B.3})$$

$$r(G) = 10f(G)^2 \quad (\text{B.4})$$

This function attributes a risk to every BG concentration G . The risk is zero at 112.5 mg/dl and increases as G deviates from this target value. This increase is asymmetric as the risk during hypoglycemia is higher than for hyperglycemia. Kovatchev et al. define the target BG range between 70 and 180 mg/dl, which corresponds to a risk value of 7.7.

The BGRI is defined as the average $r(G)$:

$$BGRI = \frac{1}{n} \sum_{i=1}^n r(G_i) \quad (\text{B.5})$$

The BGRI can be split into HBGI and LBGI such that $HBGI + LBGI = BGRI$, where the contributions to the score come from values above or below the target of 112.5 mg/dl, respectively.

The BGRI is a very convenient tool to compare algorithms applied to the same experimental scenarios. However, if the scenarios are different, the BGRI has little value.

As mentioned in section 5.3.4, Cameron et al. [2011] used a modified BGRI, proposed by Magni et al. [2007], and defined by

$$f(G) = 3.5506 [(\ln(G))^{0.8353} - 3.7932] \quad (\text{B.6})$$

$$r(G) = 10f(G)^2, \quad (\text{B.7})$$

for which zero risk is at 140 mg/dl.

B.5 RMSE

The RMSE, in mg/dl, is used to compare data fits, as well as model predictions resulting from the different investigated models. It is defined as:

$$\text{RMSE} = \sqrt{\frac{1}{N} \sum_{t=1}^N (G(t) - \hat{G}(t))^2} \quad (\text{B.8})$$

where N denotes the number of samples. It measures the square root of the mean square error between an estimated and an exact BG concentration. Hence, the lower its value is, the better are the results.

B.6 Percentage of time spent within a range of BG concentrations

A simple and comprehensive way to assess the controller performance is to compute the percentage of time within given BG concentration ranges. Common ranges are:

- target range: **70-180 mg/dl**. This is the range as much time as possible should be spent in. This is in accordance with target defined by Kovatchev et al. [2000].
- hypoglycemia: **< 70 mg/dl**. Time spent below target should be minimized as there is an increased risk of hypoglycemia.
- hyperglycemia: **> 180 mg/dl**. Time spent above target should be short in order to avoid hyperglycemia.
- severe hypoglycemia (**< 50 mg/dl**) should be avoided at all price since it puts patients in acute danger.

B.7 Mean BG concentrations

The mean BG concentration over a complete data set, pre-meal, and post-meal are given for some comparisons. The mean BG is an indicator of treatment performance, as a low mean indicates that hyperglycemia was well avoided. However, it needs to be verified that no hypoglycemia occurs. Mean pre- and post-meal BG concentrations should be low as well. They allow getting more insight into how the treatment is when it comes to meal rejection and target tracking. Average pre-meal BG corresponds to the average BG during the hour preceding the meal, while average post-meal BG is the average BG between the first and second hour after the meal.

B.8 Minimum and maximum BG concentration

These metrics simply give the minimum and the maximum BG concentration during the experiment. The minimum BG should be high, and most importantly greater than the hypoglycemic threshold, while the maximum should remain low. These two values are generally used for the Control-Variability Grid Analysis (CVGA) introduced by Magni et al. [2008] and modified by Soru et al. [2012], which plots the minimum and maximum against each other for every patient in a population. However, this metric is not used in this thesis, because the 10 patient population is too small to lead to meaningful results.

B.9 Boxplot

Boxplots are used several times in this thesis to compare data from a certain number of experiments. For each box, the central, red line is the median, the edges of the box are the 25th (q_1) and 75th (q_3) percentiles, the whiskers extend to the most extreme data points not considered outliers, and outliers are plotted individually using red crosses. Points are considered as outliers if they are larger than $q_3 + 1.5(q_3 - q_1)$ or smaller than $q_1 - 1.5(q_3 - q_1)$.

C A Minimal Exercise Extension for Models of the Glucoregulatory System

In the context of this thesis, a model extension for the effect of exercise was developed and published (Bock et al. [2011]). The development of this model is recalled and applied to the new prediction models designed in chapter 2.

C.1 Introduction

Exercise can have lowering and increasing effects on BG concentrations and patients need to adapt their treatment to stay within the above mentioned bounds if they want to exercise, as explained by Zinman et al. [2004]. However, the necessary adaptations are difficult to estimate and, thus, the risk of hypoglycemia is increased during exercise. In this context, models predicting the effect of exercise can be very useful tools for helping patients to adjust their treatment.

Only a few models for exercise are available in the literature, examples are Dalla Man et al. [2009], Roy and Parker [2007], Kim et al. [2007], Hernández-Ordoñez and Campos-Delgado [2008], Balakrishnan et al. [2013]. Their level of complexity varies strongly, but the number of parameters is typically high, which makes their identification, using only BG measurements, difficult.

For this reason, a minimal exercise extension for existing models of the glucoregulatory system that is based on observations from a clinical study is proposed. This extension introduces two additional parameters, that can be identified using only BG measurements, and one intensity-independent exercise input. Patient specific parameters are shown to be necessary to account for the considerable inter-patient variability.

This chapter is organized as follows: In Section C.2, the clinical study is described and analyzed. The model extension and the parameter identification method are described in Section C.3. Results are discussed in Section C.4, while conclusions are drawn in Section C.5.

C.2 Clinical Study

C.2.1 Protocol

Twelve patients with T1DM using continuous subcutaneous insulin injection (CSII), 6 female, 6 male, ages 20-45, were monitored during a 2-day in-patient period. During this time, BG concentrations were measured intravenously every 5 minutes and heart rate (HR) was recorded every 5 seconds. Insulin management was performed by the patients themselves. The protocol for both days was identical except for the exercise, which was executed at 65% of maximum HR for the first day and 75% for the second. These exercise periods, performed on cycle ergometers, started at 16h00 and lasted 30 minutes. Among the 12 patients recruited for this study, only 7 presented data that were not corrupted by low BG interventions.

C.2.2 Analysis

The drop in BG appears to be linear during the effort, as can be observed in figure C.1. For this reason, the most interesting parameter is the slope of the linear part, as illustrated in figure C.1. A linear regression is performed and its dependence on several factors, such as exercise intensity, gender, age, body mass index (BMI), insulin concentrations and initial BG concentrations, is tested. The slope is calculated within a time frame of 30 minutes.

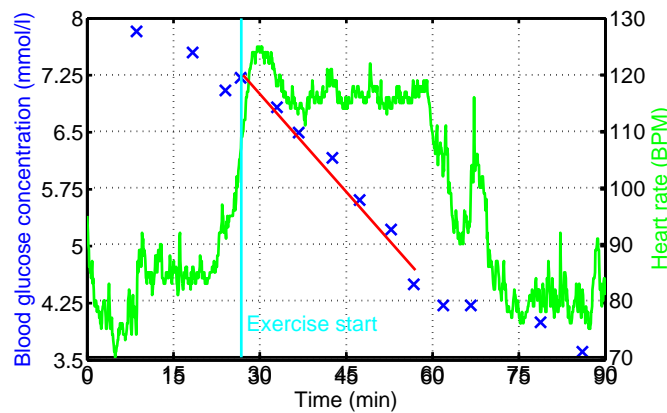


Figure C.1: Blood glucose concentration and heart rate for patient 9 on day 2. Illustration of linear regression (red line). 1 mmol/l corresponds to 18 mg/dl.

Intuitively, one would expect that the drop in BG depends on exercise intensity. In fact, this assumption, which is used by nearly all existing exercise models, is somehow contradicted by this clinical study, for the ranges of exercise intensities considered. Figure C.2 shows that the slopes for each patient, except patient 10, are similar for both intensities, and the drop in BG will be considered to be independent of the intensity. Under this assumption, two equivalent data sets are available for each patient. The results presented in figure C.2 also show that the slope varies strongly between patients. Thus, individual identification will be performed. Note

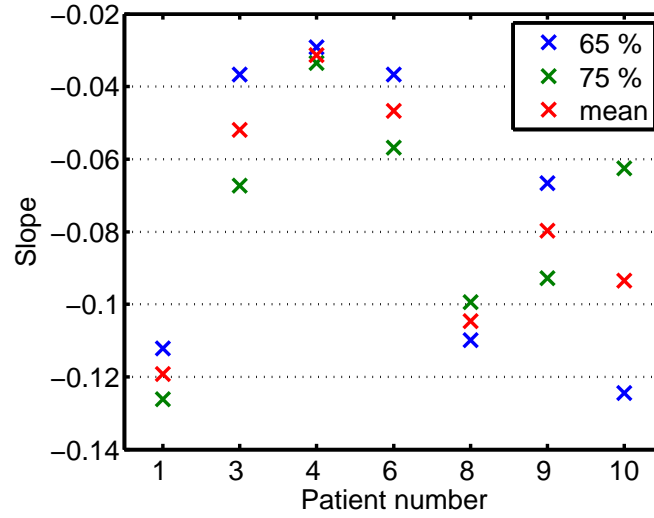


Figure C.2: Comparison of slopes for different patients. Values for both exercise sessions and their mean are shown. 1 mmol/l corresponds to 18 mg/dl.

that drawing general conclusions regarding the sensitivity of the slope to the factors discussed below would require more data.

C.3 Modeling and Parameter Estimation

C.3.1 Model Extension

According to Derouich and Boutayeb [2002], exercise leads to increases in several variables of the glucoregulatory system:

- *Insulin sensitivity*, which quantifies the effect of insulin on BG concentrations.
- *Glucose effectiveness at zero insulin*, which gives the glucose uptake.
- *Utilization of insulin*, i.e. the rate of elimination of insulin.

Trying to model all these effects simultaneously results in a model that is difficult to identify, as time constants of these effects are similar. Therefore, the effect of exercise is modeled as an increase in glucose effectiveness at zero insulin S_e , as reported by Minuk et al. [1981]. The proposed sub-model can, thus, be used as an extension for all models incorporating the concept of insulin independent glucose uptake and can be incorporated into the TPM and TPM+.

S_e should be 0 when no exercise is performed and have a positive value in the opposite case. The effect of exercise is not instantaneous and therefore a time constant for S_e is introduced.

Appendix C. A Minimal Exercise Extension for Models of the Glucoregulatory System

The dynamic behavior of S_e is defined in equation (C.1).

$$\dot{S}_e(t) = -a_e S_e(t) + K_e a_e U_e(t) \quad (C.1)$$

Where a_e (the inverse of the time constant in min^{-1}) and K_e (the exercise sensitivity in min^{-1}) are the two additional parameters that have been introduced.

As a consequence of the independence on exercise intensity, the new input $U_e = 0$ if no exercise is performed and 1 otherwise, and thus, K_e represents the amplitude of the increase in glucose uptake, while a_e shows how fast the effect appears and disappears.

C.3.2 Parameter Identification

An appropriate model of the glucoregulatory system is needed to identify the resulting new parameters. A modified version of the BMM is used. During exercise, the insulin infusion is constant. Therefore, the effect of insulin is considered constant during this period and can be combined with the glucose effectiveness at zero insulin into the new parameter S_{ins+G} . Endogenous glucose production is assumed to be constant during exercise (Minuk et al. [1981]). The complete model extension corresponds to equations (C.1) and (C.2).

$$\dot{G}(t) = -(S_{ins+G} + S_e(t)) G(t) + S_{ins+G} G_b \quad (C.2)$$

Where G is the BG in mg/dl and G_b is the basal BG chosen equal to 100 mg/dl. The term $S_{ins+G} G_b$ is the endogenous glucose production.

Firstly, S_{ins+G} is identified for each day and each patient using the data collected before the exercise session, and a standard least squares approach. This allows taking into account differences in insulin infusion that may occur from one day to another.

Then, in a second step, a_e and K_e are identified using the Iterative Two Stage (ITS) method (Vicini and Cobelli [2001]). As the exercise effect is supposed to be identical for the two days, only one couple (a_e , K_e) is identified for each patient.

However, as the sensitivity for a_e is low, an empirical value can be chosen without loss of prediction capabilities, as shown in figure C.3, and better coefficients of variation are obtained. A value of 0.1 min^{-1} is proposed.

C.4 Results and Discussion

C.4.1 Model Fits

Parameters for all 7 patients without hypoglycemic intervention are given in table C.1. These parameters are consistent as the coefficients of variation are below 100% for nearly all patients and the population mean's coefficient of variation is low. All model fits, as for example shown in figure C.3 for patient 9, are acceptable. Nevertheless, high variability within some patients can still be observed.

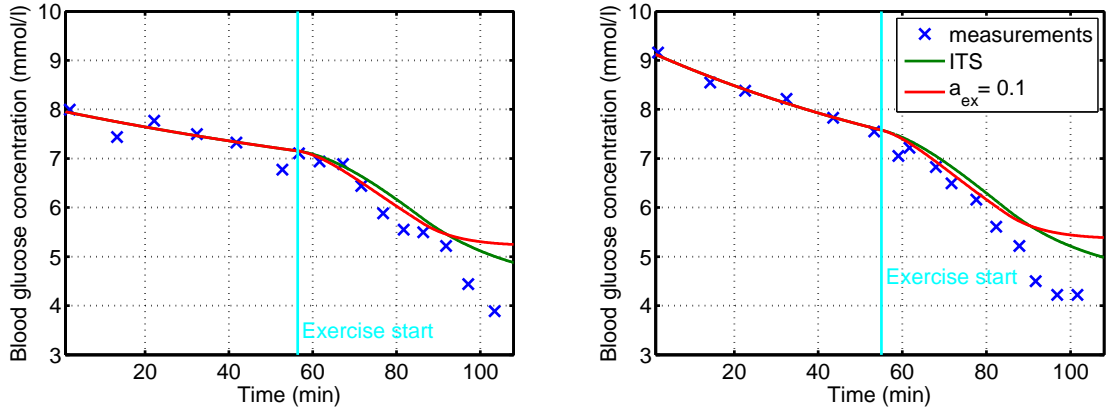


Figure C.3: Model fit for patient 9 for both days. 1 mmol/l corresponds to 18 mg/dl.

Pat. N.	1	3	4	6	8	9	10	Mean
a_e	0.0262	0.0173	0.0173	0.0289	0.0548	0.0508	0.0266	0.0317
(ITS)	(66)	(120)	(126)	(62)	(42)	(46)	(66)	(47)
K_e	0.0195	0.0089	0.0089	0.0231	0.0239	0.0206	0.0197	0.0178
(ITS)	(45)	(96)	(101)	(40)	(25)	(28)	(45)	(35)
K_e	0.0097	0.0043	0.0042	0.0117	0.0183	0.0164	0.0100	0.0107
($a_e = 0.1$)	(19)	(45)	(77)	(23)	(17)	(18)	(18)	(51)

Table C.1: Identified parameters for all patients and respective coefficients of variation (%)

C.4.2 Application to new prediction models

The minimal exercise extension can be applied to the controllers designed in chapter 2. Since the TPM+ incorporates the concept of glucose effectiveness at zero insulin, its glucose equation 2.20 can be rewritten with the exercise extension as:

$$\dot{G}(t) = -K_x X(t) - (S_G + S_e(t))G(t) + K_g U_G(t) \quad (\text{C.3})$$

The TPM is the TPM+, where $S_G = 0$. Therefore, the exercise effect can be added to the TPM by

modifying the BG equation 2.14:

$$\dot{G}(t) = -K_x X(t) + K_g U_G(t) - S_e(t) G(t) \quad (\text{C.4})$$

C.4.3 Model Limitations

The proposed model extension is strongly based on observations collected during a clinical study. However, this study only covers a small subset of possible exercise setups in terms of exercise duration or intensity and exercise types.

- Because exercise *duration* was 30 minutes, the extension is only applicable for exercise with limited durations. In fact, after about 90 minutes, the physiological processes change since the hepatic glycogen stocks are depleted Ahlborg et al. [1974]. Hence, the exercise effects are no longer captured by the proposed extension after 90 minutes.
- The *exercise intensity* was set to 65 and 75% of the maximal heart rate, i.e. in the aerobic range. However, at higher intensities, the anaerobic threshold is passed and BG dynamics change Marliss and Vranic [2002].
- The *type of exercise* that is performed might change the exercise parameters. As only data from cycling are available, this cannot be verified.
- The middle and long term effects of exercise on *insulin sensitivity* are not taken into account in this extension. However, it is shown that these changes in insulin sensitivity can be detected up to 2 days after the exercise session Mikines et al. [1988], but also over several weeks when regular exercise is performed Nishida et al. [2004].

C.5 Conclusion

A model extension for predicting the evolution of BG concentrations during exercise has been proposed. This model was found to be identifiable and in accordance with the clinical study. Additionally, as the exercise input is independent of exercise intensity, no additional measurement device is necessary. Implementations should lead to an improved quality of life for patients suffering from T1DM. Future work will include an extension of the proposed model to longer durations and a broader range of exercise intensities. For this purpose, additional clinical studies will have to be carried out. The performance of the exercise extension on the TPM and TPM+ would need to be tested as well. The alternative model, following the TPM principles can be tested as well. If the insulin and meal sub-models are not considered, the equations are

$$\dot{G}(t) = -S_e(t) \quad (\text{C.5})$$

$$\dot{S}_e(t) = -a_e S_e(t) + a_e S_{e,1}(t) \quad (\text{C.6})$$

$$\dot{S}_{e,1}(t) = -a_e S_{e,1}(t) + a_e U_e(t). \quad (\text{C.7})$$

D Additional UVa comparisons

Recently, the Doyle group published several controllers validated on 10 adults of the UVa simulator. However, the adults they considered are different from those in the 10 adult population analyzed in this thesis. Nevertheless, the comparison with the proposed controllers of chapter 5 are given below.

D.1 Wang controller

Wang et al. [2009] tested an adaptive basal therapy on 10 adults and 10 adolescents of the UVa simulator. Their scenario is described in appendix E.7. The method consists in applying standard therapy, but with a controller to adjust the basal rate. In this sense, it is close to the TPC, although the allowed variations of the basal rate are limited. Zarkogianni et al. [2011] also compared the IIAS to the results by Wang et al.

Results from all TPC versions are consistently good and slightly better than those from the IIAS. The adaptive basal therapy has the worst performance even if it performs reasonably well.

	% below tar	% above tar	% within tar	BGRI
TPC	0.13 (0.40)	0.36 (1.08)	99.51 (1.11)	0.77 (0.27)
TPC KF	0 (0)	0.65 (1.44)	99.36 (1.44)	0.79 (0.26)
TPC TPF	0 (0)	0.67 (1.48)	99.33 (1.48)	0.79 (0.27)
Adaptive basal therapy	0.5 (1.4)	1.3 (2.8)	98.2 (2.7)	1.7 (0.59)
IIAS	0 (0)	0.6 (1.52)	99.4 (1.52)	0.99 (0.43)

Table D.1: Adaptive basal therapy compared to the TPC and IIAS. Mean and standard deviation for 10 adults is given.

D.2 Grosman controller

The Zone MPC (zMPC) proposed in Grosman et al. [2010] is regularly used by the Doyle group (for instance Svensson [2013] proposes an extension of the zone MPC). The scenario is given in appendix E.8. The idea is to keep BG concentrations in a given zone rather than at a precise setpoint. In table D.2, results for announced and unannounced meals are given for different zones and a conventional MPC controller, and compared to the TPC and IIAS by Zarkogianni et al. [2011].

For unannounced meals, the zMPC is considerably better than the default standard therapy implemented in the UVa simulator. However, the TPC NM gives another important improvement over all controllers proposed by Grosman et al. and is even better than their announced-meal controllers. The huge difference suggests that Grosman et al. used a different set of 10 adults on the UVa simulator.

For announced meals, all TPC variations are considerably better than MPC and zMPC. The TPC and the IIAS are equivalent.

	mean BG	max BG	min BG	% above tar
Unannounced meals				
default open-loop (exp 1)	180 (27)	314	110	50
zMPC bounds 80-140mg/dl (exp 2)	171 (22)	291	85	44
zMPC bounds 100-120mg/dl (exp 3)	160 (23)	280	83	36
MPC setpoint 110mg/dl (exp 4)	155(23)	274	76	32
TPC NM	131 (6)	212	76	11
Announced meals				
zMPC bounds 80-140mg/dl (exp 5)	152 (28)	267	66	28 (21)
zMPC bounds 100-120mg/dl (exp 6)	141 (29)	262	62	21 (19)
MPC setpoint 110mg/dl (exp 7)	136 (29)	258	59	18 (19)
TPC	118 (5)	169	80	1.2 (2.1)
TPC KF	118 (5)	170	83	1.2 (2.0)
TPC TPF	118 (5)	170	84	1.2 (2.0)
IIAS	118 (7)	N/A	N/A	0.8 (2.1)

Table D.2: Zone MPC compared to TPC and IIAS. Mean and standard deviation for 10 adults is given.

D.3 Lee controller

The controller proposed by Lee et al. [2013] is a PID controller with feed-forward. The scenario is given in appendix E.6 and comparison results in table D.3. Two versions of the PID controller are given here: (i) ID 12 is the controller with the best performance, but was rejected because hypoglycemia was not completely avoided. (ii) ID 17 is the controller with the best performance that completely avoids hypoglycemia. This controller was considered as the best by the authors.

On the very simple proposed scenario, the TPC performs much better than the PID controller. Even when meals are not announced for the TPC, its results are superior. It can be assumed that the patients used in the UVa simulator are not the same as used for this work.

	% below tar	max BG	% above tar	% in tar
Lee ID 12	1.34 (2.9)	179 (19.3)	1.69 (2.4)	97 (4.4)
Lee ID 17	0 (0)	183 (19.6)	3.52 (5.1)	96.5 (5.1)
TPC KF	0 (0)	154 (12.1)	0 (0)	100 (0)
TPC NM	0 (0)	180 (20)	1.74 (2.1)	98.3 (2.1)

Table D.3: Controller proposed by Lee et al. compared to TPC. Mean and standard deviation for 10 adults is given.

D.4 Svensson controller

Svensson [2013] proposes a modification of the zMPC used by Grosman et al. [2010]. However, it is clear that the UVa simulator version (v3) has different subjects than the one used in this work. This becomes clear by comparing the patient characteristics given by Svensson [2013] to the ones from the version used here. Interestingly, Svensson mentions that the same CGM noise seed was used for all simulations, which no one else talks about.

E Scenarios

In this thesis, different scenarios are used in order to compare proposed controllers to published experiments. These are defined here.

E.1 Nominal Scenario

This scenario is considered as the default scenario in this thesis. It consists in two identical, consecutive days that represent a typical day. These are the default parameters, as some of them, like the sampling time, or meal announcements may change as specified in the concerned sections.

Property	
Population	10 Adults (sometimes #9 not considered)
Meal announcement	Yes
Sampling time	5 min
Initial BG	Basal BG
Duration	48 hours
Start Time	0 a.m. day 1
End time	12 p.m. day 2
Meal details	cf table E.2
CGM seed	1
Metrics	BGRI percentage in different ranges

Table E.1: Nominal scenario protocol

Time	7 a.m.	12 a.m.	4 p.m.	7 p.m.	7 a.m.	12 a.m.	4 p.m.	7 p.m.
Amount	30 g	80 g	25 g	90 g	30 g	80 g	25 g	90 g
Duration	10 min	20 min	10 min	20 min	10 min	20 min	10 min	20 min

Table E.2: Nominal scenario meal details

E.2 Zarkogianni Scenario

Zarkogianni et al. [2011] use a non linear MPC with a double deterministic model and Neural Network coupled to a fuzzy logic adaptive scheme to control blood glucose. Their scenario is summarized in tables E.3 and E.4.

Property	
Population	10 Adults
Meal announcement	Yes
Sampling time	5 min
Initial BG	Basal BG (supposedly)
Duration	48 hours
Start Time	0 a.m. day 1
End time	12 p.m. day 2
Meal duration	15 min (5 min for 5g meal) (not specified)
Meal details	cf table E.4
Metrics	% in different regions LBGI, HBGI, BGRI population mean and standard deviation

Table E.3: Zarkogianni scenario protocol

Time	7 a.m.	12 a.m.	4 p.m.	6 p.m.	11 p.m.	7:30 a.m.	1 p.m.	6:30 p.m.
Amount	45 g	70 g	5 g	80 g	5 g	40 g	85 g	60 g

Table E.4: Zarkogianni scenario meal details

E.3 Cameron Scenario

Cameron et al. [2011] tested their MPC controller on the scenario specified in tables E.5 and E.6.

E.4 Cormerais Scenario 1 day

Cormerais and Richard [2012] use two different scenarios, one of which is a one day scenario specified in tables E.7 and E.8.

E.5 Cormerais Scenario 7 days

The second scenario used in Cormerais and Richard [2012] is specified in table E.9. This scenario is quite complex with very diverse meal times and amounts. For the complete schedule, please refer to the article.

E.5. Cormerais Scenario 7 days

Property	
Population	9 Adults (#9 not considered)
Meal announcement	No
Sampling time	5 min
Initial BG	140 mg/dl
Duration	36 hours
Start Time	6 a.m. day 1
End time	6 p.m. day 2
Meal duration	20 minutes
Meal details	cf table E.6
Metrics	modified BGRI, HBGI and LBGI mean BG, pre-meal and post-meal BG percentage in different ranges

Table E.5: Cameron scenario protocol

Time	9 a.m.	1 p.m.	5:30 p.m.	8 p.m.	9 a.m.	1 p.m.
Amount	50 g	70 g	90 g	25 g	50 g	70 g

Table E.6: Cameron scenario meal details

Property	
Population	10 Adults
Meal announcement	No
Sampling time	5 min
Initial BG	100 mg/dl (from figures)
Duration	24 hours
Start Time	0 a.m. day 1
End time	12 p.m. day 1
Meal duration	20 minutes (not specified)
Meal details	cf table E.8
Metrics (per patient)	% in different regions LBGI, HBGI mean BG

Table E.7: Cormerais 1day scenario protocol

Time	7 a.m.	1 p.m.	7 p.m.
Amount	50 g	70 g	80 g

Table E.8: Cormerais 1day scenario meal details

Appendix E. Scenarios

Property	
Population	10 Adults
Meal announcement	No
Sampling time	5 min
Initial BG	100 mg/dl (from figures)
Duration	7 days
Start Time	0 a.m. day 1
End time	12 p.m. day 7
Meal duration	20 minutes (not specified)
Meal details	cf table Cormerais and Richard [2012]
Metrics (per patient)	% in different regions LBGI, HBGI mean BG

Table E.9: Cormerais 7day scenario protocol

E.6 Lee Scenario

Lee et al. [2013] tested their PID controller on the following scenario. Details are given in table E.10 and E.11.

Property	
Population	10 Adults
Meal announcement	Yes
Sampling time	5 min
Initial BG	Basal BG (supposedly)
Duration	31 hours
Start Time	0 a.m. day 1
End time	7 a.m. day 2
Meal duration	20 minutes (not specified)
Meal details	cf table E.11
Metrics	% in different regions maximum BG population mean and standard deviation

Table E.10: Lee scenario protocol

Time	7 a.m.
Amount	50 g

Table E.11: Lee scenario meal details

E.7 Wang Scenario

Wang et al. [2009] use an adaptive basal therapy as closed-loop algorithm and the scenario given in tables E.12 and E.13.

Property	
Population	10 Adults
Meal announcement	Yes
Sampling time	5 min
Initial BG	Basal BG (supposedly)
Duration	24 hours
Start Time	0 a.m. day 1
End time	12 p.m. day 1
Meal duration	20 minutes (not specified)
Meal details	cf table E.13
Metrics	% in different regions $tg=60-180$ BGRI

Table E.12: Wang scenario protocol

Time	7 a.m.	12 a.m.	6 p.m.
Amount	40 g	75 g	60 g

Table E.13: Wang scenario meal details

E.8 Grosman Scenario

Grosman et al. [2010] apply the zMPC developed by the Doyle group to the UVa simulator. They use the scenario specified in tables E.14 and E.15.

Appendix E. Scenarios

Property	
Population	10 Adults
Meal announcement	Both
Sampling time	5 min
Initial BG	Basal BG
Duration	24 hours
Start Time	0 a.m. day 1
End time	12 p.m. day 1
Meal duration	15 minutes (not specified)
Meal details	cf table E.15
Metrics	mean BG with standard deviation min and max BG time above 180 mg/dl number of hypoglycemic events

Table E.14: Grosman scenario protocol

Time	7 a.m.	1 p.m.	8 p.m.
Amount	75 g	75 g	50 g

Table E.15: Grosman scenario meal details

F Stochastic TPM equations

The covariance propagation equations for the TPM are given below. If combined with the deterministic TPM (equations 2.14 to 2.18), the complete stochastic model can be simulated. The time dependence is not indicated in order to simplify the notation.

$$\dot{P}_{G,G} = Q_{K_x,K_x} X^2 - 2Q_{K_g,K_x} XU_G + Q_{K_g,K_g} U_G^2 + 2K_g P_{G,U_G} - 2K_x P_{G,X} \quad (E1)$$

$$\begin{aligned} \dot{P}_{G,U_G} = & K_g P_{U_G,U_G} - K_x P_{U_G,X} - a_g P_{G,U_G} + a_g P_{U_G,U_{G,1}} + XQ_{a_g,K_x}(U_G - U_{G,1}) \\ & - U_G Q_{K_g,a_g}(U_G - U_{G,1}) \end{aligned} \quad (E2)$$

$$\dot{P}_{U_G,U_G} = 2a_g P_{U_G,U_{G,1}} - 2a_g P_{U_G,U_G} + Q_{a_g,a_g}(U_G - U_{G,1})^2 \quad (E3)$$

$$\begin{aligned} \dot{P}_{G,U_{G,1}} = & K_g P_{U_G,U_{G,1}} - K_x P_{U_{G,1},X} - a_g P_{G,U_{G,1}} - XQ_{a_g,K_x}(U_{CHO} - U_{G,1}) \\ & + U_G Q_{K_g,a_g}(U_{CHO} - U_{G,1}) \end{aligned} \quad (E4)$$

$$\dot{P}_{U_G,U_{G,1}} = a_g P_{U_{G,1},U_{G,1}} - 2a_g P_{U_G,U_{G,1}} - Q_{a_g,a_g}(U_{CHO} - U_{G,1})(U_G - U_{G,1}) \quad (E5)$$

$$\dot{P}_{U_{G,1},U_{G,1}} = Q_{a_g,a_g}(U_{CHO} - U_{G,1})^2 - 2a_g P_{U_{G,1},U_{G,1}} \quad (E6)$$

$$\begin{aligned} \dot{P}_{G,X} = & K_g P_{U_G,X} - K_x P_{X,X} - a_x P_{G,X} + a_x P_{G,X_1} + XQ_{K_x,a_x}(X - X_1) \\ & - U_G Q_{K_g,a_x}(X - X_1) \end{aligned} \quad (E7)$$

$$\dot{P}_{U_G,X} = a_g P_{U_{G,1},X} - a_g P_{U_G,X} - a_x P_{U_G,X} + a_x P_{U_G,X_1} + P_{U_G,X}(X - X_1)(U_G - U_{G,1}) \quad (E8)$$

$$\dot{P}_{U_{G,1},X} = a_x P_{U_{G,1},X_1} - a_x P_{U_{G,1},X} - a_g P_{U_{G,1},X} - P_{U_G,X}(X - X_1)(U_{CHO} - U_{G,1}) \quad (E9)$$

$$\dot{P}_{X,X} = 2a_x P_{X,X_1} - 2a_x P_{X,X} + Q_{a_x,a_x}(X - X_1)^2 \quad (E10)$$

$$\dot{P}_{G,X_1} = K_g P_{U_G,X_1} - K_x P_{X,X_1} - a_x P_{G,X_1} + XQ_{K_x,a_x}(X_1 - U_I) - U_G Q_{K_g,a_x}(X_1 - U_I) \quad (E11)$$

$$\dot{P}_{U_G,X_1} = a_g P_{U_{G,1},X_1} - a_g P_{U_G,X_1} - a_x P_{U_G,X_1} + Q_{a_g,a_x}(X_1 - U_I)(U_G - U_{G,1}) \quad (E12)$$

$$\dot{P}_{U_{G,1},X_1} = -a_g P_{U_{G,1},X_1} - a_x P_{U_{G,1},X_1} - Q_{a_g,a_x}(X_1 - U_I)(U_{CHO} - U_{G,1}) \quad (E13)$$

$$\dot{P}_{X,X_1} = a_x P_{X_1,X_1} - 2a_x P_{X,X_1} + Q_{a_x,a_x}(X - X_1)(X_1 - U_I) \quad (E14)$$

$$\dot{P}_{X_1,X_1} = Q_{a_x,a_x}(X_1 - U_I)^2 - 2a_x P_{X_1,X_1} \quad (E15)$$

Bibliography

- Amjad Abu-Rmileh and Winston Garcia-Gabin. Wiener sliding-mode control for artificial pancreas: A new nonlinear approach to glucose regulation. *Comput. Methods Programs Biomed.*, pages 1–14, May 2012. ISSN 1872-7565. doi: 10.1016/j.cmpb.2012.03.001.
- G Ahlborg, P Felig, L Hagenfeldt, R Hendler, and J Wahren. Substrate Turnover during Prolonged Exercise in Man. Splanchnic and leg metabolism of glucose, free fatty acids, and amino acids. *J Clin Invest*, 53(4):1080–1090, 1974. ISSN 0021-9738.
- Naviyn Prabhu Balakrishnan, Gade Pandu Rangaiah, and Lakshminarayanan Samavedham. Review and Analysis of Blood Glucose (BG) Models for Type 1 Diabetic Patients. *Ind. Eng. Chem. Res.*, 50(21):12041–12066, November 2011. ISSN 0888-5885. doi: 10.1021/ie2004779. URL <http://pubs.acs.org/doi/abs/10.1021/ie2004779>.
- Naviyn Prabhu Balakrishnan, Lakshminarayanan Samavedham, and Gade Pandu Rangaiah. Personalized Hybrid Models for Exercise, Meal and Insulin Interventions in Type 1 Diabetic Children and Adolescents. *Ind. Eng. Chem. Res.*, August 2013. ISSN 0888-5885. doi: 10.1021/ie402531k. URL <http://pubs.acs.org/doi/abs/10.1021/ie402531k>.
- F G Banting, C H Best, J B Collip, W R Campbell, and A A Fletcher. Pancreatic Extracts in the Treatment of Diabetes Mellitus. *Can. Med. Assoc. J.*, 12(3):141–6, March 1922. ISSN 0008-4409. URL <http://www.ncbi.nlm.nih.gov/pubmed/17580419>.
- Ananda Basu, Simmi Dube, Michael Slama, Isabel Errazuriz, Jose Carlos Amezcua, Yogish C Kudva, Thomas Peyser, Rickey E Carter, Claudio Cobelli, and Rita Basu. Time Lag of Glucose from Intravascular to Interstitial Compartment in Humans. *Diabetes*, pages 1–21, 2013.
- B Wayne Bequette. Challenges and recent progress in the development of a closed-loop artificial pancreas. *Annu. Rev. Control*, October 2012. ISSN 13675788. doi: 10.1016/j.arcontrol.2012.09.007. URL <http://linkinghub.elsevier.com/retrieve/pii/S1367578812000429>.
- R N Bergman, Y Z Ider, C R Bowden, and C Cobelli. Quantitative estimation of insulin sensitivity. *Am J Physiol Gastrointest Liver Physiol*, 236(6):G667–677, 1979.
- R N Bergman, L S Phillips, and C Cobelli. Physiologic Evaluation of Factors Controlling Glucose Tolerance in Man. *J Clin Invest*, 68(November 1981):1456–1467, 1981.

Bibliography

- A Bock, G François, T Prud'homme, and D Gillet. A Minimal Exercise Extension for Models of the Glucoregulatory System. In *Comput. Aided Chem. Eng.*, pages 1520–1524. 2011. doi: 10.1016/B978-0-444-54298-4.50083-0.
- A Bock, G François, and D Gillet. A Therapy Parameter-based Model for Predicting Blood Glucose Concentrations in Patients with Type 1 Diabetes. *Comput. Methods Programs Biomed.*, 2013.
- D Boiroux, D A Finan, J Bagterp Jørgensen, N Kjølstad Poulsen, and H Madsen. Optimal Insulin Administration for People with Type 1 Diabetes. Number Dycops, pages 234–239, Leuven, 2010a.
- D Boiroux, D A Finan, J B Jørgensen, N K Poulsen, and H Madsen. Meal Estimation in Nonlinear Model Predictive Control for Type 1 Diabetes. In *Symp. Nonlinear Control Syst.*, pages 1052–1057, 2010b. URL <http://scholar.google.com/scholar?hl=en&btnG=Search&q=intitle:Meal+Estimation+in+Nonlinear+Model+Predictive+Control+for+Type+1+Diabetes#8>.
- J Bondia, A J Laguna, P Rossetti, F J Ampudia-Blasco, and J Vehí. On the use of hard/soft specifications to deal with intra-patient variability in postprandial glucose control in type 1 diabetes. In *18th IFAC World Congr.*, volume 1, pages 8347–53, Milano, 2011.
- M Breton. Physical Activity - The Major Unaccounted Impediment to Closed Loop Control. *J. Diabetes Sci. Technol.*, 2:169–174, 2008.
- M Breton and B P Kovatchev. Analysis, modeling, and simulation of the accuracy of continuous glucose sensors. *J. Diabetes Sci. Technol.*, 2(5):853–62, September 2008. ISSN 1932-2968.
- Razvan Bunescu, Nigel Struble, Cindy Marling, Jay Shubbrook, and Frank Schwartz. Blood Glucose Level Prediction using Physiological Models and Support Vector Regression. *oucsace.cs.ohiou.edu*, 2013. URL <http://oucsace.cs.ohiou.edu/~razvan/papers/icmla13.pdf>.
- F Cameron. *Explicitly Minimizing Clinical Risk through Closed-loop Control of Blood Glucose in Patients with Type 1 Diabetes Mellitus*. PhD thesis, Stanford University, 2010.
- Fraser Cameron, Günter Niemeyer, Karen Gundy-Burlet, and Bruce Buckingham. Statistical hypoglycemia prediction. *J. Diabetes Sci. Technol.*, 2(4):612–21, July 2008. ISSN 1932-2968.
- Fraser Cameron, B W Bequette, D M Wilson, B A Buckingham, H Lee, and G Niemeyer. A Closed-Loop Artificial Pancreas Based on Risk Management. *J. Diabetes Sci. Technol.*, 5(2): 368–379, 2011.
- Fraser Cameron, Darrell M Wilson, Bruce A Buckingham, Hasmik Arzumanyan, Paula Clinton, H Peter Chase, John Lum, David M Maahs, Peter M Calhoun, and B Wayne Bequette. Inpatient studies of a Kalman-filter-based predictive pump shutoff algorithm. *J. Diabetes Sci. Technol.*, 6(5):1142–7, September 2012. ISSN 1932-2968. URL <http://www.pubmedcentral.nih.gov/articlerender.fcgi?artid=3570849&tool=pmcentrez&rendertype=abstract>.

- Germán Campetelli, Mercedes Lombarte, Marta S. Basualdo, and Alfredo Rigalli. Extended Adaptive Predictive Controller with Robust Filter to Enhance Blood Glucose Regulation in Type I Diabetic Subjects. *Comput. Chem. Eng.*, June 2013. ISSN 00981354. doi: 10.1016/j.compchemeng.2013.06.012. URL <http://linkinghub.elsevier.com/retrieve/pii/S0098135413002068>.
- Ismael Capel, Mercedes Rigla, Gema García-Sáez, Agustín Rodríguez-Herrero, Belén Pons, David Subías, Fernando García-García, Maria Gallach, Montserrat Aguilar, Carmen Pérez-Gandía, Enrique J Gómez, Assumpta Caixàs, and M Elena Hernando. Artificial Pancreas Using a Personalized Rule-Based Controller Achieves Overnight Normoglycemia in Patients with Type 1 Diabetes. *Diabetes Technol. Ther.*, 16(3):3–10, October 2013. ISSN 1557-8593. doi: 10.1089/dia.2013.0229. URL <http://www.ncbi.nlm.nih.gov/pubmed/24152323>.
- Marzia Cescon. *Linear Modeling and Prediction in Diabetes Physiology*. PhD thesis, Lund University, 2011.
- Marzia Cescon, Meike Stemmann, and Rolf Johansson. Impulsive predictive control of T1DM glycemia: an in-silico study. In *5th Annu. Dyn. Syst. Control Conf.*, 2012.
- Marzia Cescon, Rolf Johansson, and Eric Renard. Individualized empirical models of carbohydrate and insulin effects on T1DM blood glucose dynamics. In *IEEE Multi-Conference Syst. Control*, pages 258–263, Hyderabad, India, 2013. ISBN 9781479915576.
- W L Clarke, D Cox, L A Gonder-Frederick, W Carter, and S L Pohl. Evaluating clinical accuracy of systems for self-monitoring of blood glucose. *Diabetes Care*, 10(5):622, 1987.
- Claudio Cobelli, Eric Renard, and Boris Kovatchev. Artificial pancreas: past, present, future. *Diabetes*, 60(11):2672–82, December 2011. ISSN 1939-327X. doi: 10.2337/db11-0654.
- P Colmegna and R S Sánchez Peña. Analysis of three T1DM simulation models for evaluating robust closed-loop controllers. *Comput. Methods Programs Biomed.*, October 2013. ISSN 01692607. doi: 10.1016/j.cmpb.2013.09.020. URL <http://linkinghub.elsevier.com/retrieve/pii/S0169260713003271>.
- H Cormerais and P Richard. Artificial pancreas for type 1 diabetes: Closed-loop algorithm based on Error Dynamics Shaping. *J. Process Control*, pages 1–9, 2012. ISSN 0959-1524. doi: 10.1016/j.jprocont.2012.05.008.
- P E Cryer, S N Davis, and H Shamoon. Hypoglycemia in Diabetes. *Diabetes Care*, 26(6): 1902–1912, 2003.
- C Dalla Man, R A Rizza, and C Cobelli. Meal simulation model of the glucose-insulin system. *IEEE Trans Biomed Eng*, 54(10):1740–1749, 2007.
- C Dalla Man, M Breton, and C Cobelli. Physical Activity into the Meal Glucose-Insulin Model of Type 1 Diabetes: In Silico Studies. *J Diabetes Sci Technol*, 3:56–67, 2009.

Bibliography

- E R Damiano, F H El-Khatib, Zheng H, D M Nathan, and S J Russell. A Comparative Effectiveness Analysis of Three Continuous Glucose Monitors. *Diabetes Care*, 2012. doi: 10.2337/dc12-0070.
- Goodarz Danaei, Mariel M Finucane, Yuan Lu, Gitanjali M Singh, Melanie J Cowan, Christopher J Paciorek, John K Lin, Farshad Farzadfar, Young-Ho Khang, Gretchen A Stevens, Mayuree Rao, Mohammed K Ali, Leanne M Riley, Carolyn A Robinson, and Majid Ezzati. National, regional, and global trends in fasting plasma glucose and diabetes prevalence since 1980: systematic analysis of health examination surveys and epidemiological studies with 370 country-years and 2.7 million participants. *Lancet*, 378(9785):31–40, July 2011. ISSN 1474-547X. doi: 10.1016/S0140-6736(11)60679-X. URL <http://www.ncbi.nlm.nih.gov/pubmed/21705069>.
- E Daskalaki, A Prountzou, P Diem, and S G Mougiakakou. Real-Time Adaptive Models for the Personalized Prediction of Glycemic Profile in Type 1 Diabetes Patients. *Diabetes Technol. Ther.*, 14(2), October 2011. ISSN 1557-8593. doi: 10.1089/dia.2011.0093.
- E Daskalaki, P Diem, and S G Mougiakakou. An Actor-Critic based controller for glucose regulation in type 1 diabetes. *Comput. Methods Programs Biomed.*, April 2012. ISSN 1872-7565. doi: 10.1016/j.cmpb.2012.03.002.
- E Dassau, H Zisser, R A Harvey, M W Percival, B Grosman, W Bevier, E Atlas, S Miller, R Nimri, L Jovanovič, and F J Doyle III. Clinical Evaluation of a Personalized Artificial Pancreas. *Diabetes Care*, pages 1–9, 2012. doi: 10.2337/dc12-0948.
- Eyal Dassau, Pau Herrero, Howard Zisser, Bruce A Buckingham, Lois Jovanovič, Chiara Dalla Man, Claudio Cobelli, Josep Vehí, and Francis J Doyle III. Implications of Meal Library & Meal Detection to Glycemic Control of Type 1 Diabetes Mellitus through MPC Control. In *17th IFAC World Congr.*, pages 4228–4233, Seoul, Korea, 2008. ISBN 9781123478.
- S Del Favero, A Facchinetti, and C Cobelli. A Glucose-Specific Metric to Assess Predictors and Identify Models. *IEEE Trans. Biomed. Eng.*, (c):1–9, January 2012. ISSN 1558-2531. doi: 10.1109/TBME.2012.2185234.
- M Derouich and A Boutayeb. The effect of physical exercise on the dynamics of glucose and insulin. *J Biomech*, 35(7):911–917, 2002.
- P Dua, F J Doyle III, and E N Pistikopoulos. Model-based blood glucose control for Type 1 diabetes via parametric programming. *IEEE Trans Biomed Eng*, 53(8):1478–91, August 2006. ISSN 0018-9294. doi: 10.1109/TBME.2006.878075.
- F H El-Khatib, S J Russell, D M Nathan, R G Sutherlin, and E R Damiano. A bihormonal closed-loop artificial pancreas for type 1 diabetes. *Sci. Transl. Med.*, 2(27):27ra27, April 2010. ISSN 1946-6242. doi: 10.1126/scitranslmed.3000619.
- D Elleri, J M Allen, K Kumareswaran, L Leelarathna, M Nodale, K Caldwell, P Cheng, C Kollman, A Haidar, H R Murphy, M E Wilinska, C L Acerini, D B Dunger, and R Hovorka. Closed-Loop

- Basal Insulin Delivery Over 36 Hours in Adolescents With Type 1 Diabetes. *Diabetes Care*, 2012. doi: 10.2337/dc12-0816.
- Daniela Elleri, Janet M Allen, Marianna Nodale, Malgorzata E Wilinska, Jasdip S Mangat, Anne Mette F Larsen, Carlo L Acerini, David B Dunger, and Roman Hovorka. Automated Overnight Closed-Loop Glucose Control in Young Children with Type 1 Diabetes. *Diabetes Technol. Ther.*, 13(4), February 2011. ISSN 1557-8593. doi: 10.1089/dia.2010.0176.
- Christian Ellingsen, Eyal Dassau, Howard Zisser, Benyamin Grosman, Matthew W Percival, Lois Jovanovič, and F J Doyle III. Safety constraints in an artificial pancreatic β cell: An implementation of model predictive control with insulin on board. *J. Diabetes Sci. Technol.*, 3(3):536–544, 2009. URL <http://www.ncbi.nlm.nih.gov/pmc/articles/PMC2769860/>.
- G C Estrada, L Del Re, and E Renard. Nonlinear gain in online prediction of blood glucose profile in type 1 diabetic patients. In *49th IEEE Conf. Decis. Control*, pages 1668–1673, Atlanta, 2010.
- Andrea Facchinetti, Giovanni Sparacino, and Claudio Cobelli. Online denoising method to handle intraindividual variability of signal-to-noise ratio in continuous glucose monitoring. *IEEE Trans. Biomed. Eng.*, 58(9):2664–71, September 2011. ISSN 1558-2531. doi: 10.1109/TBME.2011.2161083. URL <http://www.ncbi.nlm.nih.gov/pubmed/21724499>.
- M Fernandez, M Villasana, and D Streja. Glucose dynamics in Type I diabetes: insights from the classic and linear minimal models. *Comput. Biol. Med.*, 37(5):611–27, May 2007. ISSN 0010-4825. doi: 10.1016/j.compbimed.2006.05.008.
- D Finan, F J Doyle III, C C Palerm, W C Bevier, H Zisser, L Jovanovic, and D E Seborg. Experimental evaluation of a recursive model identification technique for type 1 diabetes. *J. Diabetes Sci. Technol.*, 3(5):1192–202, January 2009. ISSN 1932-2968.
- D A Finan. *Modeling and monitoring strategies for type 1 diabetes*. PhD thesis, University of California, Santa Barbara, 2008. URL <http://gradworks.umi.com/33/42/3342013.html>.
- D A Finan, H Zisser, L Jovanovic, W C Bevier, and D E Seborg. Automatic Detection of Stress States in Type 1 Diabetes Subjects in Ambulatory Conditions. *Ind. Eng. Chem. Res.*, 49(17): 7843–7848, September 2010. ISSN 0888-5885. doi: 10.1021/ie901891c.
- Daniel A Finan, Howard Zisser, Lois Jovanovic, Wendy C Bevier, and Dale E Seborg. Practical issues in the identification of empirical models from simulated type 1 diabetes data. *Diabetes Technol. Ther.*, 9(5):438–50, October 2007. ISSN 1520-9156. doi: 10.1089/dia.2007.0202. URL <http://www.ncbi.nlm.nih.gov/pubmed/17931052>.
- U Fischer, W Schenk, E Salzsieder, G Albrecht, P Abel, and E-J Freyse. Does Physiological Blood Glucose Control Require an Adaptive Control Strategy? *IEEE Trans. Biomed. Eng.*, BME-34(8):575–582, 1987.

Bibliography

- G François, B Srinivasan, and D Bonvin. Convergence Analysis of Run-to-run Control for a Class of Nonlinear Systems. In *Proc. Am. Control Conf.*, volume 4, pages 3032–3037, Denver, 2003.
- G Freckmann, A Baumstark, N Jendrike, E Zschornack, S Kocher, J Tshiananga, F Heister, and C Haug. System accuracy evaluation of 27 blood glucose monitoring systems according to DIN EN ISO 15197. *Diabetes Technol. Ther.*, 12(3):221–31, 2010.
- Guido Freckmann, Stefan Pleus, Manuela Link, E Zschornack, Hans-Martin Klötzer, and Cornelia Haug. Performance evaluation of three continuous glucose monitoring systems: comparison of six sensors per subject in parallel. *J. Diabetes Sci. Technol.*, 7(4):842–853, 2013.
- M García-Jaramillo, R Calm, J Bondia, and J Vehí. Prediction of postprandial blood glucose under uncertainty and intra-patient variability in type 1 diabetes: A comparative study of three interval models. *Comput. Methods Programs Biomed.*, 2012. ISSN 0169-2607. doi: 10.1016/j.cmpb.2012.04.003.
- E Gardeñes, M A Sainz, L Jorba, R Calm, R Estela, H Mielgo, and A Trepát. Modal Intervals. *Reliab. Comput.*, 7:77–111, 2001.
- D V Goeddel, D G Kleid, F Bolivar, H L Heyneker, D G Yansura, R Crea, T Hirose, A Kraszewski, K Itakura, and A D Riggs. Expression in *Escherichia coli* of chemically synthesized genes for human insulin. *Proc. Natl. Acad. Sci. U. S. A.*, 76(1):106–10, January 1979. ISSN 0027-8424. URL <http://www.pubmedcentral.nih.gov/articlerender.fcgi?artid=382885&tool=pmcentrez&rendertype=abstract>.
- Benyamin Grosman, Eyal Dassau, Howard C Zisser, Lois Jovanovic, and Francis J Doyle III. Zone model predictive control: a strategy to minimize hyper- and hypoglycemic events. *J. Diabetes Sci. Technol.*, 4(4):961–75, July 2010. ISSN 1932-2968. URL <http://www.pubmedcentral.nih.gov/articlerender.fcgi?artid=2909531&tool=pmcentrez&rendertype=abstract>.
- Benyamin Grosman, Eyal Dassau, Howard Zisser, Lois Jovanovič, and Francis J Doyle III. Multi-Zone-MPC : Clinical Inspired Control Algorithm for the Artificial Pancreas. In *18th IFAC World Congr.*, pages 5–10, Milano, 2011.
- L Heinemann. Variability of insulin absorption and insulin action. *Diabetes Technol. Ther.*, 4(5):673–682, 2002.
- L Heinemann and J H Devries. Evidence for continuous glucose monitoring: sufficient for reimbursement? *Diabet. Med.*, October 2013. ISSN 1464-5491. doi: 10.1111/dme.12341. URL <http://www.ncbi.nlm.nih.gov/pubmed/24152416>.
- O K Hejlesen, S Andreassen, R Hovorka, and D A Cavan. DIAS - the diabetes advisory system: an outline of the system and the evaluation results obtained so far. *Comput. Methods Programs Biomed.*, 54(1-2):49–58, September 1997. ISSN 0169-2607.

- M Hernández-Ordoñez and D U Campos-Delgado. An extension to the compartmental model of type 1 diabetic patients to reproduce exercise periods with glycogen depletion and replenishment. *J Biomech*, 41(4):744–752, 2008.
- N Hernjak and F J Doyle III. Glucose control design using nonlinearity assessment techniques. *AIChE J.*, 51(2):544–554, February 2005. ISSN 0001-1541. doi: 10.1002/aic.10326.
- R Hovorka, F Shojaee-Moradie, P V Carroll, L J Chassin, I J Gowrie, N C Jackson, R S Tudor, A M Umpleby, and R H Jones. Partitioning glucose distribution/transport, disposal, and endogenous production during IVGTT. *Am. J. Physiol. Endocrinol. Metab.*, 282(5):E992–1007, 2002. ISSN 0193-1849. doi: 10.1152/ajpendo.00304.2001.
- R Hovorka, V Canonico, L J Chassin, U Haueter, M Massi-Benedetti, M O Federici, T R Pieber, H C Schaller, L Schaupp, T Vering, and M E Wilinska. Nonlinear model predictive control of glucose concentration in subjects with type 1 diabetes. *Physiol. Meas.*, 25(4):905–920, 2004. ISSN 0967-3334. doi: 10.1088/0967-3334/25/4/010.
- H-P Huang, S-w Liu, I-L Chien, and C-H Lin. A Dynamic Model with Structured Recurrent Neural Network to Predict Glucose-Insulin Regulation of Type 1 Diabetes Mellitus. In *Dyn. Control Process Syst.*, number Dycops, pages 228–233, Leuven, 2010.
- C S Hughes, S D Patek, M Breton, and B P Kovatchev. Anticipating the next meal using meal behavioral profiles: A hybrid model-based stochastic predictive control algorithm for T1DM. *Comput. Methods Programs Biomed.*, pages 1–11, June 2010. ISSN 1872-7565. doi: 10.1016/j.cmpb.2010.04.011.
- International Diabetes Foundation. IDF Diabetes Atlas, 5th edn. Technical report, International Diabetes Federation, Brussels, Belgium, 2011. URL <http://www.idf.org/diabetesatlas>.
- E P Joslin. The treatment of diabetes mellitus. *Can. Med. Assoc. J.*, pages 808–811, 1924.
- S S Kanderian, S A Weinzimer, G Voskanyan, and G M Steil. Identification of Intraday Metabolic Profiles during Closed-Loop Glucose Control in Individuals with Type 1 Diabetes. *J. Diabetes Sci. Technol.*, 3(5):1047–1057, January 2009. ISSN 1932-2968.
- Jonas Kildegaard, Jette Randløv, Jens Ulrik Poulsen, and Ole K Hejlesen. The impact of non-model-related variability on blood glucose prediction. *Diabetes Technol. Ther.*, 9(4):363–71, August 2007. ISSN 1520-9156. doi: 10.1089/dia.2006.0039.
- J Kim, G Saidel, and M Cabrera. Multi-Scale Computational Model of Fuel Homeostasis During Exercise: Effect of Hormonal Control. *Ann Biomed Eng*, 35(1):69–90, January 2007.
- Harald Kirchsteiger, Giovanna Castillo Estrada, Stephan Pölzer, Eric Renard, and Luigi del Re. Estimating Interval Process Models for Type 1 Diabetes for Robust Control Design. In *18th IFAC World Congr.*, pages 11761–6, Milano, Italy, 2011a.

Bibliography

- Harald Kirchsteiger, Stephan Pölzer, Rolf Johansson, Eric Renard, and Luigi del Re. Direct continuous time system identification of MISO transfer function models applied to type 1 diabetes. *IEEE Conf. Decis. Control Eur. Control Conf.*, (1):5176–5181, December 2011b. doi: 10.1109/CDC.2011.6161344. URL <http://ieeexplore.ieee.org/lpdocs/epic03/wrapper.htm?arnumber=6161344>.
- S Klim. *Predictive tools for designing new insulins and treatment regimens*. PhD thesis, DTU, 2009.
- Edward J Knobbe and Bruce Buckingham. The Extended Kalman Filter for Continuous Glucose Monitoring. *Diabetes Technol. Ther.*, 7(1):15–28, 2005.
- B P Kovatchev, M Straume, D J Cox, and L S Farhy. Risk analysis of blood glucose data: A quantitative approach to optimizing the control of insulin dependent diabetes. *J. Theor. Med.*, 3(1):1–10, 2000. ISSN 1027-3662.
- B P Kovatchev, M Breton, C Dalla Man, and C Cobelli. In Silico Preclinical Trials: A Proof of Concept in Closed-Loop Control of Type 1 Diabetes. *J. Diabetes Sci. Technol.*, 3(1), November 2009. ISSN 1573-4978.
- B P Kovatchev, E Renard, C Cobelli, Howard C Zisser, Patrick Keith-Hynes, Stacey M Anderson, Sue A Brown, Daniel R Chernavvsky, Marc D Breton, Anne Farret, Marie-Josée Pelletier, Jérôme Place, Daniela Bruttomesso, Simone Del Favero, Roberto Visentin, Alessio Filippi, Rachele Scotton, Angelo Avogaro, and Francis J Doyle III. Feasibility of Outpatient Fully Integrated Closed-Loop Control First studies of wearable artificial pancreas. *Diabetes Care*, 36:1851–8, 2013. doi: 10.2337/dc12-1965. URL <http://care.diabetesjournals.org/content/36/7/1851.short>.
- Kavita Kumareswaran, Hood Thabit, Lalantha Leelarathna, Karen Caldwell, Daniela Elleri, Janet M Allen, Marianna Nodale, Malgorzata E Wilinska, Mark L Evans, and Roman Hovorka. Feasibility of closed-loop insulin delivery in type 2 diabetes: a randomised controlled study. *Diabetes Care*, 2013. doi: 10.2337/dc13-1030.
- Matthew Kuure-Kinsey, Cesar C Palerm, and B Wayne Bequette. A dual-rate Kalman filter for continuous glucose monitoring. In *28th IEEE EMBS Annu. Int. Conf.*, volume 1, pages 63–6, New York City, January 2006. ISBN 1424400333. doi: 10.1109/IEMBS.2006.260057.
- Joon Bok Lee, Eyal Dassau, Dale E Seborg, and F J Doyle III. Model-Based Personalization Scheme of an Artificial Pancreas for Type 1 Diabetes Applications. In *2013 Am. Control Conf.*, pages 2917–2922, Washington, DC, USA, 2013. ISBN 9781479901760.
- E D Lehmann and T Deutsch. A Physiological Model of Glucose-Insulin Interaction. In *Physiol. Model.*, volume 13, pages 2274–75, 1991.
- Fabian León-Vargas, Fabricio Garelli, Hernán De Battista, and Josep Vehí. Postprandial blood glucose control using a hybrid adaptive PD controller with insulin-on-board limitation.

- Biomed. Signal Process. Control*, 8(6):724–732, November 2013. ISSN 17468094. doi: 10.1016/j.bspc.2013.06.008. URL <http://linkinghub.elsevier.com/retrieve/pii/S1746809413000931>.
- A Liebl, R Hoogma, E Renard, P H L M Geelhoed-Duijvestijn, E Klein, J Diglas, L Kessler, V Melki, P Diem, J-M Brun, P Schaepelynck-Bélicar, and T Frei. A reduction in severe hypoglycaemia in type 1 diabetes in a randomized crossover study of continuous intraperitoneal compared with subcutaneous insulin infusion. *Diabetes. Obes. Metab.*, 11(11):1001–8, November 2009. ISSN 1463-1326. doi: 10.1111/j.1463-1326.2009.01059.x. URL <http://www.ncbi.nlm.nih.gov/pubmed/19740082>.
- Roland Longchamp. *Commande Numérique de Systèmes Dynamiques*. Lausanne, Switzerland, ppur edition, 2010. ISBN 978-2-88074-880-7.
- Yoei M Luijff, J Hans DeVries, Koos Zwinderman, Lalantha Leelarathna, Marianna Nodale, Karen Caldwell, Kavita Kumareswaran, Daniela Elleri, Janet M Allen, Malgorzata E Wilinska, Mark L Evans, Roman Hovorka, Werner Doll, Martin Ellmerer, Julia K Mader, Eric Renard, Jerome Place, Anne Farret, Claudio Cobelli, Simone Del Favero, Chiara Dalla Man, Angelo Avogaro, Daniela Bruttomesso, Alessio Filippi, Rachele Scotton, Lalo Magni, Giordano Lanzola, Federico Di Palma, Paola Soru, Chiara Toffanin, Giuseppe De Nicolao, Sabine Arnolds, Carsten Benesch, Lutz Heinemann, and on behalf of the AP@home Consortium. Day and Night Closed-Loop Control in Adults With Type 1 Diabetes Mellitus: A comparison of two closed-loop algorithms driving continuous subcutaneous insulin infusion versus patient self-management. *Diabetes Care*, October 2013. doi: 10.2337/dc12-1956. URL <http://care.diabetesjournals.org/content/early/2013/10/22/dc12-1956.abstract>.
- Katrin Lunze, Tarunraj Singh, Marian Walter, Mathias D. Brendel, and Steffen Leonhardt. Blood glucose control algorithms for type 1 diabetic patients: A methodological review. *Biomed. Signal Process. Control*, pages 1–13, October 2012. ISSN 17468094. doi: 10.1016/j.bspc.2012.09.003.
- L Magni, D M Raimondo, L Bossi, C Dalla Man, G De Nicolao, B P Kovatchev, and C Cobelli. Model predictive control of type 1 diabetes: an in silico trial. *J. Diabetes Sci. Technol.*, 1(6): 804–812, November 2007. ISSN 1932-2968.
- L Magni, D M Raimondo, C Dalla Man, M Breton, S Patek, G De Nicolao, C Cobelli, and B P Kovatchev. Evaluating the efficacy of closed-loop glucose regulation via control-variability grid analysis. *J. Diabetes Sci. Technol.*, 2(4):630–5, July 2008. ISSN 1932-2968.
- G Marchetti, M Barolo, L Jovanovič, H Zisser, and D E Seborg. A Feedforward-Feedback Glucose Control Strategy for Type 1 Diabetes Mellitus. *J. Process Control*, 18(2):149–162, February 2008. ISSN 0959-1524. doi: 10.1016/j.jprocont.2007.07.008.
- Alan O Marcus. Continuous Subcutaneous Insulin Infusion Therapy with Rapid-Acting Insulin Analogs in Insulin Pumps: Does it Work, How Does it Work, and what Therapies Work Better than Others? *Open Diabetes J.*, 6(1):8–19, October 2013. ISSN 18765246. doi:

Bibliography

- 10.2174/1876524620130905001. URL <http://benthamscience.com/open/openaccess.php?todiaj/articles/V006/TODIAJ130905001.htm>.
- E B Marliss and M Vranic. Intense Exercise Has Unique Effects on Both Insulin Release and Its Roles in Glucoregulation. *Diabetes*, 51(suppl 1):S271–S283, 2002.
- Medtronic. Medtronic Gains Approval of First Artificial Pancreas Device System with Threshold Suspend Automation, 2013. URL <http://multimediacapsule.thomsonone.com/medtronic/medtronic-gains-approval-of-first-artificial-pancreas-device-system-with-threshold-suspend-automation->.
- K J Mikines, B Sonne, P A Farrell, B Tronier, and H Galbo. Effect of physical exercise on sensitivity and responsiveness to insulin in humans. *Am J Physiol Endocrinol Metab*, 254(3):E248–259, 1988.
- Shahar Miller, Revital Nimri, Eran Atlas, Eli A Grunberg, and Moshe Phillip. Automatic learning algorithm for the MD-logic artificial pancreas system. *Diabetes Technol. Ther.*, 13(10):983–90, October 2011. ISSN 1557-8593. doi: 10.1089/dia.2010.0216. URL <http://www.ncbi.nlm.nih.gov/pubmed/21774690>.
- H L Minuk, M Vranic, E B Marliss, A K Hanna, A M Albisser, and B Zinman. Glucoregulatory and metabolic response to exercise in obese noninsulin-dependent diabetes. *Am J Physiol Endocrinol Metab*, 240(5):E458–E464, 1981.
- D M Nathan, P A Cleary, J Y Backlund, S M Genuth, J M Lachin, T J Orchard, P Raskin, and B Zinman. Intensive diabetes treatment and cardiovascular disease in patients with type 1 diabetes. *New Engl J Med*, 353(25):2643–2653, 2005. ISSN 0028-4793.
- Revital Nimri, Ido Muller, Eran Atlas, Shahar Miller, Olga Kordonouri, Natasa Bratina, Christiana Tsioli, Magdalena A Stefanija, Thomas Danne, Tadej Battelino, and Moshe Phillip. Night glucose control with MD-Logic artificial pancreas in home setting: a single blind, randomized crossover trial-interim analysis. *Pediatr. Diabetes*, pages 1–9, August 2013. ISSN 1399-5448. doi: 10.1111/pedi.12071. URL <http://www.ncbi.nlm.nih.gov/pubmed/23944875>.
- Y Nishida, K Tokuyama, S Nagasaka, Y Higaki, Y Shirai, A Kiyonaga, M Shindo, I Kusaka, T Nakamura, S Ishibashi, and H Tanaka. Effect of Moderate Exercise Training on Peripheral Glucose Effectiveness, Insulin Sensitivity, and Endogenous Glucose Production in Healthy Humans Estimated by a Two-Compartment-Labeled Minimal Model. *Diabetes*, 53(2):315–320, 2004.
- G Nucci and C Cobelli. Models of subcutaneous insulin kinetics. A critical review. *Comput. Methods Programs Biomed.*, 62(3):249–257, 2000. ISSN 0169-2607.
- Michael J O’Grady, Adam J Retterath, D Barry Keenan, Natalie Kurtz, Martin Cantwell, Glenn Spital, Michael N Kremliovsky, Anirban Roy, Elizabeth A Davis, Timothy W Jones, and Trang T Ly. The use of an automated, portable glucose control system for overnight glucose control in adolescents and young adults with type 1 diabetes. *Diabetes Care*, 35(11):2182–7,

- December 2012. ISSN 1935-5548. doi: 10.2337/dc12-0761. URL <http://www.ncbi.nlm.nih.gov/pubmed/22875230>.
- C Owens, H Zisser, L Jovanovic, B Srinivasan, D Bonvin, and F J Doyle III. Run-to-run control of blood glucose concentrations for people with type 1 diabetes mellitus. *IEEE Trans. Biomed. Eng.*, 53(6):996–1005, 2006.
- Cesar C Palerm, Howard Zisser, Lois Jovanovič, and Francis J Doyle III. A Run-to-Run Control Strategy to Adjust Basal Insulin Infusion Rates in Type 1 Diabetes. *J. Process Control*, 18(3-4):258–265, January 2008. ISSN 0959-1524. doi: 10.1016/j.jprocont.2007.07.010. URL <http://www.pubmedcentral.nih.gov/articlerender.fcgi?artid=2516944&tool=pmcentrez&rendertype=abstract>.
- S Patek, L Magni, E Dassau, C Karvetski, C Toffanin, G De Nicolao, S Del Favero, M Breton, C Dalla Man, E Renard, H Zisser, F Doyle, C Cobelli, and B Kovatchev. Modular Closed-Loop Control of Diabetes. *IEEE Trans. Biomed. Eng.*, (c):1–14, April 2012. ISSN 1558-2531. doi: 10.1109/TBME.2012.2192930.
- Stephen D Patek, B Wayne Bequette, Marc Breton, Bruce A Buckingham, Eyal Dassau, Francis J Doyle III, John Lum, Lalo Magni, and Howard Zisser. In Silico Preclinical Trials: Methodology and Engineering Guide to Closed-Loop Control in Type 1 Diabetes Mellitus. *J. Diabetes Sci. Technol.*, 3(2):269–282, 2009.
- Stephen D Patek, Colleen S Hughes, Pavel Vereshchetin, Marc Breton, and Boris P Kovatchev. Correction Insulin Advisory System Based on Meal Behavioral Profiles. In *18th IFAC World Congr.*, pages 8354–9, Milano, Italy, 2011.
- M W Percival, W C Bevier, H Zisser, L Jovanovic, D E Seborg, and F J Doyle III. Prediction of Dynamic Glycemic Trends Using Optimal State Estimation. In *Proc. 17th World Congr. IFAC*, pages 4222–4227, Seoul, Korea, 2008. IFAC.
- M W Percival, W C Bevier, Y Wang, E Dassau, H C Zisser, Lois Jovanovič, and Doyle. Modeling the effects of subcutaneous insulin administration and carbohydrate consumption on blood glucose. *J. Diabetes Sci. Technol.*, 4(5):1214–28, January 2010. ISSN 1932-2968.
- G Pillonetto, G Sparacino, and C Cobelli. Numerical non-identifiability regions of the minimal model of glucose kinetics: superiority of Bayesian estimation. *Math. Biosci.*, 184(1):53–67, July 2003. ISSN 00255564. doi: 10.1016/S0025-5564(03)00044-0.
- Thierry Prud’homme, Alain Bock, Gregory Francois, and Denis Gillet. Preclinically assessed optimal control of postprandial glucose excursions for type 1 patients with diabetes. In *2011 IEEE Int. Conf. Autom. Sci. Eng.*, pages 702–707. IEEE, August 2011. ISBN 978-1-4577-1730-7. doi: 10.1109/CASE.2011.6042510.
- Itamar Raz, Ram Weiss, Yevgeny Yegorchikov, Gabriel Bitton, Ron Nagar, and Benny Pesach. Effect of a local heating device on insulin and glucose pharmacokinetic profiles in an

Bibliography

- open-label, randomized, two-period, one-way crossover study in patients with type 1 diabetes using continuous subcutaneous insulin infusion. *Clin. Ther.*, 31(5):980–7, May 2009. ISSN 0149-2918. doi: 10.1016/j.clinthera.2009.05.010. URL <http://www.ncbi.nlm.nih.gov/pubmed/19539098>.
- Eric Renard, Claudio Cobelli, and Boris P. Kovatchev. Closed loop developments to improve glucose control at home. *Diabetes Res. Clin. Pract.*, September 2013. ISSN 01688227. doi: 10.1016/j.diabres.2013.09.009. URL <http://linkinghub.elsevier.com/retrieve/pii/S0168822713003240>.
- A Roy. *Dynamic Modeling of Free Fatty Acid, Glucose, and Insulin during Rest and Exercise in Insulin Dependent Diabetes Mellitus Patients*. PhD thesis, University of Pittsburgh, 2008.
- A Roy and R S Parker. Dynamic Modeling of Exercise Effects on Plasma Glucose and Insulin Levels. *J Diabetes Sci Technol*, 1(3):338–347, 2007.
- A Rutscher, E Salzsieder, and U Fischer. KADIS: Model-aided education in type I diabetes. *Comput. Methods Programs Biomed.*, 41(3-4):205–215, 1994.
- Dan Simon. *Optimal State Estimation: Kalman, H Infinity, and Nonlinear Approaches*, volume 54. Wiley-Interscience, 2006. ISBN 0471708585.
- J T Sorensen. *A physiologic model of glucose metabolism in man and its use to design and assess improved insulin therapies for diabetes*. PhD thesis, Massachusetts Institute of Technology, 1985.
- P Soru, G De Nicolao, C Toffanin, C Dalla Man, C Cobelli, and L Magni. MPC based Artificial Pancreas: Strategies for individualization and meal compensation. *Annu. Rev. Control*, April 2012. ISSN 13675788. doi: 10.1016/j.arcontrol.2012.03.009.
- F Ståhl and R Johansson. Observer Based Plasma Glucose Prediction in Type I Diabetes. In *IEEE Multi-Conference Syst. Control*, volume 4, pages 1620–1625, 2010.
- Andreas Svensson. *Model Predictive Control with Invariant Sets in Artificial Pancreas for Type 1 Diabetes Mellitus*. Master, Linköping, 2013. URL <http://liu.diva-portal.org/smash/get/diva2:632180/FULLTEXT01.pdf>.
- The Diabetes Control and Complications Trial Research Group. The effect of intensive treatment of diabetes on the development and progression of long-term complications in insulin-dependent diabetes mellitus. *New Engl J Med*, 329(14):977–86, September 1993. ISSN 0028-4793. doi: 10.1056/NEJM199309303291401.
- The Doyle Group and the Sansum Diabetes Research Institute. Successful Trial of Inhaled Insulin a Major Advancement in Treatment of Type 1 Diabetes, 2013. URL <http://engineering.ucsb.edu/news/730>.
- B B Tiger. How to kiss a Stuffed cat. *Ingl. Bast.*, 14th of October 2012

- K Turksoy, E S Bayrak, L Quinn, E Littlejohn, and A Cinar. Multivariable Adaptive Closed-Loop Control of an Artificial Pancreas Without Meal and Activity Announcement. *Diabetes Technol. Ther.*, 15(5), April 2013. ISSN 1557-8593. doi: 10.1089/dia.2012.0283. URL <http://www.ncbi.nlm.nih.gov/pubmed/23544672>.
- R H Unger and S Grundy. Hyperglycemia as an inducer as well as a consequence of impaired islet cell function and insulin resistance: implications for the management of diabetes. *Diabetologia*, 28:119–121, 1985.
- K van Heusden, E Dassau, H Zisser, D Seborg, and F Doyle. Control-relevant models for glucose control using a priori patient characteristics. *IEEE Trans. Biomed. Eng.*, 7:1839–1849, November 2012. ISSN 1558-2531. doi: 10.1109/TBME.2011.2176939.
- Paul Vereshchetin, Marc Breton, and Stephen D Patek. Mealtime Correction Insulin Advisor for CGM-Informed Insulin Pen Therapy. In *2013 Am. Control Conf.*, number i, pages 2923–2928, Washington, DC, USA, 2013. ISBN 9781479901760.
- P Vicini and C Cobelli. The iterative two-stage population approach to IVGTT minimal modeling: Improved precision with reduced sampling. *Am J Physiol-Endoc M*, 280(1 43-1): E178–E186, 2001.
- J Vora and T Heise. Variability of glucose-lowering effect as a limiting factor in optimizing basal insulin therapy. A review. *Diabetes. Obes. Metab.*, March 2013. ISSN 1463-1326. doi: 10.1111/dom.12087.
- Youqing Wang, Matthew W Percival, Eyal Dassau, Howard C Zisser, Lois Jovanovic, and Francis J Doyle. A novel adaptive basal therapy based on the value and rate of change of blood glucose. *J. Diabetes Sci. Technol.*, 3(5):1099–108, September 2009. ISSN 1932-2968. URL <http://www.pubmedcentral.nih.gov/articlerender.fcgi?artid=2769919&tool=pmcentrez&rendertype=abstract>.
- Youqing Wang, Eyal Dassau, Howard Zisser, Lois Jovanovič, and Francis J Doyle. Automatic bolus and adaptive basal algorithm for the artificial pancreatic β -cell. *Diabetes Technol. Ther.*, 12(11):879–87, November 2010. ISSN 1557-8593. doi: 10.1089/dia.2010.0029. URL <http://www.ncbi.nlm.nih.gov/pubmed/20879966>.
- S A Weinzimer, G M Steil, K L Swan, J Dziura, N Kurtz, and W V Tamborlane. Fully automated closed-loop insulin delivery versus semiautomated hybrid control in pediatric patients with type 1 diabetes using an artificial pancreas. *Diabetes Care*, 31(5):934–939, 2008.
- M E Wilinska, L J Chassin, H C Schaller, L Schaupp, T R Pieber, and R Hovorka. Insulin kinetics in type-1 diabetes: continuous and bolus delivery of rapid acting insulin. *IEEE Trans. Biomed. Eng.*, 52(1):3–12, 2005.
- Malgorzata E Wilinska, Ludovic J Chassin, Carlo L Acerini, Janet M Allen, David B Dunger, and Roman Hovorka. Simulation environment to evaluate closed-loop insulin delivery

Bibliography

- systems in type 1 diabetes. *J. Diabetes Sci. Technol.*, 4(1):132–44, January 2010. ISSN 1932-2968. URL <http://www.pubmedcentral.nih.gov/articlerender.fcgi?artid=2825634&tool=pmcentrez&rendertype=abstract>.
- Konstantia Zarkogianni, Andriani Vazeou, Stavroula G Mougiakakou, Aikaterini Prountzou, and Konstantina S Nikita. An Insulin Infusion Advisory System Based on Autotuning Non-linear Model-Predictive Control. *IEEE Trans. Biomed. Eng. Eng.*, 58(9):2467–2477, 2011.
- C Zecchin, A Facchinetti, G Sparacino, G De Nicolao, and C Cobelli. Neural Network Incorporating Meal Information Improves Accuracy of Short-Time Prediction of Glucose Concentration. *IEEE Trans. Biomed. Eng.*, 59(6):1550–1560, 2012.
- C L Zhang and F A Popp. Log-normal distribution of physiological parameters and the coherence of biological systems. *Med. Hypotheses*, 43(1):11–16, July 1994. ISSN 03069877. doi: 10.1016/0306-9877(94)90042-6.
- B Zinman, N Ruderman, B N Campaigne, J T Devlin, and S H Schneider. Physical Activity/Exercise and Diabetes. *Diabetes Care*, 27(supplement 1):S59–S62, 2004.
- Howard Zisser, Lauren Robinson, Wendy Bevier, Eyal Dassau, Christian Ellingsen, Francis J Doyle III, and Lois Jovanovic. Bolus Calculator: A Review of Four "Smart" Insulin Pumps. *Diabetes Technol. Ther.*, 10(6):441–4, December 2008. ISSN 1520-9156. doi: 10.1089/dia.2007.0284. URL <http://www.ncbi.nlm.nih.gov/pubmed/19049372>.

Glossary

Several acronyms are used during this thesis. For quick reference, they are listed here with a link to their first mention and further explanations.

Acronyms

Abbreviation	Explanation	Details
AP	Artificial Pancreas	1.1.2, 5.1
AR	Autoregressive	2.2.3
ARIMA	AutoRegressive Integrated Moving Average	2.2.3
ARMAX	AutoRegressive–Moving-Average with eXogenous inputs	2.2.3
ARX	AutoRegressive with eXogenous inputs	2.2.3
BB	Basal/Bolus	5.3.4
BMM	Bergman Minimal Model	2.1,2.3.1
BG	Blood Glucose	1.1.1
BGRI	Blood Glucose Risk Index	5.2.2, B.4
CF	Correction Factor	2.3.2
CGM	Continuous Glucose Monitoring	1.1.2
CHO	Carbohydrates	1.1.2
CSII	Continuous Subcutaneous Insulin Infusion	1.1.2
CV	Coefficient of Variability	1.2.2
CVGA	Control-Variability Grid Analysis	B.8
EDS	Error Dynamics Shaping	5.3.1, 5.3.4
EGA	Error Grid Analysis	B.3
EKF	Extended Kalman Filter	1.3.3, 4.3.4
EMPC	Extended Model Predictive Control	5.3.4
FDA	Food and Drug Administration	1.2.1
GI	Glycemic Index	1.2.2
HBGI	High Blood Glucose Risk Index	B.4
HR	Heart Rate	C.2.1
I2C	Insulin-to-Carbohydrates ratio	2.3.2
IIAS	Insulin Infusion Advisory System	5.3.4
IOB	Insulin On Board	5.2.1, 5.2.2
IP	Intraperitoneal	1.1.2

Glossary

Abbreviation	Explanation	Details
IV	Intravenous	1.1.2
KF	Kalman Filter	4.1, 4.3.3
LBG	Low Blood Glucose Index	B.4
MAD	Mean Absolute Difference	2.4.4, B.1
MDI	Multiple Daily Injections	1.1.2
MISO	multiple inputs - single output	4.3.2
MM	Minimal Model	2.3.1
MPC	Model Predictive Control	2.2.3, 5.3.1
NN	Neural Networks	2.2.3
ODE	Ordinary Differential Equation	3.1
PID	Proportional-Integral-Derivative	5.3.1
R²	coefficient of determination	2.4.4, B.2
RMSE	Root Mean Square Error	
SDE	Stochastic Differential Equation	3.1
SMBG	Self Monitoring of Blood Glucose	4.3.3, B.5
SC	Subcutaneous	1.1.2
sTPC	stochastic Therapy Parameter-based Controller	5.4.3
sTPM	stochastic Therapy Parameter-based Model	3.3.2
T1DM	Type 1 Diabetes Mellitus	1.1.1
T2DM	Type 2 Diabetes Mellitus	1.1.1
TDI	Total Daily Insulin	2.2.3
TPC	Therapy Parameter-based Controller	5.3.2
TPF	Therapy Parameter-based Filter	1.3.3, 4.3.5
TPM	Therapy Parameter-based Model	2.3.1
TPM+	Extended Therapy Parameter-based Model	2.3.1
U	insulin Unit	2.3.2
UVa	University of Virginia	A.1

Variables

Variable	Units	Explanation
A	N/A	state matrix
α_d	unit-less	weight associated to day d
a_e	\min^{-1}	inverse of the exercise constant
a_g	\min^{-1}	inverse of the meal time constant
a_x	\min^{-1}	inverse of the insulin absorption/action time constant
B	N/A	input matrix
C	N/A	output matrix
CF	$\text{mg} \cdot \text{dl}^{-1} \cdot \text{U}^{-1}$	correction factor
D	unit-less	number of day
$D(s)$	N/A	TPM meal perturbation subsystem in Laplace domain
δ (discrete)	unit-less	Kronecker delta
δ (continuous)	unit-less	Dirac impulse
ΔG	$\text{mg} \cdot \text{dl}^{-1}$	BG concentration error ($G_m - G_t$)
Δ_I	$\text{mg} \cdot \text{dl}^{-1}$	insulin induced drop in BG
Δ_M	$\text{mg} \cdot \text{dl}^{-1}$	CHO induced rise in BG
e	$\text{mg} \cdot \text{dl}^{-1}$	BG concentration error
f_{det}	N/A	deterministic model function / drift function
f_{sto}	N/A	stochastic model function
g	N/A	diffusive function
G	$\text{mg} \cdot \text{dl}^{-1}$	BG concentration
Γ	N/A	discrete-time input matrix
\hat{G}	$\text{mg} \cdot \text{dl}^{-1}$	estimated BG concentration
\overline{G}	$\text{mg} \cdot \text{dl}^{-1}$	upper 95% confidence interval limit
\underline{G}	$\text{mg} \cdot \text{dl}^{-1}$	lower 95% confidence interval limit
\bar{G}	$\text{mg} \cdot \text{dl}^{-1}$	average BG
G_0	$\text{mg} \cdot \text{dl}^{-1}$	initial BG concentration
$G_{e,i}$	$\text{mg} \cdot \text{dl}^{-1}$	exact BG concentration at time t_i
G_m	$\text{mg} \cdot \text{dl}^{-1}$	measured BG concentration
G_t	$\text{mg} \cdot \text{dl}^{-1}$	target BG concentration
G_{SP}	$\text{mg} \cdot \text{dl}^{-1}$	BG concentration setpoint
G_{ss}	$\text{mg} \cdot \text{dl}^{-1}$	steady-state BG concentration
G_{TPM+}	$\text{mg} \cdot \text{dl}^{-1}$	BG concentration modeled by the TPM+
h	\min	prediction horizon
$H(s)$	N/A	system transfer function
H_{IOB}	N/A	transfer function of IOB
h_c	\min	control and prediction horizon
$I(s)$	N/A	TPM glucose-insulin subsystem in Laplace domain
\mathcal{I}	N/A	Fisher information matrix
I_{TPM+}	N/A	glucose-insulin subsystem for TPM+
$I2C$	$\text{U} \cdot \text{g}^{-1}$	insulin to CHO ratio
IOB	U	insulin on board
I_p	U/l	plasma insulin concentration
J	N/A	objective function

Glossary

Variable	Units	Explanation
J_d	$mg^2 \cdot dl^{-2}$	objective function on day d
J_{sTPM}	unit-less	risk-based cost function
K	N/A	Kalman filter gain
$K(s)$	N/A	controller transfer function
K_g	$mg \cdot dl^{-1} \cdot g^{-1}$	meal sensitivity
K_p	$U \cdot mg^{-1} \cdot dl \cdot min^{-1}$	gain of proportional controller
K_x	$mg \cdot dl^{-1} \cdot U^{-1}$	insulin sensitivity/correction factor
K_x in MM	U^{-1}	insulin sensitivity
L	N/A	Luenberger observer gain matrix
m	unit-less	number of inputs
n	unit-less	number of states
n	unit-less	number of samples
N	unit-less	number of BG measurements
N_d	unit-less	number of BG measurements on day d
N_c	unit-less	number of samples within h_c
ω_0	rad/s	system cutoff frequency
ω_c	rad/s	cutoff frequency
ω_s	rad/s	sampling frequency
p	unit-less	number of parameters
P	N/A	state covariance matrix
$p_{95\%}$	unit-less	average expected probability of being in 95% confidence interval
$p_{95\%,i}$	unit-less	expected probability of being in 95% confidence interval for $G_{m,i}$
P_{TPM+}	N/A	meal perturbation sub-system for TPM+
P_{BG}	$mg^2 \cdot dl^{-2}$	variance of BG state
$P_{BG,0}$	$mg^2 \cdot dl^{-2}$	initial variance of the BG state
Φ	N/A	discrete-time state matrix
p_2	min^{-1}	inverse of the insulin action time constant in BMM
q	unit-less	quotient of time constants
Q	N/A	process noise covariance matrix
Q_{BG}	$mg^2 \cdot dl^{-2}$	variance of process noise on BG state
r	%	relative error of BG meter
R	N/A	measurement noise covariance matrix
S	N/A	setpoint adaptation
\mathbf{S}	N/A	sensitivity of states
\mathbf{S}_{BG}	N/A	sensitivity of BG state
σ_{BG}	$mg \cdot dl^{-1}$	standard deviation of BG state
σ_{CGM}	$mg \cdot dl^{-1}$	standard deviation of CGM measurement
S_e	min^{-1}	exercise-induced increase in S_G
S_G	min^{-1}	glucose effectiveness at zero insulin
S_{ins+G}	min^{-1}	combination of insulin and S_G effect
$\sigma_{G,0}^2$	$mg^2 \cdot dl^{-2}$	variance of G_0
σ_i	$mg \cdot dl^{-1}$	standard deviation of measurement error of i^{th} data point
σ_{BG}	$mg \cdot dl^{-1}$	standard deviation of BG state
σ_{SMBG}	$mg \cdot dl^{-1}$	standard deviation of SMBG measurement
S_I	$U^{-1} \cdot min^{-1} \cdot l$	insulin sensitivity in BMM

Variable	Units	Explanation
S_{TPM+}	N/A	setpoint adaptation for the TPM+
t	min	time
θ	N/A	vector of model parameters
t_e	min	end time
t_f	min	final time
t_I	time	time of insulin bolus
t_M	time	time of meal intake
T_M	min	meal intake duration
t_{minBG}	min	time at which minimum BG is reached
t_{maxBG}	min	time at which maximum BG is reached
τ	min	proportional controller time constant
τ_{CL}	min	closed loop system time constant
τ_g	min	meal time constant
τ_x	min	insulin action time constant
T_s	min	sampling time
t_s	min	start time
u	N/A	input vector
U_0	$U \cdot min^{-1}$	feed-forward insulin injection
U_{CHO}	$g \cdot min^{-1}$	carbohydrate intake rate
$U_{CHO,tot}$	g	total amount of ingested CHO
U_e	unit-less	exercise input
U_{endo}	$mg \cdot dl^{-1} \cdot min^{-1}$	endogenous glucose production
U_G	$g \cdot min^{-1}$	gut glucose absorption
$U_{G,1}$	$g \cdot min^{-1}$	intermediate gut glucose absorption
U_I	$U \cdot min^{-1}$	subcutaneous insulin infusion rate
$U_{I,tot}$	U	total amount of infused insulin
$U_{I,corr}$	U	corrective insulin infusion
$U_{I,meal}$	U	meal rejection insulin infusion
v	N/A	measurement noise
w	N/A	process noise
W_i	unit-less	weight associated to BG measurement i
x	N/A	state vector
\hat{x}	N/A	estimated state vector
X	$U \cdot min^{-1}$	insulin action
\hat{X}	$U \cdot min^{-1}$	estimated insulin action
X in BMM	min^{-1}	insulin action
x_{BG}	$mg \cdot dl^{-1}$	BG state
\bar{x}_{BG}	$mg \cdot dl^{-1}$	lower bound of the estimated confidence interval
\underline{x}_{BG}	$mg \cdot dl^{-1}$	upper bound of the estimated confidence interval
\hat{x}_{BG}	$mg \cdot dl^{-1}$	estimated BG state
X_0	$U \cdot min^{-1}$	initial insulin action
X_1	$U \cdot min^{-1}$	intermediate insulin action
$X_{1,0}$	$U \cdot min^{-1}$	initial intermediate insulin action
\hat{X}_1	$U \cdot min^{-1}$	estimated intermediate insulin action
y	N/A	output vector

Avenue du Tir-Fédéral 79
1022 Chavannes-près-Renens
Switzerland

+41 76 4194760
alain.bock@gmail.com
ch.linkedin.com/in/alainbock

Luxembourgish (B permit)
Single
20.06.1985

ALAIN BOCK

EDUCATION	PHD IN ELECTRICAL ENGINEERING , Ecole Polytechnique Fédérale de Lausanne	2009 – 01.2014
	At the React group and the Laboratoire d'Automatique in collaboration with Roche Diagnostics	
	MSC IN MECHANICAL ENGINEERING , Ecole Polytechnique Fédérale de Lausanne	2004 - 2009
	Specialized in automatic control and production management	
	DIPLÔME DE FIN D'ÉTUDES SECONDAIRES , Lycée de Garçons, Luxembourg	1997-2004
	Mathematics and physics section	

PROJECTS	PHD THESIS: MODELS AND MODEL-BASED TOOLS TO IMPROVE TREATMENT OF TYPE 1 DIABETES
----------	---

- Design and validation of a reliable model for predictions of blood glucose concentrations
- Development of control method to improve patient safety
- Involved in planning and execution of a clinical study to test developed methods
- 6 months with Roche Diagnostics in Indianapolis, IN, USA
- Management of several Master projects

	MASTER THESIS: VIBRATION DAMPING CONTROL FOR WIRE ELECTRIC DISCHARGE MACHINING
--	---

At the **Laboratoire d'Automatique** in collaboration with **GF AgieCharmilles**, Geneva, CH

- Modeling and parameter identification of EDM process

Reduction of electrode vibration using complex robust controller design

INTERNSHIPS	DESIGN INTERNSHIP, IMAtec , Ettelbruck, Luxembourg	2006
	Design of a plastic foil packaging module using CAD software	
	TOOLING INTERNSHIP, ARCELOR , Differdange, Luxembourg	2005

LANGUAGES	ENGLISH, FRENCH, GERMAN: fluent (C2)
	SPANISH: basic (A1)
	LUXEMBOURGISH: mother tongue

SKILLS	TECHNICAL: Optimal control, optimization, parameter identification, population-based methods, data-based physiological modeling, basic and advanced control methods, stochastic modeling
	PROGRAMMING LANGUAGES: Matlab, Simulink, C, C++, Python
	SOFTWARE + OS: MS Office, LaTeX, CATIA, Inventor, Windows (XP, Vista, 7, 8), Mac OS X (10.5-8), Android

PUBLICATIONS	• Bock, A., François, G., & Gillet, D. (2013). A Therapy Parameter-based Model for Predicting Blood Glucose Concentrations in Patients with Type 1 Diabetes. <i>Comput. Methods Programs Biomed.</i>	
	• Bock, A., François, G., Prud'homme, T., & Gillet, D. (2011). A Minimal Exercise Extension for Models of the Glucoregulatory System. In <i>Comput. Aided Chem. Eng.</i> (pp. 1520–1524). doi:10.1016/B978-0-444-54298-4.50083-0	
	• Prud'homme, T., Bock, A., Francois, G., & Gillet, D. (2011). Preclinically assessed optimal control of postprandial glucose excursions for type 1 patients with diabetes. In <i>2011 IEEE Int. Conf. Autom. Sci. Eng.</i> (pp. 702–707). IEEE. doi:10.1109/CASE.2011.6042510	
	• Bock, A., Duke, D. L., & Soni, A. S. (2013). System and Method Considering the Effect of Physical Activity on the Glucoregulatory System. US 20,130,130,215.	181